Dynamics of the core planar polarity proteins and their role in morphogenesis in *Drosophila*

Samantha Jane Warrington

Submitted for the degree of Doctor of Philosophy

The University Of Sheffield.

Department of Biomedical Science
University of Sheffield

January 2014

Abstract

Signalling through the Frizzled-dependent planar polarity pathway is a conserved mechanism that polarises cells in a plane perpendicular to the apical-basal axis. Epithelial cells in many organisms exhibit planar polarity, including the *Drosophila* wing and eye, and during convergent extension movements in vertebrates.

The core planar polarity proteins involved in establishing planar polarity exhibit asymmetric subcellular localisations. Currently little is known about how the asymmetry is generated and maintained. This work uses techniques such as live imaging and FRAP of *Drosophila* epithelial tissues to study protein turnover, to understand these processes.

I focused on the core proteins Frizzled (Fz) and Flamingo (Fmi). Both proteins are localised at apical junctions in membrane subdomains (puncta). FRAP on puncta of either protein shows there is a large immobile fraction compared to surrounding junctional regions. Mutations in the other core proteins result in a loss of Fz and Fmi protein asymmetry, a loss of large puncta, as well as a reduction in the size of the immobile fraction.

My data support a model where the six known core proteins are mutually stabilised by each other into large puncta where they form intercellular asymmetric junctional complexes. These puncta represent groups of aligned intercellular protein complexes, which I propose are required for establishing and coupling cellular asymmetry.

The roles of planar polarity during coordinated cell rearrangements have not been extensively studied in *Drosophila*. This work shows that the core proteins are required for coordinated cell rearrangements during *Drosophila* embryonic tracheal cell intercalation. Regulation of the adhesion protein DE-cadherin is required for cell intercalation and this is under control of the core proteins via a RhoGEF2-dependent mechanism. Therefore this work supports a role for the core proteins in regulating cell adhesion during cell movements.

Declaration

Samantha Warrington certifies that all the material contained within this document is her own work except where it is clearly referenced to others.

No part of this thesis has been submitted for a degree, diploma or other qualification at any other university or other institute of higher learning.

All the pupal wing images in chapter 6 were dissected and immunostained by Helen Strutt, but the wings were imaged and the fluorescent intensity junctional measurements quantified by Samantha Warrington.

Figures in chapter 2 (2.4) and figures in chapters 3 (3.1 to 3.4) are reprinted from Developmental cell, 20, Strutt, H., S.J. Warrington, and D. Strutt, Dynamics of core planar polarity protein turnover and stable assembly into discrete membrane subdomains, 511-525, (2011), with permission from Elsevier.

Figures in chapter 4 (4.2 to 4.10) and in chapter 5 (5.3 to 5.12) are reprinted from Development, 140(8), Warrington, S.J., H. Strutt, and D. Strutt. The Frizzled-dependent planar polarity pathway locally promotes E-cadherin turnover via recruitment of RhoGEF2, 1693-1702, (2013), with permission from Development.

January 2014

Contents

List of Figures

CHAPTER 1

CHAPTER 2

CHAPTER 3

CHAPTER 4

CHAPTER 5

CHAPTER 6

List of Tables

List of Abbreviations

Abl	Abelson kinase
Act	Actin
Act5C	Actin5C
AJ's	Adherens Junctions
α-Cat	α-Catenin
APF	After Puparium Formation
Arg	Abl related gene
Arm	Armadillo
Baz	Bazooka
β-Cat	β-Catenin
Btl	Breathless
CA	Constitutively Active
DABCO	1,4-diazabicyclo [2.2.2] octane
DFz2	*Drosophila* Frizzled2
Dgo	Diego
Dia	Diaphanous
Dpp	Decapentaplegic
DN	Dominant Negative
Ds	Dachsous
Dsh	Dishevelled
E-cad	E-cadherin
EGFP	Enhanced Green Fluorescent Protein
En	Engrailed
EYFP	Enhanced Yellow Fluorescent Protein
FLIP	Fluorescent Loss In Photo-bleaching
Fj	Four-jointed
Fmi	Flamingo
FRAP	Fluorescent Recovery After Photobleaching
Frtz	Fritz
Ft	Fat
Fy	Fuzzy
Fz	Frizzled
GBE	Germ Band Extension
Hh	Hedgehog

hr	hour
hs	heat shock
In	Inturned
KI	Knock in
LRP6	low-density lipoprotein receptor-related protein 6
µm	micrometers
min	minute
Mwh	Multiple wing hairs
MyoII	MyosinII
NLS	Nuclear localisation signal
nm	nanometres
Pk	Prickle
Ptc	Patched
ROI's	Regions of Interest
SD	Standard deviation
sec	second
s.e.m.	Standard Error of the Mean
SFK's	Src family kinases
shg	*shotgun*
shi	*shibire*
Sp-le	Spiny-legs
Src42A	Src oncogene at 42A
Stbm	Strabismus
Stan	Starry Night
TSS	Triton Salt Solution
Ubi	Ubiquitous
Ubx	Ultrabithorax
Vangl2	Van Gogh-Like 2
Wg	Wingless
Zip	Zipper

Acknowledgments

My deepest gratitude is to my supervisor, David Strutt. I have been fortunate to have a supervisor who gave me the freedom to explore on my own, and at the same time the guidance to ensure I kept on the right track. I would like to thank him for carefully reading and commenting on the revisions of this manuscript and encouraging the use of correct grammar and consistent notation in my writings. It was this maddening attention to detail that drove me to finally learn to punctuate prose.

I am grateful to Helen Strutt for her support and practical advice. Without her our lab would not run as half as smoothly. I would also like to thank her for reading numerous thesis chapters and her helpful comments. Thanks also goes to the other members of the Strutt lab, past and present, who helped, supported, listened, laughed and comforted whenever required.

I would like to thank my advisors Anne-Galle Borycki and Alex Whitworth whom provided helpful comments and support. I am also indebted to the members of the Zeidler and Whitworth labs who provided many valuable discussions during fly meetings, which helped me to understand my research area better.

Many friends have helped me stay sane throughout these years. Their support helped me overcome setbacks and stay focused. I greatly value their friendship and appreciate their unfaltering belief in me.

Most importantly, none of this would have been possible without my family who have been a constant source of love, support and strength all these years.

Finally, I appreciate the financial support from Wellcome Trust that funded the research discussed in this thesis.

Chapter 1

General introduction- Core planar polarity protein function in *Drosophila* and vertebrates

Chapter 1

Introduction

Cell polarisation is essential for tissue morphogenesis. Almost all cells are polarised to some extent. In addition to apical-basal polarity, a cell can also be polarised along the orthogonal axis, in the plane of the epithelium. Coordination of this type of polarity across multiple cells in a tissue is known as planar polarity.

Planar polarity exists in all epithelial cells (Fanto and McNeill, 2004; Mlodzik, 2002; Veeman et al., 2003) and was first studied in the cuticle epithelium of insects such as *Rhodnius*, a blood-sucking insect (Lawrence et al., 1972), and the Milkweed bug *Oncopeltus fasciatus* (Lawrence, 1966; Locke, 1959; reviewed in Strutt, 2009). These studies support a model in which polarity establishment requires input from a hypothetical morphogenetic gradient that exists across the axis of the tissue. Studies in the genetically tractable *Drosophila* have subsequently advanced our knowledge and led to molecular detail about how polarity is established (described later).

In vertebrates, loss of the protein components required to establish planar polarity (as discussed later) are also required for rearranging groups of mesenchymal cells for example during gastrulation and neural tube closure (Heisenberg et al., 2000; Jessen et al., 2002; Montcouquiol et al., 2003; Wallingford et al., 2000; Weeraratna et al., 2002). However, in vertebrates and in *Drosophila,* there is little evidence for how these protein components required to establish planar polarity are involved at a cellular level to mediate cell rearrangements.

Therefore, the main questions that this work will try to address are: (1) how is planar polarity established? and (2) can we uncover any additional mechanisms required to promote cell rearrangements?

Drosophila development

The *Drosophila* life cycle occurs over approximately 10 days, although this can be faster with an increase in temperature. There are four parts to the life cycle: embryogenesis, larval stages, pupation and adulthood (**Figure 1.1** and Weigmann et al., 2003). During embryogenesis the embryo body plan is patterned. Once hatched, the resulting larvae undergo three larval molts taking about 5.5 to 6 days in total (**Figure 1.1**). The larvae then pupate and the initial developmental pattern of the tissues is modified to produce adult structures. Pupae eclose to form the adult fly, and 10 hours after the fly emerges, they are fertile and ready to reproduce.

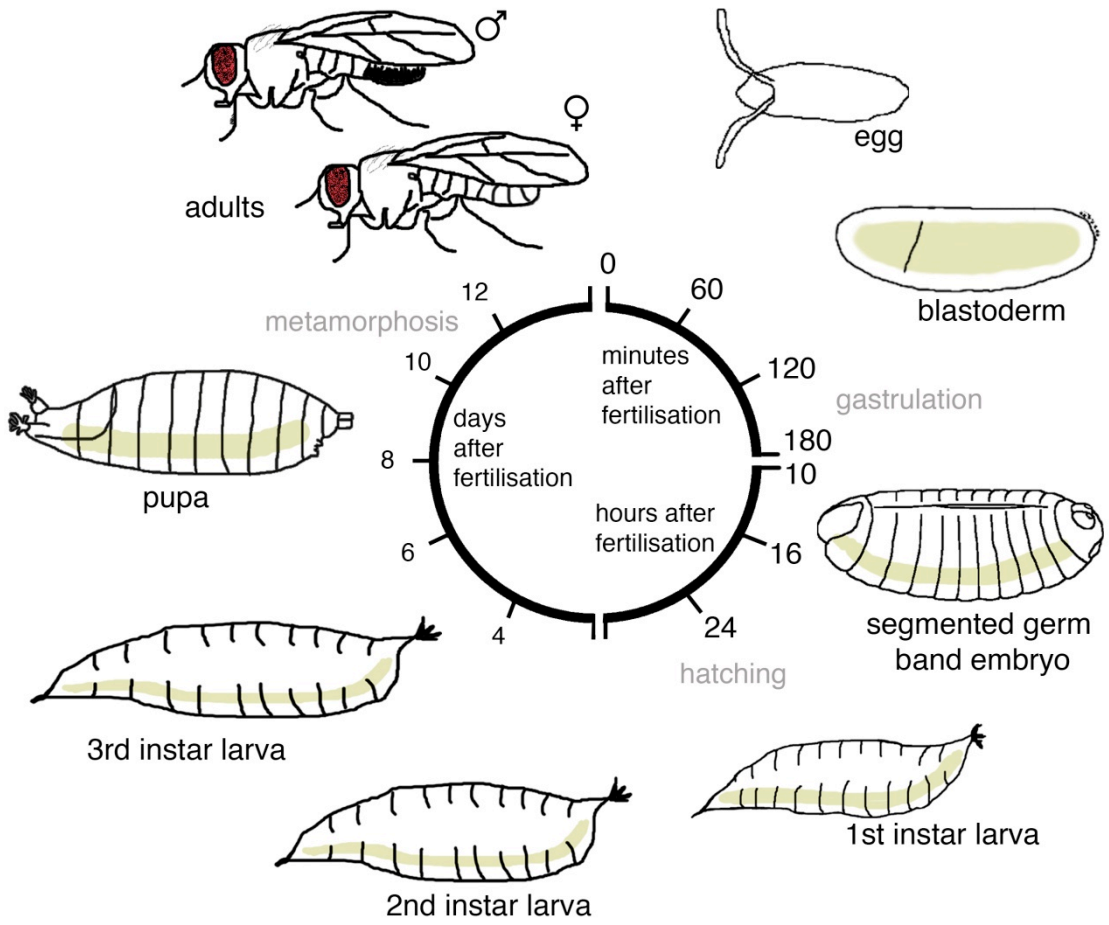

Figure 1.1: The *Drosophila* life cycle

A diagram showing the different stages of the *Drosophila* life cycle. The times for each stage are shown in minutes, hours and days. Not to scale. Anterior is to the left for each stage of development.

The establishment of planar polarity in Drosophila epithelial tissues

The establishment of planar polarity requires input from several pathways, two of these inputs are from the 'core' planar polarity proteins (core pathway) and from the Fat/Dachsous pathway. Both of these pathways consist of different groups of proteins, which act together to specify planar polarity. Molecular details will be discussed later.

Epidermal structures, for example the wing and the eye, show evident planar polarity. Both of these tissues are specified in the embryo and are formed from imaginal discs. Imaginal discs are groups of cells that invaginate from the embryonic ectoderm during embryogenesis. Imaginal discs proliferate, and continue to modify tissue patterning during larval stages, and they finish developing during pupal stages to form the fully functional organs required for adult life (Couso et al., 1993; Hartenstein, 1993).

During the pupal stage, the wing imaginal disc develops through a combination of cell rearrangements, shape changes and proliferation to become the adult wing. The wing proper forms from the wing pouch, an initially circular structure patterned along the dorsal-ventral axis by a stripe of Wingless (Wg) expression (Neumann and Cohen, 1997; Zecca et al., 1996) and the anterior-posterior axis by Decapentaplegic (Dpp) (Capdevila and Guerrero, 1994). The rest of the wing imaginal disc forms the hinge structures that attach to and form part of the notum of the fly. The morphogenesis of the wing proper is coordinated so that the wing pouch extrudes out from the flat imaginal disc folding along the Wg expression stripe of the wing disc. Therefore, a stripe of Wg expression initially crossing the wing pouch becomes located at the wing margin (Couso et al., 1994). The two layers of cells in the folded wing pouch adhere to themselves (Brower and Jaffe, 1989) to form an epithelial bilayer. Within each layer, cells in the wing adhere to each other at the level of the adherens junctions (AJ's), above the septate junctions in the subapical domain. Late in pupal development each wing cell specifies and locates an actin-rich hair at the distal edge of each wing cell that points distally (**Figure 1.2A**, Eaton et al., 1996; Gubb and Garcia-Bellido, 1982; Vinson and Adler, 1987; Wong and Adler, 1993). Interestingly, if the activity of the core planar polarity genes are disrupted, then the wing hairs (or trichomes) no longer point distally indicating that establishment of planar polarity is under genetic control (**Figure 1.2E**, Adler, 1992; Adler, 2002; Adler et al., 1990; Axelrod, 2001; Bastock et al., 2003; Das et al., 2004; Feiguin et al., 2001; Gubb and Garcia-Bellido, 1982; Rawls and Wolff, 2003; Shimada et al., 2001;

Strutt, 2001b; Strutt and Strutt, 2008; Tree et al., 2002b; Usui et al., 1999; Wong and Adler, 1993; Yan et al., 2008). Instead wing hairs arrange into reproducible swirling patterns where the hairs are localised at the centre of the cell instead of the edge (Gubb and Garcia-Bellido, 1982; Wong and Adler, 1993). In the wing the Ft/Ds pathway is required for orientating cell divisions along the proximal-distal axis as loss of *ft* results in round clones and miss polarised cell division as well as excessive cell division (Baena-Lopez et al., 2005; Mao et al., 2006). During wing formation the hinge contracts to allow wing elongation, through polarised cell divisions mediated by Ds (Aigouy et al., 2010) and increased tension on the proximal-distal axis. Loss of Ds or Ft leads to shorter broader wings (Baena-Lopez et al., 2005) suggesting that Ft and Ds are required for orientated tissue growth.

Another epithelial tissue that exhibits planar polarity patterning is the *Drosophila* eye. In the adult, the eye is made up of an array of approximately 800 ommatidia. Each ommatidium consists of a cluster of 20 cells including 8 photoreceptor cells (Tomlinson and Ready, 1987). The photoreceptor and accessory cells are specified after the morphogenetic furrow passes. Post-furrow, each newly formed pre-cluster contains 5 core photoreceptor cells (corresponding to photoreceptors 2, 3, 4, 5 and 8) (**Figure 1.2D**) and recruits the photoreceptors 1 and 7 as well as accessory cells. These clusters then rotate as a unit 90 degrees away from the eye equator and rearrange to become asymmetric, and chiral, so that the dorsal and ventral halves of the eye mirror each other (**Figure 1.2B,** Wolff and Ready, 1991). This arrangement means that each ommatidium is polarised as well as the eye as a whole.

In the *Drosophila* eye, the core pathway proteins are required to first specify the correct chirality or handedness of the ommatidial clusters, and secondly, to rotate the ommatidia 90° away from the midline (**Figure 1.2D**). Loss of the core pathway proteins results in chirality flips of the ommatidia and misrotations of the photoreceptor clusters (**Figure 1.2D**, Das *et al.*, 2002; Gubb *et al.*, 1999; Jenny *et al.*, 2005; Rawls and Wolff, 2003; Strutt *et al.*, 2002; Strutt *et al.*, 1997; Wolff and Rubin, 1998; Zheng *et al.*, 1995). The Ft/Ds pathway is also required to specify the chirality of the ommatidia and disruption to that pathway only causes chirality defects and not irregular ommatidial rotations (Rawls et al., 2002; Yang et al., 2002).

Other events that exhibit planar polarity and indeed require function of the core planar polarity pathway in *Drosophila* include the orientation of hairs and bristles on the adult abdomen (Gubb and Garcia-Bellido, 1982), the formation of *Drosophila* leg joints, as loss of planar polarity results in joint inversions (Held et al., 1986) and for

wing invagination as in the absence of planar polarity activity the wing sometimes points towards the anterior of the pupal case instead of the posterior (Lee and Adler, 2002).

The core polarity proteins are also required for cuticle ridge formation on the surface of the wing (**Figure 1.2A**). Cuticle ridges in the posterior of the wing are aligned with the proximal-distal axis and in the anterior of the wing the ridges are aligned with the anterior-posterior axis (Doyle et al., 2008). Therefore, the core proteins are involved in polarising two outcomes in the wing, the wing hairs and also the cuticle ridges.

The subcellular localisation of the core planar polarity proteins

Six proteins have been identified as components of the core polarity pathway, one of the pathways required to establish planar polarity in the *Drosophila*. In the wing this pathway orients hairs and wing ridges but does not affect the orientation of cell division. Mutations in all six proteins cause defects in ommatidial rotation and chirality in the eye, and hair polarity in the wing. In depth analysis of the subcellular localisation of the core proteins in fixed wing tissue has shown that they become asymmetrically localised to the proximal or distal cell junctions of each wing cell (**Figure 1.2C,D and G**).

Three of the core proteins are transmembrane proteins and three are cytoplasmic proteins. At the distal edge of each wing cell, the seven pass transmembrane protein Frizzled (Fz), localises with the cytoplasmic proteins Dishevelled (Dsh), a protein with PDZ, DIX and DEP domains (Axelrod, 2001; Shimada et al., 2001; Strutt, 2001b), and Diego (Dgo), an ankyrin repeat protein (Das et al., 2004; Feiguin et al., 2001). At the proximal junctions, a four pass transmembrane protein Strabismus (Stbm, also known as Van Gogh, Vang- Flybase) localises with the cytoplasmic LIM domain protein Prickle (Pk) (**Figure 1.2G**, Bastock *et al.*, 2003; Gubb *et al.*, 1999; Taylor *et al.*, 1998; Tree *et al.*, 2002b; Wolff and Rubin, 1998). Pk has two isoforms, Pk and Spiny-legs (Sple). Pk is predominantly active in the *Drosophila* wing, whereas Sple is mainly active in the *Drosophila* eye and legs (Doyle et al., 2008; Gubb and Garcia-Bellido, 1982; Gubb et al., 1999). Flamingo (Fmi, also known as Starry Night; Stan-Flybase) is an atypical cadherin which localises to proximal and distal junctions (Shimada et al., 2001; Strutt and Strutt, 2008; Usui et al., 1999) and homophillically interacts with itself in neighbouring cells (**Figure 1.2G**, Chen et al., 2008).

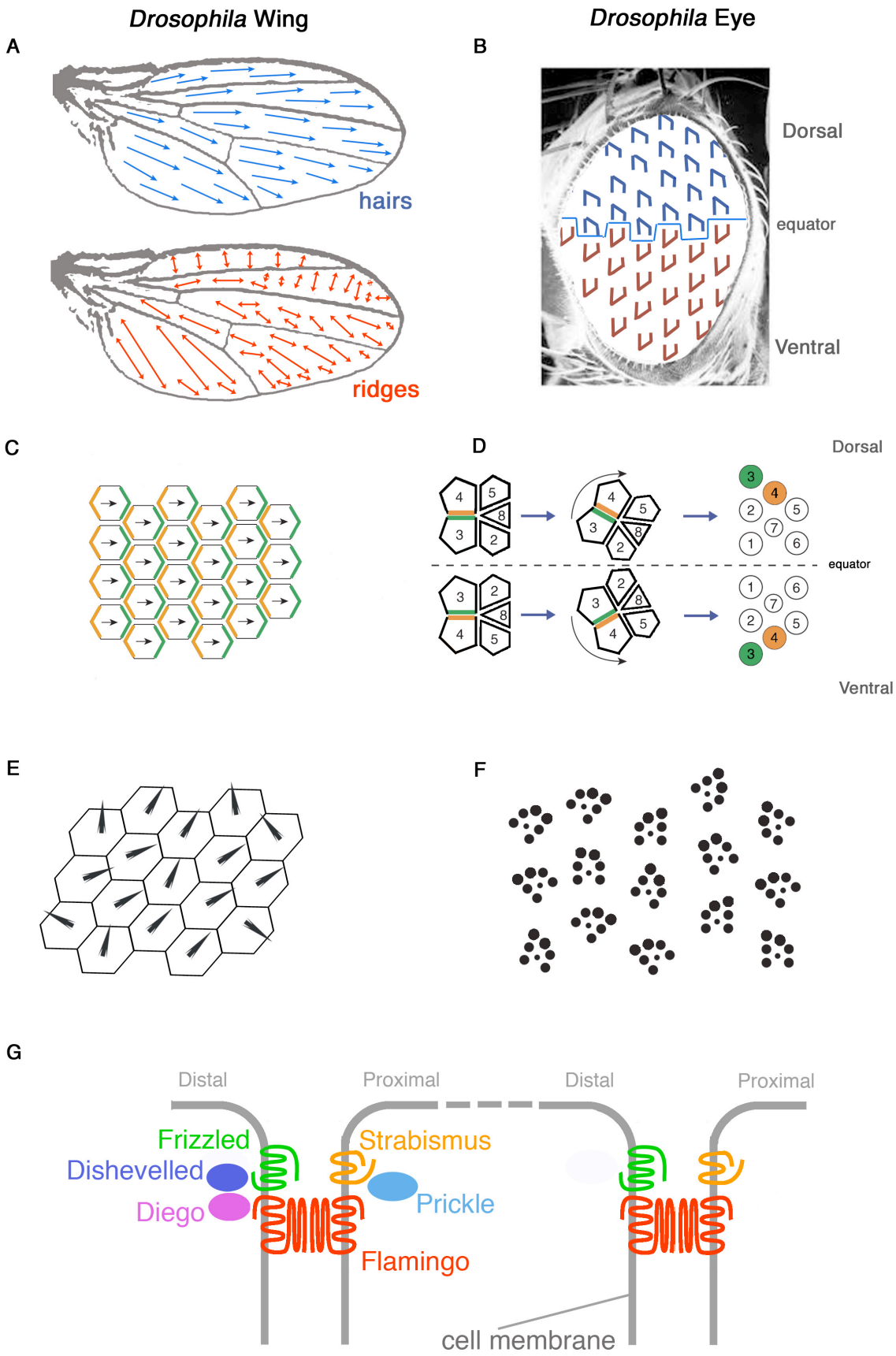

Figure 1.2: Morphological output of planar polarity establishment in the *Drosophila* wing and eye and the localisation of the core planar polarity proteins (Figure legend is on the next page).

(A) Diagram of wild-type adult *Drosophila* wings. Blue arrows indicate the direction of wing hair polarity across the wing. Red arrows indicate the direction of the wing ridges. Note wing ridges in the anterior of the wing are orientated orthogonal to the wing hairs. Proximal is to the left, anterior is up. (B) A diagram of a *Drosophila* wild-type adult eye indicating the orientation of the ommatidia in the dorsal and ventral halves of the eye. The pale blue line indicates the eye equator. (C-D) Diagrams indicating the location of the proximal (orange) and distal (green) complexes in the *Drosophila* eye and wing. (C) Wing cells, black arrows indicate the direction of polarity, proximal is to the left, Stbm containing (orange) and Fz containing (green) complexes are indicated. (D) Diagram of the formation of the ommatidia, over time. Initial ommatidial cells are recruited after the morphological furrow has passed, and consist of the photoreceptor cells R2-R5 and R8. The R3 and R4 cells in this cluster become polarised. The core protein complexes containing Fmi, Stbm and Pk (orange) localise in the R4 photoreceptor at the R3/R4 boundary, and the complexes containing Fmi, Fz, Dsh and Dgo (green) are located in the R3 cell, on the other side of the same junction. This polarisation is required for the correct rotation and chirality of the ommatidia. During the rotation photoreceptors 1, 6 and 7 are recruited to the ommatidial cluster (diagram adapted from Strutt, 2009). (E-F) Diagram of (E) the position of wing hairs and (F) ommatidia orientation in a core planar polarity mutant, shown for only the dorsal part of the eye. (G) A cartoon of the core planar polarity proteins when in the proposed asymmetric complex. Localisation of the six core planar polarity proteins at the apical junctions. Three cells are depicted to show the orientations of the predicted complex, between cells and within a cell. Cell membrane (grey), Frizzled (green), Strabismus (orange), Flamingo (red), Prickle (light blue), Dishevelled (dark blue) and Diego (pink).

In the wing, the recruitment of Fmi to the apical junctions requires both Fz and Stbm. In the absence of Fz and Stbm, Fmi is subjected to higher protein turnover and localises to the apical membrane, rather than to the junctions (Strutt and Strutt, 2008). A reduction in Fmi turnover occurs when localising with Fz and Stbm, suggesting they stabilise the Fmi homophilic interactions at the junctions (Strutt and Strutt, 2008). In addition Fz-Fmi in one cell can localise to junctions and appears to stabilise Fmi in the neighbouring cell (Strutt and Strutt, 2008). This stability further increases when Stbm is also present (Strutt and Strutt, 2008). Loss of Fmi also results in the loss of Fz and Stbm from junctions (Bastock et al., 2003; Strutt, 2001b). This suggests that all three transmembrane proteins are required for the localisation of each other at the junctions and are likely to be required to form an inner-core complex at junctions. The cytoplasmic proteins are localised by Fz, recruiting Dsh and Dgo (via Dsh) (Axelrod et al., 1998; Das et al., 2004; Jenny et al., 2005) and Stbm for recruiting Pk (Bastock et al., 2003; Jenny et al., 2003), although the cytoplasmic factors are not necessary to recruit Fmi, Fz and Stbm to the junctions. However, mutants of cytoplasmic factors do disrupt the asymmetric localisation of Fmi, Fz and Stbm (Bastock et al., 2003; Feiguin et al., 2001; Strutt, 2001b; Usui et al., 1999).

Asymmetry of the core proteins in the wing is present during early pupal wing development when polarity of the wing cells is orientated towards the wing margin (Classen et al., 2005; Strutt et al., 2011). As the pupal wing develops, the direction of polarity changes due to hinge contraction, so by the end of pupal wing development the read out of polarity, in this case the wing hairs, points towards the distal tip of the wing (Aigouy et al., 2010).

In the *Drosophila* eye the correct dorsal-ventral polarisation of photoreceptor clusters relies on precise localisation of the core proteins in the R3 and R4 photoreceptors. Specifically, Fz is required in the R3 photoreceptor (Zheng et al., 1995) and Stbm in the R4 photoreceptor (Wolff and Rubin, 1998) and they localise to the junction on either side of the R3/R4 boundary of these neighbouring ommatidial cells (**Figure 1.2D** Strutt *et al.*, 2002). Fmi is required in both the R3 and R4 photoreceptor cells (Das et al., 2002; Gubb et al., 1999; Strutt et al., 2002) and is involved in recruiting Fz and Stbm to the junctions. The activity of Fz and Stbm in the R3/R4 photoreceptors affects the Notch/Delta feedback loop across this junction (Cooper and Bray, 1999; Das et al., 2002; Fanto and Mlodzik, 1999; Strutt et al., 2002; Tomlinson and Struhl, 1999) ensuring that one photoreceptor becomes the R3 photoreceptor and the other the R4.

There are several possible mechanisms that could be responsible for the asymmetric accumulation of core proteins at the junctions. One would be for the proteins to be preferentially synthesised at those locations (Berleth et al., 1988; Davis and Ish-Horowicz, 1991; Macdonald and Struhl, 1988). A second would be for proteins to be directly trafficked to the correct side of the cell possibly via microtubules as observed in live images of Fz in pupal wings (Shimada et al., 2006; Strutt et al., 2011), as the trafficking of Fz along microtubules is lost in *dsh* and *pk* mutants, this suggests that they are involved in the polarisation of Fz at the junctions (Shimada et al., 2006). A third would be to trap proteins within membrane domains to stabilise them at the junctions (Strutt *et al.*, 2011, see chapter 4) possibly by protecting polarised complexes from endocytosis.

Movement of proteins from one side of the cell to another would require protein endocytosis and exocytosis. Both Fz and Fmi are subject to endocytosis from junctions and when lysosomal degradation is blocked they accumulate in Rab5 positive vesicles (Mottola et al., 2010; Strutt and Strutt, 2008). In addition, both, Fmi and Fz also separately localise with the endosomal marker FM4-64 and Rab5 (Shimada et al., 2006; Strutt and Strutt, 2008). Fz and Fmi are also recycled back to the junctions as they are seen in recycling endosomes containing Rab4 (Strutt and Strutt, 2008).

Intercellular signalling in the Drosophila wing

Studies in the *Drosophila* wing and eye have indicated that the core polarity proteins are not just required to polarise individual cells but also are involved in coordinating polarity between neighbouring cells.

Clones mutant for the core proteins *fz* or *stbm* are known cause non-autonomous defects of the surrounding wild-type cells in the wing and eye. For example cells that lack *fz* alter surrounding wild-type cells, so that the trichomes in the wild-type cells near the distal side of the *fz* clone point back towards the mutant tissue (**Figure 1.3A,** Adler *et al.*, 1997; Gubb and Garcia-Bellido, 1982; Vinson and Adler, 1987). This also occurs in *fz* eye clones where the surrounding ommatidia change chirality (**Figure 1.3B,** Zheng et al., 1995). These observations suggest that Fz and Stbm can alter the polarity of surrounding cells.

Closer examination of core protein localisation in wings containing *fz* mutant clones, was used to deduce that Stbm inside the clone can only form complexes with Fz located in surrounding wild-type cells outside the clone (**Figure 1.3C**).

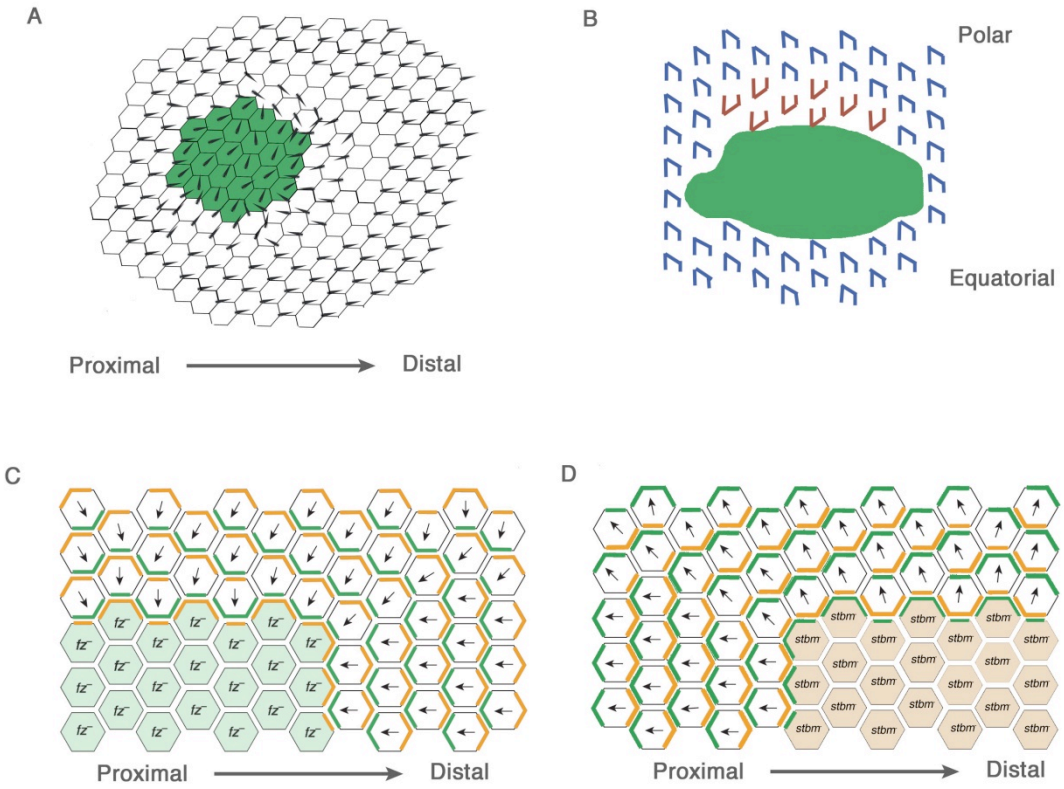

Figure 1.3: Non-autonomy phenotypes surrounding *fz* and *stbm* mutant clones

(A) A diagram of a *fz* mutant clone (marked in green) in an otherwise wild-type adult wing (cells marked in white), trichomes are depicted as black arrowheads, proximal is to the left. Note trichomes point distally except those located distal to the *fz* mutant domain point back towards the clone. (B) A diagram of a *fz* mutant clone in the dorsal half of the eye (shown in green). The correct ommatidia orientations for the dorsal half of the eye are indicated in blue. Note ommatidia on the polar side of the *fz* mutant clone reorient (indicated in red). (C-D) A diagram of a *fz* mutant clone (C) (indicated in pale green) or a *stbm* mutant clone (D) (indicated in pale orange) in a *Drosophila* pupal wing. Stbm-containing (orange) and Fz-containing (green) complexes are indicated. Black arrows indicate the direction of polarity in each cell. Note outside of the *fz* mutant clone orange and green complexes are reoriented so that the direction of polarity in the cells points towards the clone. The formation of the distal complexes requires Fz therefore, the lack of *fz* in the mutant tissue leads to only Stbm-containing (orange) complexes forming in the mutant tissue along the cell junctions at the edge of the clone. The neighbouring wild-type cells bordering the clone then localise the Fz-containing (green) complexes to junctions. This asymmetry is then propagated out from the clone (diagram adapted from Strutt, 2009). (D) Non-autonomy is also seen proximal to *stbm* mutant clones, but the hairs point away from the clone.

Consequently Fz complexes from wild-type cells are recruited to the clone boundary. This means that on the distal side of the clone, Fz in the wild-type cells is reoriented so that Fz is on the proximal side of the cell. This new polarity direction then propagates away from the clone, altering trichome localisation so that hairs point towards the clone (**Figure 1.3A**, Adler *et al.*, 2000b; Strutt and Strutt, 2007; Vinson and Adler, 1987). Mutant clones of *stbm* also exhibit non-autonomous behaviour, but this time the wild-type cells proximal to the clone are affected, and their trichomes point away from the *stbm* mutant tissue in the wing (Adler *et al.*, 2000b; Taylor *et al.*, 1998) and in the eye ommatidia change chirality on the equatorial side of the clone (Strutt and Strutt, 2007).

Interestingly, *fmi* mutant clones do not exhibit non-autonomy in surrounding wild-type cells (Chae et al., 1999; Usui et al., 1999), even though Fmi is required in both mutant and wild-type cells for the non-autonomous response of Fz and Stbm (Chen et al., 2008; Lawrence et al., 2004; Strutt and Strutt, 2007). However, Fmi has been implicated in intercellular signalling (Lawrence et al., 2004; Strutt and Strutt, 2007), Fmi lacking its intracellular C-terminus shows an increase in its distal cellular localisation (Strutt and Strutt, 2008), therefore the Fmi C-terminus is required to interact with Stbm and localise proximally. In addition, overexpression of Fmi leads to more Fz/Dsh localisation at the junctions and less Stbm/Pk (Strutt and Strutt, 2008).

This suggests that Fmi may interact more strongly with Fz than with Stbm at the junctions and Stbm may only be able to localise with junctional Fmi if Fmi is already involved in intercellular interactions with Fmi and Fz in the neighbouring cell (Strutt and Strutt, 2008). Therefore, the changes in the localisation of Fz and Stbm on the borders of clones and the observation that this localisation can be propagated away from the mutant clones, suggests that Fz and Stbm are required for cell-to-cell signalling, by setting up a local signal that can repolarise neighbouring cells. Fmi, is also required for intercellular signalling by correctly localising Fz and Stbm to the junctions on each side of the cell, but as no aberrant signal is generated, except for the first cell (as no Fmi is present at the clone boundary for Fmi homodimers to form) so the neighbouring wild-type cells are not repolarised. Importantly cell-cell signalling through Fz and Stbm has also been simulated in mathematical models via intracellular and intercellular feedback mechanisms (see below Amonlirdviman et al., 2005; Le Garrec et al., 2006).

The signalling interaction between Fz and Stbm across cell junctions may be direct, as shown *in vitro* (Wu and Mlodzik, 2008), or via Fmi (Chen et al., 2008; Lawrence et

al., 2004; Strutt and Strutt, 2008). This signal is also bidirectional (Chen et al., 2008; Struhl et al., 2012; Strutt and Strutt, 2007). A bidirectional polarity signal would require both Fz and Stbm in both neighbouring cells for the signal to be propagated across several cells. A bidirectional signalling cue was confirmed by using *fz* and *stbm* double mutant clones and observing what happens to surrounding wild-type cells. The premise was, if there was non-autonomy on the distal edge of the double mutant clone (as seen on the boundaries of *fz* mutant clones), then that would suggest that the wild-type cells do not need Stbm to be on the inside of the clone to place the Fz on the clone/wild-type border and re-orientate polarity. This would be the same with Stbm on the proximal side of the clone. Interestingly double mutant clones do not show non-autonomy of Fz or Stbm in surrounding wild-type cells (Strutt and Strutt, 2007). In addition, to support a mono-directional signalling theory the non-autonomy in the double mutant would have to be as equally strong as in the single mutants, otherwise if the non autonomy was weaker this would suggest that both Fz and Stbm would be required for signalling. Non-autonomy was found to be absent in the double mutant (Chen et al., 2008; Strutt and Strutt, 2007) taken together this suggests that, Stbm and Fz are both required to orientate polarity and signal between cells in a bidirectional manner.

Fz and Dsh involvement in canonical wnt/β-Catenin signalling

Fz, as well as its role in planar polarity, is also involved in the canonical Wnt/Fz signalling pathway, called that to distinguish it from other pathways involving Fz. In this pathway, Fz and its homologue DFrizzled2 (DFz2), both of which are redundant in canonical Wnt/β-Catenin (β-Cat) signalling (Bhanot et al., 1999; Bhat, 1998; Chen and Struhl, 1999; Kennerdell and Carthew, 1998; Muller et al., 1999), act as the receptors for Wnt ligand, Wg, together with the co-receptor, low-density lipoprotein receptor-related protein 6 (LRP6, known as Arrow in *Drosophila*)(He et al., 2004; Wehrli et al., 2000). Dsh is then recruited to the cell junctions at the same location as Fz, resulting in LRP6 phosphorylation and leading to the recruitment of the Axin complex (Klingensmith et al., 1994; Krasnow et al., 1995; Tamai et al., 2004; Tolwinski et al., 2003). Recruiting Axin to the membrane leads to the inhibition of Axin-mediated Armadillo (Arm)/β-Cat phosphorylation and degradation (He et al., 2004), therefore stabilising β-Cat and allowing it to travel into the nucleus and activate the transcription of various target genes (Macdonald and Struhl, 1988; Tolwinski *et al.*, 2003).

The two functions of Fz in canonical Wnt/β-Cat signalling and planar polarity can therefore be separated, as they have distinct outcomes. Interestingly, Fz recruits Dsh

to the junctions via the DEP domain of Dsh (Axelrod et al., 1998). The DEP domain is also required for its role in planar polarity, suggesting that junctional recruitment of Dsh is required for its polarity function, although Dsh's DEP domain is not required for Wnt/β-Cat signalling (Axelrod et al., 1998; Boutros et al., 1998). The requirement of different domains of Dsh in either planar polarity or Wnt/β-Cat signalling indicates that Dsh is the splitting point of these signalling pathways downstream of Fz, leading to different signalling outcomes. Dsh is also limiting in this context and its function can be titrated by one of the pathways at the expense of the other (Axelrod et al., 1998), therefore an increase in canonical signalling represses planar polarity.

The core planar polarity cytoplasmic factors

Interestingly, the cytoplasmic proteins, Dsh, Pk and Dgo, do not show non-autonomous cell effects on the edges of mutant clones (Lawrence et al., 2004; Strutt and Strutt, 2007) and so are presumed to be only required for autonomous cell signalling (Amonlirdviman et al., 2005; Chen et al., 2008; Strutt and Strutt, 2007). In support of this, polarity can propagate a few cells from a *fz* or *stbm* clone, in the absence of the cytoplasmic factors (Strutt and Strutt, 2007). However, in mutant wings for the cytoplasmic proteins (Pk or Dsh), polarity is not established (Axelrod et al., 1998; Gubb et al., 1999). Therefore this suggests that near a strong boundary of polarity like that on the edge of clones the cytoplasmic proteins are dispensable for propagating polarity between cells, possibly because the strong asymmetry at the boundary is enough to propagate polarity a few cells from the boundary. However, in situations where there is no strong polarity boundary, the cytoplasmic proteins are required to amplify weak asymmetry for it to be propagated between cells to make the trichomes point distally, leading to visual asymmetry of the core proteins at the junctions. This indicates that the establishment of planar polarity does not require visible asymmetry of the core proteins in the presence of a strong boundary of polarity (Strutt and Strutt, 2009).

In addition, the cytoplasmic core proteins in the wing are only required for planar polarity just before placement of the wing hairs, whereas Fmi, Fz and Stbm are required earlier in development (Strutt and Strutt, 2007; Strutt and Strutt, 2002; Wu and Mlodzik, 2008). This further suggests that the cytoplasmic proteins are likely to be required for amplifying the asymmetry of the transmembrane core proteins at the cell junctions.

Further evidence for involvement of the two phases of core protein activity in polarising wing cells comes from studying the role of planar polarity in cuticle ridge

formation on the surface of the wing. Cuticle ridges are oriented differently in different compartments of the wing. The formation of the ridges requires the same two signals from the core proteins (Doyle et al., 2008). The early signal aligns the ridges along the proximal-distal axis over the whole wing. The later signal reorientates the ridges in the anterior compartment so they align perpendicular to the posterior ridges (**Figure 1.2A**, Doyle *et al.*, 2008; Hogan *et al.*, 2011).

Evidence for the core planar polarity proteins forming a complex

All six of the known core proteins colocalise at the proximal-distal junctions (Strutt and Strutt, 2008; Strutt et al., 2011). Intriguingly, the core proteins are not uniformly localised to proximal-distal junctions as often depicted in models of core protein localisation (**Figure 1.2C**), instead they are most strongly localised to discrete membrane subdomains or "puncta" at the cell junctions (Strutt et al., 2011). These large puncta are reduced in size or absent in mutants of the core proteins, where planar polarity is lost (Strutt et al., 2011). This suggests there is a functional correlation between the presence of puncta and the establishment of planar polarity. The colocalisation of the core proteins in these membrane domains suggests that they may interact in these regions to facilitate planar polarity through cell autonomous interactions and cell-cell signalling.

Most models for how planar polarity is set up and maintained are based on the principle that the six known core proteins form a functional complex (**Figure 1.2G**). The evidence for this is mainly from *in vitro* physical interaction studies, which have often proved difficult to repeat *in vivo*. The homophilic interactions of Fmi are based on S2 cell aggregation assays (Usui et al., 1999). Other interactions have also been shown, including recruitment of Dsh to the cell membranes by Fz, and Stbm recruiting Pk (Axelrod et al., 1998; Bastock et al., 2003; Jenny et al., 2003).

However, in addition to these interactions, other *in vitro* interactions have been seen that do not correlate with *in vivo* localisation. For example, Stbm and Pk, can bind *in vitro* to Dsh or Dgo (Bastock et al., 2003; Das et al., 2004; Jenny et al., 2003; Jenny et al., 2005). One hypothesis to explain this is that these interactions only occur while core proteins are not yet asymmetrically localised at the junctions (Jenny et al., 2005; Strutt, 2003; Tree et al., 2002b).

As *in vivo* evidence in pupal wings shows that all the core proteins are required for the asymmetry and colocalisation of the other core proteins, it is therefore presumed that these proteins do interact directly or indirectly. Establishing polarity in a single

cell may require intracellular interactions between proximal and distally localised complexes. These could be negative interactions to prevent complexes of different orientations from accumulating at the same junctions, enhancing the asymmetry of the complexes. Positive interactions may also occur to cluster complexes of the same orientation when at the correct junctions. To communicate polarity to neighbouring cells intercellular interactions also occur and are mediated by the core transmembrane proteins Fz, Stbm and Fmi.

Models of planar polarity establishment in epithelial tissues

Key questions are: How are the core proteins involved in coordinating planar polarity across an epithelial tissue? Do the core proteins require an upstream signal to initially polarise cells? and is the asymmetry of these core proteins a cause or a consequence of establishing polarity?

Experiments examining coordinated tissue polarity involved cutting and rotating sections of insect cuticle prior to scale formation (e.g. Lawrence, 1966; Lawrence et al., 1972). A part of the cuticle was rotated and cells located outside of the graft then reoriented with respect to the graft boundary. These experiments suggested that the cells outside the graft region were reorienting in response to alterations to signalling gradients within the plane of the tissue.

Initial models describing how planar polarity is established in the wing

To explain the non-autonomy seen in the wing and eye of *Drosophila*, two models were initially described, both were based on the idea that to establish planar polarity a gradient was required to provide polarity information to be interpreted by the core protein Fz that was known about at that time and known to be required for the domineering non-autonomy.

One model established a graded signal by setting up a patch of cells that produced a signal that could then be passed from cell to cell in a directional manner across the tissue along the proximal-distal axis and was known as the cell-to-cell relay model (**Figure 1.4,** Adler et al., 1997). However, only passing a signal from cell-to-cell would not lead to coordinated tissue polarity, as nothing would stop the asymmetry from gradually reorientating across the tissue. Therefore, although this model via cell-cell signalling could polarise cells, an initial bias of polarity across the tissue may also be required to orientate cells to point polarity in a uniform direction.

The second model proposed to explain the non-autonomy of *fz* mutant clones relied on an upstream long range gradient, a secreted diffusible factor produced at one end of the tissue forming a gradient of this factor along the proximal-distal axis of the tissue (Adler et al., 1990). Cells could then interpret the gradient and align their polarity to the graded signal, pointing either up or down the gradient (**Figure 1.4**). As all cells would 'see' the gradient, polarity could be coordinated across the tissue.

For a cell to interpret a gradient or cue, the cell must first receive it. As Fz acts as a receptor in canonical Wnt signalling, Fz was proposed to be required to interpret and amplify a weak gradient signal across the tissue (Adler et al., 1997; Adler et al., 1990; Park et al., 1994; Zheng et al., 1995). Passing the polarity signal via Fz could produce a Fz intracellular gradient of activity within each cell, rather than a Fz gradient across the tissue. This would fit closer with the later observed asymmetric cellular localisation of the core proteins (Bastock et al., 2003; Shimada et al., 2001; Strutt, 2001b; Tree et al., 2002b; Usui et al., 1999).

The propagation of core protein asymmetric complex localisation around the boundaries of *fz* and in *stbm* mutant clones, as discussed above, suggested that cell-cell intercellular signalling is required to set up polarity. Therefore, a model arose that suggested that this cell-cell signalling occurred through local interactions between the complexes at the cell junctions (**Figure 1.5**). These interactions could be positive and/or negative interactions between the asymmetric junctional complexes, and by using feedback loops would ensure that complexes of the "wrong" orientation are removed from the junctions and degraded or moved to a "correct" junctional location, resulting in proximal complexes localising to the proximal junctions and the distal complexes at the distal junctions (**Figure 1.4**, Amonlirdviman *et al.*, 2005; Klein and Mlodzik, 2005; Le Garrec *et al.*, 2006).

Models to coordinate the establishment of planar polarity through local interactions of core protein complexes

Once the core proteins were observed to localise asymmetrically in the cell and colocalise with each other across the cell junctions (Bastock et al., 2003; Shimada et al., 2001; Strutt, 2001b; Tree et al., 2002b; Usui et al., 1999), other models emerged that relied on polarising the core protein complexes through interactions between the junctional complexes and not by interpreting signalling gradients.

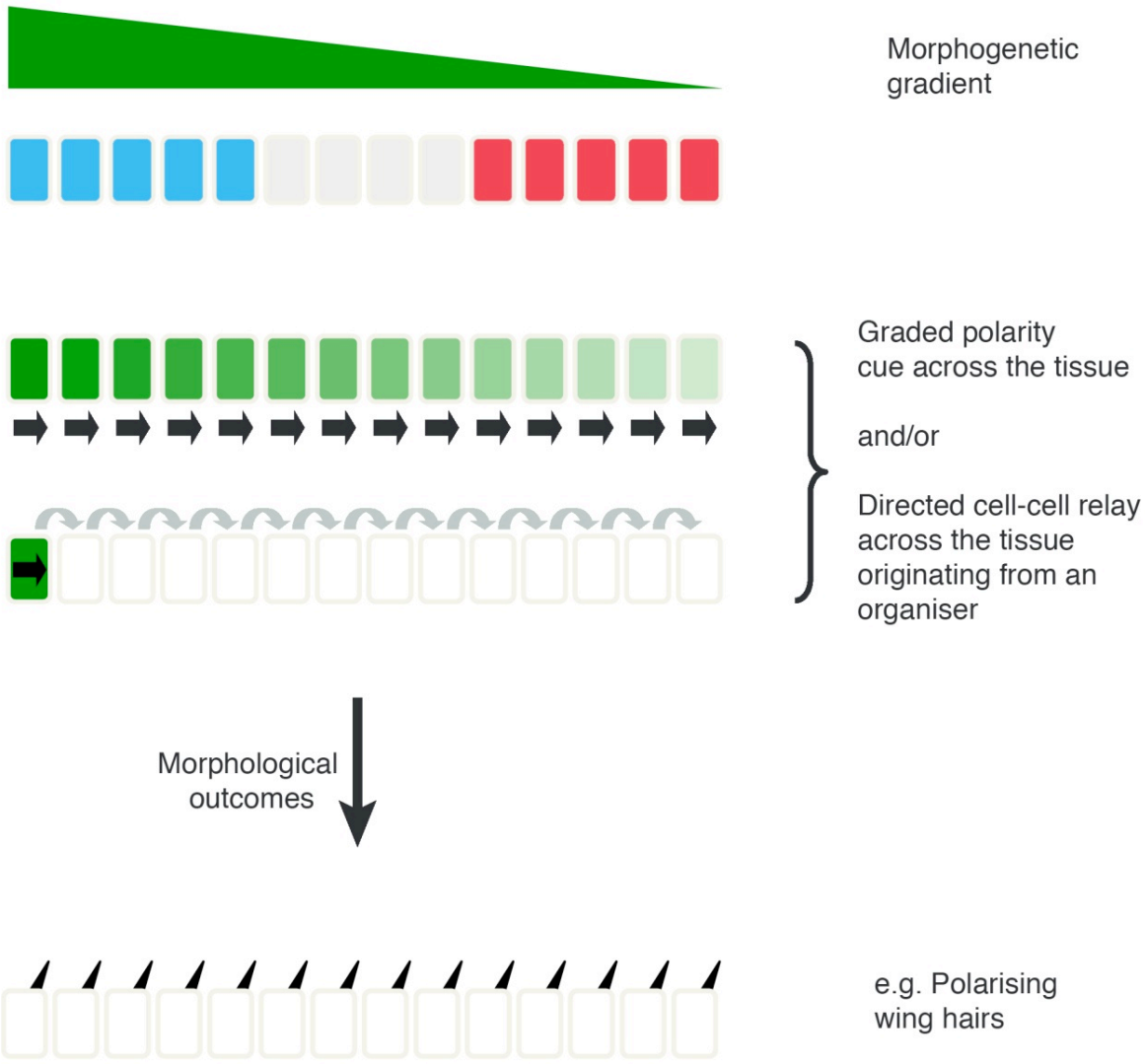

Figure 1.4: Models describing the two alternative mechanisms for establishing planar polarity in the wing

In this model a morphogen gradient is initially set up across the wing (green triangle), where different levels of the morphogen can lead to differences in cell specification (red/white/blue cells). This morphogenetic graded cue could then be interpreted as a graded polarity cue across the tissue or high levels of the morphogen could activate an organiser to initiate a cell-cell relay across the tissue. Once polarity is established this leads to morphological outcomes such as polarised wing hairs.

Any negative feedback would enhance the mobility of the proteins affected and positive feedback would result in stabilisation of proteins at the junctions. Evidence for positive interactions comes from overexpression experiments, where the over-expression of Dsh, Dgo or Pk can recruit core proteins to the junctions (Bastock et al., 2003; Feiguin et al., 2001; Tree et al., 2002b). This model also suggests that the asymmetry of the core proteins is part of the mechanism to planar polarise the cells rather than being an outcome of a gradient cue.

Linking asymmetry of the core proteins to global upstream cues

Complex formation and asymmetric localisation of the core proteins appears to be required for local coordination of polarity. However, for a whole tissue to be planar polarised in the same orientation, the initial establishment of polarity may need to be coordinated between cells, this could be imposed in the form of a polarity bias to coordinate the polarity across the tissue.

Initial suggestions for what could be providing a bias was based on gradients of a diffusible ligand that may bind to Fz. Ideas for what the diffusible molecule could be included the Wnt family of ligands, including Wingless (Wg) (Chen et al., 2008; Lawrence et al., 2002), as Fz was known as a receptor for Wnt ligands during canonical Fz signalling (Lawrence et al., 2002). However, in *Drosophila* the evidence for Wnt involvement in planar polarity activity is limited (Chen et al., 2008; Lawrence et al., 2002; Lawrence et al., 2004; Wehrli and Tomlinson, 1998; Wu et al., 2013) so it is unlikely that Wnts or Wg is the secreted factor if one does exist.

Although the polarity bias could be coordinated across the tissue, it could also be set up across each cell, possibly by polarising microtubules along the proximal-distal axis allowing directional trafficking of Fz to the distal cell junctions (Shimada et al., 2006), thereby polarising Fz in the cell. The Fat/Dachsous pathway (see later) has been implicated in polarising microtubules (Harumoto et al., 2010) and therefore could be involved in polarising the core proteins via this indirect route.

Despite the expectation that there is an upstream cue or bias that initially polarises the core protein complexes, what form the cue could take is still debated and could be either a gradient across the tissue (Lawrence et al., 2004) or the cue is generated within each cell and then amplified through local interactions between the core proteins (Amonlirdviman et al., 2005).

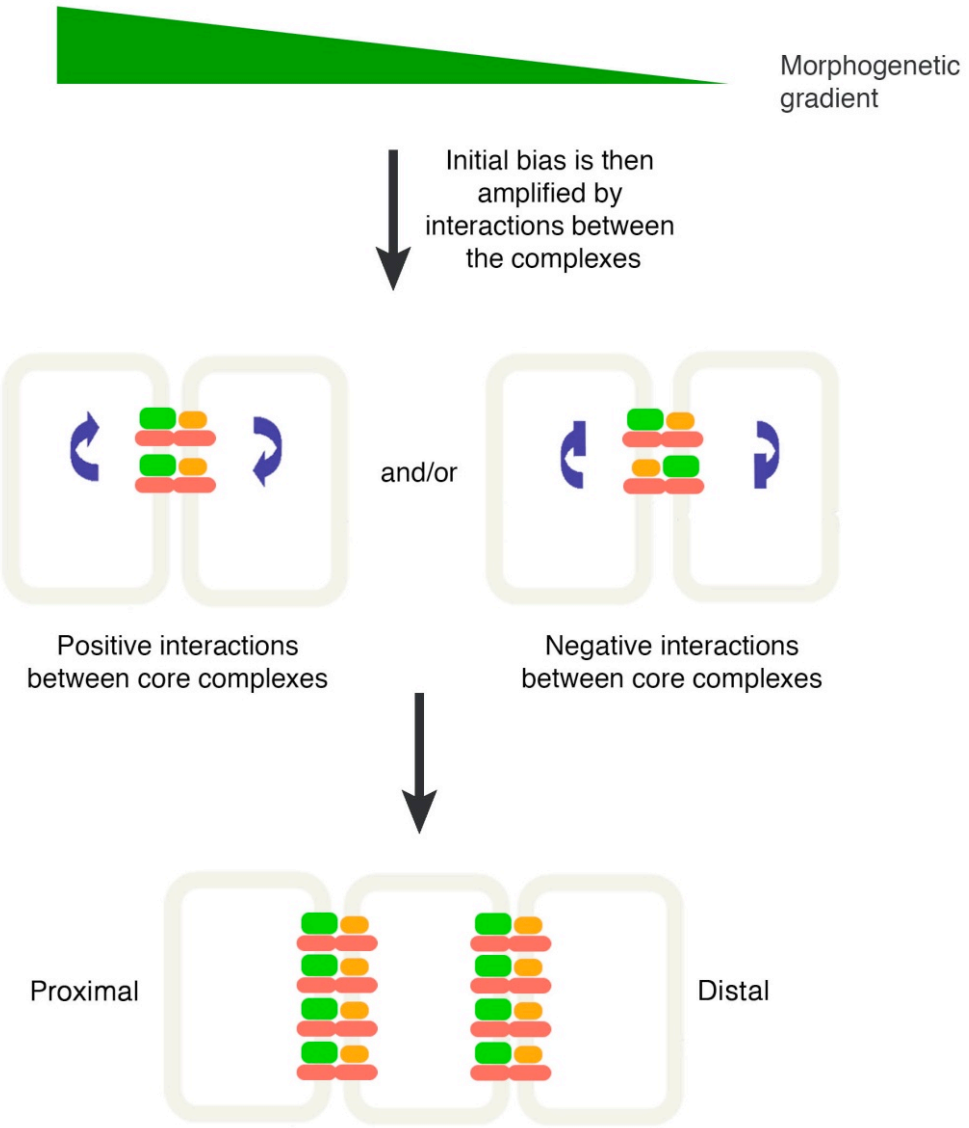

Figure 1.5: Model describing potential positive and negative interactions between core complexes as a way of establishing planar polarity in the wing

This model relies on the initial set up of a gradient either across the wing or within a cell (green triangle). This gradient may induce an initial bias of the core complexes (depicted in green (Fz), orange (Stbm) and red (Flamingo). The initial localisation of the complexes would then be modified by interactions between neighbouring complexes at the junctions (blue arrows). These interactions within the same cell may be positive and group 'like' complexes together and/or negative interactions inducing complexes of the 'wrong orientation' to be removed from the junctions. This leads to complexes of the same orientation localising together at the junctions, resulting in their asymmetric localisation.

An alternative model to explain how planar polarity is established

However, not everyone in the field believes that asymmetry of the core proteins is important to establish polarity across the wing. Therefore another model was put forward to explain how polarity could be set up without depending on establishing asymmetric complexes first. Instead, a gradient of Fz activity is established across the tissue based on a weak morphogenetic gradient. This Fz activity gradient could then be signalled to neighbouring cells through the junctional complexes on juxtaposing cell junctions, resulting in asymmetry of the core proteins and in wing hairs pointing down the Fz gradient (Lawrence et al., 2004). In this model, the asymmetry of the complexes would be a consequence of establishing polarity and not required initially to signal polarity to the neighbouring cells.

Maintenance of the polarity patterning during development

Another interesting question is: how is the long range polarity pattern maintained during development, during which cells divide and rearrange based on signals from neighbouring cells? One idea is that the polarity is set up early and then maintained as the tissue grows, then the long-range pattern could be maintained across the whole tissue (Aigouy et al., 2010; Sagner et al., 2012). The planar polarity pattern in the wing is established early during growth of the wing (Sagner et al., 2012). This early patterning could then be used to reorientate the pattern locally as the tissue grows, thereby maintaining polarisation of the tissue without the need for long-range gradients.

Fat/ Dachsous pathway as another cell polarising mechanism

In addition to the core protein involvement in establishing polarity, another system, called the Fat/Dachsous (Ft/Ds) system, is required to polarise cell division, cell dynamics and cell packing in *Drosophila* and has been suggested to also do so in vertebrates (Baena-Lopez et al., 2005; Ma et al., 2003; Saburi et al., 2008; Thomas and Strutt, 2012).

The activity of the Ft/Ds system is mediated by the interactions between the atypical cadherins Ft and Ds, that preferentially bind to each other at the apical cell surface across juxtaposing cell membranes (Ma et al., 2003; Matakatsu and Blair, 2004; Strutt and Strutt, 2002). The binding affinity of Ft to Ds is modulated by phosphorylation of their extracellular domains by the Golgi-localised kinase Four-jointed (Fj) (Brittle et al., 2010; Ishikawa et al., 2008; Simon et al., 2010; Strutt et al., 2004).

Loss of *ft* or *ds* causes non-autonomous polarity phenotypes in eye and wing similar to that of *fz* and *stbm* mutants (Adler et al., 1998; Ma et al., 2003; Rawls et al., 2002; Strutt and Strutt, 2002; Yang et al., 2002), therefore these heterophillic interactions of Ft and Ds have a role in locally signalling polarity between neighbouring cells. However, the loss of both Ft and Ds does not completely disrupt polarity formation in the eye (Brittle et al., 2012), suggesting that other polarity mechanisms may be compensating for the lack of Ft/Ds activity.

Ft and Ds, but not Fj, exhibit subcellular protein asymmetry in the wing disc when expressed at endogenous levels where Ds is found at distal cell edges and Ft at proximal cell edges (Ambegaonkar et al., 2012; Bosveld et al., 2012; Brittle et al., 2012). In the wing, Fj is expressed in a gradient and is higher distally (Strutt et al., 2004; Zeidler et al., 2000), whereas Ds is not in a gradient but is elevated in the wing hinge.

In the eye, in addition to their subcellular protein asymmetry, Ds and Fj are present in opposing gradients, whereas Ft is generally found to have uniform protein expression (Garoia et al., 2000; Strutt et al., 2004). In the eye the gradients of Fj and Ds are aligned with morphogenetic gradients. The morphogen Wg is expressed at the eye periphery where it is promotes the expression of *ds* (Clark et al., 1995; Yang et al., 2002) therefore Ds is highest at the poles. Wg is also required for the repression of *fj* expression, therefore Fj is highest at the equator (Strutt et al., 2004). This creates opposing gradients of Ds and Fj across the eye, which leads to changes in binding interactions between Ds and Ft across junctions (Brittle et al., 2010; Simon, 2004; Yang et al., 2002; Zeidler et al., 1999) and resulting in Ft subcellular asymmetry (Brittle et al., 2012).

In the wing and eye disc, Ft and Ds junctional interactions are required for the asymmetric subcellular localisation of a downstream effector Dachs, an atypical myosin, to cell edges that contain Ds (Ambegaonkar et al., 2012; Brittle et al., 2012; Mao et al., 2006; Rogulja et al., 2008). Ft is thought to degrade Dachs locally, where as Ds locally stabilises Dachs (Brittle et al., 2012). Therefore Dachs is localised at the junctions with Ds, although both Ds and Ft are required for the asymmetry of Dachs (Brittle et al., 2012).

At one time Ft/Ds activity was thought to be upstream of the core proteins and was suggested to be the unknown factor X that could polarise the core complexes (as mentioned earlier, Casal et al., 2002; Ma et al., 2003; Tree et al., 2002a; Yang et al.,

2002). Evidence for this was from experiments in the wing where in the absence of *ft* or *ds* the core protein asymmetry was misorientated, resulting in hair swirls (Ma et al., 2003; Strutt and Strutt, 2002). Interestingly, Ft/Ds can control the proximal-distal alignment of microtubules in wing cells (Harumoto et al., 2010; Shimada et al., 2006), which is reported to be required for Fz trafficking to the proximal-distal cell junctions (Shimada et al., 2006). Therefore, the core proteins could respond to Ft/Ds polarity cues, possibly through the polarisation of microtubules. However, the requirement for Ft/Ds/Fj to polarise the core protein complexes and to the extent to which they act through Dachs to achieve core protein asymmetry appears to vary between tissues.

In the wing, the gradients of Fj and the localisation of Ds does not appear to be necessary for polarising hairs as removing the gradients by uniform over-expression results in hair polarity and asymmetry appearing mostly normal except in the most proximal part of the wing boundary (Brittle et al., 2012; Matakatsu and Blair, 2004; Sagner et al., 2012; Simon, 2004). In the proximal wing Ft-Ds-Fj appear to act on the core proteins via Dachs, as *dachs* mutants alter the core protein asymmetry to the same degree as in a *ft*/*dachs* double mutant (Brittle et al., 2012). Interestingly the loss of *dachs* only affects the localisation of the core proteins in the proximal region of the wing, as in the *dachs* mutant Fz asymmetry reorients in line with the wing hinge/pouch boundary (Brittle et al., 2012). Dachs therefore appears dispensable for polarising the core proteins in the rest of the wing (Matakatsu and Blair, 2008). This suggests that the boundary of Ds expression in the proximal part of the wing enhances Dachs asymmetry but is also for Dachs to polarise core protein asymmetry in that region. As for the rest of the wing the core proteins must be polarised through another mechanism in addition to that of Ft/Ds/Fj.

In the eye disc, Ds or Ft overexpressing clones can reorientate cells surrounding the clone (Brittle et al., 2012), suggesting that these cells can respond to Ft/Ds and influence local cell polarity. However this non-autonomy surrounding Ds or Ft over-expression clones is still present in the absence of Dachs. Therefore in the eye the non-autonomy polarity effect on is not via Dachs. In addition, *dachs* mutant eyes have significantly milder ommatidial polarity phenotypes than *ft/dachs* double mutants (Brittle et al., 2012). Therefore in the eye Ft and Ds are acting on the core protein complexes but this is likely through a Dachs independent mechanism.

In the abdomen, the Ft/Ds system can influence adult abdomen bristle formation and larval denticle field polarity independently of the core pathway (Casal et al., 2006; Repiso et al., 2010).

In light of these data, the prevailing view is that in the wing and abdomen the core proteins adopt their asymmetric localisation mostly independently of Ft/Ds and Dachs. The core protein's are therefore polarised via other polarising cues, possibly with input from morphogen gradients (Casal et al., 2006), whereas in the eye evidence for Ft/Ds input into polarising the core proteins and consequently the ommatidia is fairly strong although there are possibly other patterning cues required. Therefore, the Ft/Ds and the core systems both have input into polarising the wing, eye and abdomen.

Planar polarity effector genes

In the wing, there are four known wing specific planar polarity effectors that act downstream of the core proteins and control the site of prehair initiation and the number of wing hairs (Adler et al., 2004; Collier et al., 2005; Lee and Adler, 2002; Strutt and Warrington, 2008; Wong and Adler, 1993). These include Fuzzy (Fy), a four pass transmembrane protein, and the cytoplasmic proteins Inturned (In) and Fritz (Frtz) (Collier and Gubb, 1997; Collier et al., 2005; Park et al., 1996). All three localise to the proximal side of wing cells, at the same junctional location as Stbm and Pk (Adler et al., 2004; Strutt and Warrington, 2008). These wing specific effectors require the activity of the core proteins to be localised proximally in the cell (Adler et al., 2004; Strutt and Warrington, 2008).

Mutants of *in, fy* and *frtz* affect the formation of the wing hairs and bristles, resulting in multiple hairs, which exhibit swirling patterns (Collier and Gubb, 1997; Collier et al., 2005; Gubb and Garcia-Bellido, 1982; Lee and Adler, 2002; Park et al., 1996; Wong and Adler, 1993), unlike in *fz* mutants where the hair forms in the centre of each cell (Wong and Adler, 1993).

These wing specific effector proteins restrict the subcellular localisation of another effector protein, Multiple wing hairs (Mwh), a WD40 repeat protein. Fy, In and Frtz, in conjunction with the core proteins, ensure Mwh restricts apical actin polymerisation of the newly forming wing hair to the very distal edge of the cell, allowing the production of only one hair (Strutt and Warrington, 2008; Yan et al., 2008). As for *in*, *fy* and *frtz*, in the absence of *mwh*, restriction of the hair number is lost resulting in multiple wing hairs being produced (Gubb and Garcia-Bellido, 1982). However the phenotype is also stronger, producing more hairs.

The planar polarity effectors have been placed downstream of the core proteins, as none of the confirmed effectors are required for the localisation of the core proteins

(Strutt, 2001b; Usui et al., 1999). In addition, mutants for the effector proteins *fy*, *in* or *frtz* can block Fz non-autonomy, suggesting that the effectors are acting downstream of Fz (Lee and Adler, 2002). Other work has shown that *in* acts later than the core proteins in specifying wing hair development (Adler et al., 1994). Therefore, together these data suggest that the effectors, In, Fy, Fritz and Mwh do act downstream of the core proteins in specifying and placing trichomes in the pupal wing, and also in the abdomen (Adler et al., 2004; Collier et al., 2005; Lee and Adler, 2002; Strutt and Warrington, 2008).

The planar polarity effectors are often tissue specific, this means that planar polarity can affect a range of morphological outputs in different tissues. However, many effectors have other roles in development in addition to their roles in planar polarity, making it difficult to tease apart what specific roles effectors play in mediating planar polarity outputs. One such effector is the Rho GTPase RhoA (Rho1- Flybase), which is required for actin dynamics and wing hair formation (Strutt et al., 1997), and for ommatidial rotation in the eye (Strutt et al., 1997). In the wing, RhoA is also required for cell division, which can lead to a multiple wing hair phenotype that is unrelated to planar polarity (Adler et al., 2000a). In addition RhoA can also affect core protein localisation, suggesting a role for RhoA upstream of the core proteins (Yan et al., 2009). Therefore the role of RhoA as a planar polarity effector in *Drosophila* is unclear.

Planar polarity in vertebrates

Multiple orthologs of the *Drosophila* core proteins have been found in vertebrates where the core proteins are required for a wide variety of patterning events. Examples of these include cell intercalation during gastrulation in *Xenopus* and zebrafish (*Danio rerio*) (Goto and Keller, 2002; Heisenberg et al., 2000; Jessen et al., 2002; Park and Moon, 2002; Tada and Smith, 2000; Takeuchi et al., 2003; Veeman et al., 2003; Wallingford et al., 2000), the orientation of hair cells in the mammalian cochlear (for reviews, see, Curtin et al., 2003; Ezan and Montcouquiol, 2013; Jones and Chen, 2007; Keller et al., 2000; Montcouquiol et al., 2003; Rida and Chen, 2009; Vinson and Adler, 1987; Wang and Nathans, 2007), neuronal migration (Jessen et al., 2002) and neural tube closure in the zebrafish and in the mouse (Ciruna et al., 2006; Curtin et al., 2003; Kibar et al., 2001; Murdoch et al., 2001; Wang et al., 2006a; Wang et al., 2006b).

The asymmetric localisation of the core proteins in vertebrates has not been as readily observed as it had in the *Drosophila* wing and eye. Previous attempts to

observe core proteins in zebrafish and *Xenopus* using tagged proteins failed (Carreira-Barbosa et al., 2003; Veeman et al., 2003; Wallingford et al., 2000). However, more recent attempts using GFP fusion proteins of Pk and Dsh, expressed closer to endogenous levels have shown that the core proteins are asymmetrically localised during vertebrate gastrulation (Ciruna et al., 2006; Yin et al., 2008) and in vertebrate ear patterning (Montcouquiol et al., 2003; Wang et al., 2006b). Immunolabelling for the endogenous core polarity proteins showed that they were asymmetrically localised in the vertebrate ear (Montcouquiol et al., 2006), the basal layer of the embryonic vertebrate skin (Devenport and Fuchs, 2008), also in nodal cilia thereby affecting left-right asymmetry in the mouse (Antic et al., 2010; Borovina et al., 2010; Hashimoto et al., 2010). Therefore the asymmetry of the core proteins is likely to be as important for planar polarity in vertebrates as it is in *Drosophila*.

The non-autonomous effects of the core proteins seen in the *Drosophila* wing have also been observed in the epidermis of *Xenopus* where the multi-ciliated polarised epidermal cells are surrounded by un-ciliated cells. Epithelial cells overexpressing Fz or Vangl2 (Van Gogh-like 2 ortholog of Stbm) transplanted into wild-type epidermis can cause surrounding wild-type tissue to reorientate multiciliated cells to point hairs towards high Fz and low Vangl2 activity (Mitchell et al., 2009).

The downstream effectors in the *Drosophila* wing are also conserved in vertebrates. Fritz, (Kim et al., 2010), Fuzzy (Gray et al., 2009; Heydeck et al., 2009) and Inturned (Park et al., 2006; Zeng et al., 2010) are all required for convergent extension and neural tube formation (Heydeck et al., 2009; Kim et al., 2010; Zeng et al., 2010). In vertebrates, these proteins have additional roles in facilitating cilia morphogenesis (Heydeck et al., 2009; Kim et al., 2010; Park et al., 2006). Correct cilia formation is also required for Hedgehog (Hh) signalling (Wilson and Stainier, 2010). Therefore mutations in vertebrate planar polarity effector genes also result in Hedgehog (Hh) defects due to loss of cilia formation (Gray et al., 2009; Heydeck et al., 2009; Park et al., 2006; Zeng et al., 2010).

Despite the lack of evidence for involvements of Wnts in planar polarity in *Drosophila*, work in vertebrates has showed that Wnt5 and Wnt11 regulate the core proteins during vertebrate gastrulation (Carreira-Barbosa et al., 2003). For example Wnt11 during zebrafish gastrulation causes accumulation of Fz7 at the plasma membrane (Witzel et al., 2006). In addition, Wnt11 over-expression phenotypes can be suppressed by reducing Pk, therefore in vertebrates Wnts are required for core protein localisation at the junctions although not for their asymmetry (Carreira-

Barbosa et al., 2003).

The role of the core proteins during vertebrate gastrulation is to control polarised cell intercalation during convergent-extension. In this process, cells become aligned and elongate on the medial-lateral axis, and then intercalate between neighbouring cells to elongate the tissue (**Figure 1.6**, Goto et al., 2005; Goto and Keller, 2002; Jessen et al., 2002; Veeman et al., 2003; Wallingford et al., 2000; Ybot-Gonzalez et al., 2007).

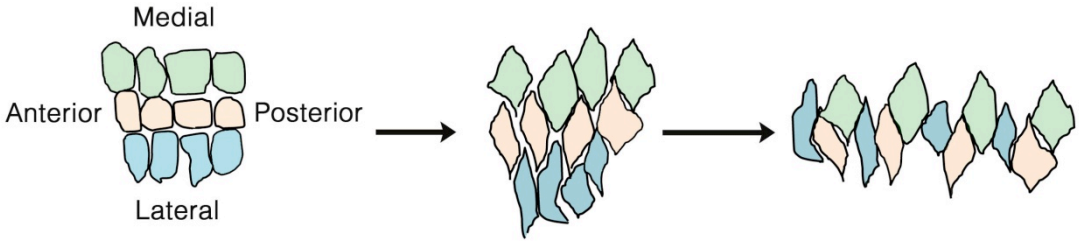

Figure 1.6 Medial-lateral cell intercalation in vertebrates

Diagram of the elongation of the tissue along the anterior-posterior axis. Cells aligned along the medial-lateral axis intercalate so that the tissue becomes shorter on that axis. Anterior is to the left.

Cell rearrangements require polarised junctional remodelling

Although core proteins are involved in cellular rearrangements in vertebrates, how these changes occur at a molecular level is relatively unknown. Similar cell rearrangements also occur in *Drosophila* although there is little evidence to show that the core proteins are involved.

In the *Drosophila* epidermis, during germ band extension (GBE), many cells converge on one axis and then extend on the other through polarised junctional shrinkage modifying cell-cell adherence, cell shape changes and through orientated cell division (**Figure 1.7A**, Bertet and Lecuit, 2009; Butler *et al.*, 2009; da Silva and Vincent, 2007; Fernandez-Gonzalez *et al.*, 2009; Irvine and Wieschaus, 1994; Zallen, 2007; Zallen and Wieschaus, 2004). The germ band elongates to approximately twice its original length on the anterior-posterior axis (da Silva and Vincent, 2007; Irvine and Wieschaus, 1994). As this occurs the posterior of the embryo folds back upon itself as it moves towards the anterior of the embryo (see chapter 5). GBE occurs in two phases an initial fast phase followed by a slower phase, both phases require cell intercalation however the increase rate of cell rearrangement during the fast phase is due to cell shape changes (Butler et al., 2009).

At the start of cell intercalation, cell junctions are aligned along the dorsal-ventral axis and are called ‘type I’ junctions (**Figure 1.7A**, reviewed in Bertet et al., 2004; Lecuit and Lenne, 2007; Zallen and Blankenship, 2008). As the cells begin remodelling their attachments to neighbouring cells these ‘type I’ junctions shrink to become ‘type II’ junctions (**Figure 1.7A, middle**), new junctions then form and extend along the perpendicular axis forming ‘type III’ junctions. These junctions now connect dorsal and ventral neighbouring cells, which were not previously in contact (**Figure 1.7A, right**). This process of shrinking junctions on one axis and establishing ‘type III’ junctions on the perpendicular axis is an irreversible process during GBE (Bertet et al., 2004), whereas in the *Drosophila pupal* wing this process can be reversed (Classen et al., 2005).

To rearrange many cells at once during GBE, groups of cells form multicellular rosettes where neighbouring cells synchronise junctional rearrangements (Blankenship et al., 2006, and **Figure 1.7B**), in a similar manner to that of 4 cells (Compare **Figures 1.7A** and **1.7B** Blankenship et al., 2006; reviewed in Lecuit and Lenne, 2007; Zallen and Blankenship, 2008).

Another well-studied example of cell intercalation in *Drosophila* occurs during

elongation of the trachea (described in chapter 4,Affolter *et al.*, 2009; Shaye *et al.*, 2008; Uv *et al.*, 2003). In both the epidermis and the trachea, cell intercalation and junctional remodelling require the modification of cell adhesion between cells (Levayer et al., 2011; Shaye et al., 2008). Cells adhere at subapical membranes where the adherens junctions are located. The main component of the adherens junctions is E-cadherin (E-cad, which is encoded by *shotgun*- FlyBase). E-cad levels are carefully regulated during cell intercalation as too much causes cells to adhere too tightly and they therefore cannot rearrange. Too little E-cad means the cells cannot adhere to their neighbours and are excluded from the epithelial layer (Cela and Llimargas, 2006; Zallen and Blankenship, 2008).

Cell adhesion is proposed to be regulated via modulating endocytic trafficking of E-cad to and from the junctions (Classen et al., 2005; Ulrich et al., 2005), and through local recycling via endosomes (Shaye et al., 2008; Shindo et al., 2008). The selective remodelling of a cell's junctions during cell intercalation, rather than general modulation of cell adhesion, suggests that there may be mechanisms to polarise E-cad turnover at a cellular level. This could be a way of regulating which junctions are modified during cell intercalation to ensure all cells within the tissue respond in the same way to allow polarised cell rearrangement (Nishimura et al., 2012). In vertebrates, Fmi and Dsh are required for vertebrate neural tube closure, by planar-polarising actin myosin contraction. In addition, cell adhesion is affected by the loss of core proteins, as a reduction in Pk levels leads to reduced junctional adhesion (Oteiza et al., 2010). However, the mechanism for how the core proteins could be regulating cell adhesion and polarising E-cad localisation has not been examined in *Drosophila*.

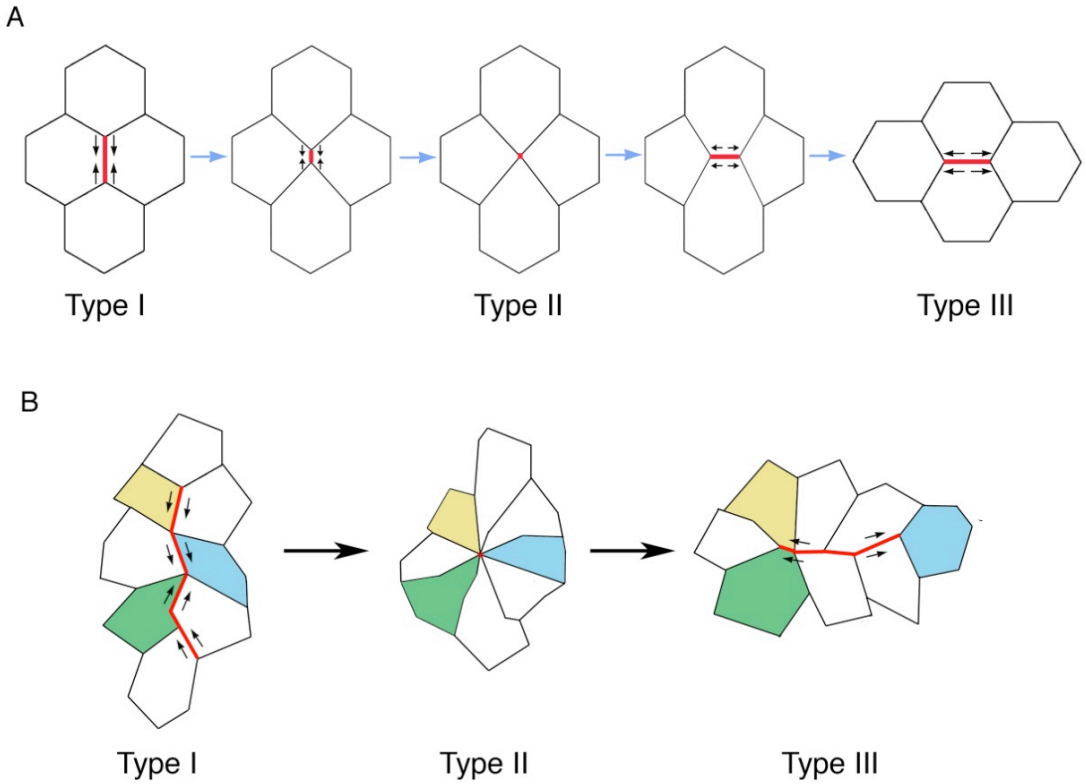

Figure 1.7: Diagram of cell rearrangements in the *Drosophila* embryonic epidermis

(A) Cell rearrangements through the shortening and lengthening of junctions between four cells. Junctions orientated along the dorsal-ventral axis, called type I junctions shrink to a point forming type II junctions. Junctions orientated along the proximal-distal axis then elongate to form type III junctions. (B) This method of converging cells on one axis and extending on another can also be applied to multiple cells intercalating at the same time. Note: The yellow and blue cells that were near each other prior to cell intercalation are separated after cell intercalation. Black arrows indicate the direction of junctional shrinkage and growth.

Aims

This work will investigate the dynamics of the core proteins as they colocalise into membrane subdomains. Previous work on the core proteins in fixed epithelial tissues, and models based on those observations, suggested that the core proteins form a junctional complex, which is required for planar polarity. However, nothing is known about these proposed complexes in terms of their persistence and stability in the cell junctions. I therefore hope to gain insight into whether these proposed complexes are functionally important and how they are maintained in polarised cells.

To study this, live imaging and Fluorescent Recovery After Photobleaching (FRAP) methods were developed to observe live localisation and stability of the core proteins at cell junctions in different epithelial derived tissues, namely the *Drosophila* pupal wing, embryonic trachea and the embryonic epidermis during GBE.

As mentioned previously, planar polarity activity is important for cell rearrangements during vertebrate development. In *Drosophila* there are a few examples of the core proteins being involved in coordinated rearrangement of groups of cells, and little has been done in either vertebrates or *Drosophila* to understand the mechanism by which planar polarity activity is linked to cellular rearrangements. To address this the role of the core proteins during polarised cellular rearrangements was studied in the *Drosophila* embryonic trachea, epidermis, and in the pupal wing. This should provide insights into the mechanism by which the core proteins coordinate polarised junctional remodelling between groups of cells, and uncover if this is a general mechanism to coordinate cell rearrangements.

Introductions to the pupal wing, the embryonic trachea, the epidermis and FRAP are provided at the beginning of the relevant chapter.

Chapter 2

The development of live-imaging and FRAP methods in the *Drosophila* pupal wing

Introduction

The transmembrane proteins Fmi, Fz and Stbm are key to the formation of proposed asymmetric complexes, and all are required for the normal localisation of these proteins to the apical junctions (Bastock et al., 2003; Strutt, 2001b; Strutt and Strutt, 2008; Strutt and Strutt, 2009; Usui et al., 1999). The cytoplasmic factors Dsh, Dgo and Pk are not necessary for Fz, Fmi and Stbm localisation at the junctions (Bastock et al., 2003; Feiguin et al., 2001; Shimada et al., 2001; Strutt, 2001a; Usui et al., 1999), or for the polarizing signal to neighbouring cells (Chen et al., 2008; Strutt and Strutt, 2007). In addition, when over expressed the cytoplasmic factors increase the levels of the other core transmembrane proteins in puncta. Therefore, the cytoplasmic factors could be required for the clustering of similar complexes at the junctions, which could make complexes more stable. Stabilizing the complexes on a specific axis could be one way to planar polarise cells. Therefore, puncta could further stabilise accumulations of correctly orientated complexes that are required to establish polarity. Alternatively, puncta could be regions of the membrane where the core proteins align in asymmetric complexes but are not stabilised.

Some of the core planar polarity proteins are known to be subject to endocytic turnover at the junctions as they are seen in endocytic vesicles and colocalise with the early endosome marker Rab5 (Mottola et al., 2010; Strutt and Strutt, 2008). If endocytic trafficking is blocked the core proteins accumulate in these vesicles (Shimada et al., 2006; Strutt and Strutt, 2008). It is yet to be determined how much protein is turned over and if this turnover is modulated by the formation of asymmetric complexes. Therefore Fluorescent Recovery After Photo bleaching (FRAP) was used as a way of measuring protein turnover in real time, to distinguish between two possibilities: that either the core proteins are stably localised to junctional puncta relative to other cell junctions; or that the protein is not preferentially stabilised in puncta and is being constantly turned over, regardless of whether the protein is localised to junctional puncta.

Live imaging of the pupal wing had been previously used to study the dynamics of cell packing in the developing wing tissue (Classen et al., 2005), and to look at the intracellular movement of Fz along microtubules (Shimada et al., 2006). We therefore employed the same imaging methods in the wing at 28hr (at 25^{o}C) after puparium formation (APF) when the core proteins are strongly asymmetric and large puncta are present (Aigouy et al., 2010; Strutt and Strutt, 2009). For the live imaging, a

fluorescently tagged protein was stably introduced into the fly stock to be imaged. Pupae from this stock were collected and aged for 27h (at 25°C), before the pupal casing above the wing was removed. The pupae were then inverted and mounted in Halocarbon oil and imaged using a fluorescence microscope (**Figure 2.1**).

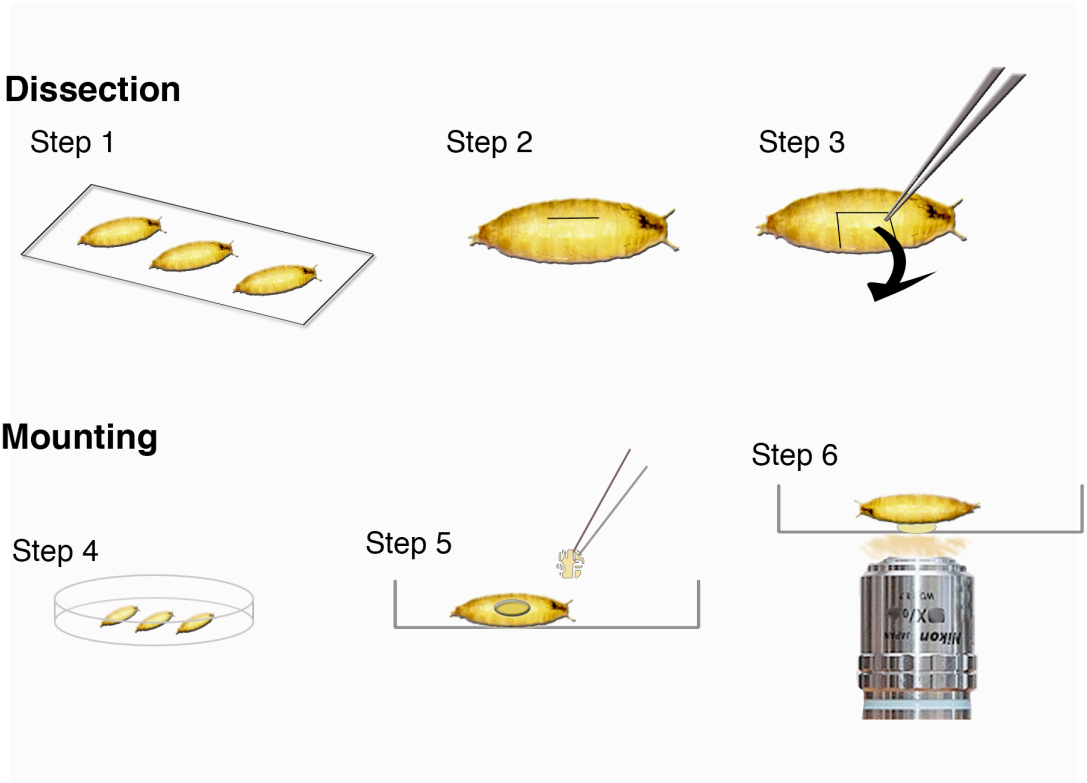

Figure 2.1: Dissection and mounting method for pupal wing live imaging

Pupae are collected at the white pre pupal stage and aged for 28h at 25°C before placing in a petri dish on double-sided tape (step 1). Pupae are then cut open along the ventral midline of the pupae starting about a third of the way down from the anterior of the pupae (step 2). A flap of cuticle is then removed using forceps (step 3). The pupae are then lifted from the double-sided tape using water and placed on a glass bottomed imaging dish (step 4). A small drop of Halocarbon 700 oil is then touched onto the cuticle opening using a pipette tip (depicted in step 5 as the pale orange blob). Individual pupae are then rotated and positioned with the wing/cuticle opening touching the glass dish and imaged from below on an inverted confocal microscope (step 6).

Establishing a method for FRAP in the pupal wing

FRAP has been typically conducted in live tissue culture cells, although FRAP *in vivo* is a better way of looking at protein turnover during a particular developmental stage or asking tissue specific questions, rather than looking at isolated cultured cells. FRAP is used to quantify the amount of protein turnover occurring within a region of a cell. It involves photo bleaching fluorescently tagged protein within a particular region in a cell and then recording how much fluorescence recovers during the length of the experiment (Axelrod et al., 1976) (See Material and methods and **Figure 2.2**).

To measure the turnover of a fluorescently tagged protein, small regions of interest (ROI's) are selected within a cell. Prebleach images are captured, to measure the base line of fluorescence in the ROI's. A laser is then used to emit intense light of a particular wavelength to bleach the fluorescent emitting part of the tag in the ROI, which renders the tag unable to emit fluorescence.

We assume the fluorescent bleaching does not destroy the protein the tag is attached to, or alter the protein's normal behaviour (Reits and Neefjes, 2001). Our experiments show that different levels of bleaching (up to 80% of initial fluorescence) result in a similar recovery, suggesting that cell damage is not occurring at these settings (**Figure 2.3A**). Another control for establishing whether cell damage is occurring is to repeat the bleaching of an ROI, and seeing the second recovery phase reach 100% of the fluorescent intensity just prior to the 2nd bleach. This should occur if the first bleach has not irreversibly damaged the region. The fluorescence reaches 100% because only unstable protein that can be turned over can be bleached during the 2nd bleach event. As recovery reached that level during the first bleach, the recovery should also be able to reach that level again after the second bleach, not being able to would show that cellular damage is occurring. Although this experiment was not conducted, the experiments that were done suggested that cellular damaged was not occurring under the experimental conditions used.

After the bleaching event, post bleach images are taken over time to measure the fluorescence recovering in the ROI's. More fluorescence recovery indicates that protein in the ROI is more susceptible to protein turnover. Less recovery suggests that the protein is more stable in that region.

The fluorescence measured in the ROI is from fluorescing protein moving into the bleached ROI, replacing the bleached protein, which would normally occur over time. The fluorescent recovery of junctional localised proteins can be from newly

synthesized protein being trafficked to the junctions, from protein trafficked from other locations within the cell to the ROI, or from diffusion of protein already within the cell or the surrounding junctions.

The amount of fluorescent recovery is assumed to be a measure of how much of the tagged protein is freely exchanging in the junctions. Any bleached protein that is not exchanged is assumed to be stably associated with the junctions and either the protein is inaccessible to endocytosis machinery, for example in a protein complex, or the protein is not subjected to protein turnover during the lifetime of the experiment, possibly due to a long protein half-life or being tethered to prevent diffusion of the protein, when in the junctions.

FRAP therefore allows us to address the question: are the core proteins persistent in puncta and if so, are they further stabilised in these puncta compared to other junctional regions? In this chapter I start to address this issue by optimizing the pupal wing live imaging and FRAP methods using the core protein Fz.

Aims

To establish a method to enable live imaging and FRAP of *Drosophila* pupal and pre-pupal wings to ascertain if Fz is persistent in junctional puncta. If this is the case, to determine if Fz is further stabilised when localised to these regions or is the protein still subjected to turnover but the structure is persistent.

Results

Live imaging in the pupal wing

For initial live imaging experiments, Fz fused to the fluorescent tag EYFP was expressed using the *Actin5C* promoter (Strutt, 2001b; Strutt et al., 1997) hereafter referred to as Fz-EYFP. This fused protein is expressed in pupal wings at a similar level to that of endogenous Fz, as shown by Western blot analysis (Strutt et al., 2011), and can rescue the fz^{P21} mutant phenotype in the wing (Strutt, 2001b; Strutt et al., 1997). In fixed pupal wings, Fz-EYFP localises asymmetrically to the junctions (Strutt, 2001b) and forms puncta as previously seen with endogenous immuno-labeled Fz (Strutt et al., 2011).

In the pupal wing, live imaging of Fz-EYFP was conducted between 28hr APF and 32h APF, when the core proteins are most asymmetric prior to actin pre-hair placement. To do this the pupae were collected and dissected as described by the Eaton lab (Classen et al., 2005) (see Materials and Methods).

Establishing a method for FRAP in the pupal wing

The imaging settings for FRAP were optimised so as many images as possible could be collected without significant photobleaching damage to the sample. A detailed explanation of FRAP can be found in Materials and Methods (and **Figure 2.2**), but an overview of optimisation in the pupal wing is described below.

For FRAP experiments, three pre-bleach images were captured 30sec apart, the regions were then bleached to approximately 80% of the regions' initial fluorescence and an immediate post-bleach image was taken before time lapse images were taken every 30sec for up to 40min. These settings were optimised to not significantly affect the fluorescence recovery of the protein (see below). Any time-lapse series that lost more than 25% of the initial fluorescent signal during the lifetime of the experiment were discarded.

Once collected, bleached regions were manually re-selected using ImageJ, to correct for tissue movement during imaging. Although minimal acquisition bleaching occurred during imaging, to correct for this control regions were selected of the same size as the bleach regions and measured. These regions were at least 2 cells away from a bleach region to avoid the initial bleaching affecting the control regions (see results below).

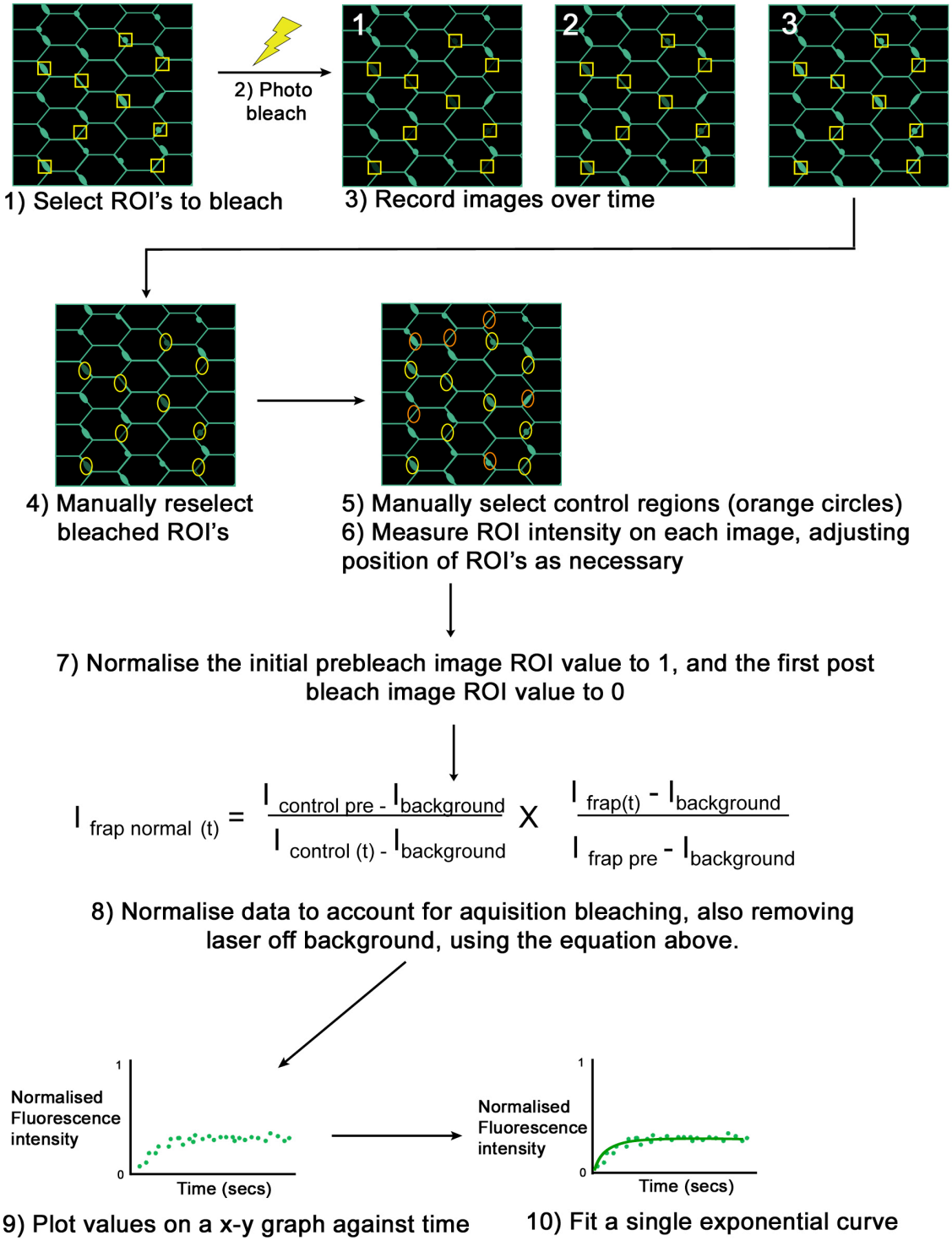

Figure 2.2: FRAP image acquisition method, and the manual image processing and data normalization steps

A simplified summary of the workflow of a FRAP experiment and subsequent analysis steps. See Materials and Methods for full method.

The mean values of the bleached ROI's were then normalised against the non-bleached control regions to correct for acquisition bleaching (Materials and Methods **Figure 2.2**). Conventional background measurements could not be taken as the wing tissue filled the field of view, therefore laser off background was subtracted instead.

Individual data sets were then normalised to allow for comparison of results between data sets. To do this the averaged pre-bleach measurement was set to 1 and the first image after bleaching was set at 0. The fluorescent measurements in between were then normalised with respect to the average prebleach value. Once normalised, the fluorescent values were then averaged across bleached regions. Multiple wings were imaged in the same manner and then averaged across wings. These data were then plotted on a graph to show the fluorescent recovery for bright and less bright regions (**Figure 2.2**). Non linear regression was then used to fit a single exponential curve to the data using Prism 5 (Graphpad). This equation is the simplest model and suggests that there is only a single phase of recovery. However it is unlikely that recovery is from a single process for example diffusion alone or from just endocytic trafficking. Therefore a more complicated model where there are two or more phases of recovery would be expected. However, the data in this work fits to a single exponential equation, suggesting that one process dominates the recovery.

Optimization of the amount of initial ROI bleaching

To obtain a high signal to noise ratio of fluorescence in the ROI during recovery, the initial bleaching must photo-bleach approximately 60-80% of the fluorescence in the ROI but at the same time must not significantly damage the sample or the amount of recovery.

To optimise the amount of initial bleaching, the laser was set at 100% and the number of laser passes was varied. Several non-overlapping regions of the same wing were photo-bleached to different degrees (**Figure 2.3A-B**). Less than 55% bleaching resulted in a low signal to noise and variable fluorescent recovery curves, whereas more than 80% resulted in a retardation of fluorescence recovery. Therefore, 20 laser passes was selected as the optimal condition, giving a bleaching level of 80%, which increased the signal to noise ratio (**Figure 2.3B**) but did not significantly inhibit the amount of fluorescence recovery (**Figure 2.3A**). Also note that as 10, 20 and 50 passes of the laser gives a similar recovery, there is therefore no evidence of photo damage under these experimental conditions.

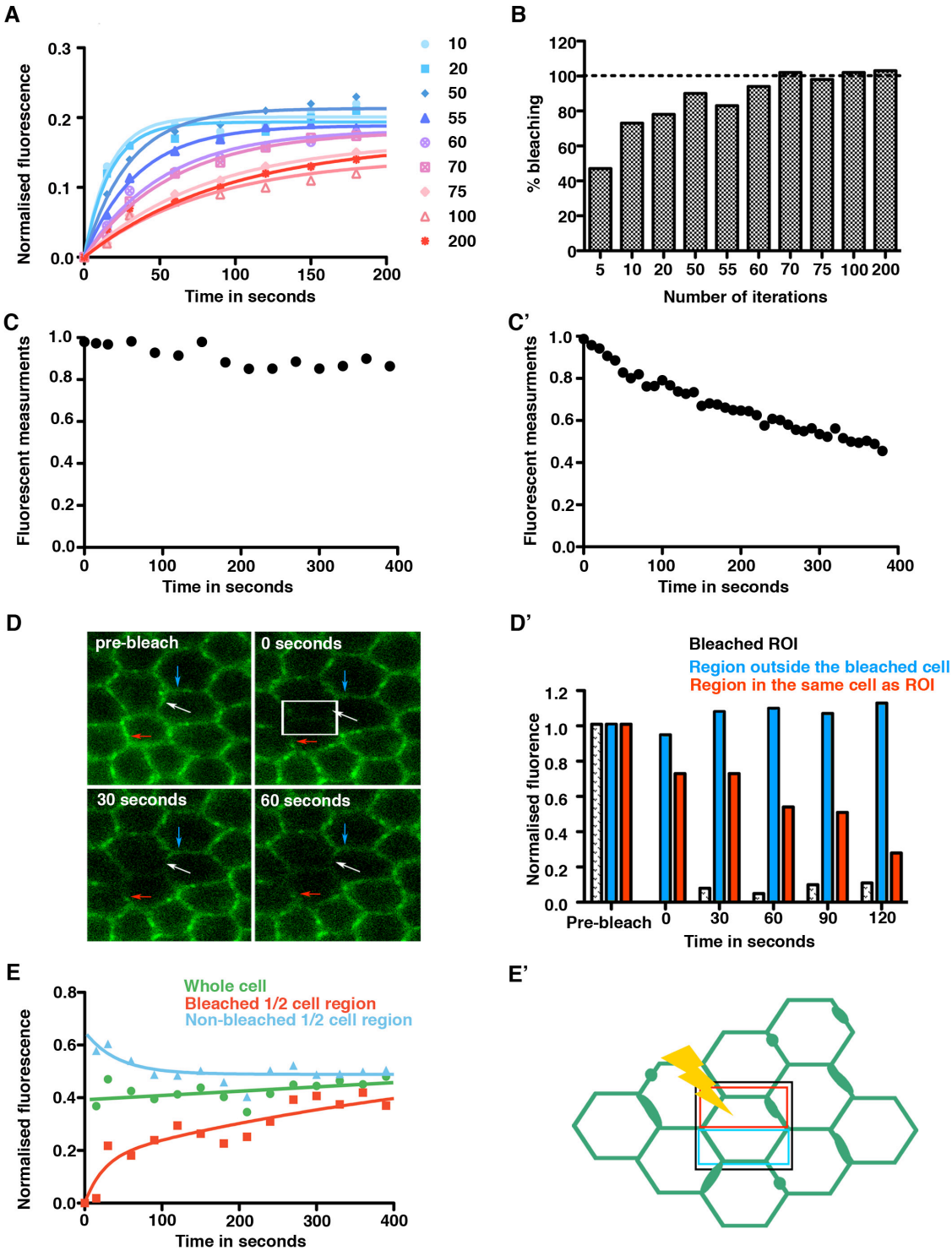

Figure 2.3: Controls for the FRAP experiments

(A) Graph of Fz-EGFP fluorescence recovery, after different amounts of bleaching. Bleaching variation was achieved by altering the number of laser passes (iterations) over the bleach region. The laser power was kept constant. This meant that the bleach time also varied, and increased with the number of laser passes (1 pass of the laser = 1.2 sec). The percentage recovery plateau was comparable when using 10-55 passes of the laser. However, increasing

the number of passes further resulted in less recovery. This could be due the protein cross-linking in the junctions when exposed to a large amount of bleaching inhibiting fluorescent recovery. Or due to the depletion of the total fluorescence in the cell, caused by unbleached protein moving into the ROI during bleaching. (B) Graph showing the percentage of bleaching in relation to the number of bleach passes of the laser. 20 passes of the laser was selected as this amount of bleaching fell between 50-80% loss of pre-bleach fluorescence which is considered optimal, to give a good signal to noise ratio and to prevent damage to the tissue. (C) Graphs showing acquisition bleaching occurring over time, comparing sampling intervals of 30sec (C) and 10sec intervals (C'). Minimal acquisition bleaching is preferred during a FRAP experiment. Note that time intervals of 30sec did not bleach more than 20% of the starting fluorescence (C), whereas the 10sec intervals increased the acquisition bleaching (C'). (D) Early recovery within the bleach region is most likely accounted for by lateral migration of Act-Fz-EYFP within the junctions. (D) Images show prebleach, 0sec, 30sec and 60sec time-lapse images. (D') shows a FRAP experiment measured in the same way as the other FRAP experiments. Bleach ROI is depicted with the white box (D), white arrow depicts part bleach region measured in D', which is bleached and then recovers over time (white patterned bars in D'). Red arrow depicts a non-bleached junctional region in the same cell (D) that loses fluorescent intensity over time as the junctional protein moves laterally into the bleached region (red bars in D'). The blue arrow is a non-bleached junctional region in a neighbouring cell with an adjoining junction to the bleached region (D), which does not lose fluorescence over time (blue bars in D'). The fluorescent intensity of Act-Fz-EYFP at the pre bleach time point is normalised to 1 and the immediate post-bleach time point (t0) is normalised to zero for the bleached region. (E-E') A half-cell bleaching experiment (E) and a diagram of the regions analysed (E'). Half a cell was bleached and the recovery measured (red line of recovery in E and the region indicated as the red box in E'), in addition the recovery of the other non-bleached half of the cell was also measured (blue line in E and the blue box in E'), as well as the fluorescence of the whole cell (green line in E and the black box in E'). Recovery of the bleached region within the first minute is accompanied by the loss of fluorescence from the non-bleach half of the cell. Recovery of Fz-EYFP is increased in this experiment to 40% but that is consistent with half of the cell being bleached rather than a small junctional region. Although, less recovery would be expected as more of the cellular pool is depleted, recovery is actually increased as the surrounding neighbouring cells with junctions bordering the bleach region also contribute to recovery.

In addition to the amount of bleaching, the length of the bleach time is also important. A long bleach time can lead to diffusion of surrounding un-bleached protein moving into the bleach region and leading to a slower recovery; as the surrounding protein that would have moved into the region, has already been bleached. This can lead to changes in rate of recovery and the final amount of recovery. As is seen when bleach times are extended (**Figure 2.3A**).

Minimizing acquisition bleaching during fluorescence recovery

To accurately measure the rate of Fz-EYFP recovery, a fast time interval between images is required. To attempt to measure the rate of Fz-EYFP in the bright and less-bright regions, the time interval between images was varied either using 10 or 30sec intervals between images. By using a 30sec time interval the amount of acquisition bleaching was 20% over 380sec allowing the GFP fluorescence to recover to 25% in the puncta (**Figure 2.3C**). However, when the time interval was reduced to 10sec the amount of acquisition bleaching increased, to 45% over 380sec, which inhibited the recovery of the fluorescence (**Figure 2.3C'**). Therefore, the 30sec time interval was used to minimize acquisition bleaching.

Lateral movement of fluorescent junctional protein accounts for some of the early fluorescence recovery in the bleached junctions

Loss of adjacent membrane fluorescence outside the bleach region was observed and I initially suspected that this was due to overspill bleaching occurring outside of the region of interest. However, this loss of fluorescence was only seen for membranes in the same cell as the bleach region and not for membranes adjoining neighbouring cells which touch the bleached membrane (**Figure 2.3D-D'**). This early loss of fluorescence surrounding bleach regions could be due to lateral diffusion of non-bleached fluorescent protein within the same cell moving into the bleach region and contributing to recovery; although, local endocytosis and exocytosis could not be ruled out. However, this meant that the selection of control ROI's must be at least two cells away from each bleach region to avoid loss of fluorescence in the control regions situated near enough to bleached regions to be subjected to local fast diffusion and trafficking.

We next wanted to ask are there other populations of fluorescent protein within the cell contributing to fluorescent recovery? To look at what happens to other populations of Fz-EYFP in the cell when a proportion is photobleached, 'Half cell' FRAP experiments on Fz-EYFP were performed. In these experiments half of a wing cell is bleached and then fluorescence intensity measurements of the bleached

region the non-bleached half of the cell and the whole cell are taken (**Figure 2.3E**). If recovery is from the other half of the cell then the fluorescent intensity of the non-bleached half will fall, on the other hand if the fluorescent intensity of the whole cell increases after bleaching then new synthesis is also occurring during the lifetime of the experiment. When half of a wing cell is photobleached the amount of fluorescence in the unbleached cell-half decreases over time suggesting that Fz-EYFP recovery is from protein diffusing or being trafficked from the unbleached half of the cell into the bleached half. However, new synthesis does not significantly contribute to Fz-EYFP recovery over the time course of the experiment, as there is no significant fluorescent increase when the whole cell is measured during the time of the experiment (**Figure 2.3E'**). In addition Huang *et. al.* (2011) suggested that the fluorescence recovery in their spot FRAP assays, which is similar to the FRAP assays presented here, came mainly from diffusion or exchange of protein, but not protein synthesis.

Discussion

Analysing the localisation and behaviour of Fz-EYFP in pupal wing cells

Fluorescently tagging a protein even if it is expressed at endogenous levels may still alter its behaviour, in terms of its localisation, transport through the cell or even resulting in cross-linking of proteins at the junctions preventing its internalization. However, a fluorescent tag is essential for FRAP experiments therefore, we can measure protein levels and look at protein localisation, but we can never be sure if the tag is altering protein behaviour or trafficking in some way.

Despite the potential problems with expression and functionality of adding a large YFP domain to a protein, results from Fz-EYFP colocalisation and rescue experiments indicate that Fz-EYFP is functional and localises asymmetrically to the junctions (Strutt et al., 2011). Western blot experiments show that Fz-EYFP is not over-expressed in relation to the endogenous protein (Strutt et al., 2011). In addition, the control experiment suggests that Fz-EYFP is not permanently cross-linked in the junctions preventing Fz turnover. Therefore, Fz-EYFP is likely to be behaving in a similar way to that of endogenous Fz, and although the tag could be altering Fz behaviour it is not altering it significantly, allowing the turnover of Fz to be monitored as accurately as it can be using this method.

Optimisation of live imaging and FRAP methods for Fz-EYFP

Imaging for FRAP experiments was optimised to reduce acquisition bleaching and to

increase the signal to noise ratio. To achieve this, I aimed to bleach 80% of the fluorescence during the initial bleach. In tissue culture cells this can be achieved by bleaching using 3-4 passes of the laser in under a few seconds. However, in the pupal wing bleaching 80% of the fluorescence is harder to achieve, as the wing develops inside a sac of fluid surrounded by a membrane. Although live imaging through this fluid is possible it results in an increase in light refraction and an increased distance between the wing membrane and the objective, reducing the amount of fluorescent signal available. So to achieve 80% bleaching in the pupal wing more laser passes are required taking up to 30sec to achieve.

Unfortunately, extended bleach times can result in a FLIP (Fluorescent Loss In Photo-bleaching) like experiment, where the recovering fluorescence is constantly being bleached, which reduces the amount of fluorescent protein available to replenish the bleach region. Although a shorter bleach time would be preferable I was unable to shorten the time and still be able to achieve sufficient bleaching to obtain a high signal to noise ratio after fluorescent bleaching. Also as the laser power had to be kept at a higher level to see enough fluorescent signal, the number of acquisition images was limited, to avoid increasing acquisition bleaching.

Due to the imaging parameters used for these FRAP experiments we were unable to extract rate measurements from the data. This was because the time interval of 30sec used to reduce acquisition bleaching during the experiment was longer than the calculated rate values from this data (see chapter 3). In addition, there is also likely to be significant fluorescent recovery in the ROI during the long initial bleaching time, which would then be subjected to bleaching, further depleting the cellular pool of fluorescent protein. Therefore, the rate values were not likely to be accurate and the FRAP experiments in this Chapter and Chapter 3 only look at the stable and unstable fractions of the recovery rather than the rate of recovery.

Depletion of the cellular pool of protein during the bleach phase results in less protein being available for recovery after the bleach. This results in a decrease in the apparent size of the stable fraction, as the recovery is reduced. However, the control experiments show that if the amount of bleaching is reduced, so that the bleaching time is limited, then a smaller amount of protein is able to move into the bleach region and so not significantly deplete the cellular pool of protein.

Fz-EYFP fluorescent recovery in FRAP ROI's comes from lateral diffusion and/or endocytic trafficking within the membrane diffusing into the ROI but also from other

cellular pools of protein. This may occur through local endocytic trafficking via Rab5 live vesicles (Shimada et al., 2006; Strutt and Strutt, 2008; Strutt et al., 2011), but does not occur through delivery of newly synthesized protein, as the levels of protein in the whole cell does not change in the half-cell FRAP experiment.

The recovery of fluorescence in the FRAP experiments shown here (**Figure 2.3A** also see FRAP graphs in chapters 4, 5 and 6) fit a single exponential curve as supposed to a biphasic recovery curve. The fitting of this type of curve suggests that there is a single mechanism that controls recovery, for example protein trafficking within the cell. Though, it is likely that protein synthesis and local diffusion are also occurring during the time frame of the experiment. Of course if the time intervals were reduced then the recovery in the first 100sec after bleaching could reveal a biphasic recovery (see Firmino *et al.*, 2013), as recovery from local diffusion would also be observed in the early phase of the experiment. However, for the data presented here, there is a 30sec time interval after the bleach, during which a lot of diffusion may occur before the first time point and so would not feature on the FRAP curve. Therefore although a single exponential curve may not be accurately depicting the different mechanisms that contribute to recovery, it does fit the later time points allowing a plateau value to be extracted from the data.

Chapter 3
Establishment of planar polarity through stabilisation of core planar polarity proteins into discrete membrane subdomains

Introduction

In the wing the core planar polarity proteins (Fz, Fmi, Stbm, Pk, Dgo and Dsh) are all asymmetrically localised at the cell junctions along the proximal-distal axis (Axelrod, 2001; Bastock et al., 2003; Das et al., 2004; Feiguin et al., 2001; Shimada et al., 2001; Strutt, 2001b; Strutt and Strutt, 2008; Tree et al., 2002b; Usui et al., 1999), at the time when the actin-rich trichome emerges from the distal end of each wing cell. The core protein asymmetry is strongest prior to wing hair formation and loss of any of the core proteins leads to a loss of this protein asymmetry and loss of the correct planar polarisation of the trichomes, suggesting that the localisation of core proteins is required for their function in polarising the trichomes.

A plausible mechanism for cell-cell communication of cell polarity to be transmitted between neighbouring cells by the core proteins would be for the core proteins to be incorporated into asymmetric complexes that span the cellular junctions. In addition, the localisation of these asymmetric complexes at the junctions would also need to be polarised within the cell. This would ensure that enough of the complexes containing Fz were at the distal edge of the cell and the Stbm containing complexes at the proximal edge of the cell.

A number of models have been presented to describe how the core planar polarity proteins might achieve asymmetric localisation within a cell (for example Amonlirdviman et al., 2005; Klein and Mlodzik, 2005; Le Garrec et al., 2006). The general assumption of these models is that the core proteins assemble into asymmetric intercellular complexes and increases the overall stability of complexes as cellular asymmetry is established. However, this is inferred from the localisation of the core planar polarity proteins in wild-type and core planar polarity mutant backgrounds, but whether the core planar polarity proteins do form asymmetric complexes within cells, which are more stable than core proteins at surrounding junctions, and how these proposed complexes are then asymmetric distributed within the cell is poorly understood.

However, there is evidence to suggest that the core planar polarity transmembrane proteins could form complexes and at least colocalise in the same place. Fmi is only found at the junctions in the presence of Fz and/or Stbm and in their absence, Fmi localises to the apical cell surface (Strutt & Strutt 2008). As Fmi is at proximal and distal junctions but Stbm is localised to the proximal junctions and Fz to the distal junctions, this agrees with the idea that the core planar polarity proteins form a

complex across the cell-cell junctions, and this may well stabilise Fmi at the junctions. As the cytoplasmic proteins Dsh, Dgo and Pk are not required for Fmi, Fz or Stbm to localise to the junctions, they are thought to have another role in complex formation possibly by clustering these proteins together. Evidence for this is that larger puncta containing Fmi, Fz and Stbm are seen at the junctions when the cytoplasmic proteins are over- expressed (Bastock et al., 2003; Feiguin et al., 2001; Tree et al., 2002b).

This chapter will examine whether the junctional puncta are persistent at the junctions. In addition whether the puncta are also stable entities, or whether puncta are no more stable than the surrounding junctions but happen to accumulate core planar polarity proteins.

Aims

To investigate the turnover of the core proteins Fz and Fmi, as key components of the intercellular complex (Strutt & Strutt 2008), the FRAP method established in chapter 2 was used to address whether Fz and Fmi are stable in junctional puncta. FRAP was further used to find out roles for the other core planar polarity proteins in either clustering Fz containing complexes into large puncta or stabilising Fz in puncta at the junctions. In addition, I investigated whether puncta containing Fz are present throughout pupal wing development and ask whether puncta retain the same stability at different stages of development, to try to gather evidence of increasing complex stability correlating with increased cellular asymmetry.

Results

Fz junctional puncta are persistent over time

The localisation of the core proteins in junctional puncta and their absence when core protein asymmetry is lost, suggests that they are important for the establishment of planar polarity. To examine these puncta further we examined transgenic flies expressing a Fz fusion to EYFP under the Actin5C (Act5C) promoter. Under these circumstances Fz-EYFP is seen to localise to junctional puncta that colocalise with the other core proteins.

To establish if Fz-EYFP junctional puncta are persistent over time, 27hr pupal wings were imaged at 5min intervals for one hour and 50min, using a pixel size of 139nm and imaging settings that avoided excessive bleaching of the sample and tissue damage (see Materials and Methods). Any time-lapse series that lost more than 25% of the initial fluorescent signal during the lifetime of the experiment were discarded. Fz-EYFP junctional puncta were found to be persistent, and retain a similar localisation over the time course of the experiment (**Figure 3.1**).

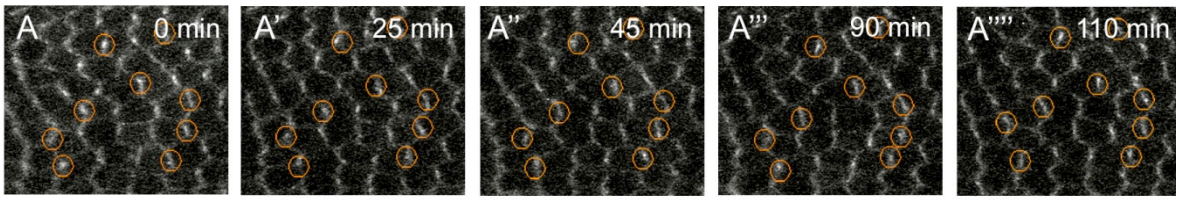

Figure 3.1: Puncta are persistent over time

(A-A'''')Time-lapse images taken between 27-29hr of pupal wing development. Several representative examples of puncta are indicated (circled in orange).

A fraction of Fz is stably localised into discrete junctional domains

FRAP analysis was conducted on pupal wings cells expressing *Act-Fz-EYFP*, using the FRAP method described in chapter 2 and in the Materials and Methods. The stability of junctional puncta and the cell junctions surrounding puncta were analysed by selecting regions at the level of the apical-lateral junctions, located on the proximal-distal junctions (**Figure 3.2A-A'''**). These regions were either enriched for large puncta with a high fluorescence signal referred to as "bright regions" or, regions of an equivalent size and also located on the proximal-distal junctions but characterized as having half as much fluorescence as the bright regions, and not

containing large puncta are referred to as “less-bright regions” (**Figure 3.2A**). However, the less-bright regions may contain some small puncta that are below the limit of resolution. The lateral or anterior-posterior junctional regions, orientated along the proximal-distal axis, which have no large puncta, were also analysed, and typically contain less fluorescence than the proximal-distal junctions (**Figure 3.2A**).

For FRAP analysis, damage to the cells and excess bleaching of the fluorescent sample must be kept to a minimum. However, at the same time the images must be bright enough and at a high enough resolution, to distinguish between bright and less-bright regions at the cell junctions. Therefore pupal wing images were collected with a scan size of 512x512 pixels using a pixel size of 139nm (**Figure 3.2A**, see Materials and Methods), so reducing the image scanning time and the amount of acquisition bleaching. Nyquist theorem states that the pixel size should be half that of the resolution of the microscope, in this case the microscope maximum theoretical resolution is 200nm so the pixel size should be 100nm, to ensure that there is at least 2x oversampling. Although the pixel size used in these FRAP experiments was 139nm it is close to the Nyquist limit, and increasing the number of pixels in the image to 2048x2048 and thereby reducing the pixel size to 34.75nm, but keeping the pixel dwell time the same, only marginally improved the image resolution, but greatly increased the amount of bleaching and the time it took to image each time point (**Figure 3.2A'**). Therefore images were taken at 512x512 pixels to minimise acquisition bleaching and to image faster.

For pupal wing FRAP, the bleach region size was fixed at 2μm^2 (11x14 pixels), which equates to 2.5 times the diameter of a typical punctum of approximately 600nm in diameter. A region of this size would ensure a whole punctum could be bleached and then tracked over time to compensate for sample movement occurring between taking initial prebleach images and the post bleach phase. This sized region, would also avoid bleaching too much of the area surrounding the selected punctum (**Figure 3.2A** green circled region), or too large a fraction of the cellular pool of Fz in the cell.

FRAP analysis of Fz-EGFP in 28hr pupal wings showed that Fz-EYFP has a stable fraction of protein at the junctions, as the fluorescence at the junctions does not recover to 100% during the lifetime of the experiment (**Figure 3.2B-C**). Interestingly in the less-bright junctional regions 53% of the fluorescence recovers during the experiment suggesting that 47% of the protein is in a stable fraction, as the bleached protein was not exchanged for fluorescing protein during the experiment (**Figure 3.2B**, black line). Furthermore, in the bright regions Fz-EYFP recovers to 26%

therefore the size of the stable fraction in the bright regions is 74%, which is larger compared to the 47% stable fraction of the less-bright regions (**Figure 3.2B**, green line). Interestingly, FRAP analysis of anterior-posterior regions, showed that the stable fraction was further reduced (**Figure3.2C**).

Most of the bright regions appears to be associated with the punctum, as there is almost no Fz protein located in the cytoplasm on either sides of the junction (**Figure 3.2A-A'**). In addition, as in the bright bleached regions, most of the fluorescence and therefore the Fz-EYFP protein, appears to be in the punctum, this allows us to infer that the size of the stable fraction in the bleach region is a close approximation to the size of the stable fraction in a punctum. Therefore these results suggest that not only are the puncta persistent entities, the junctional puncta also contain a higher proportion of stable Fz-EYFP compared to surrounding interpuncta regions. This suggests that the persistence of puncta entities is due to their containing a large stable fraction of protein.

Excess Fz at the junctions is stabilised into puncta

To investigate the effect of expressing Fz-EYFP protein in different amounts and for different times during development, Act-Fz-EYFP expression was induced using Ubx-FLP by recombining the FRT sequences flanking a *polyA* STOP cassette, in *Act-FRT-polyA-FRT-Fz-EYFP*, to enable expression of Act-Fz-EYFP from larval stages, when the *Ultrabithorax* (*Ubx*) promoter is active, instead of throughout development. Although the levels of Fz protein when measured in the pupal wing remained similar when Fz-EYFP is expressed from only larval stages or when expressed throughout development as shown by western blot (Strutt et al., 2011). FRAP experiments show that the stable fraction of Fz in bright regions is not sensitive to the timing or the level of Fz-EYFP expression, and the stable fraction of Fz-EYFP is also not affected by the absence of endogenous Fz (**Figure 3.2B**, **D-E**, green line). The similarity of levels of endogenous and EYFP tagged Fz protein when Fz-EYFP is expressed throughout development and when Fz-EYFP is only expressed at larval stages, is likely to be due to regulation of the amount of Fz protein at a post transcriptional level, since the amounts of endogenous and tagged protein are both affected, or by restricting the amount of Fz that reaches the junctions. Therefore, the levels of Fz protein are similar to that of wild-type and the tagged Fz-EYFP is probably reflecting the normal behaviour of endogenous Fz when in complexes at the junctions.

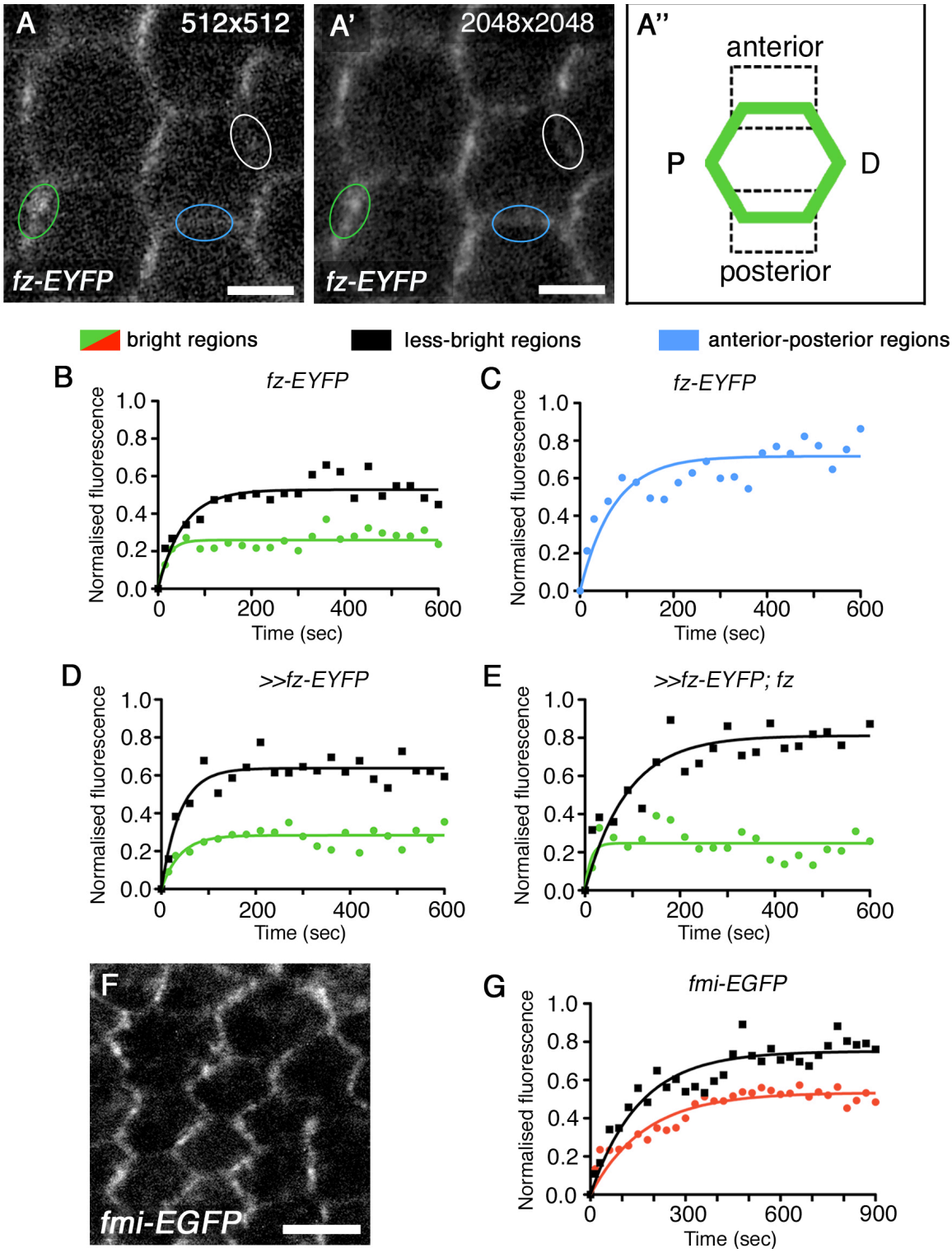

Figure 3.2: Increased expression of *ActP-fz-EYFP* in pupal wing cells results in an increase in the stable fraction of proteins at the junctions when compared using FRAP analysis

(Figure legend on next page)

Figure 3.2: Increased expression of ActP-fz-EYFP in pupal wing cells results in an increase in the stable fraction of proteins at the junctions when compared using FRAP analysis

(A-A') Live wings expressing *ActP-fz-EYFP/+* at 28hr APF. Images were taken either using (A) 512x512 pixels or (A') 2048x2048 pixels, using the same scan rate. The blue oval indicates an anterior-posterior (lateral) region, the green oval indicates a "bright" region and the black line indicates the "less bright regions". Scale bars in A-A' are 3.5μm (A'') A cartoon of the orientation of cell junctions in a wing, junctions depicted in green are marked with either with: P = proximal, D = distal, and the anterior and posterior junctions are marked with dotted lines. (B) FRAP analysis of *ActP-fz-EYFP/+*, of regions localised to the proximal-distal cell junctions, either bright regions containing mainly puncta (green line) or regions containing reduced amount of fluorescence (black line); (C) FRAP analysis of *ActP-fz-EYFP/+*, in anterior-posterior junctional regions (blue line); (D) FRAP analysis of *Ubx-FLP; ActP-FRT-polyA-FRT-fz-EYFP/+*; (E) FRAP analysis of *Ubx-FLP; ActP-FRT-polyA-FRT-fz-EYFP/+;fz^{P21}*. The stable fraction of the less-bright regions (black lines) decreases when compared to (B) *ActP-fz-EYFP/+*, when either *ActP-fz-EYFP/+* expression is delayed until pupal stages (D, *Ubx-FLP; ActP-FRT-polyA-FRT-fz-EYFP/+* P≤0.0001***) or if the dosage of *fz* is reduced (E, *Ubx-FLP; ActP-FRT-polyA-FRT-fz-EYFP/+;fz^{P21}* P≤0.0001***). When comparing (D) *Ubx-FLP; ActP-FRT-polyA-FRT-fz-EYFP/+* to (E) *Ubx-FLP; ActP-FRT-polyA-FRT-fz-EYFP/+;fz^{P21}*, comparing less-bright regions P=0.05*. (F) Live wings expressing *Arm-fmi-EGFP/+* at 28hr APF. Scale bar in F is 7μm. (G) FRAP analysis of *Arm-fmi-EGFP/+* in proximal-distal regions of the membranes, either on bright regions (red line) or less-bright regions (black line).

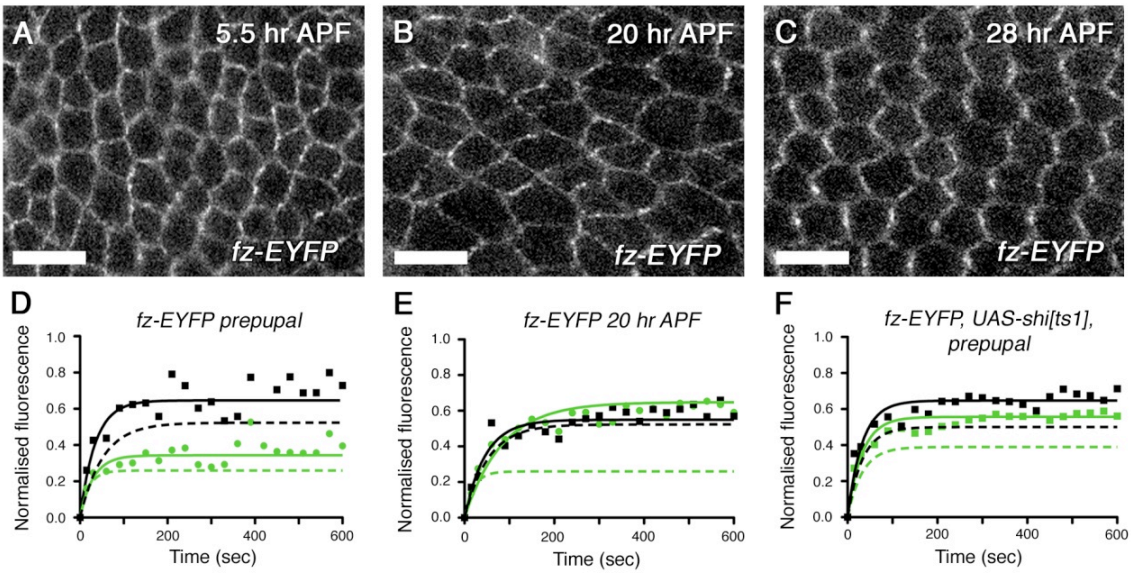

Figure 3.3: The size of the Frizzled stable fraction depends on endocytosis and the degree of cellular asymmetry

(A-C) Live wings expressing *ActP-fz-EYFP/+* in (A) prepupal wings (5.5hr), (B) at 20 hr APF and (C) at 28hr APF. Scale bars 7μm. (D) FRAP analysis of *ActP-fz-EYFP/+* in (D) prepupal wings and (E) 20hr APF wings. The dotted black and green lines are 28hr *ActP-fz-EYFP/+* wing data shown for comparison (compared to 4.2B). Comparison between the 28hr data and then prepupal and 20hr APF pupal wings show that the stable fraction of the bright regions is significantly different in each of the three time points: prepupal (5.5hr) and 20hr P≤0.0001***; 20hr and 28hr P≤0.0001***; 28hr and prepupal wings P≤0.0001***. Whereas the stable fraction of the less-bright regions is similar: prepupal (5.5hr) and 20hr P=0.1438 NS; 20hr and 28hr P=0.6919 NS; 28hr and prepupal wings P=0.0456*. (F) FRAP analysis of *ActP-fz-EYFP/ptc-GAL4, UAS-shi^{ts1}* in prepupal wings, larvae were aged at 19^{o}C before the prepupae were shifted to 30^{o}C for 30min prior to FRAP imaging. Control regions are taken from wing tissue outside of the *ptc-GAL4* domain in the same wings and are shown on the graph as dotted lines. The unstable fractions for both the bright and less-bright regions are significantly increased in the mutant tissue compared to the wild-type (P≤0.0001***).

However, when Fz is only expressed from larval stages, FRAP experiments show that the less-bright regions have a smaller stable fraction compared to Fz-EYFP expressed throughout development (**Figure 3.2D** black line compared to **Figure 3.2B** black line). If the endogenous Fz protein is also removed and Fz-EYFP is expressed from larval stages, the less-bright regions show a further reduction in the amount of stabilised Fz-EYFP (compared **Figure 3.2E** to **Figure 3.2B**). These results suggest that additional Fz protein localises at the junctions and forms additional Fz containing complexes, which stabilise into puncta too small to see, increasing the stable fraction of the less-bright regions.

To verify that the larger stable fraction in puncta is not just limited to Fz-EYFP, another core planar polarity protein was examined using FRAP. Fmi-EGFP expressed under the *armadillo* promoter also localises into puncta at the junctions (**Figure 3.2F**), and there is also a larger stable fraction of Fmi protein when localised to bright regions compared to less-bright regions (**Figure 3.2G**).

The stable fraction of Fz in puncta is reduced in size at developmental stages when planar polarity protein asymmetry is absent

To determine if the proportion of stable Fz protein within puncta varies over developmental time, I chose another two time points to FRAP in addition to the 28hr time point, the prepupal wing at 5.5hr and pupal wings at 20hr. In wing cells at 20hr there is significant junctional remodelling occurring, whereas at 5.5hr junctional remodelling is modest and just associated with cell division. Although in the cultured 5.5hr APF prepupal wings, the core planar polarity proteins show asymmetric localisation, it is not as profound as the asymmetry seen in the 28hr pupal wings although the large Fz puncta are present at the junctions (**Figure 3.3A**). In contrast, the 20hr pupal wings show symmetric Fz junctional localisation (Strutt et al., 2011). This suggests that the degree of asymmetry is reduced when cells are undergoing junctional remodelling and/or cell division.

FRAP of the Fz in bright regions in 5.5hr prepupal wings was found to have a large stable fraction (**Figure 3.3D** green line). This large stable fraction in the bright regions at 5.5hr prepupal wings was reduced in 20h pupal wings (**Figure 3.3D-E**), although Fz-EYFP still has a sizeable stable fraction, as the fluorescent recovery does not reach 100% during the lifetime of the experiment. However, the stable fraction of the bright regions in both the 5.5hr and 20hr was reduced compared to the 28hr time point (Compare the dotted and full lines in **Figure 3.3D** and **3.3E**).

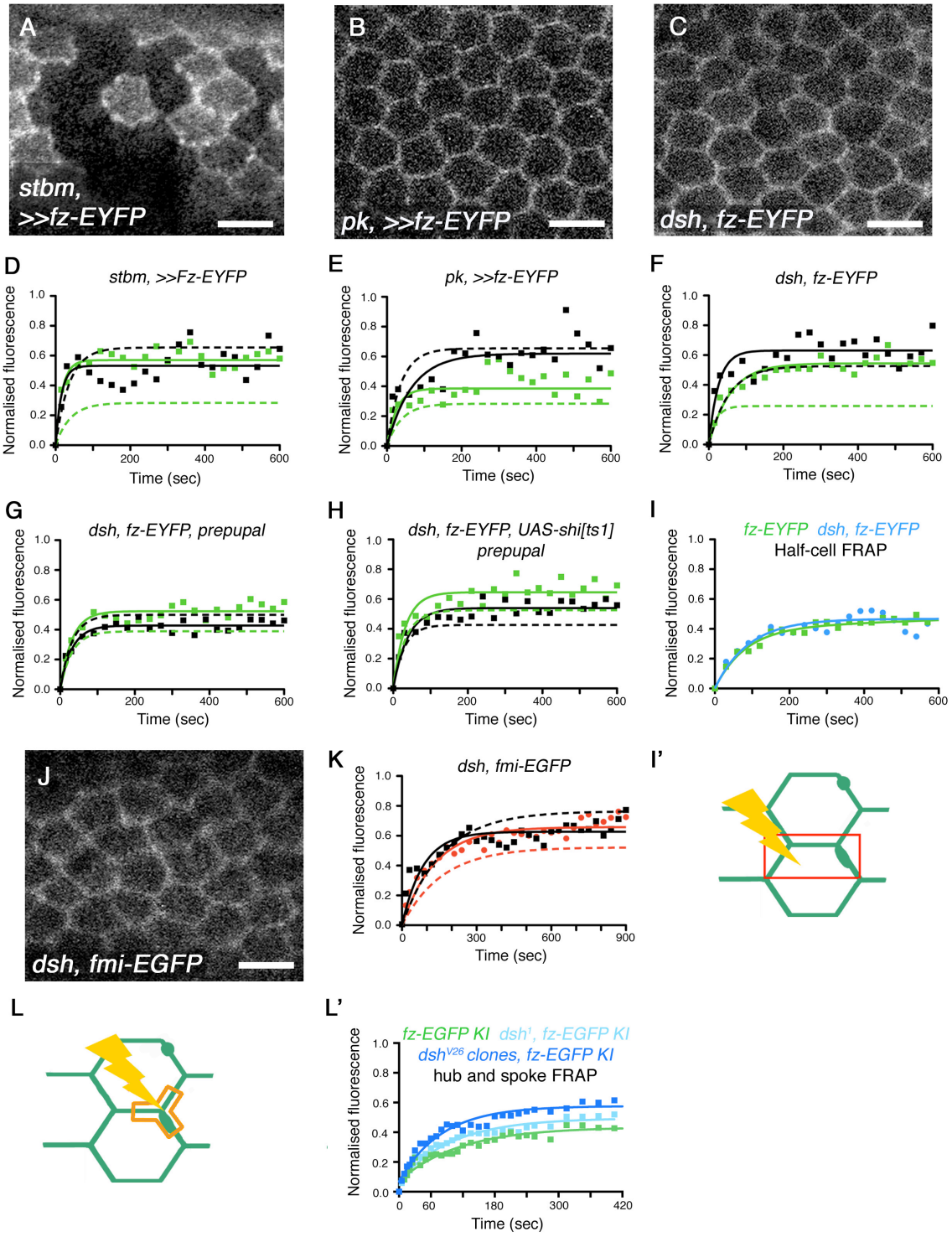

Figure 3.4: The cytoplasmic core polarity proteins are required for the increased stable fraction of Frizzled and Flamingo in junctions

(A) Image of *Ubx-FLP; ActP-FRT-polyA-FRT-fz-EYFP*, $stbm^{6}/stbm^{6}$. (B) *Ubx-FLP; ActP-FRT-polyA-FRT-fz-EYFP*, $pk^{pksple13}/pk^{pksple13}$. *(C)* dsh^{1}*; ActP-fz- EYFP/+* (D-F) FRAP analysis on live wings on bright (green) or less-bright (black) regions, (D-E) show dotted lines indicating 28hr wing data for *Ubx-FLP; ActP-FRT-polyA-FRT-fz-EYFP/+*; (F) dotted lines of 28hr wing data for *ActP -fz-EYFP/+* (legend is continued on the next page).

(D) FRAP of genotype *Ubx-FLP; ActP-FRT-polyA-FRT-fz-EYFP*, $stbm^{6}/stbm^{6}$, (puncta compared to 28h puncta in a wild-type background, see Figure 3.2D, P≤0.0001***). (E) FRAP of genotype *Ubx-FLP; ActP-FRT-polyA-FRT-fz-EYFP,* $pk^{pksple13}/pk^{pksple13}$, (puncta compared to 28h puncta in a wild-type background, see Figure 3.2D, P=0.0017*); (F) FRAP of genotype dsh^{1}*; ActP-fz- EYFP/+*, (Compare dsh^{1}*;* Fz-EYFP/+ in puncta compared to 28h puncta in a wild-type background, see Figure 3.2B, P≤0.0001***); (D-F) Comparing interpuncta in wild-type and mutant backgrounds, see Figure 3.2D to compare interpuncta in wild-type to: $stbm^{6}$ P=0.0458 NS, $pk^{pksple13}$ P=0.2675 NS and see Figure 3.2B for comparison between interpuncta regions in wild-type and dsh^{1} backgrounds P=0.6942 NS). (G-H) FRAP analysis of prepupal wings dsh^{1}*; ActP-fz-EYFP/ptc-GAL4; UAS-*shi^{ts1}/+. (G) FRAP on tissue outside of the *ptc-GAL4* domain in dsh^{1}*; ActP-fz-EYFP/ptc-GAL4; UAS-*shi^{ts1}/+ prepupal wings compared to FRAP on a region outside the *ptc-GAL4* domain in prepupal *ActP-fz-EYFP/ptc-GAL4; UAS-*shi^{ts1}/+ wings raised at the same conditions, dotted lines shown for comparison (see dotted lines on Figure 3.3F), P≤0.0001. (H) FRAP analysis on dsh^{1}*; ActP-fz-EYFP/ptc-GAL4; UAS-*shi^{ts1}/+ tissue in the *ptc-GAL4* domain; dotted lines indicate data for dsh^{1}*; ActP-fz-EYFP/ptc-GAL4; UAS-*shi^{ts1}/+ tissue in same wings for comparison (see solid lines in G). Note that in the dsh^{1}*; ActP-fz-EYFP/ptc-GAL4; UAS-*shi^{ts1}/+ bright regions have a smaller stable fraction than less-bright regions; this suggests that the remaining bright regions are not clusters of stable protein P≤0.0001. (I-I') Fluorescence recovery after half of a cell has been bleached (marked as the red box in I') (I') Cartoon of the junctions of two cells from above (green), the red box marks the half-cell bleach region. (I) FRAP of *ActP-fz-EYFP/+* (green) or dsh^{1}*; ActP-fz-EYFP/+* (blue) wings. Note that the stable fraction for *ActP-fz-EYFP/+* (0.46) is not significantly different from the stable fraction of dsh^{1}*; ActP-fz-EYFP/+* (0.47; p=0.44 NS). (J) Image of dsh^{1}*; ArmP-fmi-EGFP/+* (K) FRAP analysis of dsh^{1}*; ArmP-fmi-EGFP/+*. Dotted lines indicate 28hr data for *ArmP-fmi-EGFP/+* (compare to 4.2G). The stable fraction of Fmi-EGFP in the bright (red) and less-bright regions (black) show that there is a significant different in the wild-type compared to dsh^{1} mutant wings (P≤0.0001***). (L') FRAP of 28hr pupal wings of *fz-EGFP KI)/+* endogenously expressed (EGFP coding region knocked-in (KI) to the endogenous locus into the endogenous locus) (green), dsh^{1}*; fz-EGFP KI /+* (pale blue) and dsh^{v26}*FRT18; Ubx-FLP; fz-EGFP KI /+* clones (dark blue). Note that the stable fraction for *fz-EGFP KI/+* (0.40) is significantly different from the stable fraction of dsh^{1}*; ActP-fz-EYFP/+* (0.47; P=0.0012*), and from dsh^{v26}*FRT18; Ubx-FLP; fz-EGFP KI /+* (0.56, P≤0.0001***). (L) Cartoon of the junctions of two cells from above (green), the orange shape marks the 'hub and spoke' bleach region. Scale bars are 7μm.

Despite the changes in the stability of the bright regions the differences are not so remarkable in the less-bright regions (**Figure 3.3D-E**), signifying that the less-bright regions are not susceptible to alterations in the degree of core polarity protein asymmetry or the developmental stage. Interestingly, at 20hr, the size of the stable fractions of the bright and less-bright regions, were not significantly different (**Figure 3.3E**). So although at 20hr bright regions are present, these regions, unlike the bright regions in 5.5hr and 28hr, are no longer places in the junctions that contain proportionally more stable Fz. This suggests a correlation between the degree of asymmetry of the core proteins and the size of the stable fraction in bright regions.

Endocytosis is involved in removing unstable Fz protein from the junctions but is not required for Fz recovery

Removal of Fz from the junctions requires endocytosis (Strutt and Strutt, 2008). The Fz that is removed is likely to be excess unstable protein, not in complexes. If so, then in the absence/reduction of crucial endocytic components there might be an increase in unstable Fz at the junctions, and FRAP analysis would show an increase in the unstable fraction of junctional Fz. To test this, endocytosis was reduced by overexpressing a temperature sensitive form of *shibire* (*shi*), the *Drosophila* homology of dynamin. FRAP of Fz-EYFP in a *UAS-shi* background at the restrictive temperature of 30°C for 30min prior to imaging, showed an increase in Fz-EYFP recovery and consequently a larger unstable fraction in both the bright and less-bright regions (**Figure 3.3F**).

Although inhibiting dynamin in this manner may only partially block endocytosis, the increase in the unstable fraction of Fz indicates that endocytosis is required for the removal of unstable Fz from the junctions. In addition inhibiting dynamin is also likely to affect secretion/exocytosis events, so the loss of dynamin may also be partially blocking delivery of protein to the junctions. However, as recovery of Fz is occurring at these junctions, this suggests that the Fz protein is able to exchange bleached protein for fluorescing protein in the ROI. This recovery is likely to be from lateral diffusion of protein already in nearby junctions, and not from new synthesis, as discussed in chapter 2.

The increased stable fraction of Fz in bright regions is lost when the transmembrane protein Stbm is absent

In pupal wing cells lacking *stbm*, Fz is no longer asymmetric (Strutt, 2001b) and interestingly distinct junctional puncta are no longer evident, although membrane regions of varying brightness still persist (**Figure 3.4A**).

FRAP analysis of the brightest regions and the dimmest regions, show that they no longer show a difference in the stable fractions of Fz (**Figure 3.4D**). As brighter regions, no longer correlate to regions of increased stability, this suggests that Stbm appears to be required to concentrate the stable fraction of Fz into puncta.

Cytoplasmic planar polarity proteins are required for clustering of Fz in puncta

In the absence of the cytoplasmic core proteins (Dsh, Dgo or Pk) Fz localisation is also disrupted, and although Fz is still present at the junctions (Strutt, 2001b) its asymmetry is lost (**Figure 4.4B and C** and Strutt *et al.*, 2011), as are the larger puncta containing Fz (**Figure 3.4B and C**). Instead, Fz is localised to all junctions including the anterior-posterior ones, which normally contain a relatively small proportion of Fz compared to proximal-distal junctions (**Figure 3.3C** compared to **Figure 3.4B and C**).

This may indicate that the cytoplasmic factors could be required for the increase in the stable fraction of Fz at junctions, as in the absence of these proteins there is no longer a large stable fraction of Fz. Alternatively, Fz stability may not be affected in the absence of the cytoplasmic factors, instead, the clustering of Fz-containing complexes into puncta may have been lost, therefore explaining why the large puncta are absent. Therefore, the cytoplasmic factors may be required for one or both of these functions.

To investigate the effect of the cytoplasmic core proteins on Fz stability, FRAP analysis was performed on Fz-EYFP at 28hr in *pk* and *dsh* mutant backgrounds. Although only small puncta are present, the brightest ones were picked as the bright regions and less-bright regions from the proximal-distal junctions. FRAP of Fz-EYFP in the *pk* mutant showed a decrease of the stable fraction of Fz-EYFP in bright regions compared to Fz-EYFP in a wild-type background (compare **Figure 3.2B** and **3.4E**), although the stable fraction was still larger than that of the less-bright regions (**Figure 3.4E**). In the dsh^{1} mutant, which shows a strong loss of planar polarity (Perrimon and Mahowald, 1987; Strutt and Strutt, 2007), the Fz stable fraction of the bright regions was further decreased (**Figure 3.4F**). A similar result was also seen in dsh^{1} wings at 5.5h, where the stable fraction of the Fz-EYFP bright regions was not significantly different from the less-bright regions (**Figure 3.4G**). FRAP analysis of Fmi-EGFP in a dsh^{1} mutant background (**Figure 3.4J**) also showed that the stable fraction of Fmi-EGFP in bright regions decreased, so that the bright and less-bright regions had a stable fraction of a similar size (**Figure 3.4K**).

The smaller stable fraction of Fz and Fmi in bright regions in the absence of the core cytoplasmic proteins could be explained in two possible ways. One is that stable material has become unstable, allowing the material to be redistributed around the cell junctions via endocytosis or diffusion within the junctions. The other is that the amount of stable material does not alter in the cytoplasmic mutants but the material is no longer clustered in puncta.

As only a small region of the junctions was measured in the bright region FRAP, a dispersal of the stable fraction would reduce the size of the stable fraction present in the bright regions, unlike in the wild type background where the bright regions mostly contain puncta. A dispersal of the complexes could be achieved through either no longer clustering the complexes together, or by preventing complexes being tethered within the junctions, perhaps by altering cytoskeletal elements. Clustering of complexes could also cause a stable fraction to emerge by creating a complex that is too large to be endocytosed or diffuse in the membrane. However, the stable fraction could be independent of clustering and form by individual complexes being tethered to the cytoskeleton.

To test whether an increase in endocytosis was primarily responsible for the decrease in size of the stable fraction of Fz in bright regions, FRAP of Fz-EYFP was carried out while expressing *UAS-shi* in a *dsh* mutant background. Unsurprisingly, a slight increase in the unstable fraction of Fz-EYFP was seen in the *UAS-shi dsh*^{1} background compared with *dsh*^{1} alone (**Figure 3.4H**), although a similar increase was seen with *UAS-shi* alone (**Figure 3.3F**). This suggests that loss of endocytosis and the removal of *dsh* together has an additive rather than a synergistic effect on the stable/unstable proportion of Fz-EYFP that is in the junctions. This supports the view that Dsh does not normally increase the stable fraction of Fz by blocking endocytosis of Fz complexes from the junctions. Therefore the loss of Dsh is probably altering the mobility of the stable fraction within the junctions through either preventing complexes being tethered in the junctions or by reducing clustering of the complexes into a stable fraction.

To test directly whether the stable fraction of Fz is still present and just dispersed in the cytoplasmic component mutants, the junctions of half a cell were bleached along the horizontal axis (**Figure 3.4I'**), and the recovery of the whole region was measured. In this case, if the role of the cytoplasmic factors were to cluster an already stable fraction, then we would expect that the stable fraction of Fz would be similar in wild-type and mutant backgrounds, which was observed (**Figure 3.4I**).

The model would suggest that the stable fraction of Fz seen in wild-type is retained in the cytoplasmic mutant backgrounds, but the stable fraction is now dispersed around the cell edges. This result suggested that Dsh and possibly the other cytoplasmic factors are required for clustering Fz containing complexes together in discrete membrane subdomains but are not required for the stability of those complexes.

However, a caveat to the half-cell experiment, is that the larger ROI used to bleach is likely to be depleting the overall cellular pool of Fz. This would then reduce the amount of recovery observed, as less protein is available to exchange with the bleached protein. This could also therefore mask any differences that may occur between the wild-type and mutants, leading to the conclusion that there was no change in the stable fraction of Fz. To try to avoid bleaching the cellular pool of protein but still quantify the stable fraction of protein in half of the cell junctions, the ROI region was adjusted, so that half of the cell's junctions were bleached but the cytoplasmic area was avoided (**Figure 3.L**). Indeed, when using this ROI the stable fraction of Fz in the *dsh* mutant background was decreased compared to Fz in a wild-type background (**Figure 3.L'**), indicating that Dsh is required at least in part for the stability of Fz at the junctions, but this still may occur by clustering complexes into large puncta causing mobile complexes to become so big they are immobile, and thereby increasing the stable fraction of Fz.

Discussion

Puncta are persistent over time

Fixed imaging of the pupal wing has previously shown that the core protein Fz is asymmetrically localised to proximal-distal junctions. The development of live imaging in this work has shown that puncta are not a fixation artefact or due to cross linking of antibodies at the junctions, and are persistent over time (Chapter 3 Aigouy *et al.*, 2010; Strutt *et al.*, 2011).

A fraction of Fz is stably localised into puncta

FRAP analysis of Fz-EYFP showed that the ‘bright regions’ have a larger stable fraction of protein, compared to the ‘less-bright regions'. Therefore, if we take the behaviour of bright regions as a proxy for the behaviour of puncta, as most of the fluorescence in the bright regions appears to be in the puncta, then puncta are sites where the stable fraction of Fz is concentrated. Moreover, the ‘less-bright regions' do not fully recover to 100% of the pre-bleach fluorescence, indicating that those regions also contain a sizable stable fraction. One explanation of this is that the less-bright regions could also contain puncta, but they are smaller than the limit of resolution, and therefore cannot be distinguished. This idea is further supported by FRAP of the anterior-posterior membranes where less Fz protein is localised and the stable fraction of Fz-EYFP is further decreased. Therefore, puncta are locations where core planar polarity proteins are recruited to form asymmetric complexes spanning the junctions, and these complexes are clustered into these stable micro domains.

FRAP analysis used here shows that both Fz and Fmi when in puncta are in a larger stable fraction than junctional regions outside the large puncta. These results agree with other data using antibody internalisation assays to measure the rate of endocytosis of a particular protein (Strutt et al., 2011). In that assay Fmi in large puncta persists at the junctions, but the surrounding junctional protein is internalised during the experiment, suggesting that Fmi is indeed more stable in puncta (Strutt et al., 2011).

Interestingly, increasing the amount of Fz expressed in the cell can increase the stable fraction of Fz at the junctions in the less-bright regions, therefore showing that excess Fz present at the junctions can be incorporated into stable complexes.

Endocytosis of Fz is required for the removal of Fz at the junctions

Reducing membrane recycling using a temperature sensitive *shibire* mutant decreased the size of the stable fraction as measured with FRAP. This suggests that excess unstable Fz is removed through endocytosis. Since fluorescence recovery occurs when dynamin activity is reduced this suggests that Fz protein recovery could be from local lateral movement of protein within the junctions, as well as some residual endocytic protein transport, but the short time frame of the experiment and FRAP analysis (see chapter 2) suggests that recovery is not from new protein synthesis.

A correlation between the degree of asymmetry and the size of the Fz stable fraction in junctions

Further FRAP experiments showed that the proportion of stable Fz protein in puncta varies over developmental time. At 28hr, the degree of Fz asymmetry is at its strongest and puncta have a larger stable fraction. However, at an earlier time point of 5.5hr, core proteins show moderate asymmetry and Fz in puncta show a corresponding drop in the size of the stable fraction. At an intermediate time-point of 20hr, there is low asymmetry of the core proteins and a low stable fraction of Fz compared to 5.5hr and 28hr. Therefore there is a correlation between the increase of core protein asymmetry and the size of the stable fraction in puncta.

Stbm is required to concentrate the Fz stable fraction into puncta

FRAP experiments described in this chapter show that Stbm is required to increase the size of the stable fraction of Fz at junctions and for the incorporation of Fz into stable junctional puncta. This data is further supported by data from Fmi antibody internalisation assays where the loss of *stbm* results in an increase in the rate of Fmi internalisation from the junctions (Strutt et al., 2011). This suggests that Stbm is also required for stabilising Fmi at the junctions.

This work agrees with a model put forward that suggests that the transmembrane proteins Fz, Fmi and Stbm form an inner ‘core' (Strutt and Strutt, 2008). In that model, Fmi forms a homodimer across the junctions, the recruitment of Fz to the junctions then stabilises the Fmi dimer (Fz-Fmi::Fmi) and then the addition of Stbm further stabilises the complex across the junctions to form a Fz-Fmi::Fmi-Stbm complex (Strutt and Strutt, 2008; Usui et al., 1999). The FRAP results presented here are consistent with this model, where Fz and Fmi have a larger stable fraction when associated with puncta. In addition, the increased protein junctional stability of Fz requires the presence of Stbm as shown by the FRAP analysis and antibody

internalisation assays (Strutt et al., 2011). Therefore, Stbm appears to stabilise individual Fz-Fmi:Fmi-Stbm complexes at the junctions and clusters complexes together.

Cytoplasmic polarity proteins are required for stabilising and clustering of Fz into puncta

Interestingly, the loss of the cytoplasmic planar polarity proteins (Dsh, Pk or Dgo) does not affect the recruitment of Fz, Stbm or Fmi to the junctions (Bastock et al., 2003; Strutt, 2001b; Usui et al., 1999) but does affect their asymmetric localisation and incorporation into larger puncta (Strutt et al., 2011). In addition, both Dsh and Pk are required for the increase in the stable fraction of Fz in bright regions. This suggests that the cytoplasmic factors are required to concentrate the stable fraction of Fz into puncta.

As the larger puncta are absent in the cytoplasmic polarity mutants this suggests that Dsh, Pk and Dgo are required to cluster stable complexes together to form the large puncta. Large puncta are likely to be clusters of symmetric complexes aligned in the junctions. This is based on evidence that the core proteins all colocalise in puncta and the increase in the size of puncta correlates with the degree of asymmetry of the core proteins, suggesting that puncta are sites where the core proteins asymmetrically localise across the junctions and similar orientated complexes locally align together. Therefore in the cytoplasmic mutants a smaller stable fraction of Fz in the bright regions may be due to the dispersal of the stable fraction. Indeed, Fmi antibody internalisation experiments showed that in the absence of the cytoplasmic factors the rate of Fmi internalisation did not increase (Strutt et al., 2011). This suggests that Dsh, Dgo and Pk are not required to increase the stable fraction of Fz in junctions.

To examine if the stable protein fraction of Fz was dispersed around the cell junctions in the cytoplasmic polarity mutants, half of a cell's junctions were bleached avoiding bleaching the cellular pool of Fz using a "hub and spoke" shaped ROI. FRAP of Fz in dsh^{1} and dsh^{V26} mutant backgrounds using this shaped ROI showed that the stable fraction of Fz had decreased. Therefore, the cytoplasmic factor Dsh is required for the increase in the stable fraction of Fz at the junctions, in addition to clustering asymmetric complexes into puncta. This does not explain why in the antibody internalization assays there is no difference in the rate of endocytosis of Fmi in the cytoplasmic mutants. That may be because either the difference in rate between the wild-type and the cytoplasmic mutants is too small to measure in this assay, or that

the loss of Stbm can increase endocytosis where as the loss of Dsh causes changes to mobility of the complexes by diffusion but Fmi is protected by an unknown mechanism.

The involvement of cytoplasmic proteins in increasing the size of the stable fraction of Fz is further supported by the observation that over-expression of the cytoplasmic proteins Dsh, Dgo or Pk, leads to an increase of the other core planar polarity proteins at the junctions and the appearance of the larger puncta (Aigouy et al., 2010; Bastock et al., 2003; Feiguin et al., 2001; Tree et al., 2002b).

A requirement for puncta in planar polarity establishment

Cellular asymmetry of the core proteins is essential for planar polarity. As there is a correlation between core protein asymmetry and puncta size this suggests that the formation of puncta are necessary for planar polarity.

Clustering of similar orientated complexes by the core planar polarity cytoplasmic proteins would require interactions between the complexes. Cytoplasmic proteins could either promote inhibitory or negative interactions between differently orientated complexes or promote positive interactions between similarly orientated complexes (Das et al., 2004; Jenny et al., 2003; Jenny et al., 2005; Tree et al., 2002b).

How asymmetric complexes are clustered into puncta is currently unknown. Although there are several possible explanations, the simplest model is that the asymmetric complexes of the same orientation are grouped together by the cytoplasmic proteins reducing lateral diffusion of the complexes in the membrane. As we do not observe Fz containing complexes becoming more stable in the absence of cytoplasmic factors, it is unlikely that the cytoplasmic factors increase the diffusion and endocytosis of "wrongly orientated" complexes to shuttle them to other regions in the membrane.

Interestingly, as only the core planar polarity transmembrane proteins Fmi, Fz and Stbm are required to establish asymmetric complexes, this suggests the formation or stabilisation of these complexes do not require them to be clustered together. However, Stbm may be required for clustering as well, since there is a loss of puncta in *stbm* mutants.

Interestingly the cytoplasmic protein Dsh is required for increasing the size of the stable fraction as well as clustering the complexes. The cytoplasmic proteins are

required for intracellular establishment of visible asymmetry but not cell-cell signalling. Therefore the role of the cytoplasmic proteins in establishing visible asymmetry was thought to occur by interactions between similar or oppositely orientated junctional complexes, through either a mixture of positive and negative interactions or only negative interactions (Amonlirdviman *et al.*, 2005; Klein and Mlodzik, 2005; Le Garrec *et al.*, 2006). Tree *et. al.* (2002) showed that the cytoplasmic proteins are involved in negative interactions as *in vitro,* Pk is involved in inhibiting Dsh recruitment to the membrane via the DEP domain of Dsh and the PET domain of Pk, therefore setting up a negative feedback loop, possibly inhibiting the localisation of Dsh at the proximal cell junctions (Tree *et al.*, 2002b).

However, the FRAP data presented here suggests that the cytoplasmic proteins (Dsh and Pk) are involved in causing net positive interactions during the establishment of complex asymmetry, which was surprising. Although this does not rule out the possibility that both negative and positive interactions could be occurring, but the net result is positive ensuing like complexes cluster into puncta. Therefore the cytoplasmic core proteins are most likely required for the stability of the complexes, and this possibly involves clustering complexes together through net positive interactions.

Local self-organisation of the complexes could occur through positive interactions that would lead to a local increase in complex asymmetry. Although only local interactions between complexes would not result in cellular asymmetry of the core proteins, for that to occur an intracellular non-local signal would be required to ensure complexes of one orientation were located at the proximal end of the cell and complexes of the other orientation were at the distal end of the cell. This signal could be either in the form of a gradient across the cell, which complexes would align to, or interactions between complexes that resulted in complexes being trafficked to a ‘correct’ junctional location (Burak and Shraiman, 2009; Fischer et al., 2013). These interactions that resulted in a non-local response could feasibly self organise the complexes, although it would not be able to globally align the cells across a tissue. However, it could increase in the asymmetry of complexes in neighbouring cells. As complexes of one orientation would inhibit the formation of similar complexes forming along the neighbouring cells junctions, providing a form of long-range subcellular inhibition (Gierer and Meinhardt, 1972; Turing, 1952). Clustering of asymmetric complexes of the same orientation into puncta is therefore likely to be part of a feedback mechanism for establishing cellular asymmetry and propagating it between cells.

Chapter 4

The core planar polarity pathway promotes E-cadherin turnover through the regulation of RhoGEF2 in intercalating tracheal cells

Introduction

Core planar polarity proteins have been implicated in establishing planar polarity across groups of cells in a variety of tissues. In vertebrates planar polarisation is required for morphogenesis of three-dimensional tissues to form structures such as the cochlea, neural tube, heart vessel and kidney tubules in mice (Curtin et al., 2003; Descamps et al., 2012; Lienkamp et al., 2012; Montcouquiol et al., 2003; Saburi et al., 2008; Wang et al., 2006a) and for neural tube closure in *Xenopus* (Wallingford and Harland, 2002). However, how the polarised activity of the core proteins interacts with cellular machinery to alter cell behaviour is poorly understood. Therefore this work will try to address how core planar polarity pathway activity is involved in cell rearrangement and put forward a possible model to explain how the core proteins could be increasing junctional turnover and cell rearrangements.

Drosophila was selected as a model to avoid the protein redundancy of the planar polarity proteins observed in vertebrates. Protein redundancy can make genetic analysis difficult as multiple homologs perform the same function, whereas *Drosophila* has only one of each of the six known core proteins making genetic work simpler to interpret. *Drosophila* has been used extensively to study how the core proteins establish and maintain polarity in the plane of the tissue but limited work has been published on how these proteins could be polarising cell rearrangements of a tissue. The best characterised examples of cell rearrangements in *Drosophila* are the extension of the embryonic epidermal germ band and the formation of the embryonic trachea.

Cell rearrangements require polarised junctional remodelling

Cell rearrangement within a tissue is crucial during morphogenesis to form distinct and functional tissues. However, cells must retain contact with neighbouring cells during the reorganisation otherwise tissues would disintegrate. Cell rearrangements are often polarised so that only junctions aligned along one axis are rearranged at a time. Therefore to retain contact to neighbouring cells requires some way of ‘knowing' the orientation of the cell to be able to selectively choose which junctions to remodel and which junctions to stabilise. Polarised rearrangements can explain how the epithelia remodel junctions to allow tissues to elongate or rearrange. Nevertheless it does not explain how the polarisation is set up in the first place.

Polarised junctional cell rearrangements have been hypothesised to occur in a similar way to that of epithelial cells undergoing cell intercalation in the *Drosophila*

embryonic germband. One such example is the formation of the *Drosophila* embryonic trachea (Affolter et al., 2009; Uv et al., 2003). Tracheal cells undergo cell intercalation (Lecuit, 2005; Ribeiro et al., 2004) and could potentially rearrange their junctions in a similar way to that of that of cells in the embryonic germband (Lecuit, 2005).

Cell junctions are extensively remodelled during the formation of the trachea

Interestingly, the core proteins are required for the correct formation of the tracheal tubes and mutants of the core proteins form an elongated dorsal trunk (Chung et al., 2009; Nelson et al., 2012). However, the involvement of the core proteins in trachea formation has not been extensively investigated; therefore the trachea could be seen as a suitable model to look at how planar polarity activity is required during cell intercalation.

The embryonic tracheal system is formed from groups of epithelial cells called placodes. There are 10 placodes located down each side of the embryo, so there are 2 placodes in each of the posterior segments (the thoracic segments 2 and 3 and abdominal segments 1-8), which begin to invaginate at stage 11 of embryogenesis (reviewed in Affolter et al., 2003; Myat, 2005; Uv et al., 2003). Once invaginated, these placode cells do not divide (Samakovlis et al., 1996); but each placode rearranges to form the 6 primary tracheal branches (**Figure 4.1A**).

These branches initially bud out from the placode and then extend through the migration of the branch tip cells (**Figure 4.1A,B**). Filopodial extensions from the tip cells allow them to migrate and extend the buds into branches (Ribeiro et al., 2002; Sato and Kornberg, 2002).

During trachea tube formation the branch buds on the anterior and posterior side of the placode extend laterally along the anterior-posterior axis until they fuse with the neighbouring placode buds to form the dorsal trunk. The other budding branches erupt from the dorsal and ventral side of the placode, extending along the dorsal-ventral axis. The tip cell of each dorsal extension migrates dorsally dragging behind it the rest of the cells within the branch termed 'stalk cells. At this time the stalk cells also rearrange within the branch relative to their neighbours, allowing the branch to extend further until it fuses to the dorsal branches migrating dorsally on the other side of the embryo. The ventral buds of the placode, however, extend ventrally and bifurcate at a more ventral point. These bifurcated branches then extend rearranging the cells within the branch and then fuse with neighbouring ventral branches.

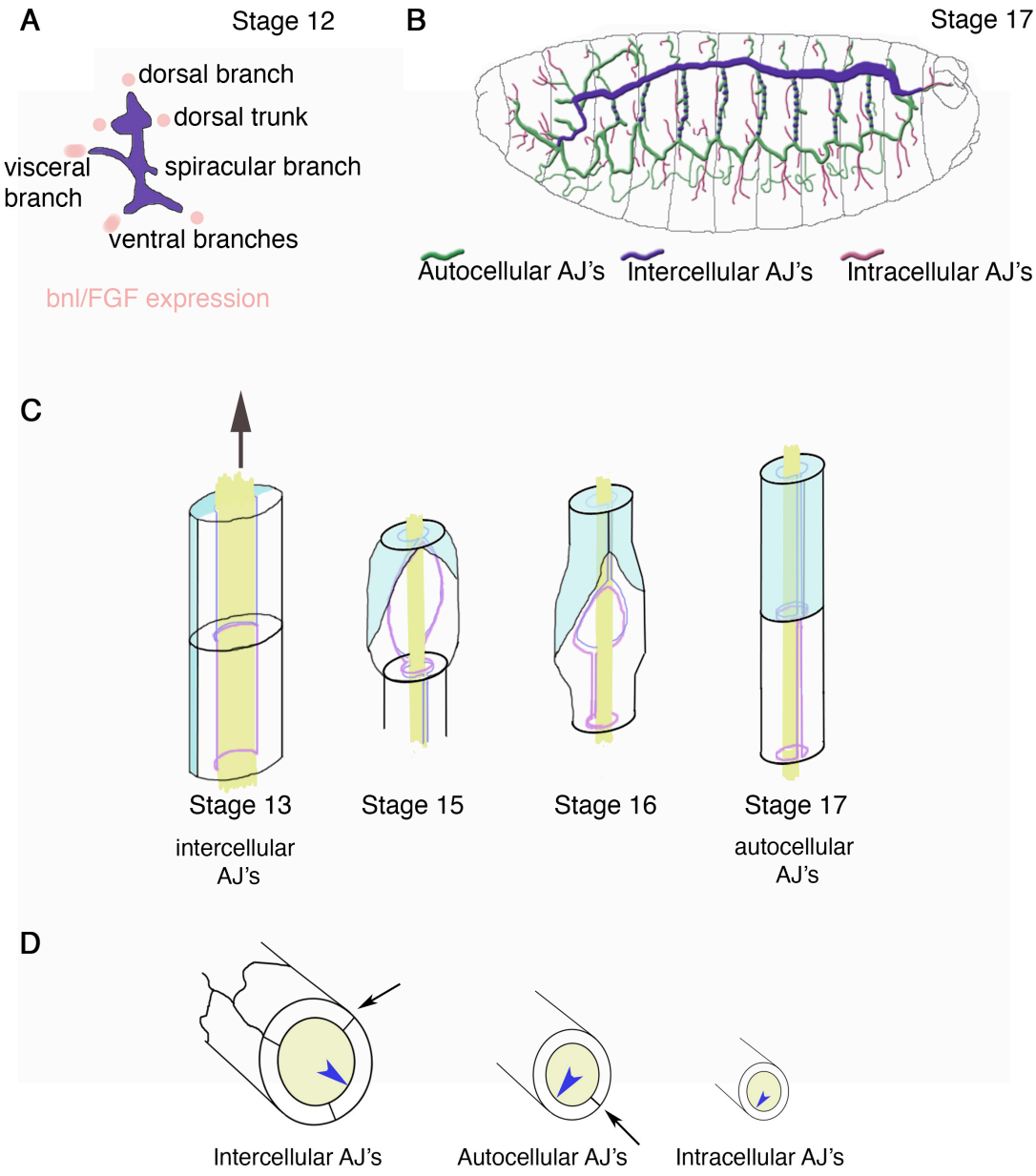

Figure 4.1: The formation of the *Drosophila* embryonic trachea

(A) A stage 12 tracheal placode, names of branches are indicated. Pink regions indicate the expression patches of Branchless (Bnl) ligand expression outside of the tracheal placode. These regions attract the migrating branches (purple) that express the receptor Breathless (btl), which is essential for the formation of the trachea. (adapted from Cabernard *et al.*, 2004). (B) Cartoon of a stage 17 Drosophila embryos labelled for the different types of adherens junctions. Autocellular in green, intercellular in dark purple, and intracellular in pink (Adapted from, Ribeiro et al., 2004; Samakovlis et al., 1996). (C) Progression of tracheal cell intercalation (proposed by, Ribeiro et al., 2004). Cells rearrange from being paired cells wrapped around a lumen (stage 13), to being single cells wrapped around the lumen (stage 17). (D) Cartoon of the three different types of adherens junctions, wrapped around the central lumen. Black arrows indicate the junctions and the blue arrowheads indicate the apical surface of the tube.

Once extended all of these branches form a network of interconnected tubes **(Figure 4.1B**, Cabernard *et al.*, 2004; Ribeiro *et al.*, 2004; Samakovlis *et al.*, 1996).

During the rearrangement of tracheal cells, some branches also modify their cellular adheren's junctions (AJ's). These include the dorsal branches and the lower ventral branches, which rearrange from initial intercellular AJ's to form autocellular AJ's, (**Figure 4.1B,** Caussinus *et al.*, 2008; Chihara *et al.*, 2003; reviewed in, Lubarsky and Krasnow, 2003; Ribeiro *et al.*, 2004; Shindo *et al.*, 2008; Uemura *et al.*, 1996). Initially in the tracheal buds, pairs of neighbouring cells adhere together with intercellular AJ's exhibiting characteristic loops of junction between the cells (**Figure 4.1C,** Ribeiro *et al.*, 2004). AJ's remodelling involves one of a pair of tracheal cells reaching around the central lumen and adhering to itself, thus displacing its neighbour in the pair, which either moves above or below the cell (**Figure 4.1C**, Ribeiro *et al.*, 2004). Disruption of tracheal cell intercalation leads to the retention of the loops of intercellular AJ's linking cells together, however the tubes are still functional (Jazwinska et al., 2003; Ribeiro et al., 2004). All of the tracheal branches are single cell walled tubes that surround a central lumen (**Figure 4.1D**). By larval stages the tracheal system is an open tubular network through which air diffuses into the larval tissues and allows waste respiratory gases to leave (Behr et al., 2007; Tsarouhas et al., 2007; Zhang and Ward, 2009).

Tension is required for cell intercalation

Tracheal cell intercalation is a consequence of increased branch tension (Caussinus et al., 2008; Ribeiro et al., 2002; Samakovlis et al., 1996). The migration of the tip cell increases branch cell tension imposing an extrinsic directional force on the stalk cells (Ribeiro et al., 2002; Samakovlis et al., 1996), cells then try to reduce this tension by remodelling junctions to rearrange cells leading to branch extension. Using cell intercalation to reduce extrinsic applied tension is not unusual and is required for convergent extension in *Xenopus laevis* (Beloussov et al., 2000). Although, in other intercalating tissues for example in *Drosophila* GBE, extrinsic forces do not appear to be essential (Irvine and Wieschaus, 1994).

Applied directional tension along a tracheal branch means cell junctions orthogonal to the direction of tension are under more stress than junctions in line with the axis of tension and may need to be strengthened to ensure branches do not snap. Whereas junctions in line with the direction of tension could remodel to allow cells to intercalate and reducing branch tension.

E-cadherin turnover is essential for cellular rearrangements

The main adhesive force between cells is established at the levels of the AJ's. A complex containing E-cad, β-Cat (Arm) and α-Catenin (α-Cat) is required for cell adhesion and is stabilised at the junctions by interactions with actin filaments (Cavey et al., 2008; Yamada et al., 2005).

The regulation of adhesion complexes is essential to ensure cells maintain adhesion to neighbours while cell intercalation is occurring. The regulation of E-cad turnover is via endocytosis (reviewed in Wirtz-Peitz and Zallen, 2009). Tight regulation of endocytosis is therefore required in tracheal cells during cell intercalation, as a loss of endocytosis leads to a disruption in cell intercalation and retention of intercellular AJ's (Shaye et al., 2008).

RhoA regulates E-cad turnover in the epithelium

In the germ band epithelium E-cad turnover is polarised by activating RhoA leading to local actin polymerisation that clusters junctional E-cad into patches. Clathrin and AP2 are recruited to increase E-cad endocytosis on epithelial anterior-posterior cell junctions (see Levayer et al., 2011).

In the *Drosophila* trachea, E-cad turnover could also be via RhoA and Rac as loss of Rac or overexpression of constitutively active or dominant negative RhoA leads to trachea disintegration (Chihara et al., 2003; Lee and Kolodziej, 2002a). This suggests that RhoA and Rac are important for cell viability and or junctional remodelling in the trachea.

RhoA can be activated by the Guanine exchange factor RhoGEF2 (Barrett et al., 1997; Grosshans et al., 2005; Mulinari et al., 2008; Nikolaidou and Barrett, 2004). Germline clones lacking *RhoGEF2* function exhibit defects in cellular rearrangements including germ band extension and invagination of the ventral furrow (Barrett et al., 1997; Mulinari et al., 2008).

Models of cell intercalation

Previous models of tracheal cell intercalation have depicted tracheal cells pairing up as they migrate in the forming branches. Ribeiro *et al.* (2004) proposed that the alignment of the paired tracheal cells prior to cell intercalation might be required to ensure cells intercalate correctly. It is therefore possible that tracheal cells are being planar polarised at this stage, allowing for specific junctional remodelling along one

cellular axis between paired cells, whilst remaining attached in the other direction to cells above and below the paired cells that are not intercalating (Ribeiro et al., 2004). If cell polarisation is required in the paired cells prior to intercalation, then cells would need to be planar polarised to distinguish between the proximal-distal AJ's of the branch that will be remodelled and the AJ's, around the circumference of the tubes, which need to be maintained during cell intercalation or the branch could break (**Figure 4.1C**).

One pathway, which could polarise cells in the plane of the tissue, is the core planar polarity pathway. Although the core proteins have not been directly implicated in tracheal cell intercalation, the core proteins are present throughout *Drosophila* embryonic development, and are required for specifying tracheal tube length, as loss of the core proteins results in a convoluted dorsal tracheal trunk through an unknown mechanism (Chung et al., 2009; Nelson et al., 2012).

Aims

Proposed mechanisms for cell intercalation in the trachea and in more widely studied convergent extension models indicate that there is a requirement for local polarisation of cells during intercalation. This work therefore sets out to address the potential role for the core planar polarity pathway in cell rearrangement and intercalation during the formation of the embryonic trachea.

Results

The results presented here, show that the core proteins are required for tracheal cell intercalation, through modulating the levels and turnover of the adhesion protein E-cad at the cell junctions. In the trachea, the core proteins may alter E-cad stability through regulating the guanine exchange factor RhoGEF2, to increased E-cad turnover at the junctions.

The core planar polarity pathway is required for cell intercalation in the embryonic trachea

The formation of the *Drosophila* trachea is tightly regulated to form an identical structure in each developing embryo. Previous work has showed that mutants of core proteins show defects in trachea formation (Chung et al., 2009; Nelson et al., 2012), which suggests that the core proteins play a role in tracheal formation. However as the maternal zygotic core planar polarity mutants are viable to adulthood it is unlikely that these tracheal defects are severe. We therefore examined the tracheal branches for subtle defects in cell rearrangement and intercalation.

Loss of the core proteins resulted in an increase in the length of the trunk, which appeared contorted (**Figure 4.2B-D**, Chung *et al.*, 2009; Nelson *et al.*, 2012). Closer examination of the dorsal and ventral branches showed that cell intercalation in these mutant backgrounds or when Fz is overexpressed, was also disrupted. Whilst in wild-type embryos, almost all of the branches had intercalated by stage 17, in the core mutants most branches had not fully intercalated and many still exhibited loops of intercellular AJ's (**Figure 4.2E-K**), indicating that cell intercalation was compromised (Ribeiro et al., 2004). However the retention of intercellular AJ's was not due to a general delay in embryogenesis as core planar polarity mutants and wild-type embryos both showed comparable development of head involution, dorsal closure and embryonic pole cell migration (**Figure 4.3A-C'**).

The core proteins do not specify the patterning of the trachea as the initial number of cells specified in the dorsal branches is comparable between wild-type and core planar polarity mutant embryos (**Figure 4.4A, B, E**). However, in the core mutants, cells are progressively lost from the branches as cell intercalation progresses until approximately 4 cells are left in a branch (**Figure 4.4E**).

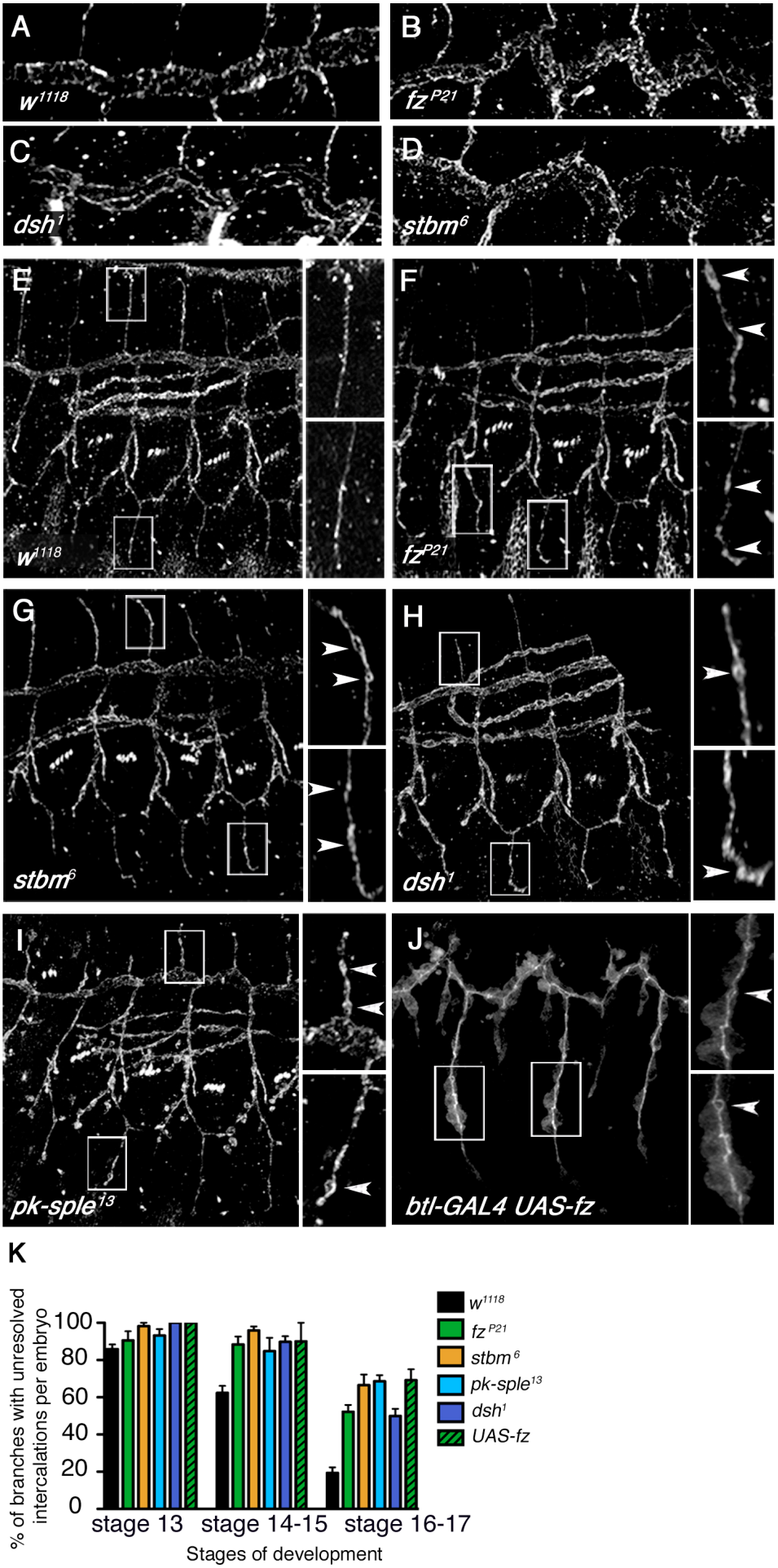
A
w1118
B
fzP21
C
dsh1
D
stbm6
E
w1118
F
fzP21
G
stbm6
H
dsh1
I
pk-sple13
J
btl-GAL4 UAS-fz
K
% of branches with unresolved intercalations per embryo
100
80
60
40
20
0
stage 13
stage 14-15
stage 16-17
Stages of development
w1118
fzP21
stbm6
pk-sple13
dsh1
UAS-fz

Figure 4.2: Core planar polarity protein mutant phenotypes in the *Drosophila* trachea

(A-D) Images of tracheal dorsal trunk immunostained with the junctional marker Crumbs in (A) wild-type (w^{1118}), (B) fz^{P21}, (C) dsh^{1} and (D) $stbm^{6}$. (E-J) Images of stage 15 embryonic trachea in (E) wild-type (w^{1118}), (F) fz^{P21}, (G) $stbm^{6}$, (H) dsh^{1}, (I) $pk\text{-}sple^{13}$ and (J) *btl-Gal4/UAS-fz*. White boxes indicate the location of the blow up regions to the right of each panel. White arrowheads indicate cells that have not completed cell intercalation. (K) Quantification of the percentage of ventral branches, which still have unresolved cell intercalations occurring at stage 13, stage 14-15 and stage 16-17. In wild-type (w^{1118}, black bars), fz^{P21} (green bars), $stbm^{6}$ (orange bars), dsh^{1} (dark blue bars), $pk\text{-}sple^{13}$ (light blue bars) and *btl-Gal4/UAS-fz* (stripy black and green bars). ANOVAs were used to compare simultaneously the control (w^{1118}) and the mutant conditions at each stage: stage 13, $P=0.0075$; stage 14-15, $P\leq0.0001$; stage 16-17, $P\leq0.0001$.

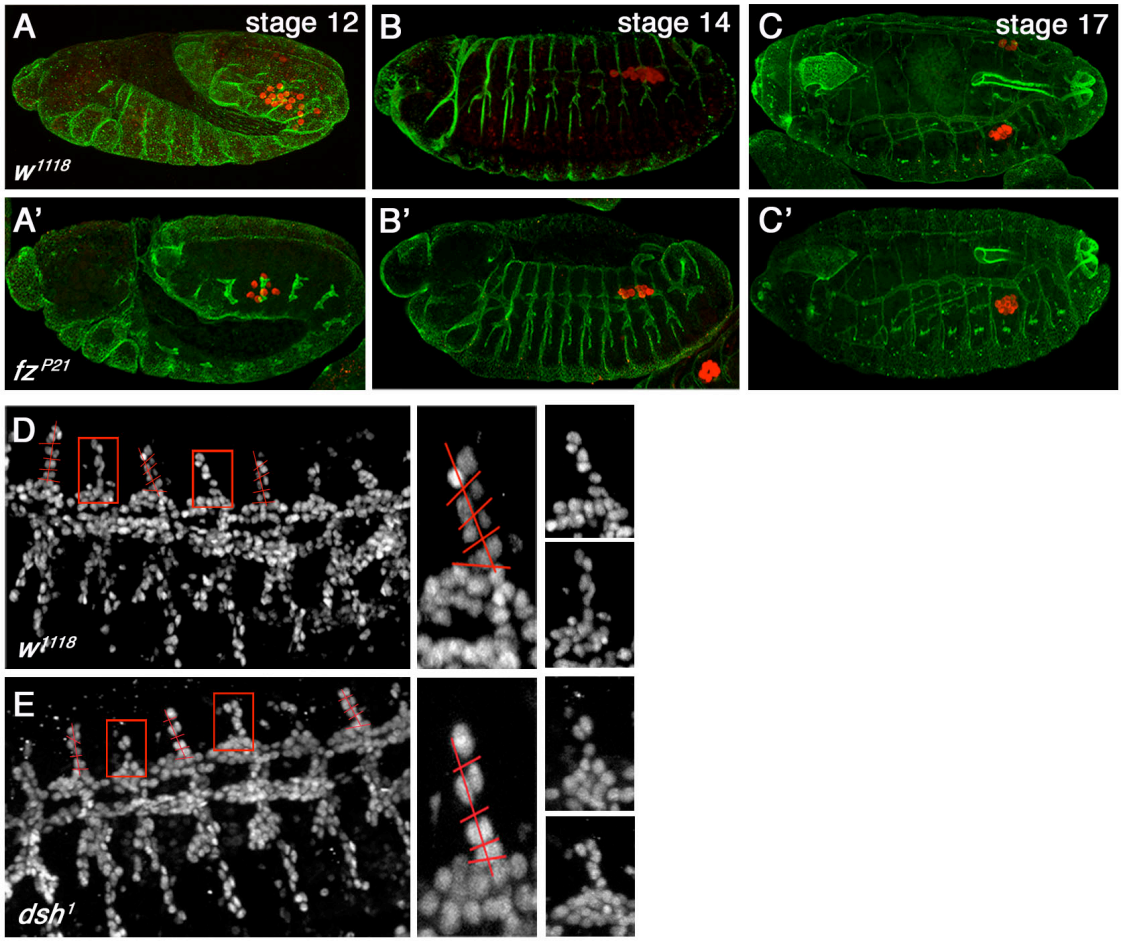

Figure 4.3: Embryo development in wild-type and core planar polarity mutants

(A-C') Dorsal closure, the migration of the embryonic pole cells and head involution occurs normally in core planar polarity mutants. All embryos are stained with the junctional marker Crumbs (green) and the pole cell marker Vasa (red). Stages 12, 14 and 17 were compared in (A-C) Wild-type (w^{1118}) and (A'-C') fz^{P21}. (D-E) Alignment of tracheal cells in the dorsal branches at stage 13 of embryonic development. Nuclei of cells are marked using expression of UAS-*red-stinger*. In (D) wild-type (w^{1118}) and (E) dsh^{1} mutant.

As previous work has shown, wild-type dorsal branches start cell intercalation with approximately 7 cells and finish with approximately 6 cells per branch (**Figure 4.4E**, Baer *et al.*, 2010; Samakovlis *et al.*, 1996). Cells that do leave are from the base of the dorsal branch and not from the branch itself (Baer et al., 2010). This suggests that these cells are either activating apoptotic pathways then leaving the branches, or the cells are being excluded as they remodel their junctions with neighbouring cells.

The remodelling of cell junctions and the contortion of the cells when under tension is likely to increase cell stress. Tracheal cells under stress are known to be able to activate apoptosis pathways prior to leaving the tracheal branches (Baer et al., 2010). To see if core planar polarity mutants cause cells to become stressed and undergo apoptosis prior to leaving the branches, a nuclear GFP marker for the early stages of apoptosis was used (Bardet et al., 2008). This construct, named UAS-Apoliner (Bardet et al., 2008) consists of a membrane tether tagged to RFP at one end, and a nuclear localisation signal tagged with GFP at the other. Between the tags is a DIAP1 fragment, which is cleaved by Caspase3 at the onset of apoptosis (Ditzel et al., 2003; Yokokura et al., 2004), thereby, allowing the GFP tag to migrate to the nucleus whilst the RFP tag remains at the cell junctions (Bardet et al., 2008).

Prior to cell intercalation, wild-type and core mutants show no GFP positive cells in the tracheal branches (**Figure 4.5A,B**). However, during cell intercalation the core pathway mutant *fz* cells have GFP positive nuclei (**Figure 4.5C,E**). This indicates that cells in *fz* mutants are stressed during cell intercalation so they turn on Caspase3 activated apoptotic pathways. Occasionally in the core mutants paired cells are observed that both have green nuclei (**Figure 4.5E**). These cells may be under stress as they try to intercalate and therefore turn on the apoptosis marker prior to intercalating, therefore providing a way to exclude cells from the branches.

Although we cannot definitively say why tracheal cells are excluded from the branches, the loss of these cells has implications on what happens to the remaining cells within a tracheal branch. If cell death is a way for stressed cells to leave the tube allowing the remaining cells to elongate the branches, then removing cell death may uncover a more severe intercalation phenotype. Interestingly if cell death is blocked in *fz* mutant tracheal branches by overexpression of the cell death inhibitor p35 (Baer et al., 2010) then tracheal branches do not extend or intercalate properly (**Figure 4.5G**). This suggests that in core mutants the exclusion of cells from the branches during cell intercalation allows the branches to continue to extend.

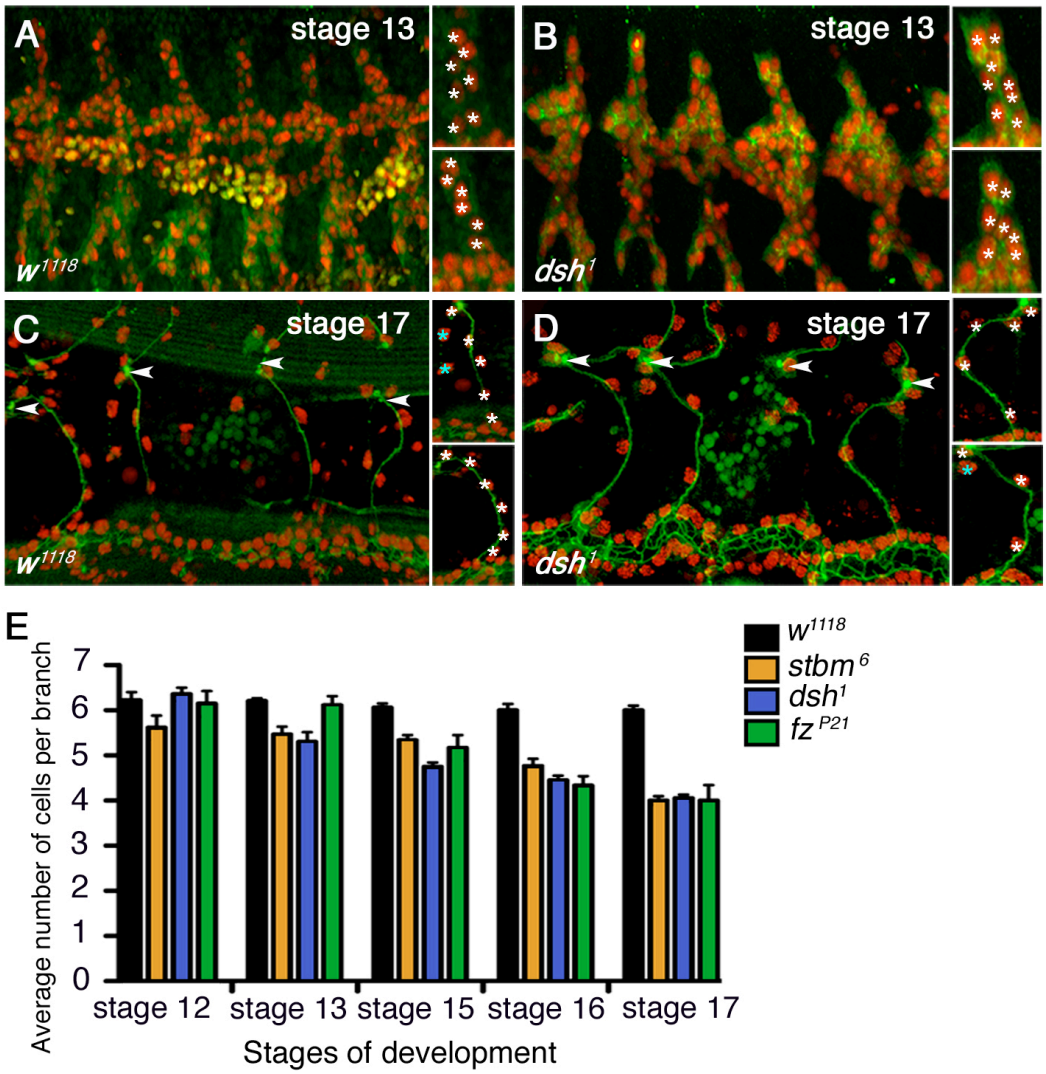

Figure 4.4: The dorsal tracheal branches have fewer cells in the core planar polarity protein mutants

(A, C) wild-type (w^{1118}) compared to (B, D) dsh^{1}. At (A-B) stage 13 and (C-D) stage 17. Tracheal branches were imaged live using *btl-Gal4 UAS-α-Cat* (green) to mark the junctions and UAS-*red stinger* (red) to mark the cell nuclei. Arrowheads indicate the location where the dorsal tracheal branches join the branches on the other side of the midline. Blue asterisk indicates a cell not part of the branch it is near. (E) Quantification of the average number of cells per branch. At stages 12,13,15,16 and 17. In wild-type (w^{1118} black bars), dsh^{1} (blue bars), $stbm^{6}$ (orange bars) and fz^{P21} (green bars). ANOVAs were used to compare the control (w^{1118}) and the mutant conditions for each stage: stage 12, P=0.078; stage 13, $P\leq$.0001; stage 15, $P\leq$0.0001; stage 16, $P\leq$0.0001; stage 17, $P\leq$0.0001. Error bars represent s.e.m.

The role of endocytosis during cell intercalation

Failure of cell intercalation in the core planar polarity mutants suggests a defect in the modification of cellular adhesion during junctional remodelling (Shaye et al., 2008; Shindo et al., 2008). One way to remodel junctions is through the endocytosis of adhesion complexes from the junctions where rearrangement is occurring (Shaye et al., 2008; Shindo et al., 2008; Tanaka-Matakatsu et al., 1996; Uemura et al., 1996), and the recycling of components back to membranes where increased adhesion is required (Shaye et al., 2008).

If the disruption of cell intercalation in the core mutants was due to a disruption in endocytosis of junctional proteins then we may expect to also see tracheal cell death in endocytic mutants. When a dominant negative form of the endocytosis factor Rab5 is overexpressed the tracheal branches do fail to complete cell intercalation (Shaye et al., 2008), but they do not turn on the apoptosis marker Apoliner in intercalating stalk cells (**Figure 4.5F**, Baer *et al.*, 2010). This suggests that disrupting endocytosis leads to incomplete cell intercalation but does not lead to cell apoptosis. Therefore it is unlikely that cell apoptosis in the core mutants is solely due to the absence of endocytosis.

Core proteins alter levels of E-cad at the junctions in the trachea

Interestingly in tracheal cells endogenous E-cad is increased in planar polarity mutants (**Figure 4.6A**), and conversely overexpression of Fz results in a reduction of endogenous E-cad protein at the junctions (**Figure 4.6B**). These results suggest that core polarity proteins normally remove E-cad protein from the AJ's. The effect is cell autonomous as only clonal cells overexpressing Fz show a decrease in E-cad protein levels (**Figure 4.6D, D'**).

However, the alteration in endogenous E-cad levels is not due to core proteins affecting E-cad transcription, as in *dsh*^{1} mutants there is no increase in the transcription of *shotgun* (*shg*), which is the gene encoding the E-cad protein in *Drosophila* (**Figure 4.6C**). Core proteins are therefore likely to be either increasing the removal of E-cad from the junctions through endocytosis or preventing exocytosis of E-cad to the junctions.

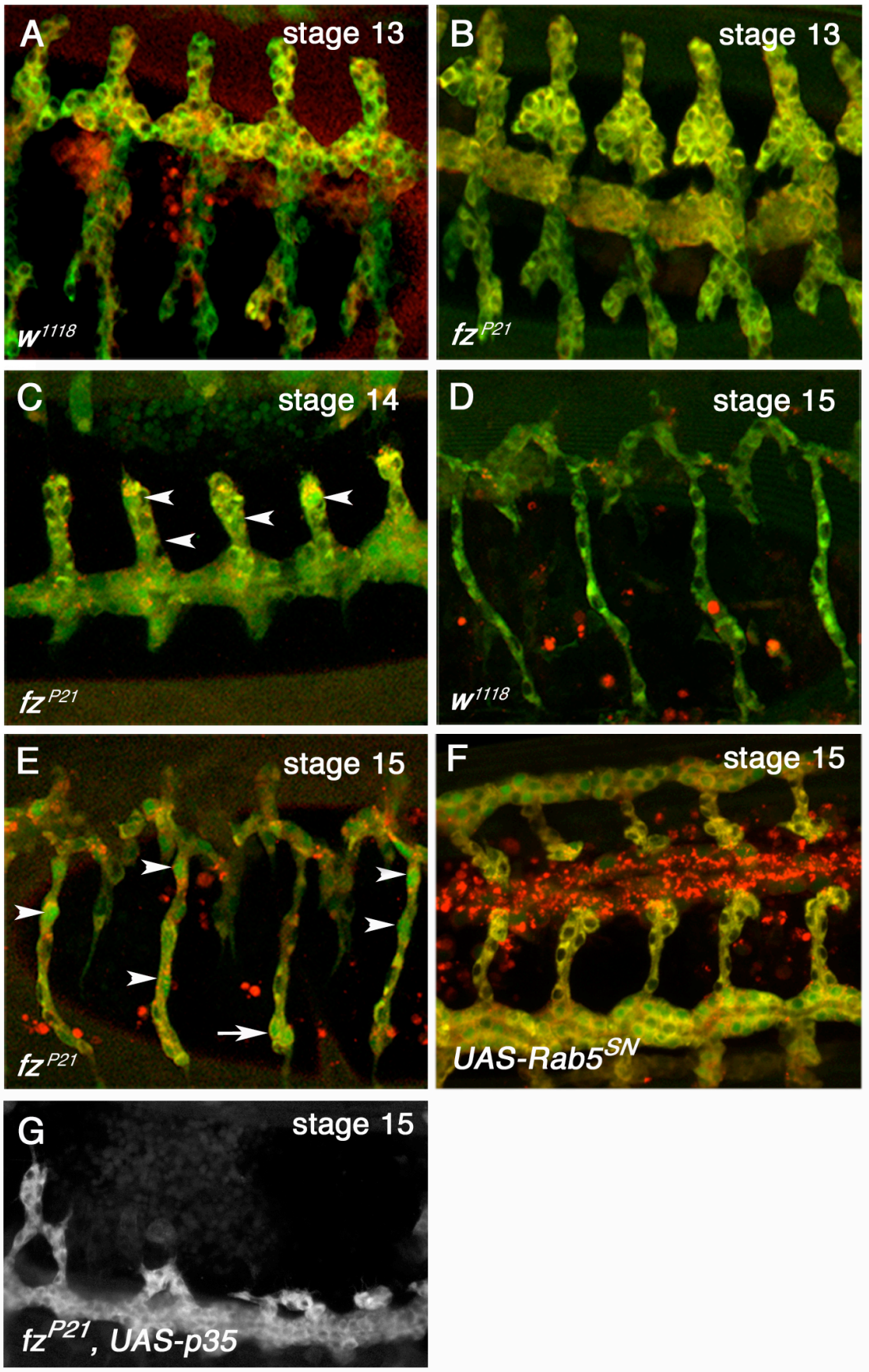

Figure 4.5: Trachea cells undergo cell apoptosis in core planar polarity protein mutants

(Figure legend is on the next page)

Figure 4.5: Trachea cells undergo cell apoptosis in core planar polarity protein mutants

Embryos expressing the *UAS-Apoliner* marker in tracheal cells using *btl-Gal4* in (A) Wild-type (w^{1118}) embryo at stage 13, (B) fz^{P21}mutant at stage 13, (C) fz^{P21} mutant at stage 14, (D) wild-type (w^{1118}) at stage 15, (E) fz^{P21} mutant at stage 15, (F) *UAS-Rab5*^{SN} at stage 15. Note: the intercalating stalk cells do not have green nuclei, although the trunk cells do, which is sometimes seen in wild-type examples (Figure 4.5F, Baer *et al.*, 2010). Arrowheads indicate cells with green nuclei, which show that those cells have activated the apoptotic pathway. Arrow indicates a pair of cells that have not intercalated but both cells have green nuclei. (G) fz^{P21} mutant at stage 15 also expressing *btl-Gal4 UAS-Apoliner* and *UAS-p35*, which blocks cell apoptosis. Error bars represent s.e.m.

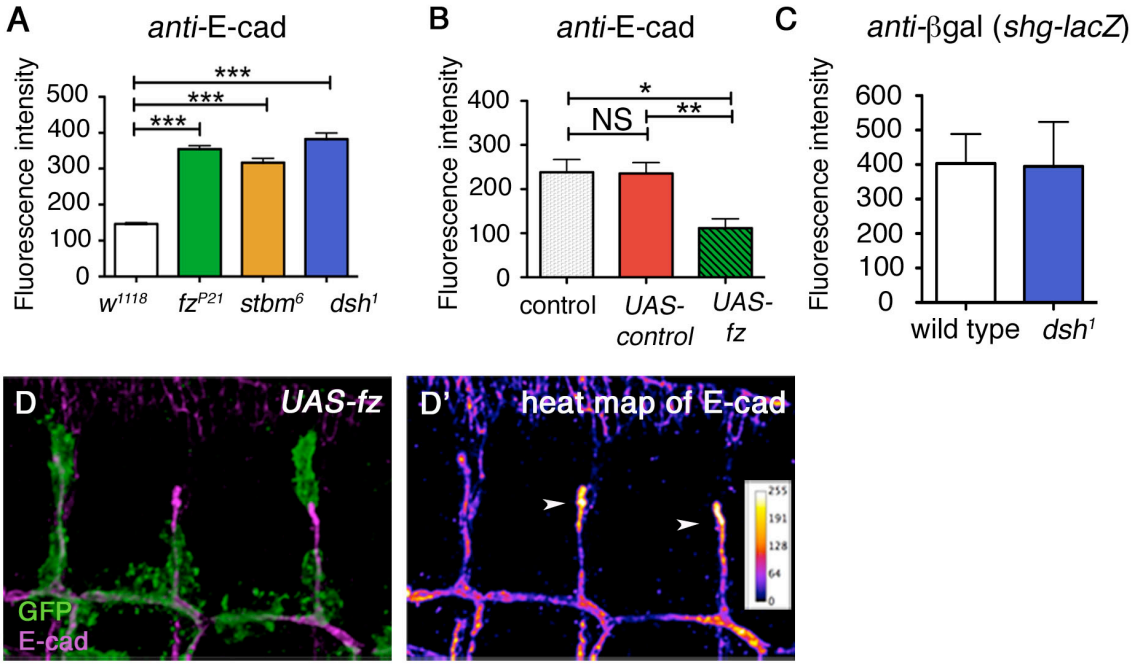

Figure 4.6: Core planar polarity proteins affect E-cad levels in the trachea

(A) Intensity measurements of endogenous E-cad levels in stage 14 tracheal branches in control (w^{1118}) (white bars) and core planar polarity mutants fz^{P21} (green bars), $stbm^{6}$ (orange bars), dsh^{1} (blue bars). (B) Endogenous E-cad levels in control (w^{1118}, white bars), UAS-control (red bars) and *btlGal4/UAS-fz* (green and black striped bars). ANOVAs were used to compare the control and mutant conditions in: (A) $P \leq 0.0001$; (B) $P=0.0002$. Asterisks on the graphs indicate individual results from a Dunnett's multiple comparison Post ANOVA test (NS, not significant; $*P \leq 0.05$, $**P \leq 0.01$, $***P \leq 0.0001$). (C) *shg* transcription is not up regulated in dsh^{1} mutants *shg-lacZ* (an enhancer trap in the locus encoding E-cad, Shindo et al., 2008) was used to quantify the levels of βgal labelling showing levels of transcription of *shg-lacZ* in control and dsh^{1} epithelial cells (t-test, P=0.90). Error bars are s.d. (D) Endogenous E-cad levels are reduced cell-autonomously in dorsal tracheal branch clones overexpressing *UAS-fz* with *UAS-GFP* to mark the clones (green), clones were induced using the *btl>stop>Gal4* driver. Branches are immunostained for E-cad (magenta in D, or shown as an intensity map in D').

Core planar polarity proteins affect E-cad stability in tracheal cells

To achieve cell intercalation, at least a proportion of junctional E-cad would have to be subjected to protein turnover (Classen et al., 2005; Gumbiner, 2005; Ulrich et al., 2005). This process is more likely to be an exchange based mechanism at the level of the junctions, rather than due to lateral diffusion within the membrane (de Beco et al., 2009).

To see how E-cad stability at the membrane was affected by the loss of core pathway components, FRAP (see the Materials and Methods section for details) was used in the trachea in a similar way to the method used in pupal wings (see Chapter 3); to measure the stable fraction of E-cad-GFP in the AJ's.

For FRAP, E-cad tagged with GFP was expressed in the tracheal system, images were taken and bleaching of the GFP fluorophore was performed on vertically orientated junctions in dorsal and ventral tracheal branches. Selected regions were imaged after bleaching, enabling the fluorescence to be quantified over time to measure the amount of recovery of GFP fluorescence at the junctions.

FRAP analysis shows that E-cad-GFP fluorescence in wild-type (w^{1118}) embryos recovered to 47% of the initial pre-bleach fluorescence, therefore the remaining 53% must be in a stable fraction that is not subjected to protein turnover during the lifetime of the experiment (**Figure 4.7A**). However in the planar polarity mutants (fz^{P21}, $stbm^{6}$, dsh^{1}) E-cad-GFP fluorescence after bleaching recovered to a lower level indicating that there is an increase in E-cad stability at the junctions in the core planar polarity mutants compared to wild-type embryos (**Figure 4.7A**). There is also an increase in total E-cad levels in the core mutants (**Figure 4.6A**), consequently there is not just more E-cad in the junctions it is also more stable. Therefore core proteins most likely promote E-cad removal from the junctions in tracheal cells.

FRAP of E-cad-GFP in cells over-expressing Frizzled showed a modest decrease in recovery compared to E-cad-GFP in a wild-type background and therefore also showed an increase in E-cad stability (**Figure 4.7B**), analogous to what is seen with the core planar polarity mutants (**Figure 4.7A**). However, with FRAP we are only measuring the relative stable proportion of protein at the junctions and not the absolute amount. If we take into account that the overall amount of E-cad fluorescence was greatly reduced in the Frizzled over expression background (**Figure 4.6B**); then the absolute stable fraction of E-cad in the Fz over-expression background is less.

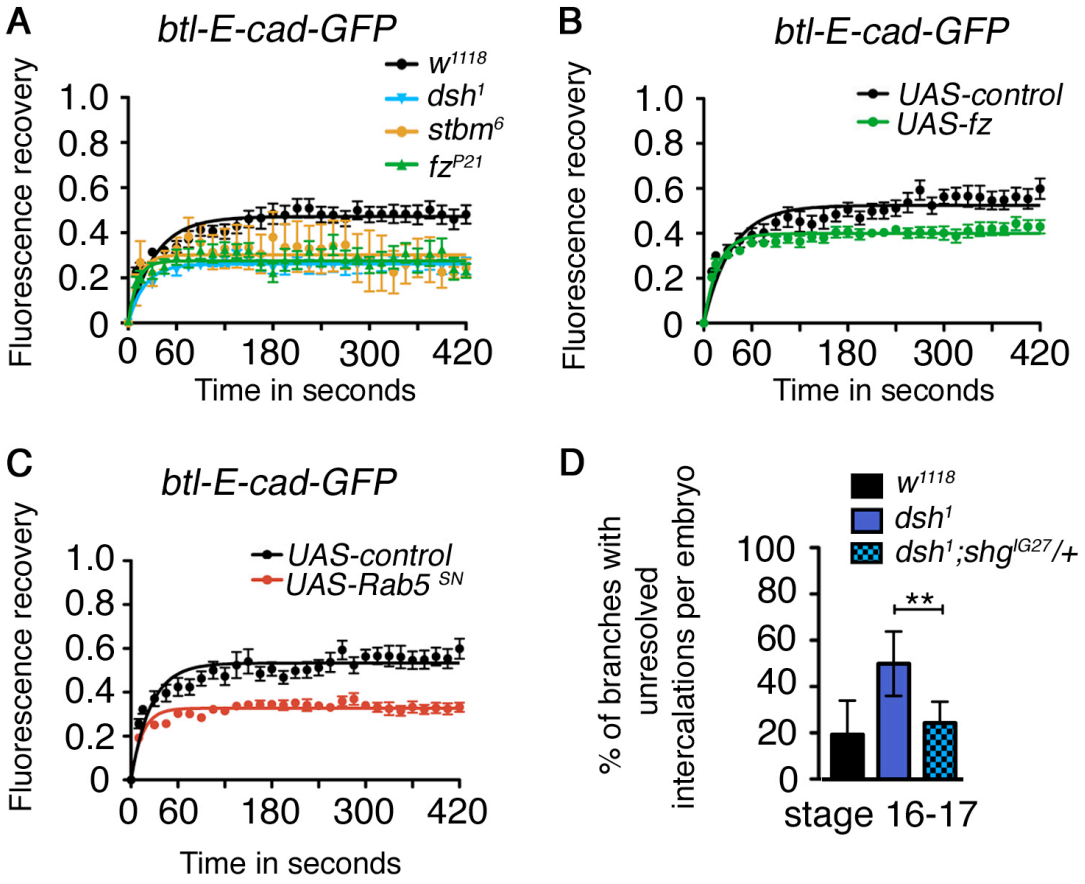

Figure 4.7: The loss of the core planar polarity proteins increase E-cad junctional stability

(A) FRAP analysis of *btl-Gal4/UAS-E-cad-GFP* on junctions of cells in dorsal tracheal branches, in wild-type or core planar polarity mutant backgrounds. (A one-way ANOVA comparing stable fractions of E-cad-GFP in wild-type (w^{1118}), fz^{P21} (green), $stbm^{6}$ (orange), dsh^{1} (blue) was performed, $P \leq 0.0001$). Half-lives could not be determined, as a proportion of fluorescence recovery had occurred prior to the first time interval, therefore the rate calculated from these graphs was not likely to be accurate. Error bars represent s.e.m. (B-C) FRAP analysis of *btl-Gal4/UAS-E-cad-GFP* co-expressed with (B) *UAS-fz* or (C) $UAS\text{-}Rab5^{SN}$. In both cases, E-cad-GFP had a larger stable fraction (i.e. less recovery) compared to the *UAS-NLS-red-stinger* control (black line in B-C) (t-test comparing the stable fractions of the control in B and C $P \leq 0.0001$). Error bars represent s.e.m. (D) Quantification of the percentage of tracheal branches with unresolved intercalations in wild-type (w^{1118}), dsh^{1} (blue bars, as shown in **Figure 4.2K**) and in dsh^{1} mutants that were also heterozygous for shg^{IG27} (blue hatched bars). A loss of a single copy of *shg* resulted in a reduction in the number of intercalations in the dsh^{1} mutant compared to dsh^{1} alone (*t*-test, $^{**}P=0.0016$). Error bars represent s.d.

Table 1: Genetic interactions of dsh^{1} with various RhoA, RhoGEF2 or Rab5 mutant alleles

Genotype	Allele	Results	Flybase reference
w;dsh^{1}[sxl-GFP]/Y		Viable, wild-type	
w;dsh^{1}[sxl-GFP]/Y; RhoA^{72AY}/+	Hypomorphic RhoA allele	Only heterozygous female embryos with the sxl-GFP balancer were seen.	FBgn0014020
w;dsh^{1}[sxl-GFP]/Y; RhoA^{72M1}/+	Hypomorphic RhoA allele	Only heterozygous female embryos with the sxl-GFP balancer were seen.	FBal0061662
w;dsh^{1}[sxl-GFP]/Y; RhoA$^{72\,36}$/+	The RhoA allele has a P element inserted into an intron 33bp upstream of the RhoA ATG start site	Only heterozygous female embryos with the sxl-GFP balancer were seen.	FBal0061657
w;dsh^{1}[sxl-GFP]/Y; RhoA^{72O}/+	RhoA putative null allele - P element excision including the translational start site	Only heterozygous female embryos with the sxl-GFP balancer were seen.	FBal0061661
w;dsh^{1}[sxl-GFP]/Y; Rab5^{00231} /+	P element insertion in the Rab5 coding region near the 5' end	All male *dsh^{1}* embryos visualised without the balancer died during germ band retraction	FBst0010827
w;dsh^{1}[sxl-GFP]/Y; RhoGEF2$^{6.5}$/+	Hypomorphic RhoGEF2 allele	*dsh^{1}* males are dead and female embryos have severely disrupted trachea when heterozygous for both *dsh^{1}* and *RhoGEF2$^{6.5}$*	FBst0009384
w;dsh^{1}[sxl-GFP]/Y; RhoGEF2^{04291}/+	Loss of function RhoGEF2 allele	Only female embryos with the sxl-GFP balancers are seen, females heterozygous for both *dsh^{1}* and *RhoGEF2^{04291}* are also severely disrupted	FBal0008055

Note: Sex lethal-GFP (Sxl-GFP) was used to distinguish males from females, as Sxl-GFP is only expressed in females.

This is because more fluorescence should have recovered if the total amount of fluorescence was similar to that of E-cad-GFP in the wild-type background. Therefore if corrected for the amount of protein present then the proportion of E-cad that is stable in a Frizzled over expression background would be decreased (compare **Figure 4.6B** and **Figure 4.7B**). This suggests that over-expressing Fz actually decreases E-cad stability.

These data so far suggest that the core polarity proteins are required to up-regulate junctional removal of E-cad, as removal of the core polarity components results in an increase in E-cad protein levels and its stability at the junctions. As inhibiting endocytosis in tracheal cells also disrupted cell adhesion (Shaye et al., 2008) by increasing junctional E-cad, we inhibited endocytosis using a dominant negative form of Rab5, which also resulted in E-cad-GFP being stabilised at the junctions (**Figure 4.7C**).

If the core proteins increase E-cad endocytosis and this is the cause of the intercalation defect at the junctions then a disruption of endocytosis in a *dsh*^{1} hemizygous background would further increase the severity of the tracheal intercalation phenotype. To test this, firstly, a mutant of Rab5 was used and secondly an over-expressed temperature sensitive allele of *shibire,* which encodes the *Drosophila* homolog of dynamin (Sever, 2002). However, both of these coupled with hemizygous *dsh*^{1} resulted in embryonic lethality prior to trachea formation (**Table 1**).

However, genetic interaction experiments performed between *dsh* and *shotgun* (the gene which encodes E-cad) showed that the *dsh*^{1} defective intercalation phenotype could be rescued by removing one gene copy of *shg* (**Figure 4.7D**). This suggests that the direct increase of E-cad at the junctions in core planar polarity mutants causes the intercalation defects.

The core pathway does not act through the wing effectors Fuzzy and Mwh to affect E-cad turnover

As the modulation of E-cad by the core proteins is unlikely to be a direct affect, we looked for what pathways could link the core proteins to E-cad.

In the adult cuticle including the *Drosophila* wing, the core pathway acts through several downstream effectors to specify the number, localisation and formation of actin-rich hairs. This process is known to involve Fuzzy (Fy), Inturned (In), Fritz (Frtz) and Multiple wing hairs (Mwh), which have roles in cellular remodelling and the actin

cytoskeleton (Adler et al., 1994; Collier and Gubb, 1997; Collier et al., 2005; Goodrich and Strutt, 2011; Strutt and Warrington, 2008).

As actin modifiers, these proteins could play a role in remodelling the actin cytoskeleton during cell intercalation and be required for E-cad turnover (Goodrich and Strutt, 2011). Fy and Mwh are expressed in the embryo during development (Adler et al., 1994; Collier and Gubb, 1997; Collier et al., 2005). However neither *fy* nor *mwh* maternal zygotic mutants showed any defects in tracheal cell intercalation compared to wild-type embryos (**Figure 4.8A-C**).

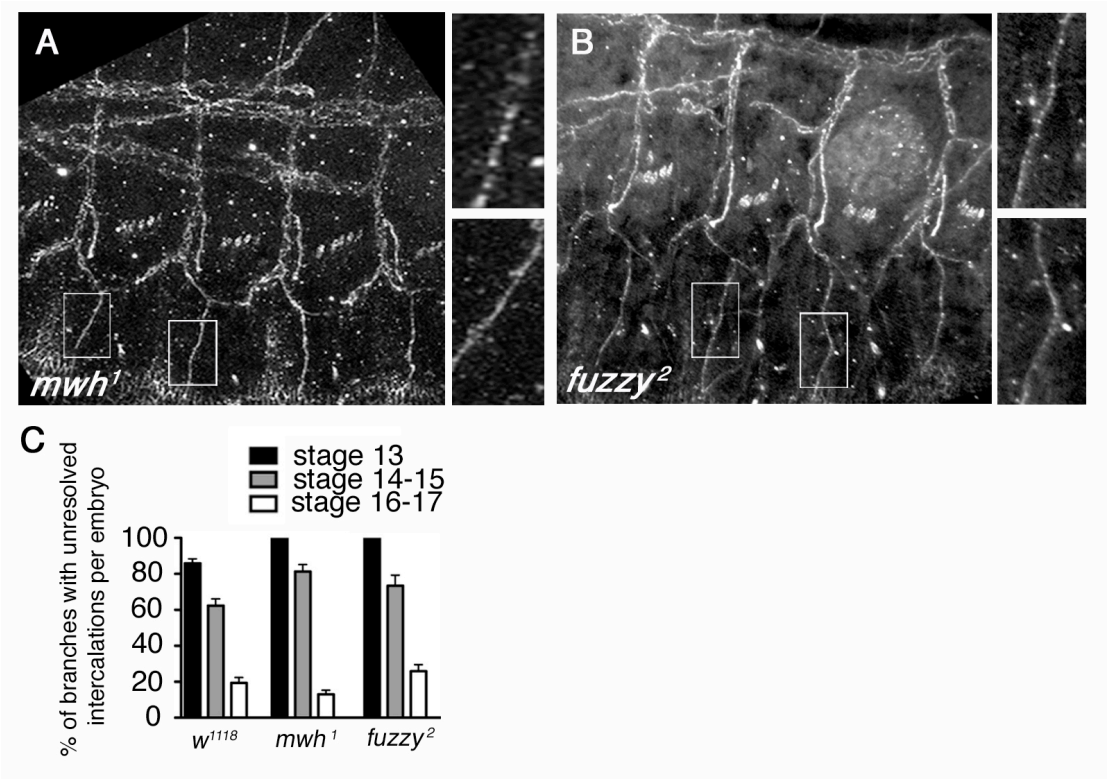

Figure 4.8: Downstream planar polarity effectors are not required for tracheal cell intercalation

(A, B) Embryonic tracheal branches at stage 15 in mutants for downstream effectors of the core proteins stained for the junctional marker Crumbs, (A) *mwh*^{1} and (B) *fuzzy*^{2}. Compared to wild-type results (also shown in **Figure 4.2K**). White boxes in A and B indicates where the magnified regions were taken from. (C) Quantification of the number of branches with unresolved intercalations, at stage 13, 14-15 and 16-17. Error bars are s.e.m. ANOVAs compared the means of the wild-type compared to the mutant backgrounds at each stage: stage 13 P=0.012; stage 14-15 P=0.072; stage 16-17 P=0.069.

RhoA activity increases E-cad turnover in the embryonic trachea

Rho acts as a downstream effector of the core polarity proteins in the *Drosophila* eye (Strutt et al., 1997), and if RhoA were acting as an effector of the core polarity proteins in the trachea then a similar tracheal intercalation defect would be expected with RhoA, as well as a decrease in E-cad levels and turnover.

Maternally depleted *RhoA* null mutants exhibit an 'anterior open' phenotype during embryogenesis (Strutt et al., 1997) which could affect the elongation of the trachea. Therefore RhoA overexpression constructs were used to either express the constitutively active (CA) or dominant negative (DN) forms of RhoA (Strutt et al., 1997).

Expression of the constitutively active RhoA construct in the tracheal branches using the tracheal specific *btl-Gal4* driver leads to general trachea disruption, including a contorted trunk and some branches failing to migrate to their final locations (**Figure 4.9A**, Lee and Kolodziej, 2002b). Dominant negative RhoA disrupts trachea formation (**Figure 4.9B**) and reduces cell adhesiveness and epithelial cells lose attachment to their neighbours and appear to undergo apoptosis (Bloor and Kiehart, 2002).

Although tracheal formation was obviously affected by the constitutively active or dominant negative forms of RhoA, the extent of the intercalation disruption meant the defects were not quantifiable in the same way as the intercalation defects were quantified in the core planar polarity mutants.

Despite the severe disruption of the trachea, the overall fluorescence level of E-cad was not significantly different (**Figure 4.9D**). However, FRAP of E-cad-GFP in a DN RhoA background (**Figure 4.9C**) found that E-cad stability was increased at the junctions similarly to that of E-cad in planar polarity mutants (compared to **Figure 4.7 A**). These results suggest that RhoA is normally increasing the turnover of E-cad in the trachea therefore acting in the same direction as the core protein pathway and is most likely an effector of that pathway in this tissue.

If RhoA acts as an effector of the core proteins then removal of RhoA in a dsh^1 mutant background would increase the severity of the disrupted trachea phenotype. To establish if RhoA and indeed its activator RhoGEF2 were acting downstream of the core proteins to increase E-cad turnover, we attempted to use genetic interaction experiments. The aim was to remove one copy of a null RhoA allele in a hemizygous dsh^1 background and to score the trachea for cell intercalation defects. As decreasing

E-cad levels or increasing its turnover in a *dsh*^{1} background decreases the severity of the *dsh*^{1} intercalation phenotype, an increase in junctional E-cad or decreasing turnover would be expected to enhance the phenotype. However the combination of *dsh*^{1} and the null *RhoA* allele resulted in embryonic lethality. We also examined a variety of RhoA hypomorphic and null alleles as well as the hypomorphic RhoGEF2 allele separately in the hemizygous *dsh*^{1} background (see **Table 1**), however all RhoA and RhoGEF2 alleles tested resulted in embryonic lethality and so could not be scored for tracheal defects (see **Table 1**).

As expression of a constitutively active RhoA allele caused lethality in the hemizygous *dsh*^{1} background, a more gentle approach was used to subtly increase the levels of active RhoA in the *dsh*^{1} hemizygous background. To do this the Gal4-UAS system was used in conjunction with temperature sensitive Gal80. At lower temperatures Gal80 forms a complex that competes for binding with Gal4 to the UAS promoter site, thereby reducing the activation of UAS expression by Gal4 (McGuire et al., 2003). At higher temperatures the Gal80 complex is unstable and degrades, allowing Gal4 to bind to the UAS binding site, increasing UAS expression. A constitutively active RhoA form of RhoA, *RhoA*^{V14} was expressed in embryos along with *btl-Gal4*, Gal80^{TS} and hemizygous *dsh*^{1}; however even at lower temperatures (18°C) there was still early embryonic lethality.

RhoGEF2 positively regulates E-cad turnover in the trachea

To see if RhoGEF2 is also activating RhoA in tracheal cells and affecting junctional remodelling, embryos expressing an antimorphic version of the RhoGEF2 protein were assayed for tracheal intercalation defects. As with the core pathway mutants, RhoGEF2 antimorphic embryos also exhibited loops of intercellular AJ's (**Figure 4.9 E, F**) and an increase in E-cad levels (**Figure 4.9G**), suggesting intercalation is also compromised in these embryos. In agreement with this, FRAP shows that there is an increase in the stability of E-cad at the junctions when expressing the antimorphic *RhoGEF2* (**Figure 4.9H**).

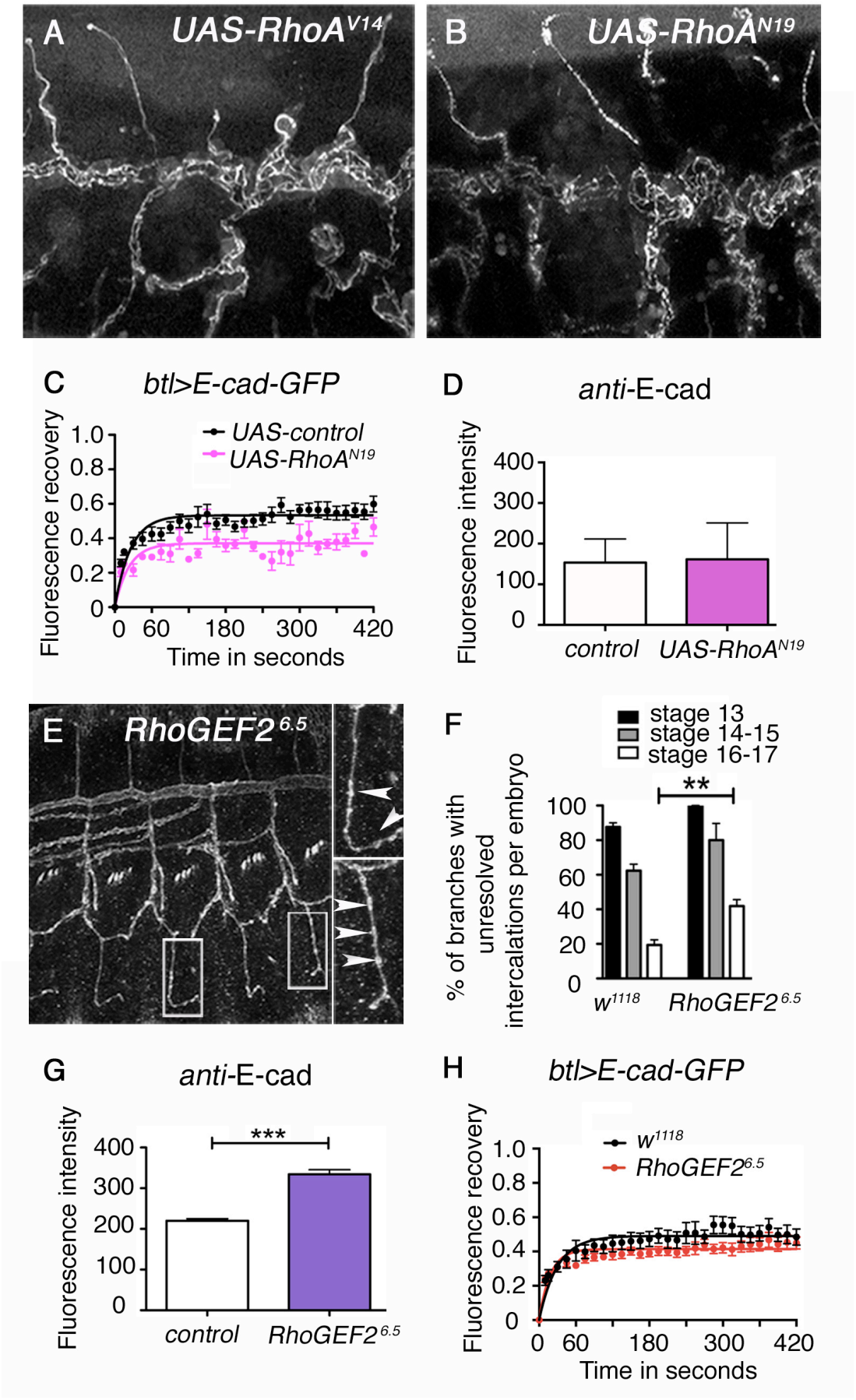

Figure 4.9: RhoA and RhoGEF2 are required for tracheal cell intercalation

(Figure legend is on the next page)

Figure 4.9: RhoA and RhoGEF2 are required for tracheal cell intercalation

(A-B) Lateral view of the tracheal branches immunostained with Crumbs, in which (A) activated $RhoA^{V14}$ or (B) the dominant negative $RhoA^{N19}$ was overexpressed using btl-Gal4. (C) FRAP of btl-Gal4/UAS-E-cad-GFP co-expressing UAS-$RhoA^{N19}$. Overexpression of $RhoA^{N19}$ leads to an increase in the stable fraction of E-cad-GFP (pink line) when compared to the UAS-NLS-red-stinger control (black line) (t-test comparing stable fractions, $P \leq 0.0001$). (D) Intensity measurements of junctional E-cad in stage 14 tracheal branches expressing UAS-$RhoA^{N19}$ compared to the wild-type (w^{1118}) control, (t-test, P=0.21). (E) Lateral view of tracheal branches immunostained for Crumbs in embryos expressing the $RhoGEF2^{6.5}$ heterozygous antimorphic allele. Smaller images are magnifications of the white boxes shown in E. (F) Quantification of the intercalation phenotype in embryos expressing the heterozygous $RhoGEF2^{6.5}$ allele, (t-test comparing w^{1118} and $RhoGEF2^{6.5}$ at stage 16-17 P=0.0029). (G) Intensity measurements of junctional E-cad in stage 14 tracheal branches expressing heterozygous $RhoGEF2^{6.5}$ compared to w^{1118} (t-test, $P \leq 0.0001$). (H) FRAP analysis of dorsal tracheal branches btl-Gal/UAS-E-cad-GFP when expressing heterozygous $RhoGEF2^{6.5}$ (t-test, $P \leq 0.0001$).

Proposed asymmetric localisation of proteins in the trachea

RhoGEF2 has been reported to be asymmetrically localised in the embryonic epidermis and regulates polarised E-cad turnover (Levayer et al., 2011). In support of the idea that the core proteins could be directly recruiting RhoGEF2 to the junctions and that RhoGEF2 then alters E-cad levels we looked for asymmetry of the core proteins in tracheal cells. The core proteins are known to be asymmetrically localised to the proximal and distal membranes in the pupal wing (see Chapter 3, Strutt and Strutt, 2009) and could also be asymmetrically localised in tracheal cells.

The endogenous Fz is present in the tracheal cell junctions in the branches and trunk (**Figure 4.10A-A''**, antibody control in **Figure 4.10B-B''**) and colocalises with E-cad (**Figure 4.10A-A''**) and in a similar junctional location as another apical junctional marker Crumbs (Warrington et al., 2013). Junctional localisation in tracheal cells has also been shown for the core proteins Fmi and Stbm in the tracheal trunk and branches (Chung et al., 2009; Forster and Luschnig, 2012; Nelson et al., 2012).

If the core proteins were asymmetrically localised then we would expect their enrichment on junctions aligning along the dorsal ventral axis, which are remodelled during cell intercalation. These junctions would then have an increase in E-cad turnover to allow cells to remodel their junctions. However, asymmetric localisation of any of the core proteins was not observed in the trachea, looking at the endogenous protein (**Figure 4.10A-A''**). This might be because either the core proteins are not asymmetrically localised in tracheal cells; or because the proteins are asymmetrically localised but the localisation is transient or weak and therefore hard to observe.

If asymmetric localisation of the core proteins is transient in intercalating tracheal cells, then another way of observing it could be to look for a phenotype that may be a read out of a response to polarisation. Previous work has suggested that paired cells align prior to cell intercalation (Ribeiro et al., 2004). If this polarised alignment requires the core proteins then, then this may be disrupted in their absence. However, despite a published model depicting aligned paired cells (Ribeiro et al., 2004), it was not possible to consistently observe that paired cells were aligned prior to intercalation in wild-type branches by using the alignment of the tracheal cell nuclei as a proxy for cell alignment (**Figure 4.3D**), and there was no significant difference in the *dsh*^{1} mutants (**Figure 4.3E**). This indicates that either nuclei do not align consistently, paired cells do not need to be polarise prior to cell intercalation or that pairing of cells is not dependent on the planar polarity pathway.

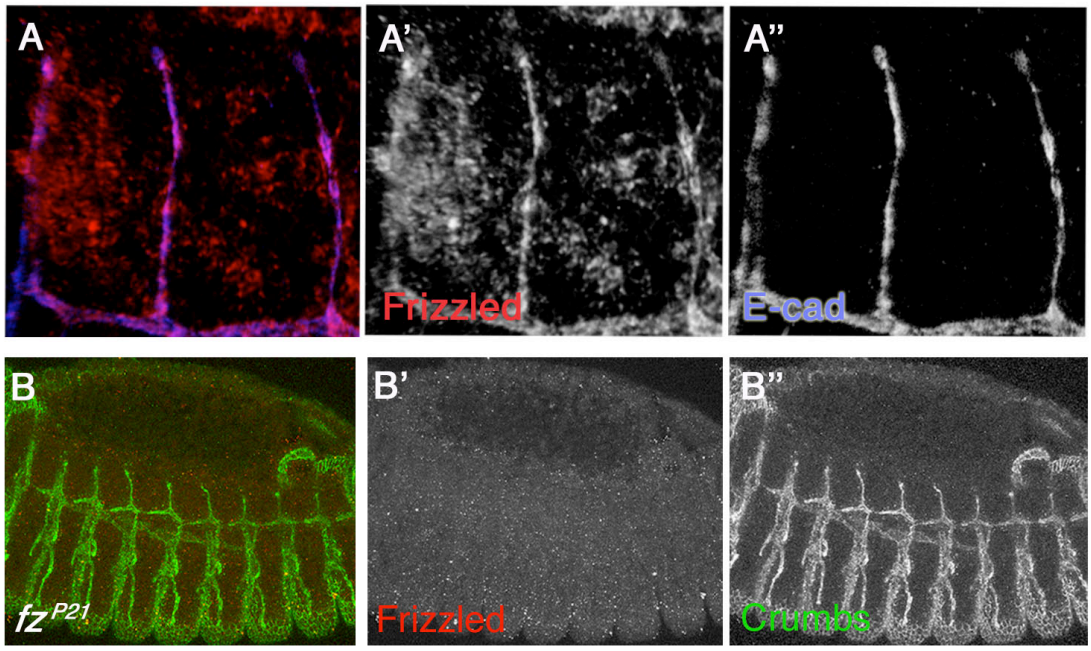

Figure 4.10: Frizzled is localised to adherens junctions in tracheal cells

(A) Dorsal branches of stage 15 tracheal branches immunostained for endogenous Fz (red in A or white in A') and E-cad (blue in A or white in A'') at junctions. (B) Tracheal branches in fz^{P21} mutants, immunostained for endogenous Fz (red in B, while in B') and the junctional marker Crumbs (green in B, white in B'').

Discussion

This work has shown that the core proteins are required for tracheal cell intercalation, as loss of the core proteins leads to a disruption in cell rearrangements and a loss of cells from the tracheal branches due to apoptosis. However, the core proteins are not required for tracheal branch specification, therefore are most likely required during cell intercalation.

In addition, the loss of core proteins leads to an increase in levels of the adhesion protein E-cad at the junctions, whereas over-expression of the core proteins causes a decrease in E-cad levels. This change in E-cad levels is likely due to regulation of E-cad at a post-transcriptional level, as E-cad transcription is not affected in core planar polarity mutants. This suggests that the core proteins are normally involved in removing E-cad from the junctions. Furthermore, the increase in E-cad at the junctions seen in a *dsh*^{1} mutant can be rescued by removing a copy of *shg.* This indicates that the increased level of E-cad causes the defects in cell intercalation seen in the core planar polarity mutants.

Furthermore, FRAP analysis showed that E-cad turnover is affected in core planar polarity mutants, as the loss of core proteins results in an increase in E-cad stability. Therefore, the core proteins are required to reduce the stable fraction of E-cad protein at the junctions, to increase the removal of E-cad from the junctions.

Tracheal cell intercalation is known to require the modulation of junctional E-cad levels, through delivery and removal of protein (Shaye et al., 2008). In addition FRAP analysis showed that overexpressing a dominant negative version of Rab5 results in an increase in the E-cad stable fraction at the junctions. Consequently, as the core protein mutants increase the amount of stable E-cad at the junctions, they may also be required in the regulation of E-cad turnover through modulating endocytosis.

The regulation of E-cad turnover by the core proteins does not occur through the downstream wing-specific effectors Fy and mwh. In the *Drosophila* epidermis, the turnover of E-cad is proposed to require RhoGEF2 to locally activate RhoA and then through downstream pathways regulate E-cad removal from the junctions (Levayer et al., 2011). This could also be occurring in the trachea, as RhoGEF2 can physically interact with Dsh in *Drosophila* S2 cells (Warrington et al., 2013), in which case the core proteins could be acting via Dsh. Interestingly disruption of both RhoGEF2 and RhoA activities in tracheal cells also increases junctional E-cad levels, and increases

the amount of stable junctional E-cad. In addition the loss of either RhoGEF2 or RhoA causes a delay in cell intercalation; and causes similar phenotypes to that of core planar polarity mutants and when endocytosis is inhibited.

Interestingly, in addition to the increase in E-cad at the junctions in core planar polarity mutants, tracheal cells are also lost from the branches as intercalation proceeds. This result initially seems at odds with the data showing that E-cad is increased in the absence of the core proteins, as how can cells leave the branches if they have increased cell-cell adhesion? Therefore the cell intercalation defects cannot be as simple as generally inhibiting endocytosis or increasing the levels of E-cad at junctions. Indeed, reducing endocytosis, and therefore increasing E-cad levels at the junctions does not induce tracheal cell apoptosis (Shaye et al., 2008), which does occur in tracheal cells of the core planar polarity mutants.

Instead the core proteins may be locally altering E-cad junctional turnover in a more subtle way possibly allowing only particular junctions to remodel at one time, ensuring branch integrity is maintained (**Figure 4.11**). Therefore in the core planar polarity mutants the cells may become stressed during cell intercalation due to the increase in E-cad at all junctions and the absence of the local increase in E-cad turnover, as all junctions try to intercalate at once. This may result in cells either not intercalating, or cells apoptosing due to stress. Apoptosis may allow cells to leave the branches as during apoptosis E-cad activity at the junctions is reduced (Steinhusen et al., 2001) leading to less cell-cell adhesion allowing the apoptotic cell to be excluded from the branches (**Figure 4.11**).

If the core proteins were involved in locally promoting cell intercalation on a particular axis by polarising cells, we would expect to see an asymmetric localisation of the core proteins at the junctions, to allow a local increase in turnover. However, despite the core proteins showing asymmetric localisation in the wing and eye (Axelrod, 2001; Bastock et al., 2003; Chae et al., 1999; Feiguin et al., 2001; Shimada et al., 2001; Strutt, 2001b; Strutt and Strutt, 2008; Tree et al., 2002b; Usui et al., 1999), we could not find any evidence for the core proteins being asymmetric in the trachea. However, these results are consistent with other reports and in other dynamic cell rearranging contexts (Chung et al., 2009; Forster and Luschnig, 2012; Nelson et al., 2012), this may mean that asymmetry is either absent in tracheal cells or the asymmetry is transient and hard to observe. Therefore, we cannot rule out a model where the core proteins are uniformly increasing junctional E-cad turnover rather than potentially locally modulating E-cad turnover in the trachea.

In summary the activity of the core planar polarity proteins possibly promotes E-cad endocytosis via Dsh's interaction with RhoGEF2 through the activation of RhoA activity (Levayer et al., 2011), allowing junctional remodelling and cell intercalation to occur. My data suggest a novel role for the core planar polarity pathway in promoting planar-polarised cellular rearrangements through E-cad turnover in the *Drosophila* embryonic trachea.

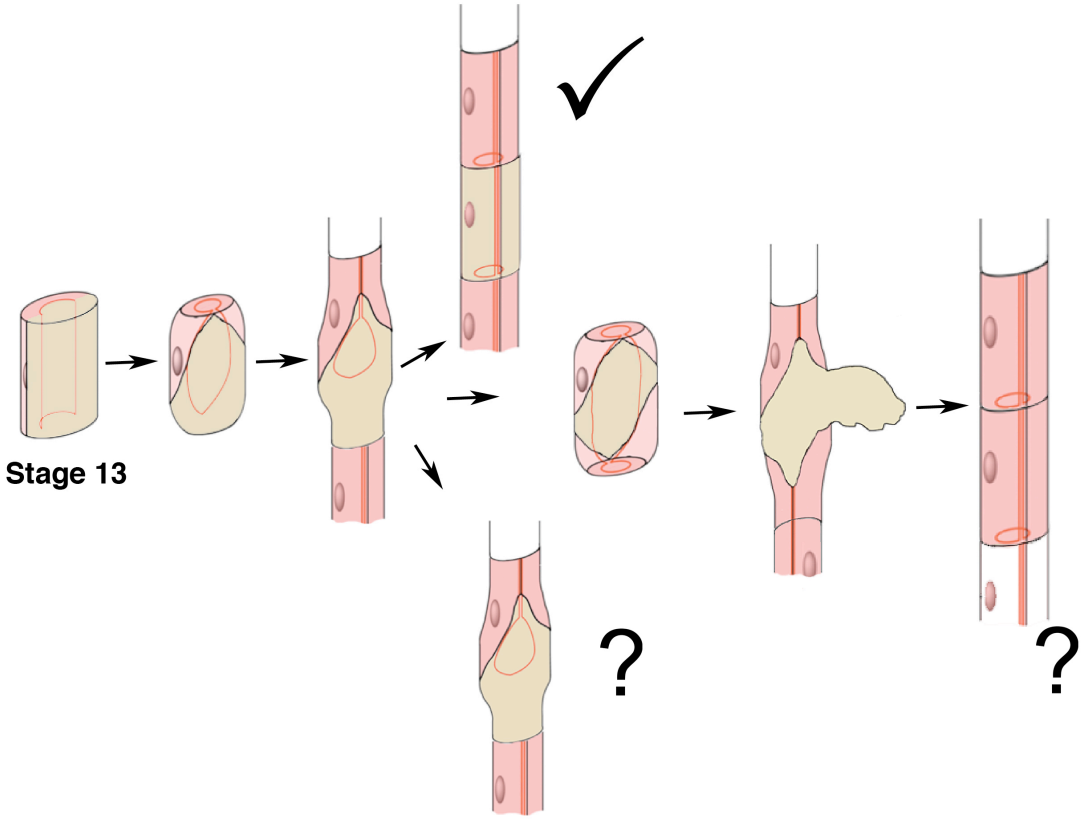

Figure 4.11: Cell intercalation model of how cells in tracheal branches could be excluded from the branches

Stage 13 indicates when the cells are in a paired orientation. Cells then begin to intercalate and would normally form a tube with single cells surrounding a lumen (indicated by black tick, also see Ribeiro et al., 2004). However, in core planar polarity mutants cell intercalation does not proceed as normal and results in cells leaving the branches or cells being unable to intercalate further, models for how this may occur are indicated by question marks. Either the cells become stuck and are unable to intercalate further, or a cell maybe excluded resulting in branches that appear to have undergone cell intercalation.

Chapter 5

Asymmetric core planar polarity protein localisation in the epidermis reduces E-cad stability through the asymmetric localisation of RhoGEF2

Chapter 5

Introduction

Data from Chapter 4 of this work, using tracheal cell intercalation as a model for cell rearrangement, indicate a requirement for activity of the core planar polarity proteins in regulating E-cad protein levels and turnover by acting through RhoGEF2. Removal of E-cad from the cell junctions during cell intercalation is most likely a polarised process (Levayer et al., 2011) to allow some junctions to remodel while others stay attached to their neighbours. In the trachea it was not possible to observe whether the core proteins modulate E-cad trafficking in a polarised manner, therefore the embryonic epidermis was used instead, which is a well characterised model of cell intercalation in which E-cad is asymmetrically planar polarised (Blankenship et al., 2006).

Junctional remodelling is required for cell intercalation in the epidermis

Germ band extension (GBE) occurs during *Drosophila* embryogenesis and requires junctional cell rearrangements and cell intercalation of the ventral-lateral epithelial cells (Irvine and Wieschaus, 1994) but not cell division (Edgar and O'Farrell, 1989; Zallen and Wieschaus, 2004). Epithelial cells converge together on the dorsal-ventral axis and then extend along the anterior-posterior axis allowing the germ band to almost double in length as it extends from the posterior of the embryo (**Figure 5.1** and Irvine and Wieschaus, 1994). Restrained by the vitelline membrane, the germ band curves back on itself and migrates approximately 75% of the embryo length towards the anterior (**Figure 5.1**).

In the epidermis convergent extension involves the rearrangement of junctions between many cells at once. To do this cells form multi-cellular rosettes, where neighbouring cells synchronise junctional rearrangements (Blankenship *et al.*, 2006, and **Figure 1.1a**) in a similar manner to that by which four neighbouring cells rearrange (Compare **Figures 1.7A and 1.7B**). Where ‘type I' vertical cell junctions align along the dorsal-ventral axis, these junctions shrink to form ‘type II' junctions and then new junctions extend along the perpendicular axis to form ‘type III' junctions, and in the epidermis this process is irreversible, (**Figure 1.1a,** Bertet *et al.*, 2004; Reviewed in,Lecuit and Lenne, 2007; Zallen and Blankenship, 2008). This is contrary to what can happen in the *Drosophila* wing where the original junction can re-expand, although this could be due to the lack of dramatic tissue morphogenetic changes in the wing (Classen et al., 2005).

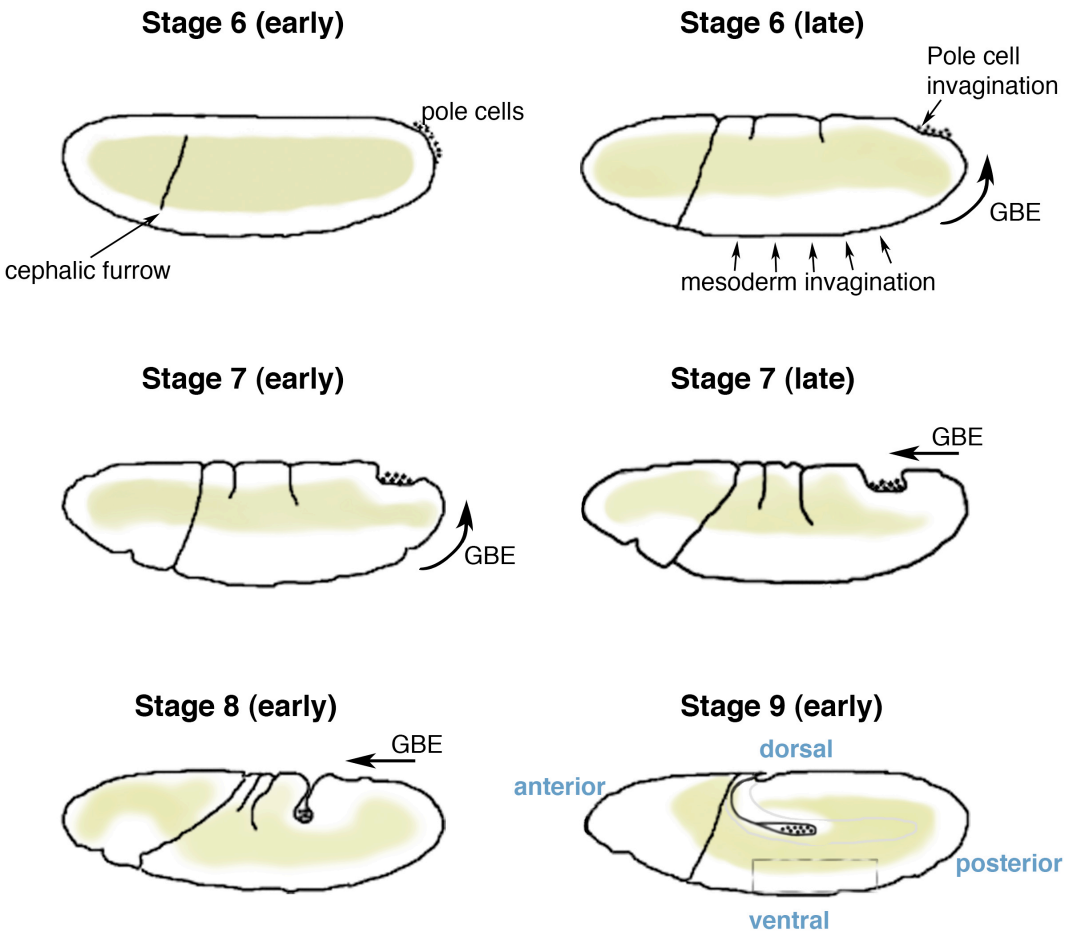

Figure 5.1: Progression of germ band extension from stage 6 to stage 9

Adapted from (Lye and Sanson, 2011). Anterior is left and dorsal is up. Arrows indicate movement of the germ band as the posterior of the embryo elongates and folds over and is constrained by the vitelline membrane (not indicated) and migrates towards the anterior of the embryo. Cells undergoing convergent extension are located on the ventral-lateral sides of the embryo at stage 7. The box in stage 9 indicates the ventral-lateral region of the embryo.

The rearrangement of junctions through cell intercalation is thought to require the modulation of cell adhesion between cells, in order for cells to exchange neighbouring junctions (Wirtz-Peitz and Zallen, 2009). The adherens junctions are principally comprised of the adhesion protein E-cad, and the cytosolic proteins Arm and α-Cat, all three proteins are required for cell intercalation in the epidermis as discussed in Chapter 4. During GBE in the ventral-lateral region (**Figure 5.1** see stage 9), junctional E-cad protein is planar polarised (Blankenship et al., 2006) and increased on the horizontal junctions (aligned along the anterior-posterior axis). This polarisation of E-cad localisation is thought to occur by locally increasing E-cad endocytosis on the vertical junctions (aligned along the dorsal-ventral axis) (Levayer et al., 2011), and through recycling of E-cad, which is increased on the vertical junctions in the wing (Levayer et al., 2011). E-cad is recycled back to the junctions through Rab11 containing endosomes (Classen et al., 2005), and this delivery is polarised via increased Sec5 mediated exocyst activity at the vertical junctions (Classen et al., 2005). These processes increase E-cad turnover and reduces E-cad stability (de Beco et al., 2009; Georgiou et al., 2008; Leibfried et al., 2008; Levayer et al., 2011).

Models of junctional rearrangement in which E-cad modulation is required

Several models describe how epithelial cellular rearrangements could be occurring during GBE by modulating E-cad levels and turnover. A model put forward by Levayer *et. al.* (2011) proposes that E-cad localisation is polarised through increased Clathrin mediated endocytosis at vertical junctions (Levayer et al., 2011). For this to occur, the formin Diaphanous (Dia) and the non-muscle myosin, MyosinII (MyoII) are recruited to the vertical junctions (Levayer et al., 2011). Their activities and localisation are controlled by the guanine exchange factor RhoGEF2, which is also planar polarised and increased at vertical junctions (Levayer et al., 2011). Dia and MyoII are proposed to be required for E-cad turnover by increasing clustering of E-cad complexes. The E-cad complex clusters are then thought to recruit AP2 and the Clathrin coat proteins to promote endocytosis. Increasing E-cad turnover on the vertical junctions is proposed to cause preferential shrinkage of those junctions in a MyoII dependent manner (Levayer et al., 2011).

A second mechanism by which cell rearrangement is controlled involves the Abelson kinase. In *Drosophila*, Abelson kinase (Abl) is localised to the vertical epithelial adherens junctions (Fox and Peifer, 2007) and is involved in promoting endocytosis of Arm and also E-cad in intercalating cells (Tamada et al., 2012). Abl is known to phosphorylate Arm at cell junctions that are shrinking (Tamada et al., 2012).

This phosphorylation appears to be important for Arm removal from the junctions, as in Arm mutants that cannot be phosphorylated, Arm remains at the junctions (Tamada et al., 2012), resulting in defects in multi-cell rosette formation during cell intercalation and disrupted GBE (Tamada et al., 2012). As Arm is planar polarised and localises to the horizontal junctions in the epidermis (Blankenship et al., 2006), Abl kinase could be locally altering Arm dynamics and polarising cell adhesion. Arm and E-cad interact at the junctions (Huang et al., 2011); (Drees et al., 2005; Yamada et al., 2005) therefore Abl could be indirectly affecting E-cad turnover at the junctions.

E-cad turnover is also modulated by Src kinases at junctions in the *Drosophila* epidermis (Shindo et al., 2008; Takahashi et al., 2005; Thomas and Brugge, 1997). There are two known Src family kinases (SFKs); *Src42A* and *Src64B* both are expressed in the epidermis. Src, a non-receptor protein tyrosine kinase, is localised to adherens junctions in a complex with E-cad and Arm (Takahashi et al., 2005). Src is proposed to affect cell intercalation by modulating E-cad levels in two opposite ways. Firstly, it is thought to reduce E-cad levels at the junctions, by increasing E-cad endocytosis (Behrens et al., 1993; Fujita et al., 2002). Secondly, Src activates Arm, which traffics to the nucleus and activates E-cad transcription, thereby increasing the levels of E-cad at the junctions (Peifer et al., 1991). Src is therefore likely to be involved in increasing turnover of E-cad at the junctions during junctional remodelling.

Interestingly, in vertebrates the RhoGEF2-related protein PDZ-RhoGEF can be recruited to the junctions by the vertebrate homolog of Fmi, known as Celsr1 and acts with DAAM1 to regulate cell adhesion in neuro-epithelial cells (Nishimura et al., 2012). In *Drosophila*, RhoGEF2 can directly interact with the core protein Dsh (Warrington et al., 2013). Therefore, there is evidence on which to base a model where the core polarity proteins could be modulating E-cad turnover through localising the activity of RhoGEF2, which, through RhoA, activates other downstream pathways. Although this model is attractive, the other models could also explain how cell adhesion is modulated to allow cell intercalation to occur.

Core proteins regulate cell-cell adhesion

In vertebrates, the core proteins have been implicated in regulating cell-cell adhesion as, in the absence of the core protein Pk, local adhesion forces at the junctions are increased; suggesting Pk normally reduces cell adhesion in this context (Oteiza et al., 2010). In the vertebrate neural tube the Stbm homologue, Vang-like2 (Vangl2) is required to positively regulate cell-cell adhesion and is proposed to polarise Rac1 localisation. Overexpression of Vangl2 disrupts cell-cell adhesion in tissue culture

cells (Lindqvist et al., 2009) and removal of Rac1 in a Vangl2 over-expression background restores cell-cell adhesion (Lindqvist et al., 2009).

There is further evidence, which implicates the core proteins in modulating cell adhesion in the *Drosophila* wing, where the inhibition of endocytosis causes holes to form in the tissue during cell rearrangements, as cell adhesion modulation is reduced (Classen et al., 2005). Interestingly, the core polarity mutants enhance the formation of these holes (Classen et al., 2005), suggesting that core proteins normally promote the turnover of adhesion complexes in the wing. However, the core protein mutants alone do not cause holes to form in the wing. Therefore, the core proteins are not involved in cell-cell adhesion but may be involved in polarising the turnover of cell adhesion molecules.

As the core proteins exhibit asymmetric localisation in the wing as well as in other *Drosophila* epithelial tissues, the core proteins could be locally activating cell adhesion where the core proteins are localised.

As the core proteins modulate E-cad trafficking in the *Drosophila* trachea, and E-cad trafficking is important for germband elongation, we decided to investigate whether the core proteins modulate E-cad localisation in the germband and whether this depends on the asymmetric localisation of the core proteins.

The *Drosophila* epidermis was initially discounted as a suitable model to characterise core protein asymmetry, because it was reported that the core proteins are not visibly asymmetric when epithelial cells are intercalating during GBE, and during dorsal closure (Kaltschmidt et al., 2002; Morel and Arias, 2004). In addition, the core planar polarity mutants do not exhibit obvious defects in GBE (Zallen and Wieschaus, 2004). Conversely, late embryonic epithelial cells producing actin denticles, have been shown to exhibit planar polarised core protein localisation (Price et al., 2006). Therefore, it is possible that there is subtle asymmetry at earlier times in development, which could be detected by more quantitative methods.

Aims

The aim of this chapter was to establish if core polarity proteins are required for polarised E-cad endocytosis during cell intercalation in the epidermis, and if polarised E-cad is essential for cell intercalation during GBE. In addition, I aimed to investigate which pathways the core proteins act to modulate E-cad localisation and turnover.

Note: All the wing images in this chapter were dissected and immunostained by Helen Strutt, but the wings were imaged and the fluorescent intensity junctional measurements quantified by Samantha Warrington.

Results

Core proteins are asymmetrically localised in polarising cells in the epidermis

In contrast to previous reports (Price et al., 2006; Shaye et al., 2008), the core proteins Fz, Stbm and Fmi show planar polarised asymmetry in epidermal cells (**Figure 5.2A''-C',C''**). At stage 8, when the epithelium is still polarising and there are no mature adherens junctions or septate junctions, Frizzled is subtly increased on the vertical junctions (crossing the anterior-posterior axis) compared to horizontal junctions (crossing the dorsal-ventral axis) (**Figure 5.2A"-B**). Furthermore, by stage 15, when intercalation has finished, and the epithelium is fully polarised, with mature adherens and septate junctions, the asymmetry of the core proteins is even more pronounced (**Figure 5.2C**, Price *et al.*, 2006).

E-Cad asymmetric localisation is lost in core polarity mutants

E-cad asymmetry increases over time and by stage 14, when the adherens junctions have matured, the asymmetry of E-cad can now be seen clearly without quantification (**Figure 5.2A',C**). Interestingly this enrichment of endogenous E-Cad on the horizontal junctions is lost in the core polarity mutants (**Figure 5.2D**) and instead E-cad levels increase at all cell junctions (**Figure 5.2D**). This suggests the core proteins are required for the polarised localisation of junctional E-cad in intercalating epithelial cells.

Strikingly this difference in E-cad junctional stability on the horizontal and vertical junctions is lost in the core polarity mutants, (*fz*^{P21}*, stbm*^{6}*, dsh*^{1} and *fmi*^{E59}) (**Figure 5.3B-E**) and in ventral-lateral regions of the embryo at stage 15 epithelial cells over-expressing Fz (**Figure 5.3F-G**). This again indicates that E-cad is preferentially stabilised at the horizontal junctions and removed from the vertical junctions and this increase in turnover requires polarised core proteins.

The asymmetric localisation of junctional RhoGEF2 in the epidermis is lost in core polarity mutants

In epithelial cells the asymmetric localisation of E-cad requires RhoGEF2 (Levayer et al., 2011). RhoGEF2 localisation is increased on the vertical junctions at the same location as the core proteins (**Figure 5.2E-G**), a reciprocal localisation to that of E-cad (**Figure 5.2A**, Blankenship *et al.*, 2006; Levayer *et al.*, 2011). Intriguingly this enrichment of RhoGEF2 on the vertical junctions is also abolished in *fz* mutants and the remaining RhoGEF2 is less tightly localised to the junctions (**Figure 5.2F-G**).

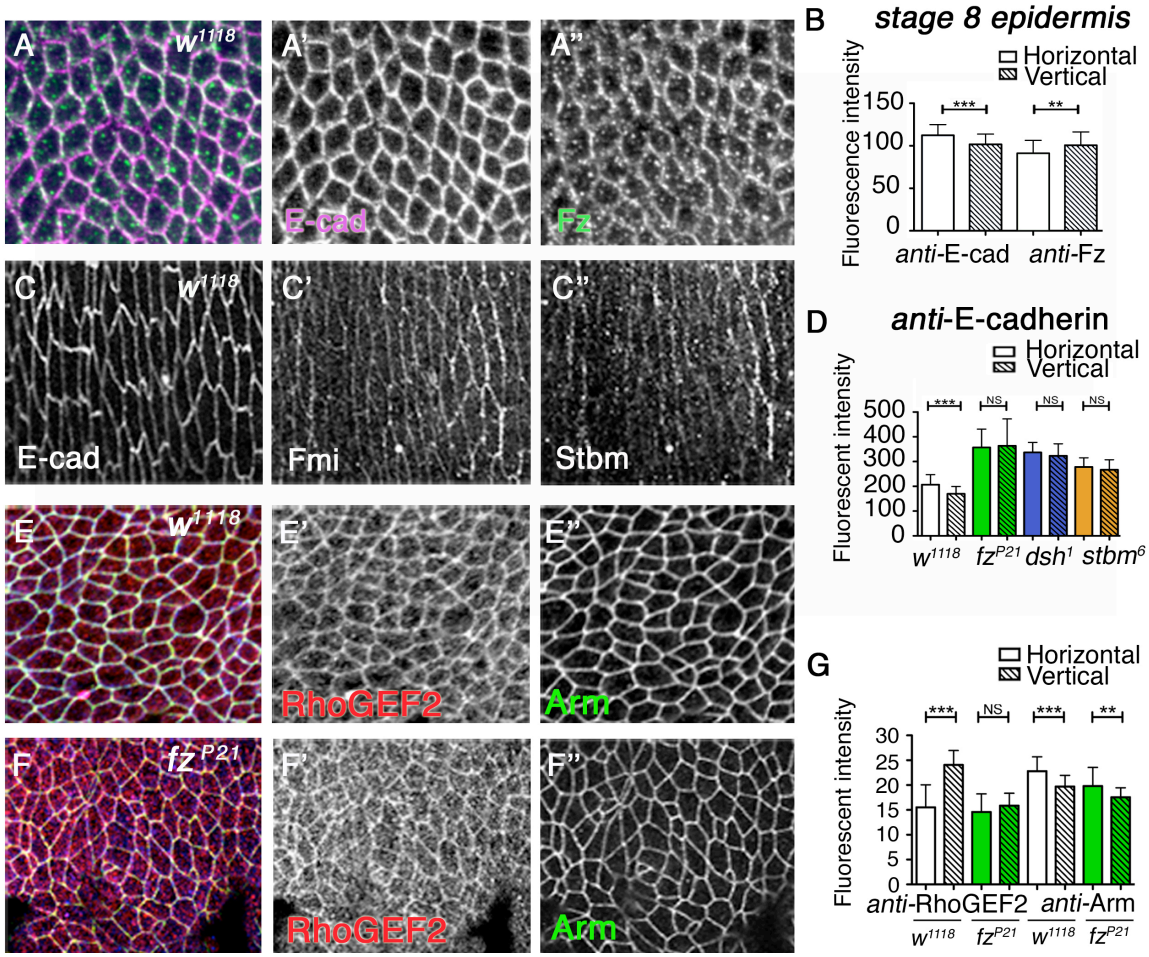

Figure 5.2: The core proteins are required for the planar asymmetric localisation of E-cad and RhoGEF2 in the embryonic epidermis

(A-A'') Wild-type (w^{1118}) stage 8 ventral-lateral epidermis, labelled for E-cad (Magenta in A and white in A') and Fz (green in A and white in A''). (B) Quantification of fluorescent intensity at the vertical and horizontal junctions in stage 8 ventral-lateral cells in w^{1118}. Stars indicate results of a Student's T-test comparing horizontal and vertical junctions, Fz P=0.0035**, E-cad P≤0.0001***. (C-C'') Localisation of (C) E-cad, (C') Fz and (C'') Stbm in the ventral-lateral epidermis of stage 15 w^{1118} embryos. (D) Quantification of endogenous E-cad fluorescent intensity at horizontal and vertical junctions in stage 15, w^{1118} embryos (white) and fz^{P21} (green), dsh^{1} (blue) and $stbm^{6}$ (orange). ANOVA test comparing the horizontal intensity mean values of mutants to w^{1118} gives P≤0.0001. Asterisks show individual results from a Bonferroni multiple comparison test. (NS= not significant, P<0.05*, P<0.01**, P<0.0001***). (E-F'') Localisation of RhoGEF2 (red in E, F and white in E', F') and Arm (green in E,F, white in E'', F'') in (E-E'') w^{1118} and (F-F") fz^{P21} ventral-lateral cell junctions in stage 8 embryos. (G) Quantification of fluorescent intensity of RhoGEF2 and Arm (white bars indicate w^{1118} and green bars indicate fz^{P21}) at non ventral-lateral junctions of stage 8 embryos. T-test comparing horizontal and vertical junctions. RhoGEF2 in w^{1118} P<0.0001*** and fz^{P21} P=0.26, Arm in w^{1118} P<0.0001 and in fz^{P21} P=0.0035**. Error bars s.d.

As RhoGEF2 is required for regulating E-cad asymmetry, RhoGEF2 might also be required for correct E-cad turnover at junctions, and a loss of E-cad stability may be expected if RhoGEF2 function is removed. Indeed, FRAP of Ubi-E-cad-GFP in an antimorphic *RhoGEF2* background (Levayer et al., 2011) resulted in E-cad stability no longer being polarised at the cell junctions (**Figure 5.3H**).

E-Cad stability in the epidermis is polarised through activity of core polarity proteins

The enrichment of E-cad at horizontal junctions suggests E-cad is more stable at those junctions compared to vertical junctions. To confirm this, FRAP was carried out on E-Cad-GFP expressed under the control of a ubiquitous promoter (here after named Ubi-E-cad-GFP) in stage 8 ventral epidermal cells to (see Chapter 2 and 3 for detail and discussion of FRAP). In wild-type epithelial cells junctional Ubi-E-cad-GFP shows less recovery on horizontal junctions than on vertical junctions (**Figure 5.3A**), suggesting that horizontal junctions have a larger stable fraction of E-cad.

It is worth noting that in the core mutants the amount of Ubi-E-cad-GFP at the junctions is decreased relative to that at wild-type junctions (**Figure 5.3I**). This is in contrast to the level of endogenous E-cad, which is increased in the core mutants (**Figure 4.6A**). This maybe because E-cad-GFP is less able to compete for junctional access compared to E-cad, and therefore E-cad-GFP is decreased at the junctions in the presence of increased E-cad. Nevertheless the important result is that the difference in E-cad stability between the vertical and horizontal junctions is lost in the core polarity mutants (**Figure 5.3B-E**).

To circumvent the reduced E-cad expression seen at the junctions with the Ubi-E-cad-GFP construct, an E-cad::GFP knock in was obtained (Huang et al., 2009), which tagged the endogenous E-cad. FRAP was performed on endogenous E-cad::GFP heterozygotes, which confirmed there was still a difference between the vertical and horizontal E-cad junctional recovery (**Figure 5.3J**). This difference in E-cad::GFP stability was lost in a *dsh*^{1} mutant (**Figure 5.3K**). Therefore both Ubi-E-cad-GFP and the E-cad::GFP knock in give the same overall result; that E-cad is less stable on the vertical junctions in a wild-type background compared to horizontal junctions and this reduced stability of junctional E-cad of the vertical junctions is lost in the core polarity mutants.

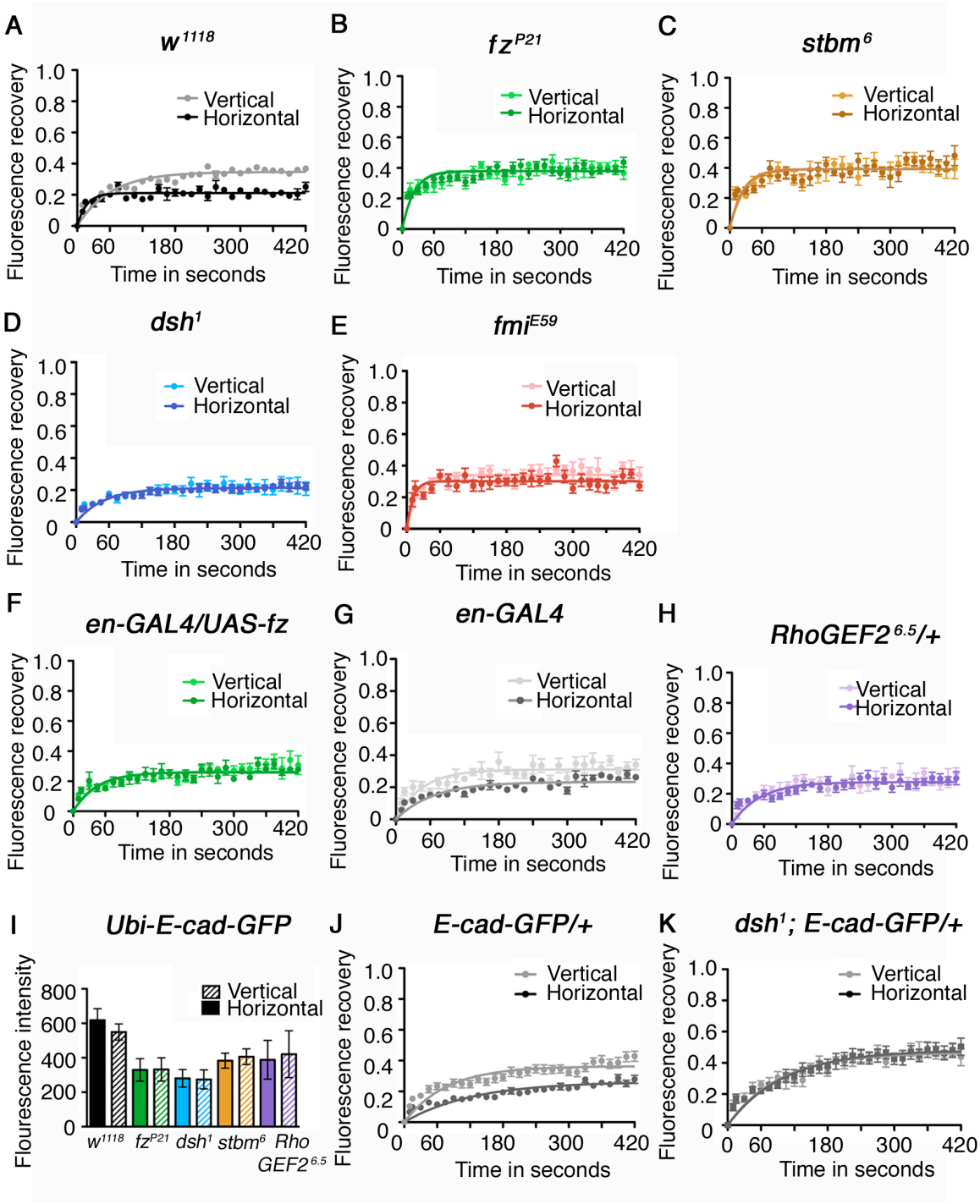

Figure 5.3: E-cad asymmetric junctional stability is lost in core polarity mutants

(Figure legend on next page)

Figure 5.3: E-cad asymmetric junctional stability is lost in core polarity mutants

Graphs show FRAP analysis of E-cad-GFP expressed under the control of the Ubiquitin promoter in stage 8 epithelial cells, except where indicated. Comparing horizontal and vertical junctions using students T-test (A) wild-type (w^{1118}) (P≤0.0001), (B) fz^{P21} (P=0.28), (C) $stbm^{6}$ (P=0.13), (D) dsh^{1} (P=0.83), (E) fmi^{E59} (P=0.13), (F) *en-Gal4/UAS-fz* at stage 15 ventral-lateral side of the embryo (P=0.064) (G) *en-Gal4* control at stage 15 ventral-lateral side of the embryo (P≤0.0001), (H) $RhoGEF2^{6.5}$/+ antimorph (P=0.084). (I) Intensity measurements of Ubi-E-cad-GFP in the epidermis at stage 8, on vertical and horizontal junctions in wild-type (w^{1118} black bars), and the core polarity mutant's fz^{P21} (green bars), dsh^{1} (blue bars), $stbm^{6}$ (orange bars) and $RhoGEF2^{6.5}$/+ (purple bars). Note that the increase in E-cad on the horizontal junctions is lost in the core polarity mutants, but the level of E-cad in the mutants is also reduced. This may be due to competition between the endogenous and tagged forms of E-cad. (J-K) FRAP analysis of E-cad::GFP expressed under its endogenous promoter, with one copy of E-cad::GFP and one copy of the wild-type E-cad either (J) in the wild-type background or (K) in a dsh^{1} mutant background. In the wild-type background E-cad has a larger stable fraction on the horizontal junctions compared to the vertical junctions (compared using Student's t-test P≤0.0001). But this increase is lost in the dsh^{1} mutant (compared using Student's t-test P=0.63).

The core polarity proteins are required for the asymmetric localisation of Zipper and Bazooka, but not Arm, at the junctions in the epidermis

Other apical junctional proteins required for cell rearrangements during GBE also exhibit planar polarised cell-junctional localisation (Bertet et al., 2004; Blankenship et al., 2006; Levayer et al., 2011; Zallen and Wieschaus, 2004). The *Drosophila* protein Bazooka (Baz)/Par3, like E-cad, is increased on the horizontal junctions (**Figure 5.4A,** Zallen and Wieschaus, 2004). However, Zipper (Zip), which encodes the Myosin-II heavy chain (Young et al., 1993), is enriched on the vertical junctions (**Figure 5.4B** and Zallen and Wieschaus, 2004). Interestingly, the asymmetries of Baz and Zip are lost in the core polarity mutants (**Figure 5.4A-B**). This suggests that the polarisation of Baz and MyoII localisation at the junctions requires input from the core proteins.

Arm is asymmetrically enriched at the same location as E-cad (**Figure 5.2G**, Blankenship *et al.*, 2006). Surprisingly the asymmetric localisation of Arm remains unchanged in the core polarity mutants (**Figure 5.2G**).

Src kinase acts in a parallel polarity to the core polarity proteins

To ascertain if Src kinase was involved in the asymmetry of junctional E-cad in the epidermis, E-cad::GFP was examined in the epidermis in the $Src42A^{F80}$ mutant, which is null for the kinase activity of Src42A, although protein levels and localisation is unaffected (Forster and Luschnig, 2012). In the $Src42A^{F80}$ mutant, E-cad was still present at the junctions, although large aggregates of E-cad::GFP could be seen at some junctions (**Figure 5.5B'**). Moreover, FRAP of E-cad::GFP at the vertical and horizontal junctions in the $Src42A^{F80}$ mutant (avoiding the large clumps of junctional E-cad, **Figure 5.5C**) showed that E-cad still exhibited asymmetric junctional stability, with more stable E-cad on the horizontal junctions (**Figure 5.5C**). It is worth noting that there is an increase in the amount of E-cad::GFP recovery at all junctions in the $Src42A^{F80}$ mutant compared to wild-type (compare **Figure 5.3A** to **Figure 5.5C**), therefore E-cad is still asymmetrically polarised in the Src42A mutant but there is a smaller stable fraction.

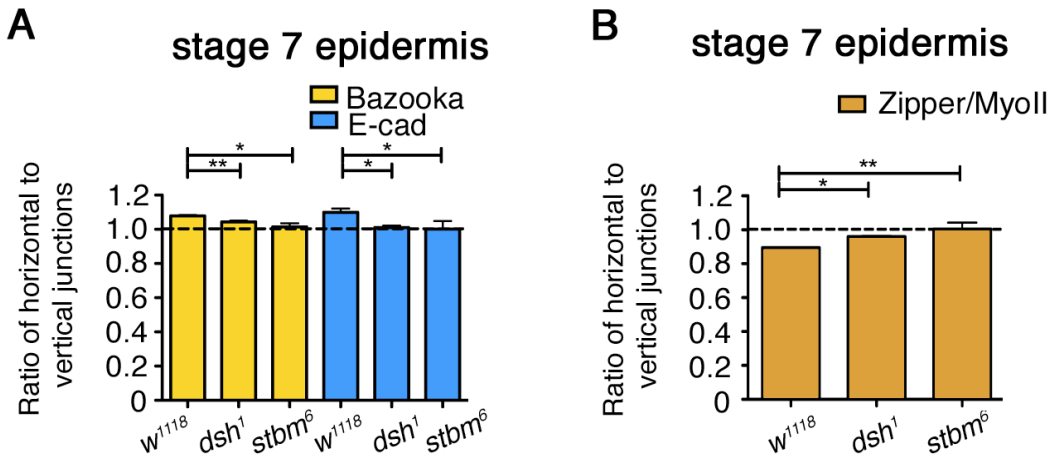

Figure 5.4: Asymmetric localisation of Baz and Zipper is lost in core polarity mutants

(A) Quantified asymmetric localisation of Bazooka (yellow bars), and E-cad (blue bars) on horizontal and vertical cell junctions of the ventral-lateral embryonic epidermis in wild-type (w^{1118}), dsh^{1} and $stbm^{6}$ mutants at stage 7. Shown as a ratio of horizontal to vertical junctional intensity, a value of 1 equals symmetric localisation. (B) Quantified asymmetric localisation of Zipper in stage 7 ventral-lateral embryonic epidermis in w^{1118}, dsh^{1} and $stbm^{6}$ mutants. Asterisk above each bar indicates single results from the Dunnett's multiple comparison tests (*P≤0.05, **P≤0.01).

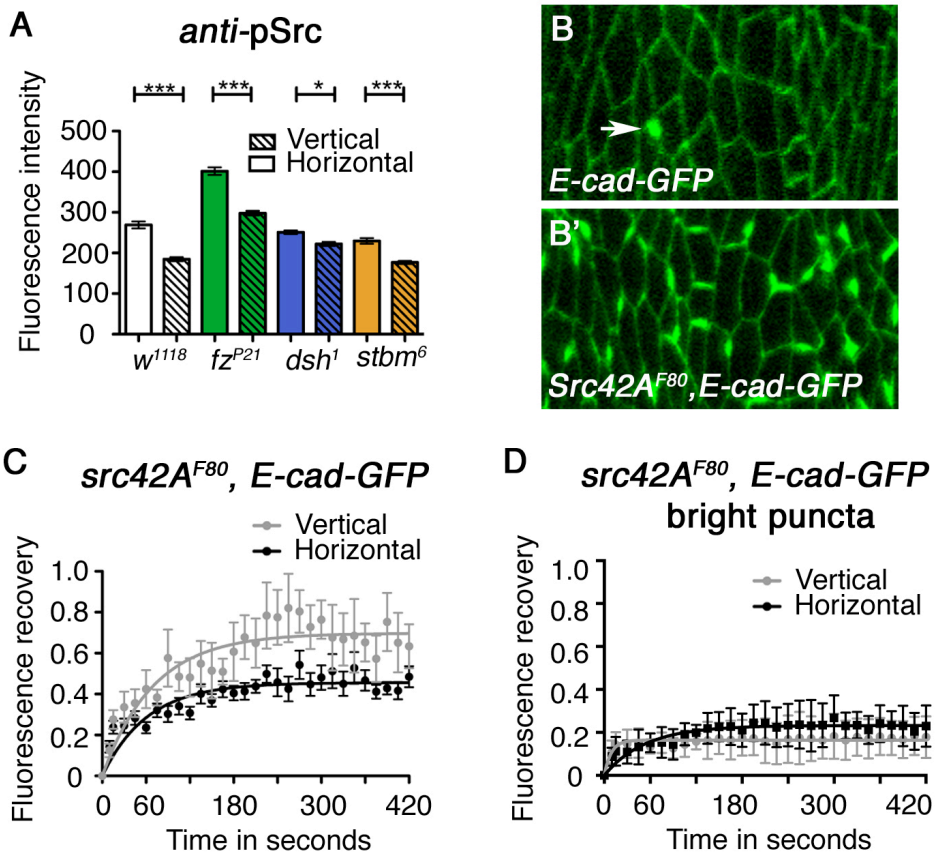

Figure 5.5: The effect of Src on E-cad turnover in the epidermis is not required for the asymmetric localisation and stability of E-cad

(A) Quantified fluorescent intensity of pSrc at apical junctions on vertical and horizontal junctions, in w^{1118} (white bars), fz^{P21} (green bars), dsh^{1} (blue bars), $stbm^{6}$ (orange bars). pSrc remains higher on horizontal compared to vertical junctions in the absence of core protein activity, although the overall levels of pSrc do increase. Src asymmetry therefore does not require the core proteins to asymmetrically localise. The additional Src may be recruited by E-cad at the horizontal junctions in core polarity mutant backgrounds, consistent with the previous reports on interactions between Src and E-cad (Takahashi et al., 2005). ANOVA comparing all intensities shows that there is variation in intensities, P<0.0001***. Asterisks above the chart show individual results from the ANOVA P=0.0123* P≤0.0001***. (B-B') Endogenous E-cad::GFP localisation in stage 8 ventral-lateral epidermal cells in (B) wild-type (w^{1118}), (B'') $Src42^{F80}$ zygotic mutant. Arrow indicates a sensory organ precursor. (C) FRAP analysis of vertical and horizontal junctions in $Src42A^{F80}$ mutants in regions of the junctions containing E-cad-EGFP but away from the large aggregates of E-cad at the junctions. E-cad recovery still shows a difference between vertical and horizontal junctions in Src42A mutant embryos (Student's t-test P≤0.0001***). (D) FRAP analysis on the bright puncta seen in B'. E-cad in these bright puncta is more stable, but there is still a difference in stability between the horizontal and vertical junctions (compare black and grey lines in D, Student's t-test P≤0.0001***).

These results are in contrast to a previous report where E-cad stability in the embryonic trachea was increased in the *Src42A*^{F80} mutant (Forster and Luschnig, 2012). Interestingly, FRAP of the large aggregates of E-cad::GFP seen in the membranes (**Figure 5.5B'**) showed that they were more stable (**Figure 5.5D**). This suggests that Src42A is normally active in a subset of the junctions, to decrease E-cad turnover but not to polarise it.

In the epidermis active phospho-Src is asymmetrically localised to the vertical junctions (**Figure 5.5A**) and this asymmetry remains in core polarity mutants (**Figure 5.5A**), suggesting that the core proteins are not required for Src asymmetry in the epidermis. Next we checked if Src was instead acting upstream of the core proteins. Src42A increases E-cad transcription at the cell junctions (Forster and Luschnig, 2012), therefore if Src acted through the core pathway then the core proteins would also increase E-cad turnover. However, the core mutants do not alter E-cad transcription in the trachea (**Figure 4.6C**). This indicates that Src is not acting upstream of the core proteins to alter E-cad transcription at least in the trachea, therefore suggesting that Src and the core proteins act in parallel to regulate E-cad turnover at the junctions.

Core proteins regulate polarised distribution of E-cad in the pupal wing

As in the epidermis, E-cad is also asymmetrically localised in 28hr wing cells and is subtly but significantly increased on horizontal junctions, which cross the anterior-posterior axis of the wing (**Figure 5.6A',B**). Furthermore, E-cad asymmetric localisation at 28hr is lost in the core polarity mutants *stbm*^{6}, *fz*^{P21} and *fmi*^{E59} (**Figure 5.6A-I**), indicating that in the wing the core proteins are also required for E-cad asymmetry.

In the wing the asymmetric localisation of E-cad is reciprocal to the localisation of Fmi and Stbm, which is increased on the vertical (crossing the proximal-distal) junctions in 28hr in pupal wing cells (**Figure 5.7C**). Interestingly, at earlier time points (20hr and 24hr) Fmi still shows significant polarised localisation, whereas the asymmetric localisation of E-cad is absent or reduced respectively (**Figure 5.7A-B**). Therefore E-cad asymmetry increases as core protein asymmetry increases. As in the epidermis, FRAP of Ubi-E-cad-GFP in the wing showed that E-cad stability is increased on the horizontal junctions compared to the vertical junctions (**Figure 5.8 A**), and this asymmetric stabilisation is lost in core protein mutants (**Figure 5.8B-C**).

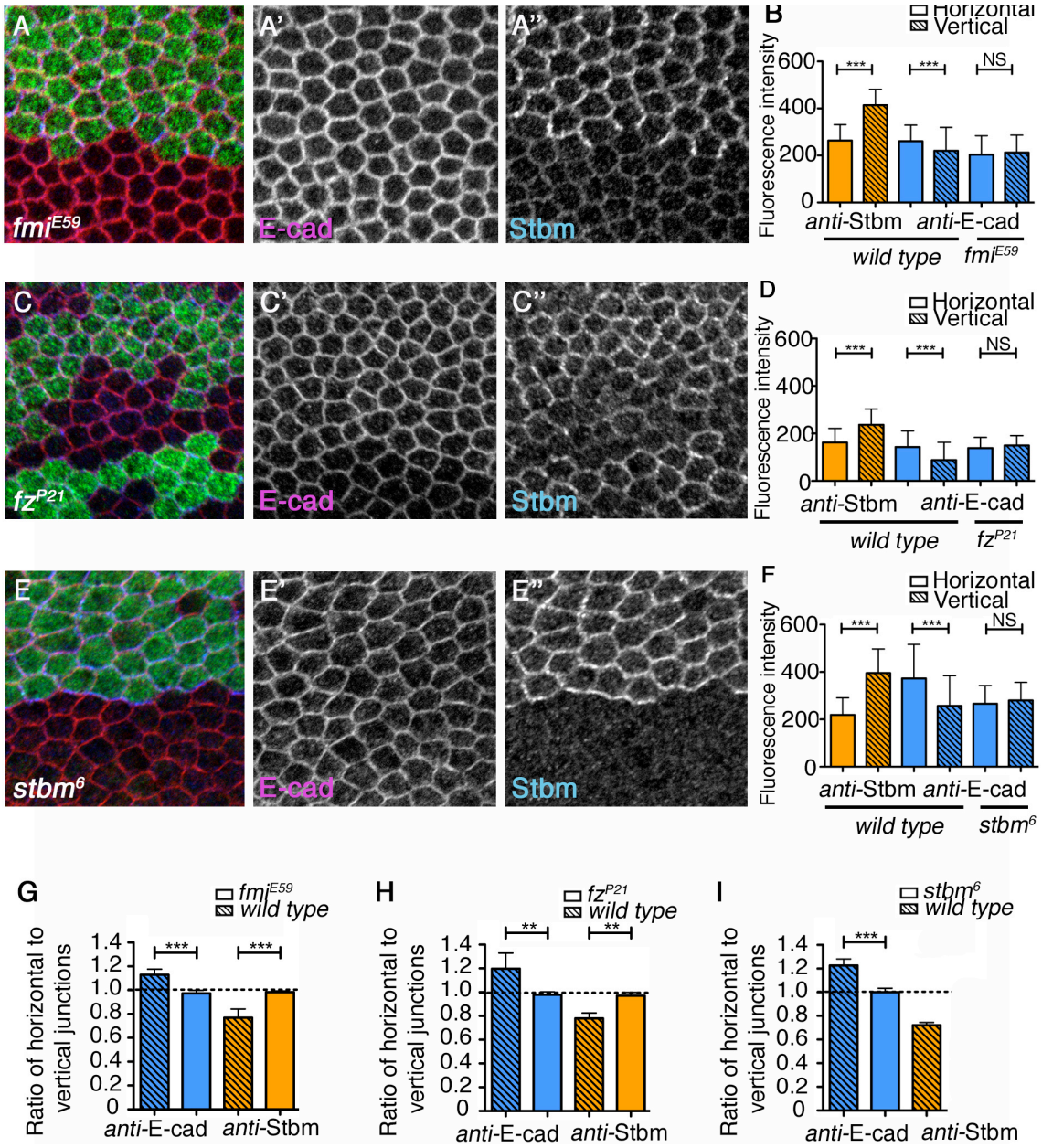

Figure 5.6: Core polarity proteins affect E-cad localisation in the wing

(A-A'', C-C'', E-E''') Core polarity mutant clones (A-A'') *fmi*^{E59}, (C-C'') *fz*^{P21} and (E-E'') *stbm*^{6}, immunostained for E-cad (magenta in A, C, E, white in A', C', E') and Stbm (blue in A, C, E, white in A'', C'', E''). Clones are indicated by the absence of *lacZ* expression in green. Distal is to the right. (B) Quantification of A-A'' for the localisation of Stbm (orange bars), E-cad in wild-type and inside *fmi*^{E59} clonal cells. (D) Quantification of C-C'' for the localisation of Stbm (orange bars in wild-type cells, E-cad in wild-type and inside *fz*^{P21} clonal cells. (F) Quantification of E-E'' for the localisation of Stbm (orange bars in wild-type, E-cad in wild-type and inside *stbm*^{6} clonal cells. (G-I) Ratios of the fluorescent intensity of E-cad and Stbm on horizontal and vertical junctions in *fmi*^{E59}, *fz*^{P21}and *stbm*^{6} mutants compared to wild type, a value of 1 indicates symmetric junctional localisation. An increase in the ratio above 1 indicates a higher intensity of fluorescence is on the horizontal junctions. A decrease in the ratio indicates that there is more fluorescence on the vertical junctions.

Next, the localisation of RhoGEF2 was examined to see if it is also asymmetrically localised in wing cells. Indeed this was found to be the case; RhoGEF2 is increased on the proximal-distal junctions in the wing (**Figure 5.9A', B**), localising to the same junctions as the core proteins. In the absence of core proteins, RhoGEF2 asymmetry at the cell junctions is lost (**Figure 5.9**). Therefore, as in the epidermis, the activity of the core proteins is required to polarise RhoGEF2 localisation in wing cells.

Interestingly, an increase in core protein activity can recruit excess RhoGEF2 to the junctions. Overexpression of Pk, can increase the clustering of the core complexes at the cell junctions (Bastock et al., 2003; Feiguin et al., 2001; Shimada et al., 2001; Tree et al., 2002b). Pk over-expression was therefore used to see if RhoGEF2 could also be recruited to the cell junctions. This was indeed found to be the case (**Figure 5.10A'', B**). This suggests that the asymmetric localisation of RhoGEF2 is a direct result of RhoGEF2 being asymmetrically recruited to the junctions by the core proteins.

RhoGEF2 is also required in the wing for asymmetric localisation of E-cad at the junctions as reducing RhoGEF2 using RNAi results in a loss of E-cad asymmetry (**Figure 5.10C-D**). However, despite the loss of RhoGEF2 in the wing cells, there is no significant impact on cell packing, which could be expected if the adhesion properties of these cells had been significantly affected (**Figure 5.10E**).

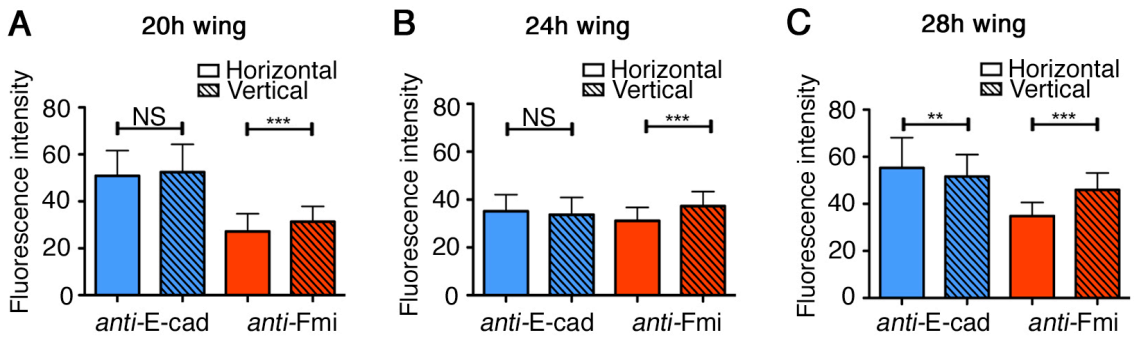

Figure 5.7: E-cad asymmetry increases as Fmi becomes more asymmetric in the pupal wing

(A-C) Quantification of the junctional fluorescence intensity of E-cad (blue bars) and Fmi (red bars) on horizontal and vertical junctions in pupal wings at: (A) 20hr, (B) 24hr, (C) 28hr. Intensities of E-cad on horizontal and vertical junctions were compared using Student's t-test (NS = not significant, P<0.05*, P<0.01**, P<0.0001***). Error bars are s.d.

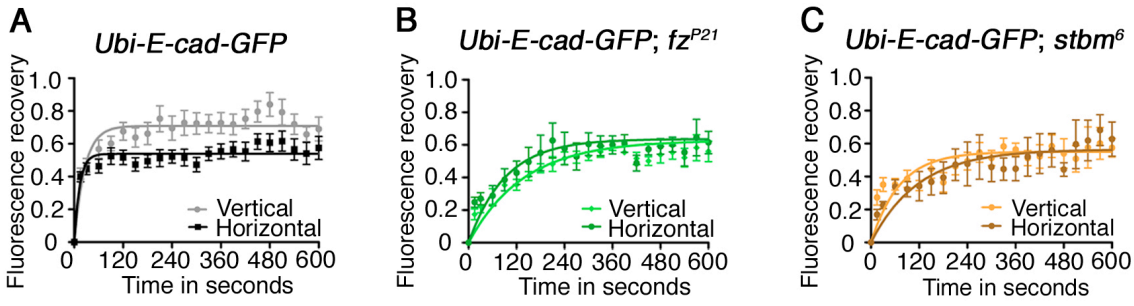

Figure 5.8: FRAP analysis of Ubi-E-cad-GFP on dorsal-ventral and proximal-distal junctions in the wing

(A) FRAP analysis of junctions in wild-type pupal wings at 28hr, showing a difference between horizontal and vertical junctions. (B-C) This asymmetry is lost in the (B) fz^{P21} mutant and the (C) $stbm^{6}$ mutant. Student's T-test comparing the plateau values for horizontal and vertical junctions: w^{1118} P≤0.0001***, fz^{P21} P=0.79, $stbm^{6}$ P=0.36. Error bars are s.e.m.

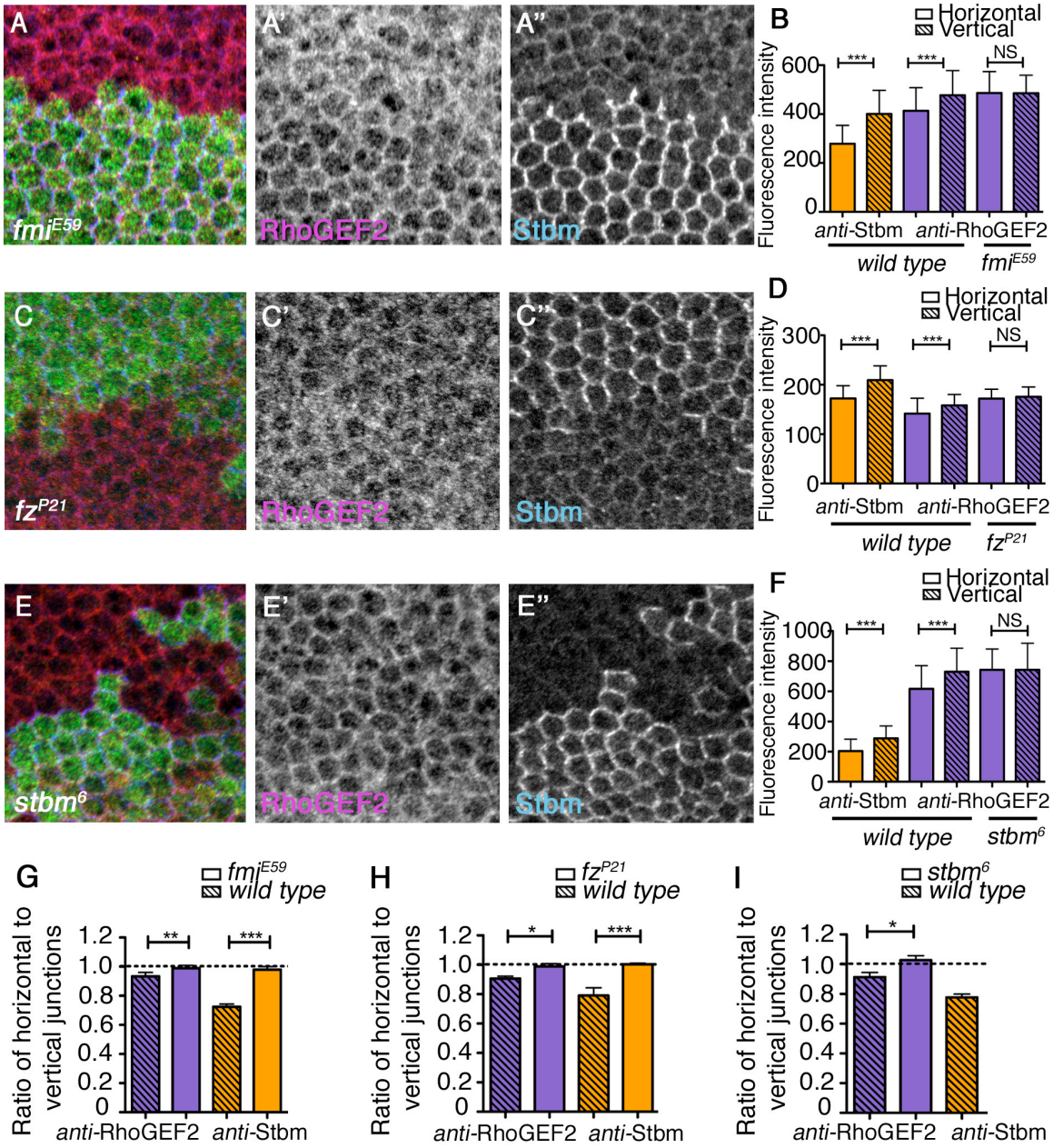

Figure 5.9: Core polarity proteins affect RhoGEF2 localisation in the wing

(A-A'', C-C'', E-E'') Core polarity mutant clones (A-A'') *fmi*^{E59}, (C-C'') *fz*^{P21} and (E-E'') *stbm*^{6}, immunostained for E-cad (magenta in A, C, E, white in A', C', E') and Stbm (blue in A, C, E, white in A'', C'', E''). Clones are indicated by the absence of *lacZ* expression in green. Distal is to the right. (B) Quantification of A-A'' for the intensity of: Stbm (orange bars) in wild-type, RhoGEF2 in wild-type and inside *fmi*^{E59} clonal cells. (D) Quantification of C-C'' for the localisation of Stbm (orange bars) in wild-type. RhoGEF2 in wild-type and inside *fz*^{P21} clonal cells. (F) Quantification of E-E'' for the localisation of Stbm (orange bars) in wild-type. RhoGEF2 in wild-type and inside *stbm*^{6} clonal cells. (G-I) Ratios of the fluorescent intensity of RhoGEF2 and Stbm on horizontal and vertical junctions in *fmi*^{E59}, *fz*^{P21} and *stbm*^{6} mutants compared to wild-type, a value of 1 indicates symmetric junctional localisation. An increase in the ratio above 1 indicates a higher fluorescent intensity on the horizontal junctions. A decrease in the ratio indicates that there is more fluorescence on the vertical junctions.

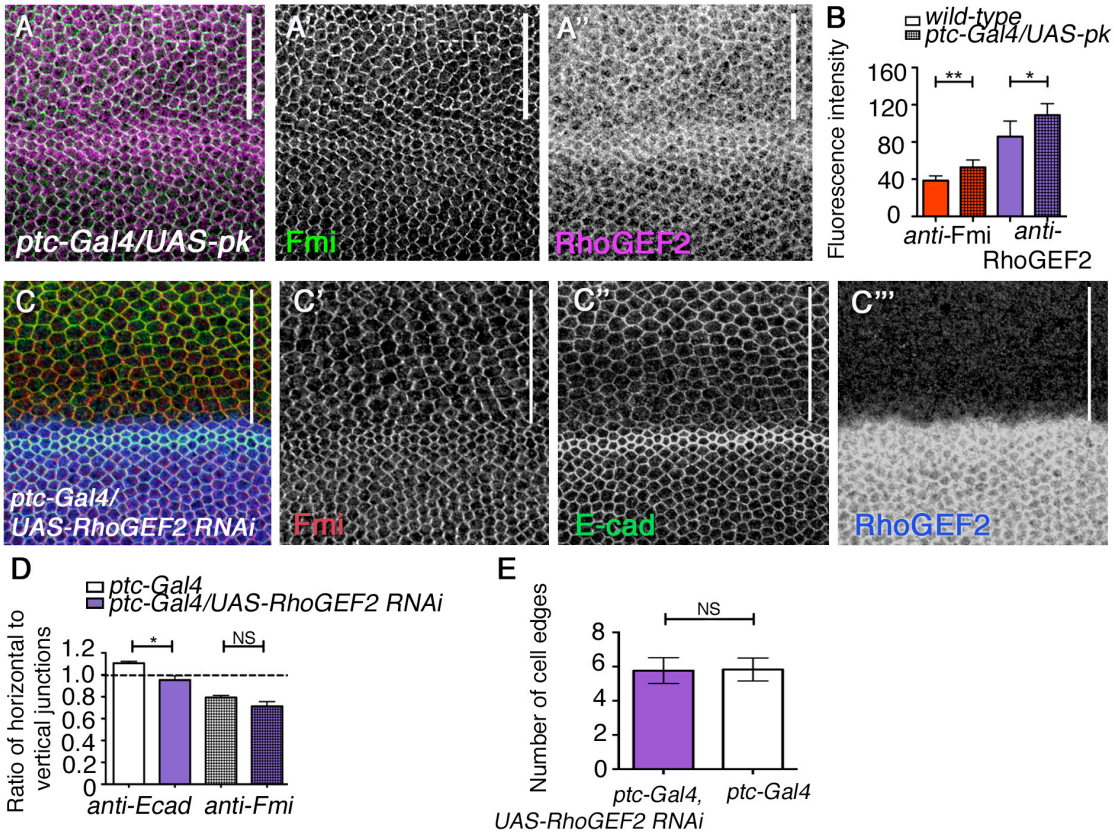

Figure 5.10: The recruitment of RhoGEF2 to the apical junctions

(A) Overexpression of *UAS-pk* expressed between veins 3 and 4 (region indicated by white bar) using *ptc-Gal4*, increases Fmi (green in A, white in A') and increases RhoGEF2 (magenta in A, white in A''). (B) Quantification of fluorescence intensity of Fmi (red bars) and RhoGEF2 (purple bars). t-tests comparing large regions of the wing in either wild-type or *ptc-Gal4/UAS-pk* over-expression wings, Fmi P<0.0042**, RhoGEF2 P=0.0388*. Error bars are s.d. n=6. (C) Loss of RhoGEF2 results in loss of E-cad asymmetry but not a loss of Fmi asymmetry. Fmi (red in C, white in C'), E-cad (green in C and white in C'') and RhoGEF2 (blue in C, white in C'''). (D) Quantification of C, ratios of E-cad and Fmi levels in wild-type and *UAS-RhoGEF2-RNAi* cells. E-cad asymmetry is lost while Fmi asymmetry is retained. n=4 wings. Asterisks above the charts show individual results from *t*-tests (NS, not significant; $P \leq 0.05$*). (E) Quantification of the number of cell edges for each wing cell in a defined region, using Packing Analyzer v2.0 (Aigouy et al., 2010). Comparing regions of the patch domain expressing *ptc-GAl4/UAS-RhoGEF2 RNAi* region (mean number of cell sides=5.762, s.d.=0.754) with *ptc-GAL4* only domains, (mean number of cell sides =5.831, s.d.=0.671; *t*-test, P=0.0655, n=4 wings, ~600 cells per wing). Note cells normally have approximately 6 sides allowing cells to tessellate and pack together.

Chapter 5

Discussion

Here I show that in two cell types, the embryonic epidermis and in the pupal wing, the core proteins are required for E-cad asymmetry at the junctions. In addition, E-cad asymmetry increases over time as core protein asymmetry increases. Like E-cad, RhoGEF2 is also asymmetrically localised in epithelial cells (Levayer et al., 2011), and is required for the asymmetry of E-cad at junctions (Levayer et al., 2011, this work). In this work I show that the core proteins are also required for the asymmetry and enrichment of RhoGEF2 at the junctions. This is likely to occur by recruiting RhoGEF2 to the junctions (Warrington et al., 2013) through interactions with Dsh, as Dsh can directly interact with RhoGEF2 in tissue culture cells (Warrington et al., 2013).

Although regulation of E-cad turnover is clearly required in the trachea (see Chapter 4), a requirement is less obvious in the epidermis and wing, where there appears to be no consequences of failing to asymmetrically localise junctional E-cad in those tissues. For example, in core polarity mutants, which clearly disrupt E-cad asymmetry, there is no appreciable GBE phenotype in the epidermis (**Figure 5.11** and Zallen and Wieschaus, 2004).

A previous study on E-cad turnover, suggested that polarised removal of E-cad from the junctions may be required for GBE. However, the loss of E-cad asymmetry was not proved as the cause of the GBE defects (Levayer et al., 2011). Therefore, polarised E-cad turnover regulated by the core proteins may not be essential for, or the only way of polarising cell intercalation. So, a GBE defect in the core proteins may be masked by the presence of other E-cad regulatory pathways during cell intercalation.

Another way of regulating E-cad is through Src, which regulates E-cad turnover and E-cad transcription (Forster and Luschnig, 2012), potentially modulating adhesion junctions and allowing cell intercalation to occur. However, the core polarity mutants do not affect Src localisation in the epidermis. Moreover, Src mutants do not affect core protein asymmetry or alter planar polarised wing hair orientation (Forster and Luschnig, 2012), suggesting that Src is not acting upstream of the core proteins. Therefore, the core proteins and Src are probably working in parallel to regulate E-cad junctional turnover.

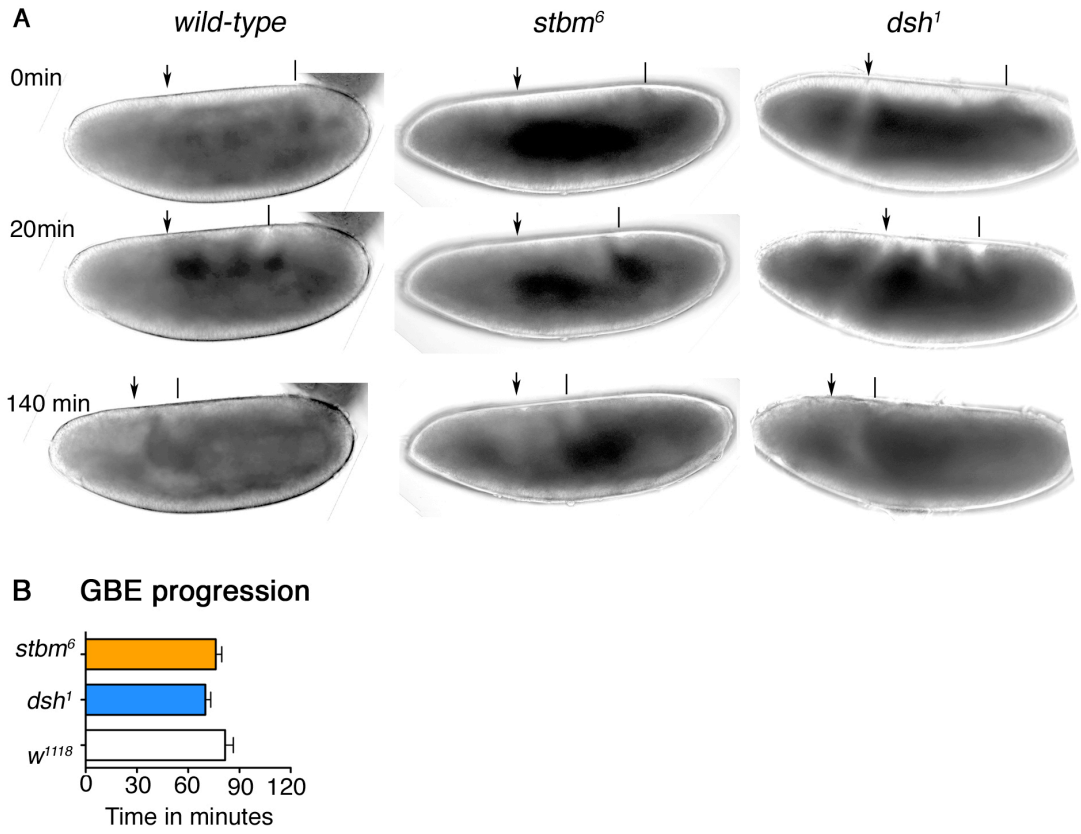

Figure 5.11: Germ band extension is not significantly affected by the loss of the core proteins

(A) GBE images of wild-type (w^{1118}), *dsh*^{1} and *stbm*^{6} mutant embryos at 0min, 20min and 140min. Arrows indicate anterior furrow and lines indicate the progress of the posterior of the germ band. (B) The time taken for the fast phase of GBE to occur in wild-type (w^{1118}), *dsh*^{1} and *stbm*^{6} embryos. ANOVA P=0.3411, wild-type is not significantly different from the mutants.

Abl a non-receptor tyrosine kinase is another protein involved in epithelial remodelling (Grevengoed et al., 2001), and mutant mice lacking the genes *Abl* and *Arg* (Abl related gene) do not complete cell rearrangements such as neural tube closure (Koleske et al., 1998). Abl is known to be required for regulating Arm at the junctions (Grevengoed et al., 2001). As Arm and E-cad interact at the junctions, Abl may be involved in regulating E-cad junctional asymmetry. Abl may also interact with the core proteins, this is indicated from experiments using *Drosophila* S2 cells, where Abl is required for Dsh phosphorylation on the Tyr473 residue, which in the pupal wing, is functionally important for the localisation and activity of Dsh (Singh et al., 2010). However, as mutants for the core proteins do not disrupt Arm localisation, the core proteins are not likely to be working in the same pathway as Abl to regulate E-cad endocytosis, although Abl could be involved in Dsh regulation.

Nemo has been linked to AJ remodelling through Arm and E-cad phosphorylation by increasing their junctional turnover in the *Drosophila* eye (Mirkovic et al., 2011). Nemo can also interact with the core proteins Stbm and Pk *in vitro* (Mirkovic et al., 2011). This suggests that Nemo could be required downstream of the core proteins to polarise the turnover of the Arm/E-cad junctional complex at least in the compound eye. However, if this were the case we would expect Arm asymmetric localisation to be disrupted as well as the asymmetric localisation of E-cad. As Arm localisation is not affected in the absence of the core proteins, Nemo is unlikely to be acting downstream of the core proteins in this context to regulate Arm localisation and E-cad turnover, although Nemo could be acting in parallel to the core proteins.

The stability of the AJ's is largely thought to be due to the stable association of Arm and E-cad at these junctions, as described in mammalian cells with mature AJ's (Yamada et al., 2005). The extent of the interaction between Arm and E-cad is largely dependent on the extent of cell polarisation (Huang et al., 2011). In early embryos where cells are still polarising, the interaction between Arm and E-cad can be disrupted *in vitro,* as shown in protein pull-down assays under mild acidic conditions (Huang et al., 2011). This suggests the interaction between Arm and E-cad is weaker when cells are still polarising, compared to later stages where acid washes have no effect of the Arm/E-cad interaction (Huang et al., 2011). FRAP experiments on polarising epidermal cells show that membrane associated Arm is also less stable compared to E-cad (Huang et al., 2011). However, FRAP experiments on polarised epithelial cells in late embryos, show that Arm and E-cad have similar junctional stability (Huang et al., 2011), suggesting Arm is only stably associated with E-cad in polarised cells. Consequently Arm in the polarising cells of the germ band is less likely to be in stable complexes with E-cad (Drees et al., 2005; Yamada et al., 2005). Therefore, the asymmetric localisation of Arm may not be significantly affected by the loss of E-cad asymmetry in the absence of the core proteins. This means if Arm regulates E-cad turnover Arm could be working in parallel to that of the core proteins.

Interestingly, previous work using FRAP on Ubi-E-cad-EGFP conducted at stage 16 showed that at this later time point the horizontal junctions recovered more than the vertical junctions (Bulgakova *et al.*, 2013), the opposite to what is observed at stage 8. However, I do not observe this reversal of recoveries for E-cad-EGFP on the horizontal and vertical junctions at stage 15 (**Figure 5.3G**). This may be because of differences in the FRAP methods used, and/or the staging of the embryos, as stage 15 embryos were used in this work. In addition the stage 15 FRAP in this work was conducted nearer the lateral side of the embryo and not the ventral side, which could

also possibly explain the differences seen in the fluorescence recovery in these FRAP experiments compared to the FRAP on E-cad-EGFP at stage 16 observed by others (Bulgakova *et al.*, 2013).

In summary there are many pathways involved in regulating E-cad localisation and turnover at the junctions, and not all affect the asymmetry of E-cad (Grevengoed et al., 2001; Huang et al., 2011; Mirkovic et al., 2011), the activity of the core proteins may be redundant with other regulatory pathways to regulate E-cad turnover. Although, we did not look at all pathways known to modulate E-cad at the junctions, we did establish that Src and Arm are not acting in the same pathway as the core proteins, nevertheless they could still be acting in parallel. Therefore, this complexity of parallel pathways required for GBE could be compensating in the absence of the core proteins and may explain why mutants for the core proteins do not appear to have a GBE phenotype.

E-cad polarisation in the pupal wing

Interestingly E-cad and RhoGEF2 are also asymmetrically localised in the pupal wing, with RhoGEF2 enriched on the vertical junctions and E-cad enriched on the horizontal junctions. Both E-cad and RhoGEF2 asymmetries are lost in core mutants and in the wing E-cad asymmetric turnover is lost in the absence of the core proteins. During wing development the asymmetry of E-cad correlates with that of the asymmetry of Fmi during development, suggesting that E-cad requires the core proteins for its junctional asymmetry. This suggests that a similar mechanism that requires the core proteins to asymmetrically polarise E-cad turnover in the epidermis, is also occurring in the wing.

One unresolved question in the wing is: why is E-cad polarised in a tissue where the cells are not significantly intercalating? Despite no longer intercalating after 22h APF, wing cells do continue to remodel their junctions at this stage as they “jiggle” around in the tissue (Aigouy et al., 2010; Classen et al., 2005). But if Levayer et. al. (2011) is correct and junctions with less E-cad are always shrinking, as polarised MyoII flows towards the vertical junctions is increased (Levayer et al., 2011), then why do vertical junctions in the wing not preferentially shrink compared to horizontal junctions? Although, these issues are unresolved I would speculate that either the cue to polarised E-cad is remaining from an earlier time during wing development, when these cells are intercalating, and after cell intercalation vertical junctional shrinkage is inhibited; or that junctional shrinkage is not totally dependent on polarised E-cad turnover.

Chapter 6
General Discussion

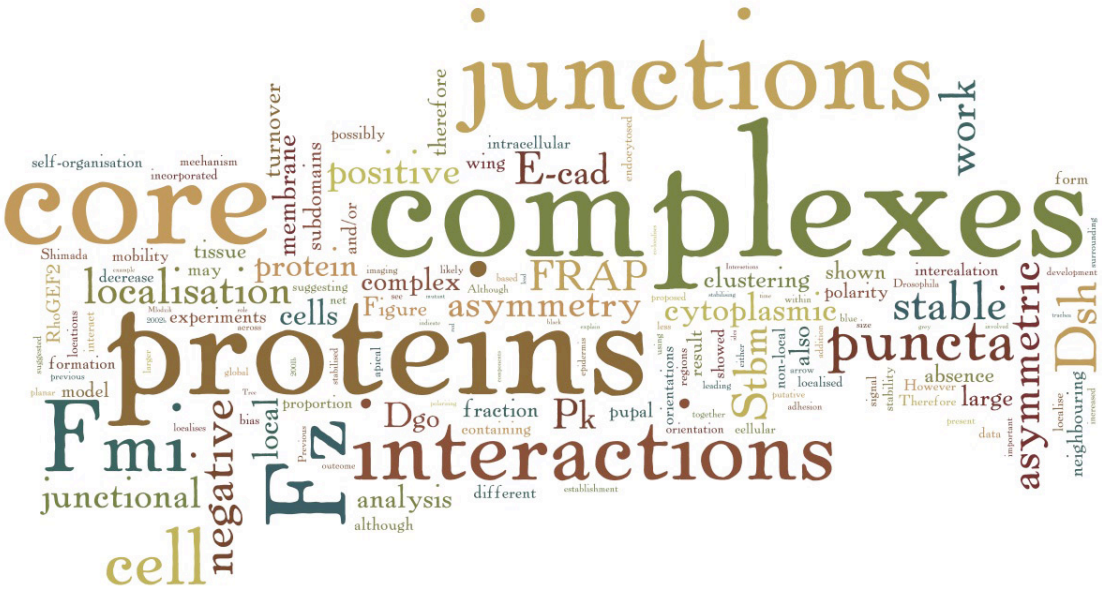

Core planar polarity proteins are stabilised into membrane subdomains

Previous work on understanding whether the core proteins (Fz, Fmi, Stbm, Pk, Dgo and Dsh) form a functional complex at the junctions relied on fixed tissue analysis and colocalisation studies. Live imaging and FRAP analysis presented here have shown that stable populations of Fz and Fmi are incorporated into junctional subdomains (puncta), which are persistent over time. In addition, during the formation of asymmetric asymmetry of the core proteins, the proportion of stable Fz within puncta increases compared to surrounding junctional regions, as well as an increase in the size of the puncta. This suggests that the formation of large puncta is linked to the asymmetric localisation of the core proteins.

Previous work supported an argument that the core proteins form a complex, which spans the junctions between two neighbouring cells. Fixed tissue localisation experiments showed that Fmi localises proximally and distally at cell junctions (Shimada et al., 2001; Strutt and Strutt, 2008; Usui et al., 1999) and form homodimers across junctions between cells (Chae *et al.*, 1999; Usui *et al.*, 1999). Fmi at distal junctions co-localises with Fz (Strutt, 2001b) and Fmi also physically associates with Fz in co-immunoprecipitation experiments (Chen *et al.*, 2008), therefore, suggesting that Fz-Fmi:Fmi interact at the junctions (where '-' denotes proteins binding within a cell and ':' denotes binding across a junction).

Furthermore there is other evidence to support the existence of a larger complex consisting of Dgo-Dsh-Fz-Fmi:Fmi-Stbm-Pk. Colocalisation experiments showed that Dsh, Dgo and Stbm localise to the same membrane subdomains spanning cell junctions as Fz and Fmi (Axelrod, 2001; Bastock *et al.*, 2003; Feiguin *et al.*, 2001; Shimada *et al.*, 2001; Strutt, 2001b). In addition, some of the cytoplasmic core proteins have been shown to directly interact *in vitro* with other core proteins (Jenny *et al.*, 2003; Jenny *et al.*, 2005; Tree *et al.*, 2002b; Wong *et al.*, 2003; Wu and Mlodzik, 2008). While Stbm and Fmi have not been shown to interact in *Drosophila*, a direct interaction has been shown between them in vertebrate cells using co-immunoprecipitation assays (Devenport and Fuchs, 2008). Therefore, the evidence that these six proteins colocalise together at the apical cell junctions and the *in vitro* interactions between these proteins, although not verified *in vivo*, supports an idea that these core proteins form a complex that localises to discrete puncta.

Some of the components of this putative complex (the cytoplasmic components Dgo, Dsh and Pk) seem to be required for asymmetric localisation but dispensable for cell-cell signalling, as polarity can propagate a few cells from a *fz* or *stbm* clone, in the

absence of the cytoplasmic factors (Strutt and Strutt, 2007), although Dgo, Dsh and Pk are required for the formation of large puncta. This suggests that clustering of the complexes into large puncta is not required for cell-cell signalling. Since Dgo, Dsh and Pk are required for asymmetric localisation of the core proteins and the formation of large puncta they are possibly required for the assembly of the complexes into ordered arrays of the same polarity in puncta to establish cellular asymmetry.

Cellular asymmetry would logically require these asymmetric complexes to be mostly aligned with the same polarity, into ordered arrays of asymmetric complexes, at the proximal and distal membranes. The alignment of these complexes seems to be concentrated into puncta (Strutt *et al.*, 2011).

As these complexes are asymmetric across the cell junctions, the accumulation of Fz containing complexes in one cell would lead to an increase in accumulation of Stbm containing complexes in the neighbouring cell. So aligned complexes in one cell would affect the alignment of the complexes in the neighbouring cell, but would also inhibit the localisation of complexes of the opposite orientation, resulting in a form of long range intercellular inhibition (**Figure 6.1**, Strutt *et al.*, 2011). This may be part of a mechanism for amplifying cellular asymmetry and thus coupling asymmetric localisation of the core proteins in neighbouring cells.

Puncta may therefore be a consequence of aligning complexes of the same orientation. However, smaller puncta still exist in the absence of the core cytoplasmic proteins e.g. Pk. These smaller puncta may not contain aligned complexes as they would lack one of the six core proteins and may not be the same as the large ‘polarised’ complexes that appear when cellular asymmetry occurs.

This work therefore set out to try to understand more about why the core proteins localise to these membrane subdomains, and ask are these regions of the membrane functionally important? Or are these subdomains just locations that are less occupied by other proteins, for example regions that do not colocalise with adherens junctions? One approach to address this was to ask if the core proteins Fz and Fmi are stably incorporated into these Puncta? If so, this would explain why the core proteins accumulate in these regions. Or are the core proteins in constant flux and only accumulate at the junctions where the protein is transported, and so puncta are not special junctional locations? For example, Fz is transported distally along microtubules (Shimada *et al.*, 2006), which might be sufficient for the formation of asymmetry even if the transported Fz is not stably localised. To analyse the turnover

and stability of Fz and Fmi at the junctions, either localised in puncta or in surrounding junctional regions, a FRAP analysis method using the pupal wing was established. FRAP analysis was further used to uncover roles for the other core planar polarity proteins in clustering core proteins into large puncta.

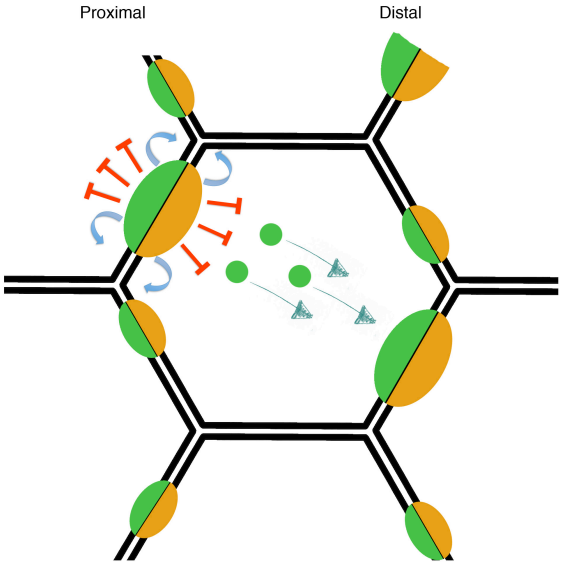

Figure 6.1: Model for how puncta contribute to cellular asymmetry

The alignment of distal containing complexes (green) results in the increased accumulation of proximal complexes (orange) in the neighbouring cell (cells separated by the black lines). Positive interactions (blue arrows) promote the clustering of like complexes. Non-local inhibition of complexes (red arrows) prevent complexes of the opposite orientation from localising at that membrane and instead are proposed to be trafficked to the distal side of the cell (green arrows) via microtubules (Shimada *et al.*, 2006). Proximal is to the left.

Proposed model for the formation of complexes and their asymmetric localisation

Previous data from our lab showed that Fmi, in fixed tissue, is increased at the apical junctions when Fz is present in the cell. Furthermore, in the absence of Fz, Fmi shows reduced localisation at the junctions and instead a proportion of Fmi accumulates at the apical membrane (Strutt and Strutt, 2008, and **Figure 6.2**).

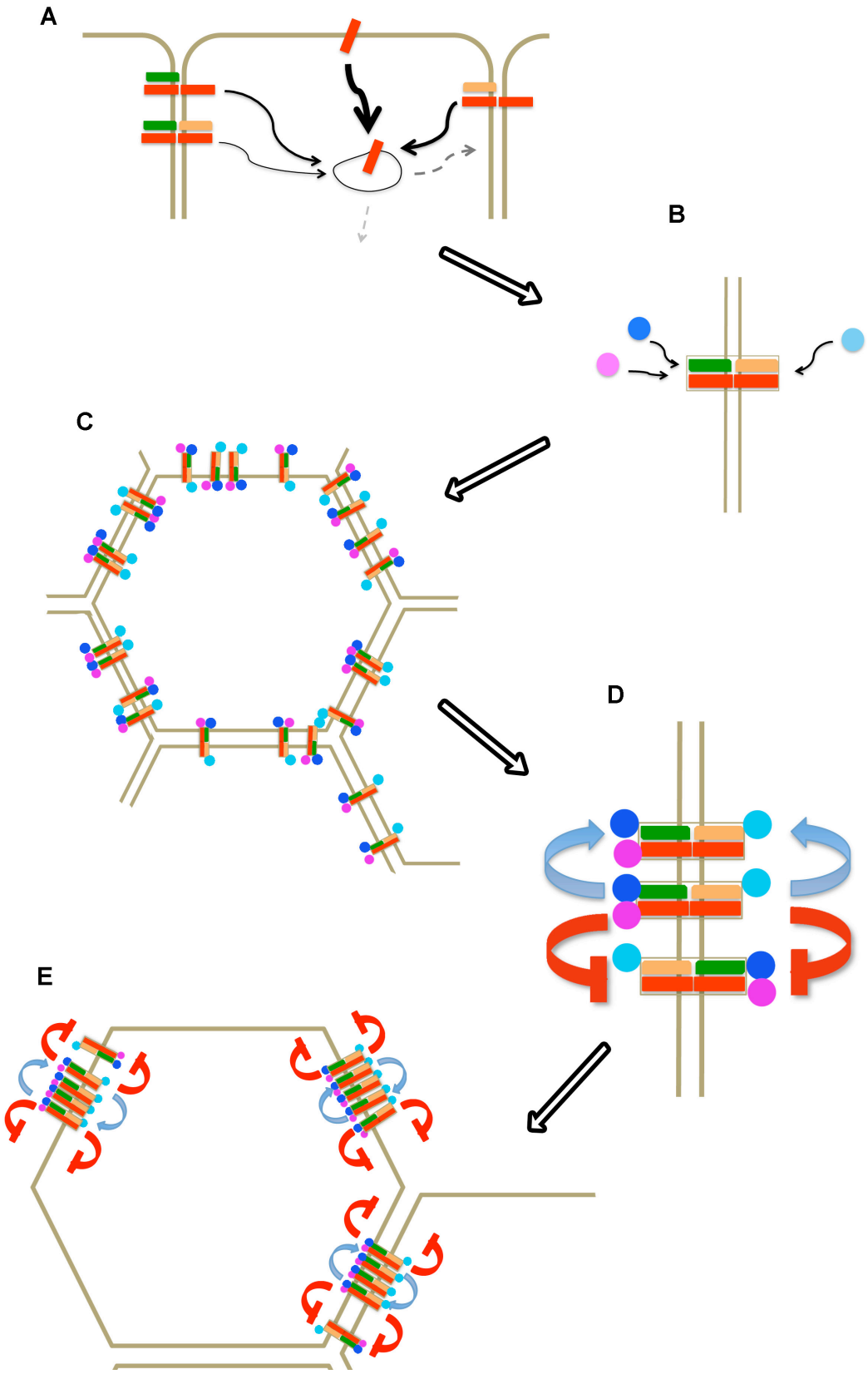

Figure 6.2: Model of proposed interactions between core protein complexes resulting in local self-organisation of asymmetric complexes at the junctions

(See next pages for figure legend)

Model of proposed interactions between core protein complexes resulting in local self-organisation of asymmetric complexes at the junctions

(A) Fmi (red) localises to the apical membrane in the absence of Fz (green) and Stbm (orange), but is readily endocytosed from the junctions as indicated by the large black arrow (Strutt and Strutt, 2008). Interactions with the core proteins Fz and Stbm decrease the ability of Fmi to be endocytosed (indicated by the decrease in thickness of the black arrows) and therefore Fmi is further stabilised at the junctions (Strutt et al., 2011). The grey dotted arrows indicate that Fmi after being endocytosed can be recycled back to the membrane (dark grey arrow, Strutt and Strutt, 2008) or degraded (light gray arrow, Shimada et al., 2006; Strutt and Strutt, 2008). (B) The cytoplasmic proteins Pk (pale blue), Dsh (dark blue) and Dgo (pink) are also present at the junctions when Fmi, Stbm and Fz are present. They are possibly required to modify positive and/or negative interactions between complexes of the same or opposite orientations. (C) Asymmetric junctional complexes containing Fmi, Stbm and Fz start out randomly oriented, the cytoplasmic factors enter the complexes, which are required for the putative positive or negative local interactions between the complexes. These interactions could amplify an initial bias of polarity or in the absence of a bias, a non-local intracellular signal might suffice to promote cellular asymmetry (see text). (D) Complexes undergoing positive (blue) and/or negative (red) interactions between complexes. Positive interactions would stabilise or decrease mobility of the complexes and negative interactions would destabilise complexes or increase complex mobility. (E) These local interactions would result in clustering of ‘like’ complexes and the repulsion of different orientated complexes coupled with a global bias or a non-local signal/inhibition would lead to asymmetric localisation of the core proteins within a cell. These interactions would also alter the localisation of the asymmetric complexes in the neighbouring cells as the complexes span the junctions, leading to establishment of planar polarity between neighbouring cells based on local interactions and an initial bias.

The reduction of Fmi at junctions and the relocalisation of Fmi to the apical membrane also occurs, although to a lesser extent, in *stbm* mutants, where more Fmi in the *stbm* mutant remains at the junctions (Strutt and Strutt, 2008). When both Stbm and Fz are absent Fmi localises apically (Strutt and Strutt, 2008). This suggests that Fz and Stbm are both required for localising Fmi to the junctions, although Fz seems to be more important than Stbm for Fmi junctional localisation (Strutt and Strutt, 2008).

In agreement with this, Stbm cannot recruit and stabilise Fmi homodimers at the junctions, demonstrated by previous work from our lab, showing that Stbm-Fmi at the junctions in *fz* mutant cells could not recruit Fmi in the neighbouring *fz- stbm-* double mutant cells at the clone boundary. Whereas Fz-Fmi at junctions in a *stbm* mutant background could stabilise Fmi from the neighbouring cells at the *fz- stbm-* clone boundary into Fmi:Fmi homodimers (Strutt and Strutt, 2008). Therefore, Stbm also requires the presence of Fz at the junctions to stabilise Fmi homodimers (**Figure 6.2A**). Both Stbm and Fz are required to reduce Fmi endocytosis from the junctions, since Fmi can be endocytosed more readily from the cell junctions in the absence of Fz or Stbm (Strutt and Strutt, 2008), although the increase in Fmi endocytosis was inferred from observations of more Fmi being sent for degradation (Strutt and Strutt, 2008). Nevertheless, Stbm and Fz are involved in reducing Fmi intracellular trafficking and therefore increasing its stability at the membrane.

Thus, these prior data are in agreement with our current findings where FRAP analysis of fluorescently tagged Fz and Fmi, showed that both had a larger stable proportion of protein when localised in puncta compared to surrounding junctional membrane. Therefore, the core proteins are more stable when localised in puncta. In addition, FRAP analysis (this work) and previous antibody internalisation experiments (Strutt et al., 2011) showed that Stbm is required to increase the stable fraction of Fz and Fmi in junctional puncta. Therefore, the presence of the core proteins Fz, Stbm and Fmi are required for all the core proteins to be mutually stabilised into puncta, resulting in reduced turnover of Fz and Fmi, and possibly other core complex components at the junctions.

Further FRAP analysis in this work showed that the cytoplasmic core proteins Dsh and Pk are required to increase the stable fraction of Fz at the junctions. This agreed with Strutt & Strutt (2009) where cytoplasmic proteins (Dsh and Pk) were required for further stabilising Fz into complexes at the cell junctions (**Figure 6.2B**). The cytoplasmic proteins also appear to be required to cluster the core proteins into large

puncta (Bastock *et al.*, 2003; Feiguin *et al.*, 2001; Tree *et al.*, 2002b). This is inferred from experiments where the large puncta are lost in the cytoplasmic mutants (**Figure 6.1**, also see Strutt *et al.*, 2011) although the small puncta that are left are not complete complexes (as one protein is absent) and therefore may not be aligned with other complexes. Dsh and Pk are possibly required to cluster aligned complexes together to form larger puncta.

The asymmetric complexes are hypothesised to also include Dgo, as Dgo co-localises with the other core proteins at the junctions and although Dgo was not looked at in these experiments, it is likely to behave like the other cytoplasmic proteins and stabilise core proteins into puncta.

Interactions between complexes are proposed to be required to correctly localise core complexes at junctions

The complexes in puncta are therefore likely to be complete asymmetric complexes associating with the reciprocal complex in the neighbouring cell, which may confer a greater degree of complex stability. Compared to membrane regions between the puncta that may contain partial or unaligned complexes that are subjected to a greater degree of turnover.

Aligning complexes in large puncta may be achieved through local positive and/or negative interactions between complexes of opposite orientations within the cell. Positive interactions would result in stabilising and clustering complexes of the same orientation and would lead to the formation of large puncta. Negative interactions within a cell would be expected to increase the mobility between complexes of the opposite orientation. However, this would not be expected to occur in puncta (**Figure 6.2E**), as ‘large puncta’ are likely to consist of complexes with the same alignment, therefore negative interactions would not alter the stable protein fraction in puncta. Furthermore, unaligned regions outside puncta may contain complexes of opposite orientations, where negative interactions would result in the segregation of complexes with opposite orientations, thus increasing stability of regions where complexes are aligned. Therefore resulting in the same net outcome induced by positive interactions.

The cytoplasmic components (Dsh, Pk, Dgo) are required to form large puncta which are proposed to contain aligned complexes, therefore, the cytoplasmic proteins could be modifying local interactions between complexes of the same or opposite orientations within a cell to cluster complexes with the same orientation into large puncta and increase cellular asymmetry (**Figure 6.2C-D**).

FRAP half-cell experiments suggest that the local interactions between the complexes are likely to be positive, since in the absence of one of the other core proteins, Fz at the junctions becomes less stable and only small puncta are seen that possibly do not contain whole complexes. The idea of only having positive local interactions would be interesting to pursue as most models for how the complexes achieve asymmetry are based on a mixture of positive and negative interactions or only negative interactions (Amonlirdviman *et al.*, 2005; Klein and Mlodzik, 2005; Le Garrec *et al.*, 2006). These local interactions result in an overall outcome where there is an increase in cellular asymmetry. However, the data in this work suggests that complexes undergo positive interactions, which may result in an increase in cellular asymmetry and an increase in the size of the protein stable fraction.

Nevertheless, it has been suggested that only local interactions either positive and/or negative between complexes would not predict cellular asymmetry of the core proteins (Burak and Shraiman, 2009; Le Garrec *et al.*, 2006), instead patches of complexes of the same orientation would arise at all cell junctions. Burak *et.al.* 2009 suggest a mathematical model where a non-local inhibition signal was modelled in the form of a ‘messenger molecule’ that would ensure the repulsion of differently orientated complexes so that they end up at opposite ends of the cell (Burak and Shraiman, 2009). They propose that this ‘messenger molecule’ may be a diffusible factor whose activity could be modulated across the cell. However, they also suggest that the complex core proteins themselves could be directly modified and affecting their affinity for binding to oppositely orientated complexes.

Therefore a non-local intracellular signal would be required to ensure complexes are localised proximally and distally in the cell with complexes of different orientations being localised at different ends of the cell. This could be achieved by either an intracellular non-local signal within each cell, allowing self-organisation of the asymmetric complexes even in the absence of a global cue (Burak and Shraiman, 2009; Fischer et al., 2013), or the complexes could respond to a gradient across each cell and reposition the complexes in line with the gradient. However, establishment of polarity would not be through self-organisation of the complexes. Indeed a non-local intracellular signal would not coordinate polarity across the tissue so an upstream global cue would still be required in this model (Burak and Shraiman, 2009; Fischer et al., 2013).

Future work

Further exploration of the localisation and stability of the core proteins (Stbm, Dgo, Dsh, Pk, Fz and Fmi) using live imaging and FRAP should provide a fruitful area for future investigation. Indeed preliminary FRAP analysis with the five other core proteins has shown that they all have a stable fraction when in puncta. Alterations of the current FRAP method for faster imaging would allow rate of turnover data to be collected and will give insights into the behaviour of the mobile fraction of core proteins, which was not addressed in this work. A change in core protein turnover in the absence of one or other of the core proteins may indicate their involvement in modulating the mobility of the core proteins, although this may not be necessary for the establishment of multiple complexes aligning in large puncta.

In some models describing the self-organisation of complexes, the cytoplasmic proteins are thought to be involved in negative interactions between complexes to establish intracellular core protein asymmetry (Amonlirdviman *et al.*, 2005; Le Garrec *et al.*, 2006). However, this work has shown that Dsh and Pk are required to increase the stable proportion of Fz in puncta, therefore suggesting that Dsh and Pk are involved in positive interactions and clustering of correctly orientated Fz containing complexes. FRAP analysis of Fz in core protein mutant backgrounds so far has only shown the net affect of removing one of the core proteins throughout development. It is possible that Dsh and/or Pk participate in negative interactions at some point during asymmetry establishment but those negative interactions result in a net positive outcome and complex clustering. A way to test if there are negative interactions occurring during an earlier phase of establishing asymmetry involving Fz and Dsh, would be to induce Dsh expression in a *dsh* mutant background during pupal wing development and then measure the stable fraction of Fz at the junctions using half-cell FRAP, to measure general levels of turnover. If negative interactions are required at an earlier phase of asymmetry establishment to destabilise complexes in the ‘wrong’ place, then this may be seen prior to complexes being stabilised when in the correct locations.

Core proteins promote asymmetric E-cad turnover via RhoGEF2 in the trachea, epidermis and in the pupal wing

This work has additionally uncovered a role for the core proteins during cell intercalation in the *Drosophila* embryonic trachea, epidermis and the pupal wing. The core proteins are required for increased E-cad turnover at cell junctions, thereby suggesting a role for the core proteins in regulating the level of adhesion between cells. Our data supports a model where core proteins acting via Dsh alter E-cad

turnover by recruiting RhoGEF2 to the junctions and activating its downstream target RhoA.

I show here that, in the epidermis and in the pupal wing the core proteins recruit RhoGEF2 to the same junctions as the core proteins at the proximal-distal junctions. The core proteins are required for the asymmetric localisation of RhoGEF2 and E-cad. This reduces E-cad at those junctions resulting in E-cad accumulation on the dorsal-ventral junctions. Why E-cad asymmetry is seen in the late pupal wing is unclear, since this tissue is no longer undergoing cell intercalation. Although the mechanism could be left over from a previous time in development, it does not explain why the proximal-distal junctions are not shrinking. This would be expected based on the prevailing model (Levayer et al., 2011) where the removal and recycling of E-cad from the shrinking junctions is required at some level for cell intercalation to occur. Indeed loss of E-cad asymmetry through removal of the core proteins does not result in GBE defects (this work and Zallen and Wieschaus, 2004). Consequently an intriguing possibility arises that junctional length shrinkage is not totally dependent on polarised E-cad turnover.

As embryos develop from early to late stages, the epidermis changes. In early embryos (stages 7-11) cells are still polarising and there are no mature adherens junctions or septate junctions. In contrast, by late stages (stages 14-16) the epithelium has become polarised, the adherens junctions have matured and septate junctions have formed. Interestingly, other work from Bulgakova and Brown (2013) shows that at later stages E-cad-EGFP on the horizontal junctions recovers more than the vertical junctions, the opposite to what has been observed at stage 8 (this work and Cavey *et al.*, 2008), or what was observed in more lateral regions of the epidermis at stage 15. This could be due to differences in the experimental methods applied or the location of the bleach regions in the epidermis. However, if E-cad is more stable on vertical junctions of the epidermis at later stages of embryogenesis; then are the core proteins still actively involved in increasing E-cad turnover at the vertical junctions at later stages, or is another mechanism required to increase E-cad turnover on the horizontal junctions?

Final conclusions

The work in this thesis has provided insight into the formation of stable asymmetric core protein complexes at the junctions, and has demonstrated that the stability and clustering of these complexes requires the core cytoplasmic proteins. In addition the asymmetric localisation of the core proteins is required for the asymmetric localisation

of RhoGEF2 that activates RhoA (Levayer et al., 2011) leading to the modulation of E-cad mediated cell adhesion during cell intercalation. This work therefore incorporates the core proteins into a mechanism for polarising cell adhesion during cell intercalation and tissue remodelling. This provides a general tissue mechanism, at least in *Drosophila,* for polarising E-cad localisation and endocytosis during junctional remodelling.

Chapter 7
Materials and methods

Fly stocks and genetics

The mutant alleles used in the work are described in Table 2 and FlyBase. The core pathway mutants were crossed out for several generations prior to use, to reduce the effects of background mutations on the strength of the embryonic phenotypes. The *fz*, *stbm*, *pk*, *fy* and *mwh* mutant embryos were maternal-zygotic mutants for null alleles, for *dsh* the embryos were either mutant for the dsh^{V26} null allele or maternal-zygotic mutants for the planar polarity specific allele dsh^{1}, and *fmi* and *Src42A* embryos were zygotic mutants for null alleles. The antimorphic $RhoGEF2^{6.5}$ allele was lethal when homozygous and was therefore examined in heterozygous embryos.

Mitotic clones were induced using the FLP/FRT system (Xu and Rubin, 1993) using either *Ubx-FLP* (Emery et al., 2005) or *hs-FLP* (Golic and Lindquist, 1989). Over-expression of Shi was achieved by using the GAL4-UAS system (Brand and Perrimon, 1993). UAS-shi^{ts1} flies were crossed the *Patch-GAL4* (*Ptc-Gal4*) driver to express the UAS-Shi^{ts1} in a stripe orientated along the proximal distal axis in the wing. Larvae were aged at 19°C and prepupae shifted to 30°C for 30min before imaging for FRAP.

Over-expression of Fz in the trachea was done by crossing *UAS-fz* flies to *hs-FLP; btl >y+>GAL4* (Ribeiro et al., 2004) and subjecting the embryos to a 15min heat shock at 38°C, 1hr before imaging, to allow time for expression of the *UAS-fz*.

For prepupal wing imaging, white pupae were collected and aged at 25°C for 5.5hr before dissecting and imaging. Pupal wings were aged for 28hr at 25°C before imaging, unless otherwise indicated.

Antibodies

Primary antibodies used were rabbit anti-GFP (1:1000, Abcam), rabbit anti-Fz (1:200 Bastock et al., 2003), rabbit anti-RhoGEF2 (1:25, gift from J. Grosshans, Göttingen, Germany, Grosshans et al., 2005), rabbit anti-pSrc42A (pY148) (1:200, Invitrogen), mouse monoclonal anti-βgal (1:400, Promega), rabbit anti-Vasa (1:100, gift from Ralf Jauch, Alf Herzig and Ralf Pflanz, Göttingen, Germany). The mouse monoclonal anti-Crumbs (1:10, DSHB, Tepass et al., 1990), mouse monoclonal anti-Fmi (1:10, DSHB, Usui et al., 1999), mouse anti-Arm (1:200, DSHB, Peifer et al., 1994), rat monoclonal anti-E-cad (1:25, DSHB, Oda et al., 1994), and mouse anti-Myc 9E10 (1:25, BioServ), rabbit anti-Zipper/MyoII (1:100, gift from Thomas Lecuit Levayer et al., 2011), guinea pig anti-Bazooka (1:250, gift from Jennifer Zallen Blankenship et al., 2006). Rabbit anti-Stbm was generated against a His-tagged fusion protein

corresponding to amino acids 406-584, used at 1:1000. Secondary antibodies were anti-mouse Cy2, anti-rat Cy5, anti-rabbit rhodamine red-X (Jackson Immuno Research); anti-rat Alexa568 and anti-rabbit Alexa568 (Molecular Probes) all used at 1:250.

Fixation and immunolabelling of Drosophila embryos

Embryos were collected overnight at 25^{o}C on agar plates containing apple juice, then dechorionated in 50% bleach and fixed in 4% formaldehyde in PBS and devitellinised either by hand or in 1:1 heptane:95% methanol.

To devitillinise by hand, embryos were placed in a loose-bottomed basket with a removable nylon mesh at the base. After the embryos are dechorionated the mesh (containing the embryos) was removed, dabbed on a tissue to take away excess moisture, and placed embryo side up on an apple juice plate. Embryos were picked up from the mesh using a bent needle and placed on double sided Sellotape, located in a petri dish and ddH_20 was applied to the embryos. The embryos were then removed from the vitiline membrane by gently pressing on the embryo at the posterior end, using a bent needle, thereby breaking the vitiline membrane and the embryo pops out.

For methanol devilitisation, embryos were fixed for 20min in a 1:1 solution of heptane and 4% formaldehyde. After fixing, the formaldehyde was substituted for methanol and vortexed for 1min to remove the vitiline membrane. The heptane was then removed and embryos were stored in methanol at -20°C. For anti-RhoGEF2 immunostaining embryos were dechorionated in 50% bleach, and then heat fixed by placing embryos in Triton Salt Solution (Triton X-100 0.3%, NaCl 4% w/v) heated to 100^{o}C, for 45sec, then adding ice cold TSS and incubating on ice for a minimum of 5min. Embryos were then removed from the TSS and washed in H_2O before devitellinisation. After heat-fixing, embryos can be stored in methanol for up to a year and rehydrated before use, however for embryos to be stained with phalloidin or anti-RhoGEF2 the embryos were used immediately as any storage resulted in poor antibody staining.

For immunostaining, all antibody incubations and washes were done using PBS/0.1% Triton X-100. Normal goat serum (10%) was added when incubating with antibodies to reduce non-specific binding of the antibody. Antibody immunostaining was done either over night at 4^{o}C or for 3h at room temperature, and 3 washes of 10min each, were done between the antibody incubations. After staining, embryos were placed in

50% glycerol and mounted on glass slides, covered with No 1.5, 20x20mm sized coverslips and sealed with nail varnish.

Confocal images of fixed embryos were taken either using a Nikon A1 LSM confocal microscope with a 40x NA1.2 oil plan apochromatic objective at 2x zoom, or a Leica SP1 confocal microscope with a 40x NA1.32 oil plan apochromatic objective at 2x zoom. For lateral views of tracheal branches stacks of ~50 slices were taken, the interval between slices was 0.5μm.

Fixation and immunolabelling of Drosophila pupal wings

Pupal wings were dissected at 28hr after prepupal formation at 25°C and immunolabelled by Helen Strutt, as previously described (Strutt, 2001b). Wings were then mounted in 10% glycerol in PBS with 2.5% DABCO (1,4-diazabicyclo [2.2.2] octane). Fixed wings were imaged on a Nikon A1 LSM confocal microscope with a 60x NA1.4 oil plan apochromatic objective at 3x zoom. Stacks of 8-10 slices 0.5μm apart were imaged and then 3-4 slices were selected coinciding with the level of the adheren's junctions and using ImageJ an average stack projection was applied.

Live imaging in pupal and prepupal wings

Pupae to be imaged at 28hr APF were collected at the white prepupal stage and aged at 25°C for 27 ½hr and then dissected before imaging, adapting the Classen method for dissection (Classen et al., 2008). Embryos were placed on double-sided tape in a petri dish and a square of cuticle was removed from above the developing wing with a razor blade and forceps. The pupa was then inverted and mounted in a drop of Halocarbon 700 oil in a 2.5cm glass-bottomed dish (Iwaki). Pupae were retained after imaging and allowed to develop, >95% eclose, suggesting minimal tissue damage during dissection and imaging.

Prepupal wings were dissected in Schneider's medium/Fetal bovine serum (SM/FBS) (Classen et al., 2008) and placed in a glass-bottomed dish with ~20μl of SM/FCS surrounded by a gasket of parafilm. A round coverslip was then placed on top and a ring of wet paper tissue was added to prevent evaporation. Alternatively wings were placed in a ~5μl SM/FCS containing 1% methylcellulose on a slide surrounded by Sellotape Diamond tape. A round coverslip was then placed on top and nail varnish applied to prevent evaporation, in this case samples were imaged no more than 1hr after dissection to prevent evaporation of the liquid surrounding the wing tissue.

Wing samples were imaged on an inverted Zeiss LSM 510 confocal microscope, with

a Zeiss 63x NA 1.4 oil apochromatic objective lens at 2x zoom, pixel size of 139nm, or for **Figure 3.4L** a Nikon A1 confocal microscope was used, with a Nikon 60x 1.3NA oil apochromatic objective lens at 4x zoom, pixel size of 103.6nm.

These settings were used to optimize the resolution of the microscope available, while also reducing damage to the sample by over bleaching. The pinhole was also open to maximise the light detected, this step was also essential as the florescence from the pupal wing could not be seen clearly when the pinhole is set to 1 Airy unit using the Zeiss microscope. The 488nm Argon laser was used at an output of 20% with the gain set at 500-600 and a band pass 505-550nm filter was used for detection. Single images with no averaging were taken to reduce acquisition bleaching.

FRAP of pupal and prepupal wings

For wing FRAP, pupae were dissected and mounted for imaging as described in the live imaging section above. FRAP analysis of trafficking mutants was carried out in prepupal wings, as pupal wing tissue was unhealthy under the same conditions. In these experiments wild-type and mutant tissue from the same wings were analysed. Wing cell plasma membrane regions containing concentrated protein (bright regions) or diffuse protein (less-bright regions) were selected and bleached, using the 488nm Argon laser at 100% laser power and passing 20 times over a region of interest (ROI) of 2μm^2 this is smaller than half of the distal membrane in a *Drosophila* pupal wing cell, and about twice as large as a typical punctum at 28hr APF.

The size of the ROI could not be reduced, as tissue movement makes the ROI hard to track over time. No laser bleaching occurs outside the ROI, indicating that loss of fluorescence outside the ROI (but within the same cell) and rapid recovery inside the ROI is likely to be due to lateral protein diffusion (see chapter 2).

Three pre-bleach images were captured, as well as an immediate post-bleach image and then images on the Zeiss 510 confocal were taken at a rate of 1 frame per sec, every 30sec for up to 40min. Microscope settings were: 20% of the 488nm laser, gain 500, 0 offset, 2x zoom with an open pinhole. However, for **Figure 3.4L** the Nikon Al was used, taking 3 prebleach images, and then bleaching using 100% to scan 13 passes at a rate of 2 frames per sec. Then the post bleach images were taken using 5x5sec, 10x10sec, 10x15sec and 7x30sec intervals. Imaging settings were, 5% of the 488nm laser, gain120, -9 offset, 4x zoom, 1.2AU, images were taken at a rate of 1 frame every 4sec.

For the FRAP experiments conducted on the Zeiss 510 confocal, faster image acquisition was attempted but this led to increased acquisition bleaching (see Chapter 2). Pixel size of 136nm was used, 512x512 images at the expense of the resolution (compare 512 images by 2048 images **Figure 3.2A-A'**). Any data set that contained regions seen to be moving out of focus were discarded. A background measurement of an in-focus wing but with the lasers were off was then measured, to detect any noise picked up by the detector. Unfortunately fluorescence noise that may have been fluctuating during the experiment could not be removed.

Analysis of FRAP data

For data analysis Volocity (v.4.4 Improvision) was used to manually re-select and quantify the fluorescence of at least 10 of the $2\mu m^2$ bleached regions at each time-point, and laser-off background was subtracted. To measure acquisition bleaching, readings were collected from 4 non-bleached control regions (for each of the bright or less-bright regions) $2\mu m^2$ in size, at least two cells away from a bleach region. Data were then corrected for acquisition bleaching and normalised against an average of the pre-bleached values. Data were transferred to Prism (v.5 Graphpad), plotted on an X-Y graph and a one-phase exponential association curve fitted. An extra sum-of-squares F test was performed to see if the curve plateau (Y^{max}) was different among data sets. Note that in most cases the half-life of recovery was less than the acquisition interval (30sec) and thus the rate of recovery could not be accurately determined.

Live imaging of embryos

For live imaging of the embryonic trachea, embryos were collected in cages overnight at 25^{o}C, collected and dechorionated in 4% bleach, and placed on a glass coverslip (20 x 50 mm). Prior to the addition of the embryos, each coverslip was coated in heptane glue and a square frame of parafilm was placed on the glue forming a gasket, in which the embryos were placed. Once on the slide the embryos were then covered with halocarbon oil. Embryos were imaged for a maximum of 3hr, but the slides were retained after imaging to ensure embryos were still viable and later hatched as larvae.

Embryos were imaged on an inverted Zeiss LSM 510 scanning confocal microscope, using a 488nm laser with a band pass 505-550nm filter and a 561nm laser with a long pass 575nm filter. The lasers were set at an output of ~20% intensity, and the pinhole was set to 1 Airy unit. Images were taken using a 63x NA 1.4 oil apochromatic objective lens at 2x zoom with the gain set at 300-400 for detection.

Single images with no averaging were taken to reduce acquisition bleaching.

Drosophila embryo FRAP

For FRAP of cellular junctions in the epidermis and of tracheal cells at stage 14/15 of embryonic development, 2μm^2 regions (106 pixels) were selected on junctions which were angled vertically. These junctions were bleached with a Zeiss 40x NA 1.2 oil apochromatic objective lens at 2x zoom using the 488nm laser with 50% laser intensity can passing the laser 20 over the image during bleaching.

Images after bleaching were captured using 512x512 pixels as single image slices with no averaging, Three prebleach images were collected, then an immediate post bleach image was taken and then images were taken once every 15sec for up to 30min. Analysis of FRAP data used the same method as for pupal wing FRAP (see above).

Quantifying tracheal phenotypes

Tracheal dorsal and ventral branches were assayed for the presence of cell intercalations by immunolabelling embryos for Crumbs distribution to highlight the adheren's junctions and blind scoring for the percentage of branches in each embryo, which show incomplete intercalations. The data were then averaged across embryos. The number of nuclei per dorsal tracheal branch was counted using live embryos expressing *btl-GAL4/UAS-α-Cat* to mark the junctions and *UAS-NLS-red-stinger* to mark the nucleus, excluding the branches at the very anterior and posterior of each embryo. ANOVAs were used to compare the control and the mutant conditions for each stage

Cell junction intensity measurements

To measure the fluorescent intensity of junctions in live or fixed tissue, images were taken at constant settings. Image stacks comprised of ~20 images at 1μm apart were taken and 3 slices of the greatest intensity were averaged. To measure intensity of the junctions, the ImageJ line measurement tool was set to the width of the junctions (approximately a width of 100nm or 6 pixels) and used to measure the mean intensity of each junction. The measured mean values were then normalised by subtracting the laser off background and the intensities were then averaged across at least 4 images. Statistics were performed using Prism (v.5 GraphPad) and multiple genotypes were compared to control (w^{1118}) embryos using an AVOVA and Dunnett's Multiple Comparison Test or an unpaired two-tailed Student's t-test if only two

genotypes were compared.

For intensity measurements of the junctions in the epidermis a measurement of the junction angle was also recorded. Intensity measurements were grouped by angle into groups containing 0-<45 and >135-180 degrees relative to the anterior-posterior axis (horizontal junctions), or crossing the anterior-posterior axis (vertical junctions) with an angle of >45-<135 relative to the anterior-posterior axis.

The two groups were compared using an unpaired two-tailed Student's t-test if only two genotypes were compared or using an ANOVA and the Dunnett's Multiple Comparison Test to compare multiple groups to a control genotype (w^{1118}). The error bars on all graphs are shown as Standard Error of the Mean (s.e.m.) unless stated.

Table 2: List of mutant alleles and transgenic constructs used

Name of gene	Allele	Class	Comments	Flybase reference
white	w^{1118}	n/a *(crossed out to Oregon R)*	Used as wild type	FBgn0003996
frizzled	fz^{P21}	Null allele	Crossed out to wild type	FBal0004937
strabismus (van gogh)	$stbm^{6}$	Null allele	Crossed out to wild type	FBal0062423
dishevelled	dsh^{V26} *(also known as* dsh^{3}*)*	Strong loss of function allele	Crossed out to wild type	FBal0003140
	dsh^{1}	Strong allele for planar polarity function	Crossed out to wild type	FBal0003138
prickle-spiny-legs	$pk\text{-}sple^{13}$	Null allele	Crossed out to wild type	FBal0060943
flamingo (starry night)	fmi^{E59}	Null allele		FBal0101421
multiple wing hairs	mwh^{1}	Null allele	Crossed out to wild type	FBal0012675
fuzzy	$fuzzy^{2}$	Null allele	Crossed out to wild type	FBal0004916
RhoGEF2	$RhoGEF2^{6.5}$	Antimorphic allele	Zygotic mutants die early	FBal0085926
shotgun	shg^{IG27}	P-element loss of function allele		FBgn0003391
Src42A	$Src42A^{F80}$	Amino acid substitution in the kinase domain		FBal0277626
Shibire	shi^{ts1}	Temperature sensitive allele of *shi*	Heat shock to disrupt Shi activity	FBal0246565

Name of construct	Comments	Flybase reference
fz-EGFP	EGFP recombined into the C terminus of the endogenous Fz locus	
Ubi-E-cad-GFP	E-Cadherin tagged with GFP expressed under control of the *ubiquitin* promoter	FBtp0014096
E-cad::GFP	Knock-in of GFP into the endogenous *E-cadherin* (*shotgun*) locus FBal0247908	FBal0247908
hs-FLP	Yeast FLP recombinase under control of a *heat-shock* promoter	FBst0005256
btl>y+>GAL4	*breathless* promoter upstream of the GAL4 coding sequence, separated by an FRT cassette containing a yellow transgene	FBtp0020129
ptc-GAL4	Gal4 driven by the patched promoter	FBal0040487
UAS-pk	UAS-driven expression of Prickle	FBal0101220
Ubx-FLP	UAS-driven expression of yeast FLP recombinase	FBst0042718
UAS-shi^{ts1}	UAS-driven expression of temperature-sensitive shibire	FBst0030010
ActP-fz-EYFP	*frizzled* tagged with YFP expressed under control of the *actin* promoter	FBtp0014596
ArmP-Fmi-EGFP	*flamingo* tagged with GFP expressed under control of the *armadillo* promoter	
ActP-FRT-polyA-FRT-fz-EYFP	*actin* promoter upstream of the *fz-EYFP* coding sequence, separated by an FRT cassette containing a polyA sequence	

Name of construct	Comments	Flybase reference
UAS-fz	UAS-driven expression of *frizzled*	FBal0060399
en-Gal4^{e16E}	Gal4 driven by the *engrailed* promoter	FBal0052377
shg-lacZ	*lacZ* enhancer trap insertion in the *shotgun* (*E-Cad*) locus	FBtp0039292
btl-Gal4	Gal4 expression by the *breathless* promoter	FBti0072919
UAS-Apoliner^{5}	UAS-driven expression of Apoliner on II	FBti0131165
UAS-red-stinger	UAS-driven expression of red stinger-NLS on III	FBtp0018199
UAS-α-Cat-GFP	UAS-driven expression of α-Catenin tagged with GFP	FBti0015823
UAS-Rab5^{SN}	UAS-driven expression of Rab5 dominant negative	FBal0189754
UAS-shg-DEFL$^{6.3}$ *(GFP)*	UAS-driven expression of E-*Cad* tagged with GFP	FBti0015825
UAS-RhoGEF2^{5}	UAS-driven expression of RhoGEF2	FBal0190772
RhoGEF2$^{IR\text{-}HMS01118}$	UAS-driven expression of RNAi targeting RhoGEF2	FBtp0065361
UAS-RhoA^{V14}	UAS-driven expression of RhoAV14 dominant active	FBal0105124
UAS-RhoA^{N19}	UAS-driven expression of RhoAN19 dominant negative	FBtp0008154
dsh-GFP	Dishevelled tagged with GFP expressed under its endogenous promoter	FBti0017855

Chapter 8
Bibliography

Bibliography

Adler, P.N. 1992. The genetic control of tissue polarity in Drosophila. *Bioessays*. 14:735-741.

Adler, P.N. 2002. Planar signaling and morphogenesis in Drosophila. *Dev Cell*. 2:525-535.

Adler, P.N., Charlton, J., and Liu, J. 1998. Mutations in the cadherin superfamily member gene dachsous cause a tissue polarity phenotype by altering frizzled signaling. *Development*. 125:959-968.

Adler, P.N., Charlton, J., and Park, W.J. 1994. The Drosophila tissue polarity gene inturned functions prior to wing hair morphogenesis in the regulation of hair polarity and number. *Genetics*. 137:829-836.

Adler, P.N., Krasnow, R.E., and Liu, J. 1997. Tissue polarity points from cells that have higher Frizzled levels towards cells that have lower Frizzled levels. *Curr Biol*. 7:940-949.

Adler, P.N., Liu, J., and Charlton, J. 2000a. Cell size and the morphogenesis of wing hairs in Drosophila. *Genesis*. 28:82-91.

Adler, P.N., Taylor, J., and Charlton, J. 2000b. The domineering non-autonomy of frizzled and van Gogh clones in the Drosophila wing is a consequence of a disruption in local signaling. *Mech Dev*. 96:197-207.

Adler, P.N., Vinson, C., Park, W.J., Conover, S., and Klein, L. 1990. Molecular structure of frizzled, a Drosophila tissue polarity gene. *Genetics*. 126:401-416.

Adler, P.N., Zhu, C., and Stone, D. 2004. Inturned localizes to the proximal side of wing cells under the instruction of upstream planar polarity proteins. *Curr Biol*. 14:2046-2051.

Affolter, M., Bellusci, S., Itoh, N., Shilo, B., Thiery, J.P., and Werb, Z. 2003. Tube or not tube: remodeling epithelial tissues by branching morphogenesis. *Dev Cell*. 4:11-18.

Affolter, M., Zeller, R., and Caussinus, E. 2009. Tissue remodelling through branching morphogenesis. *Nat Rev Mol Cell Biol*. 10:831-842.

Aigouy, B., Farhadifar, R., Staple, D.B., Sagner, A., Roper, J.C., Julicher, F., and Eaton, S. 2010. Cell flow reorients the axis of planar polarity in the wing epithelium of Drosophila. *Cell*. 142:773-786.

Ambegaonkar, A.A., Pan, G., Mani, M., Feng, Y., and Irvine, K.D. 2012. Propagation of Dachsous-Fat planar cell polarity. *Curr Biol*. 22:1302-1308.

Amonlirdviman, K., Khare, N.A., Tree, D.R., Chen, W.S., Axelrod, J.D., and Tomlin, C.J. 2005. Mathematical modeling of planar cell polarity to understand domineering nonautonomy. *Science*. 307:423-426.

Antic, D., Stubbs, J.L., Suyama, K., Kintner, C., Scott, M.P., and Axelrod, J.D. 2010. Planar cell polarity enables posterior localization of nodal cilia and left-right axis determination during mouse and Xenopus embryogenesis. *PLoS One*. 5:e8999.

Axelrod, D., Koppel, D.E., Schlessinger, J., Elson, E., and Webb, W.W. 1976. Mobility measurement by analysis of fluorescence photobleaching recovery kinetics. *Biophys J*. 16:1055-1069.

Axelrod, J.D. 2001. Unipolar membrane association of Dishevelled mediates Frizzled planar cell polarity signaling. *Genes Dev*. 15:1182-1187.

Axelrod, J.D., Miller, J.R., Shulman, J.M., Moon, R.T., and Perrimon, N. 1998. Differential recruitment of Dishevelled provides signaling specificity in the planar cell polarity and Wingless signaling pathways. *Genes Dev*. 12:2610-2622.

Baena-Lopez, L.A., Baonza, A., and Garcia-Bellido, A. 2005. The orientation of cell divisions determines the shape of Drosophila organs. *Curr Biol*. 15:1640-1644.

Baer, M.M., Bilstein, A., Caussinus, E., Csiszar, A., Affolter, M., and Leptin, M. 2010. The role of apoptosis in shaping the tracheal system in the Drosophila embryo. *Mech Dev*. 127:28-35.

Bardet, P.L., Kolahgar, G., Mynett, A., Miguel-Aliaga, I., Briscoe, J., Meier, P., and Vincent, J.P. 2008. A fluorescent reporter of caspase activity for live imaging. *Proc Natl Acad Sci U S A*. 105:13901-13905.

Barrett, K., Leptin, M., and Settleman, J. 1997. The Rho GTPase and a putative RhoGEF mediate a signaling pathway for the cell shape changes in Drosophila gastrulation. *Cell*. 91:905-915.

Bastock, R., Strutt, H., and Strutt, D. 2003. Strabismus is asymmetrically localised and binds to Prickle and Dishevelled during Drosophila planar polarity patterning. *Development*. 130:3007-3014.

Behr, M., Wingen, C., Wolf, C., Schuh, R., and Hoch, M. 2007. Wurst is essential for airway clearance and respiratory-tube size control. *Nat Cell Biol*. 9:847-853.

Behrens, J., Vakaet, L., Friis, R., Winterhager, E., Van Roy, F., Mareel, M.M., and Birchmeier, W. 1993. Loss of epithelial differentiation and gain of invasiveness correlates with tyrosine phosphorylation of the E-cadherin/beta-catenin complex in cells transformed with a temperature-sensitive v-SRC gene. *J Cell Biol*. 120:757-766.

Beloussov, L.V., Louchinskaia, N.N., and Stein, A.A. 2000. Tension-dependent collective cell movements in the early gastrula ectoderm of Xenopus laevis embryos. *Dev Genes Evol*. 210:92-104.

Berleth, T., Burri, M., Thoma, G., Bopp, D., Richstein, S., Frigerio, G., Noll, M., and Nusslein-Volhard, C. 1988. The role of localization of bicoid RNA in organizing the anterior pattern of the Drosophila embryo. *EMBO J*. 7:1749-1756.

Bertet, C., and Lecuit, T. 2009. Planar polarity and short-range polarization in Drosophila embryos. *Semin Cell Dev Biol*. 20:1006-1013.

Bertet, C., Sulak, L., and Lecuit, T. 2004. Myosin-dependent junction remodelling controls planar cell intercalation and axis elongation. *Nature*. 429:667-671.

Bhanot, P., Fish, M., Jemison, J.A., Nusse, R., Nathans, J., and Cadigan, K.M. 1999. Frizzled and Dfrizzled-2 function as redundant receptors for Wingless during Drosophila embryonic development. *Development*. 126:4175-4186.

Bhat, K.M. 1998. frizzled and frizzled 2 play a partially redundant role in wingless signaling and have similar requirements to wingless in neurogenesis. *Cell*. 95:1027-1036.

Blankenship, J.T., Backovic, S.T., Sanny, J.S., Weitz, O., and Zallen, J.A. 2006. Multicellular rosette formation links planar cell polarity to tissue morphogenesis. *Dev Cell*. 11:459-470.

Bloor, J.W., and Kiehart, D.P. 2002. Drosophila RhoA regulates the cytoskeleton and cell-cell adhesion in the developing epidermis. *Development*. 129:3173-3183.

Borovina, A., Superina, S., Voskas, D., and Ciruna, B. 2010. Vangl2 directs the posterior tilting and asymmetric localization of motile primary cilia. *Nat Cell Biol*. 12:407-412.

Bosveld, F., Bonnet, I., Guirao, B., Tlili, S., Wang, Z., Petitalot, A., Marchand, R., Bardet, P.L., Marcq, P., Graner, F., and Bellaiche, Y. 2012. Mechanical control of morphogenesis by Fat/Dachsous/Four-jointed planar cell polarity pathway. *Science*. 336:724-727.

Boutros, M., Paricio, N., Strutt, D.I., and Mlodzik, M. 1998. Dishevelled activates JNK and discriminates between JNK pathways in planar polarity and wingless signaling. *Cell*. 94:109-118.

Brand, A.H., and Perrimon, N. 1993. Targeted gene expression as a means of altering cell fates and generating dominant phenotypes. *Development*. 118:401-415.

Brittle, A., Thomas, C., and Strutt, D. 2012. Planar polarity specification through asymmetric subcellular localization of Fat and Dachsous. *Curr Biol*. 22:907-914.

Brittle, A.L., Repiso, A., Casal, J., Lawrence, P.A., and Strutt, D. 2010. Four-jointed modulates growth and planar polarity by reducing the affinity of dachsous for fat. *Curr Biol*. 20:803-810.

Brower, D.L., and Jaffe, S.M. 1989. Requirement for integrins during Drosophila wing development. *Nature*. 342:285-287.

Bulgakova, N.A., Grigoriev, I., Yap, A.S., Akhmanova, A., and Brown, N.H. 2013. Dynamic microtubules produce an asymmetric E-cadherin-Bazooka complex to maintain segment boundaries. *J Cell Biol*. 201:887-901.

Burak, Y., and Shraiman, B.I. 2009. Order and stochastic dynamics in Drosophila planar cell polarity. *PLoS Comput. Biol.* 5:e1000628.

Butler, L.C., Blanchard, G.B., Kabla, A.J., Lawrence, N.J., Welchman, D.P., Mahadevan, L., Adams, R.J., and Sanson, B. 2009. Cell shape changes indicate a role for extrinsic tensile forces in Drosophila germ-band extension. *Nat Cell Biol*. 11:859-864.

Cabernard, C., Neumann, M., and Affolter, M. 2004. Cellular and molecular mechanisms involved in branching morphogenesis of the Drosophila tracheal system. *J Appl Physiol*. 97:2347-2353.

Capdevila, J., and Guerrero, I. 1994. Targeted expression of the signaling molecule decapentaplegic induces pattern duplications and growth alterations in Drosophila wings. *EMBO J*. 13:4459-4468.

Carreira-Barbosa, F., Concha, M.L., Takeuchi, M., Ueno, N., Wilson, S.W., and Tada, M. 2003. Prickle 1 regulates cell movements during gastrulation and neuronal migration in zebrafish. *Development*. 130:4037-4046.

Casal, J., Lawrence, P.A., and Struhl, G. 2006. Two separate molecular systems, Dachsous/Fat and Starry night/Frizzled, act independently to confer planar cell polarity. *Development*. 133:4561-4572.

Casal, J., Struhl, G., and Lawrence, P.A. 2002. Developmental compartments and planar polarity in Drosophila. *Curr Biol*. 12:1189-1198.

Caussinus, E., Colombelli, J., and Affolter, M. 2008. Tip-cell migration controls stalk-cell intercalation during Drosophila tracheal tube elongation. *Curr Biol*. 18:1727-1734.

C andavey, M., Rauzi, M., Lenne, P.F., and Lecuit, T. 2008. A two-tiered mechanism for stabilization and immobilization of E-cadherin. *Nature*. 453:751-756.

Cela, C., and Llimargas, M. 2006. Egfr is essential for maintaining epithelial integrity during tracheal remodelling in Drosophila. *Development*. 133:3115-3125.

Chae, J., Kim, M.J., Goo, J.H., Collier, S., Gubb, D., Charlton, J., Adler, P.N., and Park, W.J. 1999. The Drosophila tissue polarity gene starry night encodes a member of the protocadherin family. *Development*. 126:5421-5429.

Chen, C.M., and Struhl, G. 1999. Wingless transduction by the Frizzled and Frizzled2 proteins of Drosophila. *Development*. 126:5441-5452.

Chen, W.S., Antic, D., Matis, M., Logan, C.Y., Povelones, M., Anderson, G.A., Nusse, R., and Axelrod, J.D. 2008. Asymmetric homotypic interactions of the atypical cadherin flamingo mediate intercellular polarity signaling. *Cell*. 133:1093-1105.

Chihara, T., Kato, K., Taniguchi, M., Ng, J., and Hayashi, S. 2003. Rac promotes epithelial cell rearrangement during tracheal tubulogenesis in Drosophila. *Development*. 130:1419-1428.

Chung, S., Vining, M.S., Bradley, P.L., Chan, C.C., Wharton, K.A., Jr., and Andrew, D.J. 2009. Serrano (sano) functions with the planar cell polarity genes to control tracheal tube length. *PLoS Genet*. 5:e1000746.

Ciruna, B., Jenny, A., Lee, D., Mlodzik, M., and Schier, A.F. 2006. Planar cell polarity signalling couples cell division and morphogenesis during neurulation. *Nature*. 439:220-224.

Clark, H.F., Brentrup, D., Schneitz, K., Bieber, A., Goodman, C., and Noll, M. 1995. Dachsous encodes a member of the cadherin superfamily that controls imaginal disc morphogenesis in Drosophila. *Genes Dev*. 9:1530-1542.

Classen, A.K., Aigouy, B., Giangrande, A., and Eaton, S. 2008. Imaging Drosophila pupal wing morphogenesis. *Methods Mol Biol*. 420:265-275.

Classen, A.K., Anderson, K.I., Marois, E., and Eaton, S. 2005. Hexagonal packing of Drosophila wing epithelial cells by the planar cell polarity pathway. *Dev Cell*. 9:805-817.

Collier, S., and Gubb, D. 1997. Drosophila tissue polarity requires the cell-autonomous activity of the fuzzy gene, which encodes a novel transmembrane protein. *Development*. 124:4029-4037.

Collier, S., Lee, H., Burgess, R., and Adler, P. 2005. The WD40 repeat protein fritz links cytoskeletal planar polarity to frizzled subcellular localization in the Drosophila epidermis. *Genetics*. 169:2035-2045.

Cooper, M.T., and Bray, S.J. 1999. Frizzled regulation of Notch signalling polarizes cell fate in the Drosophila eye. *Nature*. 397:526-530.

Couso, J.P., Bate, M., and Martinez-Arias, A. 1993. A wingless-dependent polar coordinate system in Drosophila imaginal discs. *Science*. 259:484-489.

Couso, J.P., Bishop, S.A., and Martinez Arias, A. 1994. The wingless signalling pathway and the patterning of the wing margin in Drosophila. *Development*. 120:621-636.

Curtin, J.A., Quint, E., Tsipouri, V., Arkell, R.M., Cattanach, B., Copp, A.J., Henderson, D.J., Spurr, N., Stanier, P., Fisher, E.M., Nolan, P.M., Steel, K.P., Brown, S.D., Gray, I.C., and Murdoch, J.N. 2003. Mutation of Celsr1 disrupts planar polarity of inner ear hair cells and causes severe neural tube defects in the mouse. *Curr Biol*. 13:1129-1133.

da Silva, S.M., and Vincent, J.P. 2007. Oriented cell divisions in the extending germband of Drosophila. *Development*. 134:3049-3054.

Das, G., Jenny, A., Klein, T.J., Eaton, S., and Mlodzik, M. 2004. Diego interacts with Prickle and Strabismus/Van Gogh to localize planar cell polarity complexes. *Development*. 131:4467-4476.

Das, G., Reynolds-Kenneally, J., and Mlodzik, M. 2002. The atypical cadherin Flamingo links Frizzled and Notch signaling in planar polarity establishment in the Drosophila eye. *Dev Cell*. 2:655-666.

Davis, I., and Ish-Horowicz, D. 1991. Apical localization of pair-rule transcripts requires 3' sequences and limits protein diffusion in the Drosophila blastoderm embryo. *Cell*. 67:927-940.

de Beco, S., Gueudry, C., Amblard, F., and Coscoy, S. 2009. Endocytosis is required for E-cadherin redistribution at mature adherens junctions. *Proc Natl Acad Sci U S A*. 106:7010-7015.

Descamps, B., Sewduth, R., Ferreira Tojais, N., Jaspard, B., Reynaud, A., Sohet, F., Lacolley, P., Allieres, C., Lamaziere, J.M., Moreau, C., Dufourcq, P., Couffinhal, T., and Duplaa, C. 2012. Frizzled 4 regulates arterial network

organization through noncanonical Wnt/planar cell polarity signaling. *Circ Res*. 110:47-58.

Devenport, D., and Fuchs, E. 2008. Planar polarization in embryonic epidermis orchestrates global asymmetric morphogenesis of hair follicles. *Nat Cell Biol*. 10:1257-1268.

Ditzel, M., Wilson, R., Tenev, T., Zachariou, A., Paul, A., Deas, E., and Meier, P. 2003. Degradation of DIAP1 by the N-end rule pathway is essential for regulating apoptosis. *Nat Cell Biol*. 5:467-473.

Doyle, K., Hogan, J., Lester, M., and Collier, S. 2008. The Frizzled Planar Cell Polarity signaling pathway controls Drosophila wing topography. *Dev Biol*. 317:354-367.

Drees, F., Pokutta, S., Yamada, S., Nelson, W.J., and Weis, W.I. 2005. Alpha-catenin is a molecular switch that binds E-cadherin-beta-catenin and regulates actin-filament assembly. *Cell*. 123:903-915.

Eaton, S., Wepf, R., and Simons, K. 1996. Roles for Rac1 and Cdc42 in planar polarization and hair outgrowth in the wing of Drosophila. *J Cell Biol*. 135:1277-1289.

Edgar, B.A., and O'Farrell, P.H. 1989. Genetic control of cell division patterns in the Drosophila embryo. *Cell*. 57:177-187.

Emery, G., Hutterer, A., Berdnik, D., Mayer, B., Wirtz-Peitz, F., Gaitan, M.G., and Knoblich, J.A. 2005. Asymmetric Rab 11 endosomes regulate delta recycling and specify cell fate in the Drosophila nervous system. *Cell*. 122:763-773.

Ezan, J., and Montcouquiol, M. 2013. Revisiting planar cell polarity in the inner ear. *Semin Cell Dev Biol*. 24:499-506.

Fanto, M., and McNeill, H. 2004. Planar polarity from flies to vertebrates. *J Cell Sci*. 117:527-533.

Fanto, M., and Mlodzik, M. 1999. Asymmetric Notch activation specifies photoreceptors R3 and R4 and planar polarity in the Drosophila eye. *Nature*. 397:523-526.

Feiguin, F., Hannus, M., Mlodzik, M., and Eaton, S. 2001. The ankyrin repeat protein Diego mediates Frizzled-dependent planar polarization. *Dev Cell*. 1:93-101.

Fernandez-Gonzalez, R., Simoes Sde, M., Roper, J.C., Eaton, S., and Zallen, J.A. 2009. Myosin II dynamics are regulated by tension in intercalating cells. *Dev Cell*. 17:736-743.

Firmino, J., Tinevez, J.Y., and Knust, E. 2013. Crumbs affects protein dynamics in anterior regions of the developing Drosophila embryo. *PLoS One*. 8:e58839.

Fischer, S., Houston, P., Monk, N.A., and Owen, M.R. 2013. Is a persistent global bias necessary for the establishment of planar cell polarity? *PLoS One*. 8:e60064.

Forster, D., and Luschnig, S. 2012. Src42A-dependent polarized cell shape changes mediate epithelial tube elongation in Drosophila. *Nat Cell Biol*. 14:526-534.

Fox, D.T., and Peifer, M. 2007. Abelson kinase (Abl) and RhoGEF2 regulate actin organization during cell constriction in Drosophila. *Development*. 134:567-578.

Fujita, Y., Krause, G., Scheffner, M., Zechner, D., Leddy, H.E., Behrens, J., Sommer, T., and Birchmeier, W. 2002. Hakai, a c-Cbl-like protein, ubiquitinates and induces endocytosis of the E-cadherin complex. *Nat Cell Biol*. 4:222-231.

Garoia, F., Guerra, D., Pezzoli, M.C., Lopez-Varea, A., Cavicchi, S., and Garcia-Bellido, A. 2000. Cell behaviour of Drosophila fat cadherin mutations in wing development. *Mech Dev*. 94:95-109.

Georgiou, M., Marinari, E., Burden, J., and Baum, B. 2008. Cdc42, Par6, and aPKC regulate Arp2/3-mediated endocytosis to control local adherens junction stability. *Curr Biol*. 18:1631-1638.

Gierer, A., and Meinhardt, H. 1972. A theory of biological pattern formation. *Kybernetik*. 12:30-39.

Golic, K.G., and Lindquist, S. 1989. The FLP recombinase of yeast catalyzes site-specific recombination in the Drosophila genome. *Cell*. 59:499-509.

Goodrich, L.V., and Strutt, D. 2011. Principles of planar polarity in animal development. *Development*. 138:1877-1892.

Goto, T., Davidson, L., Asashima, M., and Keller, R. 2005. Planar cell polarity genes regulate polarized extracellular matrix deposition during frog gastrulation. *Curr Biol*. 15:787-793.

Goto, T., and Keller, R. 2002. The planar cell polarity gene strabismus regulates convergence and extension and neural fold closure in Xenopus. *Dev Biol*. 247:165-181.

Gray, R.S., Abitua, P.B., Wlodarczyk, B.J., Szabo-Rogers, H.L., Blanchard, O., Lee, I., Weiss, G.S., Liu, K.J., Marcotte, E.M., Wallingford, J.B., and Finnell, R.H. 2009. The planar cell polarity effector Fuz is essential for targeted membrane trafficking, ciliogenesis and mouse embryonic development. *Nat Cell Biol*. 11:1225-1232.

Grevengoed, E.E., Loureiro, J.J., Jesse, T.L., and Peifer, M. 2001. Abelson kinase regulates epithelial morphogenesis in Drosophila. *J Cell Biol*. 155:1185-1198.

Grosshans, J., Wenzl, C., Herz, H.M., Bartoszewski, S., Schnorrer, F., Vogt, N., Schwarz, H., and Muller, H.A. 2005. RhoGEF2 and the formin Dia control the formation of the furrow canal by directed actin assembly during Drosophila cellularisation. *Development*. 132:1009-1020.

Gubb, D., and Garcia-Bellido, A. 1982. A genetic analysis of the determination of cuticular polarity during development in Drosophila melanogaster. *J Embryol Exp Morphol*. 68:37-57.

Gubb, D., Green, C., Huen, D., Coulson, D., Johnson, G., Tree, D., Collier, S., and Roote, J. 1999. The balance between isoforms of the prickle LIM domain protein is critical for planar polarity in Drosophila imaginal discs. *Genes Dev*. 13:2315-2327.

Gumbiner, B.M. 2005. Regulation of cadherin-mediated adhesion in morphogenesis. *Nat Rev Mol Cell Biol*. 6:622-634.

Hartenstein, V. 1993. Atlas of Drosophila development. Cold Spring Harbor Laboratory Press, Cold Spring Harbor, NY,.

Harumoto, T., Ito, M., Shimada, Y., Kobayashi, T.J., Ueda, H.R., Lu, B., and Uemura, T. 2010. Atypical cadherins Dachsous and Fat control dynamics of noncentrosomal microtubules in planar cell polarity. *Dev Cell*. 19:389-401.

Hashimoto, M., Shinohara, K., Wang, J., Ikeuchi, S., Yoshiba, S., Meno, C., Nonaka, S., Takada, S., Hatta, K., Wynshaw-Boris, A., and Hamada, H. 2010. Planar polarization of node cells determines the rotational axis of node cilia. *Nat Cell Biol*. 12:170-176.

He, X., Semenov, M., Tamai, K., and Zeng, X. 2004. LDL receptor-related proteins 5 and 6 in Wnt/beta-catenin signaling: arrows point the way. *Development*. 131:1663-1677.

Heisenberg, C.P., Tada, M., Rauch, G.J., Saude, L., Concha, M.L., Geisler, R., Stemple, D.L., Smith, J.C., and Wilson, S.W. 2000. Silberblick/Wnt11 mediates convergent extension movements during zebrafish gastrulation. *Nature*. 405:76-81.

Held, L.I., Jr., Duarte, C.M., and Derakhshanian, K. 1986. Extra joints and misoriented bristles on Drosophila legs. *Prog Clin Biol Res*. 217A:293-296.

Heydeck, W., Zeng, H., and Liu, A. 2009. Planar cell polarity effector gene Fuzzy regulates cilia formation and Hedgehog signal transduction in mouse. *Dev Dyn*. 238:3035-3042.

Hogan, J., Valentine, M., Cox, C., Doyle, K., and Collier, S. 2011. Two frizzled planar cell polarity signals in the Drosophila wing are differentially organized by the Fat/Dachsous pathway. *PLoS Genet*. 7:e1001305.

Huang, J., Huang, L., Chen, Y.J., Austin, E., Devor, C.E., Roegiers, F., and Hong, Y. 2011. Differential regulation of adherens junction dynamics during apical-basal polarization. *J Cell Sci*. 124:4001-4013.

Huang, J., Zhou, W., Dong, W., and Hong, Y. 2009. Targeted engineering of the Drosophila genome. *Fly (Austin)*. 3:274-277.

Irvine, K.D., and Wieschaus, E. 1994. Cell intercalation during Drosophila germband extension and its regulation by pair-rule segmentation genes. *Development*. 120:827-841.

Ishikawa, H.O., Takeuchi, H., Haltiwanger, R.S., and Irvine, K.D. 2008. Four-jointed is a Golgi kinase that phosphorylates a subset of cadherin domains. *Science*. 321:401-404.

Jazwinska, A., Ribeiro, C., and Affolter, M. 2003. Epithelial tube morphogenesis during Drosophila tracheal development requires Piopio, a luminal ZP protein. *Nat Cell Biol*. 5:895-901.

Jenny, A., Darken, R.S., Wilson, P.A., and Mlodzik, M. 2003. Prickle and Strabismus form a functional complex to generate a correct axis during planar cell polarity signaling. *Embo J*. 22:4409-4420.

Jenny, A., Reynolds-Kenneally, J., Das, G., Burnett, M., and Mlodzik, M. 2005. Diego and Prickle regulate Frizzled planar cell polarity signalling by competing for Dishevelled binding. *Nat Cell Biol*. 7:691-697.

Jessen, J.R., Topczewski, J., Bingham, S., Sepich, D.S., Marlow, F., Chandrasekhar, A., and Solnica-Krezel, L. 2002. Zebrafish trilobite identifies new roles for Strabismus in gastrulation and neuronal movements. *Nat Cell Biol*. 4:610-615.

Jones, C., and Chen, P. 2007. Planar cell polarity signaling in vertebrates. *Bioessays*. 29:120-132.

Kaltschmidt, J.A., Lawrence, N., Morel, V., Balayo, T., Fernandez, B.G., Pelissier, A., Jacinto, A., and Martinez Arias, A. 2002. Planar polarity and actin dynamics in the epidermis of Drosophila. *Nat Cell Biol*. 4:937-944.

Keller, R., Davidson, L., Edlund, A., Elul, T., Ezin, M., Shook, D., and Skoglund, P. 2000. Mechanisms of convergence and extension by cell intercalation. *Philos Trans R Soc Lond B Biol Sci*. 355:897-922.

Kennerdell, J.R., and Carthew, R.W. 1998. Use of dsRNA-mediated genetic interference to demonstrate that frizzled and frizzled 2 act in the wingless pathway. *Cell*. 95:1017-1026.

Kibar, Z., Vogan, K.J., Groulx, N., Justice, M.J., Underhill, D.A., and Gros, P. 2001. Ltap, a mammalian homolog of Drosophila Strabismus/Van Gogh, is altered in the mouse neural tube mutant Loop-tail. *Nat Genet*. 28:251-255.

Kim, S.K., Shindo, A., Park, T.J., Oh, E.C., Ghosh, S., Gray, R.S., Lewis, R.A., Johnson, C.A., Attie-Bittach, T., Katsanis, N., and Wallingford, J.B. 2010. Planar cell polarity acts through septins to control collective cell movement and ciliogenesis. *Science*. 329:1337-1340.

Klein, T.J., and Mlodzik, M. 2005. Planar cell polarization: an emerging model points in the right direction. *Annual Review of Cell Developmental Biology*. 21:155-176.

Klingensmith, J., Nusse, R., and Perrimon, N. 1994. The Drosophila segment polarity gene dishevelled encodes a novel protein required for response to the wingless signal. *Genes Dev*. 8:118-130.

Koleske, A.J., Gifford, A.M., Scott, M.L., Nee, M., Bronson, R.T., Miczek, K.A., and Baltimore, D. 1998. Essential roles for the Abl and Arg tyrosine kinases in neurulation. *Neuron*. 21:1259-1272.

Krasnow, R.E., Wong, L.L., and Adler, P.N. 1995. Dishevelled is a component of the frizzled signaling pathway in Drosophila. *Development*. 121:4095-4102.

Lawrence, P.A. 1966. Development and determination of hairs and bristles in the milkweed bug, Oncopeltus fasciatus (Lygaeidae, Hemiptera). *J Cell Sci*. 1:475-498.

Lawrence, P.A., Casal, J., and Struhl, G. 2002. Towards a model of the organisation of planar polarity and pattern in the Drosophila abdomen. *Development*. 129:2749-2760.

Lawrence, P.A., Casal, J., and Struhl, G. 2004. Cell interactions and planar polarity in the abdominal epidermis of Drosophila. *Development*. 131:4651-4664.

Lawrence, P.A., Crick, F.H., and Munro, M. 1972. A gradient of positional information in an insect, Rhodnius. *J Cell Sci*. 11:815-853.

Le Garrec, J.F., Lopez, P., and Kerszberg, M. 2006. Establishment and maintenance of planar epithelial cell polarity by asymmetric cadherin bridges: a computer model. *Dev. Dynam.* 235:235-246.

Lecuit, T. 2005. Adhesion remodeling underlying tissue morphogenesis. *Trends Cell Biol*. 15:34-42.

Lecuit, T., and Lenne, P.F. 2007. Cell surface mechanics and the control of cell shape, tissue patterns and morphogenesis. *Nat Rev Mol Cell Biol*. 8:633-644.

Lee, H., and Adler, P.N. 2002. The function of the frizzled pathway in the Drosophila wing is dependent on inturned and fuzzy. *Genetics*. 160:1535-1547.

Lee, S., and Kolodziej, P.A. 2002a. The plakin Short Stop and the RhoA GTPase are required for E-cadherin-dependent apical surface remodeling during tracheal tube fusion. *Development*. 129:1509-1520.

Lee, S., and Kolodziej, P.A. 2002b. Short Stop provides an essential link between F-actin and microtubules during axon extension *Development*. 129:1195-1204.

Leibfried, A., Fricke, R., Morgan, M.J., Bogdan, S., and Bellaiche, Y. 2008. Drosophila Cip4 and WASp define a branch of the Cdc42-Par6-aPKC pathway regulating E-cadherin endocytosis. *Curr Biol*. 18:1639-1648.

Levayer, R., Pelissier-Monier, A., and Lecuit, T. 2011. Spatial regulation of Dia and Myosin-II by RhoGEF2 controls initiation of E-cadherin endocytosis during epithelial morphogenesis. *Nat Cell Biol*. 13:529-540.

Lienkamp, S.S., Liu, K., Karner, C.M., Carroll, T.J., Ronneberger, O., Wallingford, J.B., and Walz, G. 2012. Vertebrate kidney tubules elongate using a planar cell polarity-dependent, rosette-based mechanism of convergent extension. *Nat Genet*. 44:1382-1387.

Lindqvist, M., Horn, Z., Bryja, V., Schulte, G., Papachristou, P., Ajima, R., Dyberg, C., Arenas, E., Yamaguchi, T.P., Lagercrantz, H., and Ringstedt, T. 2009. Vang-like protein 2 and Rac1 interact to regulate adherens junctions. *J Cell Sci*. 123:472-483.

Locke, M. 1959. The cuticular pattern in an insect, *Rhodnius Prolixus Stal The Journal of Experimental Biology*. 36:459-477.

Lubarsky, B., and Krasnow, M.A. 2003. Tube morphogenesis: making and shaping biological tubes. *Cell*. 112:19-28.

Lye, C.M., and Sanson, B. 2011. Tension and epithelial morphogenesis in Drosophila early embryos. *Curr Top Dev Biol*. 95:145-187.

Ma, D., Yang, C.H., McNeill, H., Simon, M.A., and Axelrod, J.D. 2003. Fidelity in planar cell polarity signalling. *Nature*. 421:543-547.

Macdonald, P.M., and Struhl, G. 1988. cis-acting sequences responsible for anterior localization of bicoid mRNA in Drosophila embryos. *Nature*. 336:595-598.

Mao, Y., Rauskolb, C., Cho, E., Hu, W.L., Hayter, H., Minihan, G., Katz, F.N., and Irvine, K.D. 2006. Dachs: an unconventional myosin that functions downstream of Fat to regulate growth, affinity and gene expression in Drosophila. *Development*. 133:2539-2551.

Matakatsu, H., and Blair, S.S. 2004. Interactions between Fat and Dachsous and the regulation of planar cell polarity in the Drosophila wing. *Development*. 131:3785-3794.

Matakatsu, H., and Blair, S.S. 2008. The DHHC palmitoyltransferase approximated regulates Fat signaling and Dachs localization and activity. *Curr Biol*. 18:1390-1395.

McGuire, S.E., Le, P.T., Osborn, A.J., Matsumoto, K., and Davis, R.L. 2003. Spatiotemporal rescue of memory dysfunction in Drosophila. *Science*. 302:1765-1768.

Mirkovic, I., Gault, W.J., Rahnama, M., Jenny, A., Gaengel, K., Bessette, D., Gottardi, C.J., Verheyen, E.M., and Mlodzik, M. 2011. Nemo kinase phosphorylates beta-catenin to promote ommatidial rotation and connects core PCP factors to E-cadherin-beta-catenin. *Nat Struct Mol Biol*. 18:665-672.

Mitchell, B., Stubbs, J.L., Huisman, F., Taborek, P., Yu, C., and Kintner, C. 2009. The PCP pathway instructs the planar orientation of ciliated cells in the Xenopus larval skin. *Curr Biol*. 19:924-929.

Mlodzik, M. 2002. Planar cell polarization: do the same mechanisms regulate Drosophila tissue polarity and vertebrate gastrulation? *Trends Genet*. 18:564-571.

Montcouquiol, M., Rachel, R.A., Lanford, P.J., Copeland, N.G., Jenkins, N.A., and Kelley, M.W. 2003. Identification of Vangl2 and Scrb1 as planar polarity genes in mammals. *Nature*. 423:173-177.

Montcouquiol, M., Sans, N., Huss, D., Kach, J., Dickman, J.D., Forge, A., Rachel, R.A., Copeland, N.G., Jenkins, N.A., Bogani, D., Murdoch, J., Warchol, M.E., Wenthold, R.J., and Kelley, M.W. 2006. Asymmetric localization of Vangl2 and Fz3 indicate novel mechanisms for planar cell polarity in mammals. *J Neurosci*. 26:5265-5275.

Morel, V., and Arias, A.M. 2004. Armadillo/beta-catenin-dependent Wnt signalling is required for the polarisation of epidermal cells during dorsal closure in Drosophila. *Development*. 131:3273-3283.

Mottola, G., Classen, A.K., Gonzalez-Gaitan, M., Eaton, S., and Zerial, M. 2010. A novel function for the Rab5 effector Rabenosyn-5 in planar cell polarity. *Development*. 137:2353-2364.

Mulinari, S., Barmchi, M.P., and Hacker, U. 2008. DRhoGEF2 and diaphanous regulate contractile force during segmental groove morphogenesis in the Drosophila embryo. *Mol Biol Cell*. 19:1883-1892.

Muller, H.A., Samanta, R., and Wieschaus, E. 1999. Wingless signaling in the Drosophila embryo: zygotic requirements and the role of the frizzled genes. *Development*. 126:577-586.

Murdoch, J.N., Doudney, K., Paternotte, C., Copp, A.J., and Stanier, P. 2001. Severe neural tube defects in the loop-tail mouse result from mutation of Lpp1, a novel gene involved in floor plate specification. *Hum Mol Genet*. 10:2593-2601.

Myat, M.M. 2005. Making tubes in the Drosophila embryo. *Dev Dyn*. 232:617-632.

Nelson, K.S., Khan, Z., Molnar, I., Mihaly, J., Kaschube, M., and Beitel, G.J. 2012. Drosophila Src regulates anisotropic apical surface growth to control epithelial tube size. *Nat Cell Biol*. 14:518-525.

Neumann, C.J., and Cohen, S.M. 1997. Long-range action of Wingless organizes the dorsal-ventral axis of the Drosophila wing. *Development*. 124:871-880.

Nikolaidou, K.K., and Barrett, K. 2004. A Rho GTPase signaling pathway is used reiteratively in epithelial folding and potentially selects the outcome of Rho activation. *Curr Biol*. 14:1822-1826.

Nishimura, T., Honda, H., and Takeichi, M. 2012. Planar cell polarity links axes of spatial dynamics in neural-tube closure. *Cell*. 149:1084-1097.

Oda, H., Uemura, T., Harada, Y., Iwai, Y., and Takeichi, M. 1994. A Drosophila homolog of cadherin associated with armadillo and essential for embryonic cell-cell adhesion. *Dev Biol*. 165:716-726.

Oteiza, P., Koppen, M., Krieg, M., Pulgar, E., Farias, C., Melo, C., Preibisch, S., Muller, D., Tada, M., Hartel, S., Heisenberg, C.P., and Concha, M.L. 2010. Planar cell polarity signalling regulates cell adhesion properties in progenitors of the zebrafish laterality organ. *Development*. 137:3459-3468.

Park, M., and Moon, R.T. 2002. The planar cell-polarity gene stbm regulates cell behaviour and cell fate in vertebrate embryos. *Nat Cell Biol*. 4:20-25.

Park, T.J., Haigo, S.L., and Wallingford, J.B. 2006. Ciliogenesis defects in embryos lacking inturned or fuzzy function are associated with failure of planar cell polarity and Hedgehog signaling. *Nat Genet*. 38:303-311.

Park, W.J., Liu, J., and Adler, P.N. 1994. Frizzled gene expression and development of tissue polarity in the Drosophila wing. *Dev Genet*. 15:383-389.

Park, W.J., Liu, J., Sharp, E.J., and Adler, P.N. 1996. The Drosophila tissue polarity gene inturned acts cell autonomously and encodes a novel protein. *Development*. 122:961-969.

Peifer, M., Pai, L.M., and Casey, M. 1994. Phosphorylation of the Drosophila adherens junction protein Armadillo: roles for wingless signal and zeste-white 3 kinase. *Dev Biol*. 166:543-556.

Peifer, M., Rauskolb, C., Williams, M., Riggleman, B., and Wieschaus, E. 1991. The segment polarity gene armadillo interacts with the wingless signaling pathway in both embryonic and adult pattern formation. *Development*. 111:1029-1043.

Perrimon, N., and Mahowald, A.P. 1987. Multiple functions of segment polarity genes in Drosophila. *Dev Biol*. 119:587-600.

Price, M.H., Roberts, D.M., McCartney, B.M., Jezuit, E., and Peifer, M. 2006. Cytoskeletal dynamics and cell signaling during planar polarity establishment in the Drosophila embryonic denticle. *J Cell Sci*. 119:403-415.

Rawls, A.S., Guinto, J.B., and Wolff, T. 2002. The cadherins fat and dachsous regulate dorsal/ventral signaling in the Drosophila eye. *Curr Biol*. 12:1021-1026.

Rawls, A.S., and Wolff, T. 2003. Strabismus requires Flamingo and Prickle function to regulate tissue polarity in the Drosophila eye. *Development*. 130:1877-1887.

Reits, E.A., and Neefjes, J.J. 2001. From fixed to FRAP: measuring protein mobility and activity in living cells. *Nat Cell Biol*. 3:E145-147.

Repiso, A., Saavedra, P., Casal, J., and Lawrence, P.A. 2010. Planar cell polarity: the orientation of larval denticles in Drosophila appears to depend on gradients of Dachsous and Fat. *Development*. 137:3411-3415.

Ribeiro, C., Ebner, A., and Affolter, M. 2002. In vivo imaging reveals different cellular functions for FGF and Dpp signaling in tracheal branching morphogenesis. *Dev Cell*. 2:677-683.

Ribeiro, C., Neumann, M., and Affolter, M. 2004. Genetic control of cell intercalation during tracheal morphogenesis in Drosophila. *Curr Biol*. 14:2197-2207.

Rida, P.C., and Chen, P. 2009. Line up and listen: Planar cell polarity regulation in the mammalian inner ear. *Semin Cell Dev Biol*. 20:978-985.

Rogulja, D., Rauskolb, C., and Irvine, K.D. 2008. Morphogen control of wing growth through the Fat signaling pathway. *Dev Cell*. 15:309-321.

Saburi, S., Hester, I., Fischer, E., Pontoglio, M., Eremina, V., Gessler, M., Quaggin, S.E., Harrison, R., Mount, R., and McNeill, H. 2008. Loss of Fat4 disrupts PCP signaling and oriented cell division and leads to cystic kidney disease. *Nat Genet*. 40:1010-1015.

Sagner, A., Merkel, M., Aigouy, B., Gaebel, J., Brankatschk, M., Julicher, F., and Eaton, S. 2012. Establishment of global patterns of planar polarity during growth of the Drosophila wing epithelium. *Curr Biol*. 22:1296-1301.

Samakovlis, C., Hacohen, N., Manning, G., Sutherland, D.C., Guillemin, K., and Krasnow, M.A. 1996. Development of the Drosophila tracheal system occurs by a series of morphologically distinct but genetically coupled branching events. *Development*. 122:1395-1407.

Sato, M., and Kornberg, T.B. 2002. FGF is an essential mitogen and chemoattractant for the air sacs of the drosophila tracheal system. *Dev Cell*. 3:195-207.

Sever, S. 2002. Dynamin and endocytosis. *Curr Opin Cell Biol*. 14:463-467.

Shaye, D.D., Casanova, J., and Llimargas, M. 2008. Modulation of intracellular trafficking regulates cell intercalation in the Drosophila trachea. *Nat Cell Biol*. 10:964-970.

Shimada, Y., Usui, T., Yanagawa, S., Takeichi, M., and Uemura, T. 2001. Asymmetric colocalization of Flamingo, a seven-pass transmembrane cadherin, and Dishevelled in planar cell polarization. *Curr Biol*. 11:859-863.

Shimada, Y., Yonemura, S., Ohkura, H., Strutt, D., and Uemura, T. 2006. Polarized transport of Frizzled along the planar microtubule arrays in Drosophila wing epithelium. *Dev Cell*. 10:209-222.

Shindo, M., Wada, H., Kaido, M., Tateno, M., Aigaki, T., Tsuda, L., and Hayashi, S. 2008. Dual function of Src in the maintenance of adherens junctions during tracheal epithelial morphogenesis. *Development*. 135:1355-1364.

Simon, M.A. 2004. Planar cell polarity in the Drosophila eye is directed by graded Four-jointed and Dachsous expression. *Development*. 131:6175-6184.

Simon, M.A., Xu, A., Ishikawa, H.O., and Irvine, K.D. 2010. Modulation of fat:dachsous binding by the cadherin domain kinase four-jointed. *Curr Biol*. 20:811-817.

Singh, J., Yanfeng, W.A., Grumolato, L., Aaronson, S.A., and Mlodzik, M. 2010. Abelson family kinases regulate Frizzled planar cell polarity signaling via Dsh phosphorylation. *Genes Dev*. 24:2157-2168.

Steinhusen, U., Weiske, J., Badock, V., Tauber, R., Bommert, K., and Huber, O. 2001. Cleavage and shedding of E-cadherin after induction of apoptosis. *J Biol Chem*. 276:4972-4980.

Struhl, G., Casal, J., and Lawrence, P.A. 2012. Dissecting the molecular bridges that mediate the function of Frizzled in planar cell polarity. *Development*. 139:3665-3674.

Strutt, D. 2001a. Planar polarity: getting ready to ROCK. *Curr Biol*. 11:R506-509.

Strutt, D. 2003. Frizzled signalling and cell polarisation in Drosophila and vertebrates. *Development*. 130:4501-4513.

Strutt, D. 2009. Gradients and the specification of planar polarity in the insect cuticle. *Cold Spring Harb Perspect Biol*. 1:a000489.

Strutt, D., Johnson, R., Cooper, K., and Bray, S. 2002. Asymmetric localization of frizzled and the determination of notch-dependent cell fate in the Drosophila eye. *Curr Biol*. 12:813-824.

Strutt, D., and Strutt, H. 2007. Differential activities of the core planar polarity proteins during Drosophila wing patterning. *Dev Biol*. 302:181-194.

Strutt, D., and Warrington, S.J. 2008. Planar polarity genes in the Drosophila wing regulate the localisation of the FH3-domain protein Multiple Wing Hairs to control the site of hair production. *Development*. 135:3103-3111.

Strutt, D.I. 2001b. Asymmetric localization of frizzled and the establishment of cell polarity in the Drosophila wing. *Mol Cell*. 7:367-375.

Strutt, D.I., Weber, U., and Mlodzik, M. 1997. The role of RhoA in tissue polarity and Frizzled signalling. *Nature*. 387:292-295.

Strutt, H., Mundy, J., Hofstra, K., and Strutt, D. 2004. Cleavage and secretion is not required for Four-jointed function in Drosophila patterning. *Development*. 131:881-890.

Strutt, H., and Strutt, D. 2002. Nonautonomous planar polarity patterning in Drosophila: dishevelled-independent functions of frizzled. *Dev Cell*. 3:851-863.

Strutt, H., and Strutt, D. 2008. Differential stability of flamingo protein complexes underlies the establishment of planar polarity. *Curr Biol*. 18:1555-1564.

Strutt, H., and Strutt, D. 2009. Asymmetric localisation of planar polarity proteins: Mechanisms and consequences. *Semin Cell Dev Biol*. 20:957-963.

Strutt, H., Warrington, S.J., and Strutt, D. 2011. Dynamics of core planar polarity protein turnover and stable assembly into discrete membrane subdomains. *Dev Cell*. 20:511-525.

Tada, M., and Smith, J.C. 2000. Xwnt11 is a target of Xenopus Brachyury: regulation of gastrulation movements via Dishevelled, but not through the canonical Wnt pathway. *Development*. 127:2227-2238.

Takahashi, M., Takahashi, F., Ui-Tei, K., Kojima, T., and Saigo, K. 2005. Requirements of genetic interactions between Src42A, armadillo and shotgun, a gene encoding E-cadherin, for normal development in Drosophila. *Development*. 132:2547-2559.

Takeuchi, M., Nakabayashi, J., Sakaguchi, T., Yamamoto, T.S., Takahashi, H., Takeda, H., and Ueno, N. 2003. The prickle-related gene in vertebrates is essential for gastrulation cell movements. *Curr Biol*. 13:674-679.

Tamada, M., Farrell, D.L., and Zallen, J.A. 2012. Abl regulates planar polarized junctional dynamics through beta-catenin tyrosine phosphorylation. *Dev Cell*. 22:309-319.

Tamai, K., Zeng, X., Liu, C., Zhang, X., Harada, Y., Chang, Z., and He, X. 2004. A mechanism for Wnt coreceptor activation. *Mol Cell*. 13:149-156.

Tanaka-Matakatsu, M., Uemura, T., Oda, H., Takeichi, M., and Hayashi, S. 1996. Cadherin-mediated cell adhesion and cell motility in Drosophila trachea regulated by the transcription factor Escargot. *Development*. 122:3697-3705.

Taylor, J., Abramova, N., Charlton, J., and Adler, P.N. 1998. Van Gogh: a new Drosophila tissue polarity gene. *Genetics*. 150:199-210.

Tepass, U., Theres, C., and Knust, E. 1990. crumbs encodes an EGF-like protein expressed on apical membranes of Drosophila epithelial cells and required for organization of epithelia. *Cell*. 61:787-799.

Thomas, C., and Strutt, D. 2012. The roles of the cadherins Fat and Dachsous in planar polarity specification in Drosophila. *Dev Dyn*. 241:27-39.

Thomas, S.M., and Brugge, J.S. 1997. Cellular functions regulated by Src family kinases. *Annu Rev Cell Dev Biol*. 13:513-609.

Tolwinski, N.S., Wehrli, M., Rives, A., Erdeniz, N., DiNardo, S., and Wieschaus, E. 2003. Wg/Wnt signal can be transmitted through arrow/LRP5,6 and Axin independently of Zw3/Gsk3beta activity. *Dev Cell*. 4:407-418.

Tomlinson, A., and Ready, D.F. 1987. Cell fate in the Drosophila ommatidium. *Dev Biol*. 123:264-275.

Tomlinson, A., and Struhl, G. 1999. Decoding vectorial information from a gradient: sequential roles of the receptors Frizzled and Notch in establishing planar polarity in the Drosophila eye. *Development*. 126:5725-5738.

Tree, D.R., Ma, D., and Axelrod, J.D. 2002a. A three-tiered mechanism for regulation of planar cell polarity. *Semin Cell Dev Biol*. 13:217-224.

Tree, D.R., Shulman, J.M., Rousset, R., Scott, M.P., Gubb, D., and Axelrod, J.D. 2002b. Prickle mediates feedback amplification to generate asymmetric planar cell polarity signaling. *Cell*. 109:371-381.

Tsarouhas, V., Senti, K.A., Jayaram, S.A., Tiklova, K., Hemphala, J., Adler, J., and Samakovlis, C. 2007. Sequential pulses of apical epithelial secretion and endocytosis drive airway maturation in Drosophila. *Dev Cell*. 13:214-225.

Turing, A.M. 1952. The chemical basis of morphogenesis. *Phil. Trans. R. Soc. Lond.* B:37 – 72.

Uemura, T., Oda, H., Kraut, R., Hayashi, S., Kotaoka, Y., and Takeichi, M. 1996. Zygotic Drosophila E-cadherin expression is required for processes of dynamic epithelial cell rearrangement in the Drosophila embryo. *Genes Dev*. 10:659-671.

Ulrich, F., Krieg, M., Schotz, E.M., Link, V., Castanon, I., Schnabel, V., Taubenberger, A., Mueller, D., Puech, P.H., and Heisenberg, C.P. 2005. Wnt11 functions in gastrulation by controlling cell cohesion through Rab5c and E-cadherin. *Dev Cell*. 9:555-564.

Usui, T., Shima, Y., Shimada, Y., Hirano, S., Burgess, R.W., Schwarz, T.L., Takeichi, M., and Uemura, T. 1999. Flamingo, a seven-pass transmembrane cadherin, regulates planar cell polarity under the control of Frizzled. *Cell*. 98:585-595.

Uv, A., Cantera, R., and Samakovlis, C. 2003. Drosophila tracheal morphogenesis: intricate cellular solutions to basic plumbing problems. *Trends Cell Biol*. 13:301-309.

Veeman, M.T., Slusarski, D.C., Kaykas, A., Louie, S.H., and Moon, R.T. 2003. Zebrafish prickle, a modulator of noncanonical Wnt/Fz signaling, regulates gastrulation movements. *Curr Biol*. 13:680-685.

Vinson, C.R., and Adler, P.N. 1987. Directional non-cell autonomy and the transmission of polarity information by the frizzled gene of Drosophila. *Nature*. 329:549-551.

Wallingford, J.B., and Harland, R.M. 2002. Neural tube closure requires Dishevelled-dependent convergent extension of the midline. *Development*. 129:5815-5825.

Wallingford, J.B., Rowning, B.A., Vogeli, K.M., Rothbacher, U., Fraser, S.E., and Harland, R.M. 2000. Dishevelled controls cell polarity during Xenopus gastrulation. *Nature*. 405:81-85.

Wang, J., Hamblet, N.S., Mark, S., Dickinson, M.E., Brinkman, B.C., Segil, N., Fraser, S.E., Chen, P., Wallingford, J.B., and Wynshaw-Boris, A. 2006a. Dishevelled genes mediate a conserved mammalian PCP pathway to regulate convergent extension during neurulation. *Development*. 133:1767-1778.

Wang, Y., Guo, N., and Nathans, J. 2006b. The role of Frizzled3 and Frizzled6 in neural tube closure and in the planar polarity of inner-ear sensory hair cells. *J Neurosci*. 26:2147-2156.

Wang, Y., and Nathans, J. 2007. Tissue/planar cell polarity in vertebrates: new insights and new questions. *Development*. 134:647-658.

Warrington, S.J., Strutt, H., and Strutt, D. 2013. The Frizzled-dependent planar polarity pathway locally promotes E-cadherin turnover via recruitment of RhoGEF2. *Development*. 140:1045-1054.

Weeraratna, A.T., Jiang, Y., Hostetter, G., Rosenblatt, K., Duray, P., Bittner, M., and Trent, J.M. 2002. Wnt5a signaling directly affects cell motility and invasion of metastatic melanoma. *Cancer Cell*. 1:279-288.

Wehrli, M., Dougan, S.T., Caldwell, K., O'Keefe, L., Schwartz, S., Vaizel-Ohayon, D., Schejter, E., Tomlinson, A., and DiNardo, S. 2000. arrow encodes an LDL-receptor-related protein essential for Wingless signalling. *Nature*. 407:527-530.

Wehrli, M., and Tomlinson, A. 1998. Independent regulation of anterior/posterior and equatorial/polar polarity in the Drosophila eye; evidence for the involvement of Wnt signaling in the equatorial/polar axis. *Development*. 125:1421-1432.

Weigmann, K., Klapper, R., Strasser, T., Rickert, C., Technau, G., Jackle, H., Janning, W., and Klambt, C. 2003. FlyMove--a new way to look at development of Drosophila. *Trends Genet*. 19:310-311.

Wilson, C.W., and Stainier, D.Y. 2010. Vertebrate Hedgehog signaling: cilia rule. *BMC Biol*. 8:102.

Wirtz-Peitz, F., and Zallen, J.A. 2009. Junctional trafficking and epithelial morphogenesis. *Curr Opin Genet Dev*. 19:350-356.

Witzel, S., Zimyanin, V., Carreira-Barbosa, F., Tada, M., and Heisenberg, C.P. 2006. Wnt11 controls cell contact persistence by local accumulation of Frizzled 7 at the plasma membrane. *J Cell Biol*. 175:791-802.

Wolff, T., and Ready, D.F. 1991. The beginning of pattern formation in the Drosophila compound eye: the morphogenetic furrow and the second mitotic wave. *Development*. 113:841-850.

Wolff, T., and Rubin, G.M. 1998. Strabismus, a novel gene that regulates tissue polarity and cell fate decisions in Drosophila. *Development*. 125:1149-1159.

Wong, H.C., Bourdelas, A., Krauss, A., Lee, H.J., Shao, Y., Wu, D., Mlodzik, M., Shi, D.L., and Zheng, J. 2003. Direct binding of the PDZ domain of Dishevelled to a conserved internal sequence in the C-terminal region of Frizzled. *Mol Cell*. 12:1251-1260.

Wong, L.L., and Adler, P.N. 1993. Tissue polarity genes of Drosophila regulate the subcellular location for prehair initiation in pupal wing cells. *J Cell Biol*. 123:209-221.

Wu, J., and Mlodzik, M. 2008. The frizzled extracellular domain is a ligand for Van Gogh/Stbm during nonautonomous planar cell polarity signaling. *Dev Cell*. 15:462-469.

Wu, J., Roman, A.C., Carvajal-Gonzalez, J.M., and Mlodzik, M. 2013. Wg and Wnt4 provide long-range directional input to planar cell polarity orientation in Drosophila. *Nat Cell Biol*. 15:1045-1055.

Xu, T., and Rubin, G.M. 1993. Analysis of genetic mosaics in developing and adult Drosophila tissues. *Development*. 117:1223-1237.

Yamada, S., Pokutta, S., Drees, F., Weis, W.I., and Nelson, W.J. 2005. Deconstructing the cadherin-catenin-actin complex. *Cell*. 123:889-901.

Yan, J., Huen, D., Morely, T., Johnson, G., Gubb, D., Roote, J., and Adler, P.N. 2008. The multiple-wing-hairs gene encodes a novel GBD-FH3 domain-containing protein that functions both prior to and after wing hair initiation. *Genetics*. 180:219-228.

Yan, J., Lu, Q., Fang, X., and Adler, P.N. 2009. Rho1 has multiple functions in Drosophila wing planar polarity. *Dev Biol*. 333:186-199.

Yang, C.H., Axelrod, J.D., and Simon, M.A. 2002. Regulation of Frizzled by fat-like cadherins during planar polarity signaling in the Drosophila compound eye. *Cell*. 108:675-688.

Ybot-Gonzalez, P., Savery, D., Gerrelli, D., Signore, M., Mitchell, C.E., Faux, C.H., Greene, N.D., and Copp, A.J. 2007. Convergent extension, planar-cell-polarity signalling and initiation of mouse neural tube closure. *Development*. 134:789-799.

Yin, C., Kiskowski, M., Pouille, P.A., Farge, E., and Solnica-Krezel, L. 2008. Cooperation of polarized cell intercalations drives convergence and extension of presomitic mesoderm during zebrafish gastrulation. *J Cell Biol*. 180:221-232.

Yokokura, T., Dresnek, D., Huseinovic, N., Lisi, S., Abdelwahid, E., Bangs, P., and White, K. 2004. Dissection of DIAP1 functional domains via a mutant replacement strategy. *J Biol Chem*. 279:52603-52612.

Young, P.E., Richman, A.M., Ketchum, A.S., and Kiehart, D.P. 1993. Morphogenesis in Drosophila requires nonmuscle myosin heavy chain function. *Genes Dev*. 7:29-41.

Zallen, J.A. 2007. Planar polarity and tissue morphogenesis. *Cell*. 129:1051-1063.

Zallen, J.A., and Blankenship, J.T. 2008. Multicellular dynamics during epithelial elongation. *Semin Cell Dev Biol*. 19:263-270.

Zallen, J.A., and Wieschaus, E. 2004. Patterned gene expression directs bipolar planar polarity in Drosophila. *Dev Cell*. 6:343-355.

Zecca, M., Basler, K., and Struhl, G. 1996. Direct and long-range action of a wingless morphogen gradient. *Cell*. 87:833-844.

Zeidler, M.P., Perrimon, N., and Strutt, D.I. 1999. The four-jointed gene is required in the Drosophila eye for ommatidial polarity specification. *Curr Biol*. 9:1363-1372.

Zeidler, M.P., Perrimon, N., and Strutt, D.I. 2000. Multiple roles for four-jointed in planar polarity and limb patterning. *Dev Biol*. 228:181-196.

Zeng, H., Hoover, A.N., and Liu, A. 2010. PCP effector gene Inturned is an important regulator of cilia formation and embryonic development in mammals. *Dev Biol*. 339:418-428.

Zhang, L., and Ward, R.E.t. 2009. uninflatable encodes a novel ectodermal apical surface protein required for tracheal inflation in Drosophila. *Dev Biol*. 336:201-212.

Zheng, L., Zhang, J., and Carthew, R.W. 1995. frizzled regulates mirror-symmetric pattern formation in the Drosophila eye. *Development*. 121:3045-3055.